Public Version – Chapter 5 is confidential and will be available on December 16th, 2024

N° d'ordre : 388

CENTRALE LILLE

THESE

présentée en vue
d'obtenir le grade de

DOCTEUR

en

Spécialité : Génie Electrique

par

Ragavendran RAMACHANDRAN

DOCTORAT DELIVRE PAR CENTRALE LILLE

Titre de la thèse:

Control and Power Management of an Offshore Wind Power Plant with a Diode Rectifier Based HVDC Transmission

Gestion des Flux Energétiques d'une Ferme Eolienne en Mer Connectée à un Système HVDC au travers d'un Redresseur à Diodes

Soutenue 16 Décembre 2019 devant le jury d'examen :

Président	*Pascal MAUSSION, Professor, Toulouse INP, ENSEEIHT, LAPLACE*
Rapporteur	*Salvy BOURGUET, Associate Professor, University of Nantes, IREENA*
Rapporteur	*Lieven VANDEVELDE, Professor, Gent University, EELAB*
Examinatrice	*Héloïse DUTRIEUX BARAFFE, Dr.Engineer, EDF R&D*
Invité	*Abdelkrim BENCHAIB, R&D Manager, SuperGrid Institute*
Invité	*Serge POULLAIN, R&D Manager, SuperGrid Institute*
Directeur de thèse	*Bruno FRANCOIS, Professor, Centrale Lille, L2EP*
Co-encadrant	*Seddik BACHA, Professor, Grenoble Alpes University, G2E Lab*

Thèse préparée dans le Laboratoire L2EP
Ecole Doctorale SPI 072 (Lille I, Lille III, Artois, ULCO, UVHC, EC Lille)

N° d'ordre : 388

CENTRALE LILLE

THESE

présentée en vue
d'obtenir le grade de

DOCTEUR

en

Spécialité : **Génie Electrique**

par

Ragavendran RAMACHANDRAN

DOCTORAT DELIVRE PAR CENTRALE LILLE

Titre de la thèse:

Control and Power Management of an Offshore Wind Power Plant with a Diode Rectifier Based HVDC Transmission

Gestion des Flux Energétiques d'une Ferme Eolienne en Mer Connectée à un Système HVDC au travers d'un Redresseur à Diodes

Soutenue 16 Décembre 2019 devant le jury d'examen :

Président	*Pascal MAUSSION, Professor, Toulouse INP, ENSEEIHT, LAPLACE*
Rapporteur	*Salvy BOURGUET, Associate Professor, University of Nantes, IREENA*
Rapporteur	*Lieven VANDEVELDE, Professor, Gent University, EELAB*
Examinatrice	*Héloïse DUTRIEUX BARAFFE, Dr.Engineer, EDF R&D*
Invité	*Abdelkrim BENCHAIB, R&D Manager, SuperGrid Institute*
Invité	*Serge POULLAIN, R&D Manager, SuperGrid Institute*
Directeur de thèse	*Bruno FRANCOIS, Professor, Centrale Lille, L2EP*
Co-encadrant	*Seddik BACHA, Professor, Grenoble Alpes University, G2E Lab*

Thèse préparée dans le Laboratoire L2EP
Ecole Doctorale SPI 072 (Lille I, Lille III, Artois, ULCO, UVHC, EC Lille)

Abstract

Energy Transition for a more sustainable world is now the priority in societies. Many countries are adopting the increase of their renewable energy capacity as one of the core strategies towards reaching this need. Especially in Europe, the offshore wind energy development has been fast and is playing an important part in the energy transition. Offshore Wind Power Plants continue to get larger and farther from the shore and, hence, Voltage Source Converter (VSC) based High Voltage DC (HVDC) Transmission has become the prominent solution for grid integration. On the Wind Generator (WG) side, the machines are still growing in size and the Type 4 (Full Scale Converter) with a Permanent Magnet Synchronous Generator (PSMG) is the norm for capacities greater than 5 MW. The drive towards decreasing the overall cost of Offshore Wind Power Projects led recently to a breakthrough in the HVDC transmission, with the use of Diode Rectifier Unit (DRU), replacing the large offshore VSC stations by multiple Diode Rectifier (DR) stations that are more compact, robust and cheaper but cannot control the power transfer as done by a VSC station.

This thesis focusses on various technological and scientific problems involved in the control system of the Offshore Wind Power Plant with a Diode Rectifier based HVDC transmission, namely: the WG control and grid forming, black start of the offshore AC power system, fault studies and integration into the Multi Terminal DC (MTDC) grid.

These challenges are first reviewed in detail along with the state of the art. Dynamic analyses are conducted for the offshore AC system for both islanded and connected (normal) mode of operation. According to characteristics of the offshore network, it is observed that the active power and AC voltage of the offshore network are coupled (P-V) and also that the reactive power and the frequency are coupled (Q-f), provided that an instantaneous means of synchronization in an arbitrary dq frame is in place. Based on the analysis, a grid forming control scheme is proposed by using the P-V and Q-f dynamic relationships.

Following this, some of the selected control solutions for the DR-HVDC offshore wind power plant topology are reviewed, compared and assessed by using time domain simulations of a study case. Further, an analysis is conducted on one control solution to understand how to dispatch reactive power sharing to the WGs, by setting droop coefficients. This part of the

analysis cements the understanding of the various existing grid forming approaches, the operation of the offshore system and can provide useful insights for future control innovations and enhancements.

The challenge of black start of the offshore AC power system is then tackled. The different alternatives to the currently existing black start solution are compared using different qualitative criteria. The energy requirements of the offshore wind power system are briefly presented and selected solutions are examined further using these requirements. Then a black start strategy is devised for the offshore wind power system and implemented in a case study.

Following this, the various faults in the offshore system are analyzed, with support from the literature. Then, the above designed Grid forming control scheme is enhanced with Fault Ride through (FRT) capability, for offshore AC grid faults. Finally, a brief analysis is done on the challenges for the integration of this OWPP topology into an MTDC network.

Acknowledgment

The PhD thesis has been an enriching journey, both personally and professionally, with the opportunity to work with the French industry and the Academia. I am immensely grateful for each and every one who have been with me, guided me along, provided those lighter moments and kept me going.

First up, I am deeply thankful to my thesis Director Professor Francois, who has been the guiding light throughout the thesis work. Every time I visited Lille for his guidance, I was more than satisfied and indeed his warmth and simplicity transcends cultures and motivated me throughout. My equally sincere gratitude goes to Professor Bacha for being supportive and helpful, affirming his onsite presence at SuperGrid Institute. Indeed, my supervisors Mr. Serge Poullain and Mr. Abdelkrim Benchaib have been instrumental in guiding me with their strong industrial perspective of the subject matter. I had so much to learn from all these four giants and it has been a genuine pleasure to have worked alongside them.

I would like to thank Miguel, whose expertise guided me in writing one of the major chapters of this thesis. I will always cherish to have known and worked with Christopher, during his short stint as an intern. We three together, had quite a run !

The formal and informal discussions during the course of a PhD always provide a wider perspective and allows one to zoom out, to assure oneself of the progress or sometimes stumble upon new ideas. I will always be grateful to those conversations with Juan Carlos, Kosei and other colleagues who were kind enough to be constructive in their opinion. Thanks to Léo for pitching in with his views and especially helping out with my French writing. And that doesn't mean, those lighter moments and gestures, coffee time conversation meant less. My colleagues have been always warm and encouraging during my journey and for this I will be eternally grateful to them. I wish each and everyone of them all success in their professional and personal endeavors. A special mention definitely goes to the people I got to know from Program 1 and Program 3.

During this journey I had the good fortune of having colleagues from many parts of the world. I have surely made new friends and I am glad to stay back in Lyon for my career after the PhD.

I thank all the colleagues at SuperGrid Institute who have been very kind and accommodating

and having seamlessly handled all the administrative activities concerning me. Thanks to Mr. Hubert de la Grandiere and Mr. Bruno Luscan for having provided me this opportunity to work at this institute. I would also like to thank Centrale Lille and L2EP for enabling this work. Special thanks to Artur, Taoufik, Martin and Xin for their help during the defense. I wish them all success in their careers.

I am gifted to have had the support of my friends, old and new, along this journey - friends from India, whose thoughts and good wishes always followed me around; friends I made along the way, who are all around the world. Thanks to Prasaant, Somya, Naveen, Udhayan, Hariharan, Araksia, Shan, Katya, Madhusudhan, Nisith, Subanesh, Swann, Sivaramakrishnan, Brida and many more who have been my well wishers all along.

I am deeply thankful to my family to have supported me throughout. They have been the steady beacons in my life. Everything I have achieved and will achieve, I dedicate and owe it all to them.

Résumé de la Thèse

Transition Énergétique - Nécessité Impérieuse

Partout dans le monde, des efforts sont faits pour relever l'un des défis les plus importants de notre époque : la lutte contre le changement climatique. Plusieurs stratégies sont possibles pour réduire les émissions de gaz à effet de serre et promouvoir le développement durable, comme la conservation de l'énergie, l'amélioration de l'efficacité des systèmes, la réduction de la consommation de combustibles fossiles, la séquestration du carbone, pour n'en nommer que quelques-uns. Le développement des énergies renouvelables a été adopté comme l'une des principales stratégies de décarbonisation du mix énergétique par de nombreux pays à travers le monde. Cela s'est manifestement reflété dans la capacité cumulative d'énergie renouvelable dans les pays du monde entier, comme indiqué pour les différents continents, dans la Figure 1(source: Agence internationale pour les énergies renouvelables - IRENA). En plus de réduire la consommation de combustibles fossiles, le développement des énergies renouvelables, s'il est bien planifié, peut conduire à des améliorations socio-économiques (promouvoir la croissance de l'emploi, un environnement sain et l'économie), l'ajout de capacités durables, entre d'autres avantages [1].

L'objectif fixé par la directive de l'UE sur les énergies renouvelables est de fournir 20% de la consommation d'électricité grâce aux sources renouvelables [3]. En conséquence de quoi l'UE a investi massivement dans le secteur des énergies renouvelables entre 2005 et 2012 [4]. L'objectif en matière d'énergies renouvelables a récemment été porté à 30% de l'approvisionnement total en énergie en 2030. La plupart des pays seraient sur la bonne voie alors que l'UE dans son ensemble devrait atteindre l'objectif de 20% de l'approvisionnement en énergie issu de sources renouvelables.

Énergie Éolienne Offshore - Contexte Actuel

L'éolien offshore est un secteur industriel qui a connu une croissance rapide en raison de la directive de l'UE sur les énergies renouvelables. À ce jour en Europe, la capacité totale installée

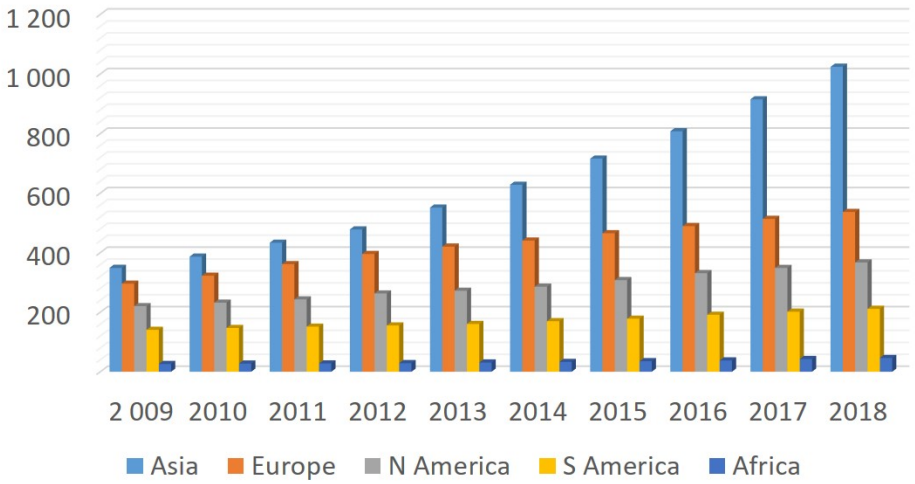

Figure 1: Capacité d'énergie renouvelable (GW) installée sur différents continents | source: base de données chez IRENA[2]

dépasse 20 GW (WindEurope). Le développement de l'éolien offshore a été assez impressionnant (comme illustré dans la Figure 1, provenant de [2]), en raison des innovations dans les turbines, les fondations, les technologies de transmission parmi d'autres facteurs [5]. En plus de ces efforts, le fait que l'énergie éolienne terrestre soit confrontée à des problèmes tels que les coûts d'implantation élevés, une opposition publique croissante résultant de divers facteurs, notamment des aspects visuels [5], a fait de l'éolien offshore le pilier central de nombreux pays européens pour atteindre l'objectif actuel et poursuivre les engagements futurs.

Un rapport de WindEurope ou anciennement de l'Association européenne de l'énergie éolienne (EWEA) [6] prévoit une capacité éolienne offshore comprise entre 49 GW et 99 GW à l'horizon 2030. La Figure 3 compare la capacité cumulée en 2018 pour certains pays européens et la projection pour 2030 selon [6], compte tenu de certains facteurs favorables. Certains pays comme la France, par exemple, devraient rapidement développer et mettre en service davantage d'éoliennes offshore dans les années à venir, y compris flottantes.

A l'extérieur de l'Europe, le développement de l'éolien offshore a déjà été énorme et s'accélère encore. En Chine par exemple (voir Figure 2), la capacité installée de l'éolien offshore a fortement augmenté et s'élève aujourd'hui à 4,59 GW. Le développement de l'éolien offshore aux États-Unis, bien qu'il semble être à la traîne avec une seule centrale éolienne offshore installée à ce jour (le Rhode Island de 30 MW) a une capacité installée projetée de 22 GW à l'horizon 2030 [7].

Selon des statistiques récentes de WindEurope [8], la taille moyenne d'une centrale éolienne a augmenté au-delà de 500 MW et la taille moyenne des éoliennes installées en 2018 est de 6,8 MW. Le Tableau 1 présente la liste des plus grandes éoliennes disponibles aujourd'hui sur le marché, avec le générateur synchrone à aimant permanent (PMSG) de type 4 comme technolo-

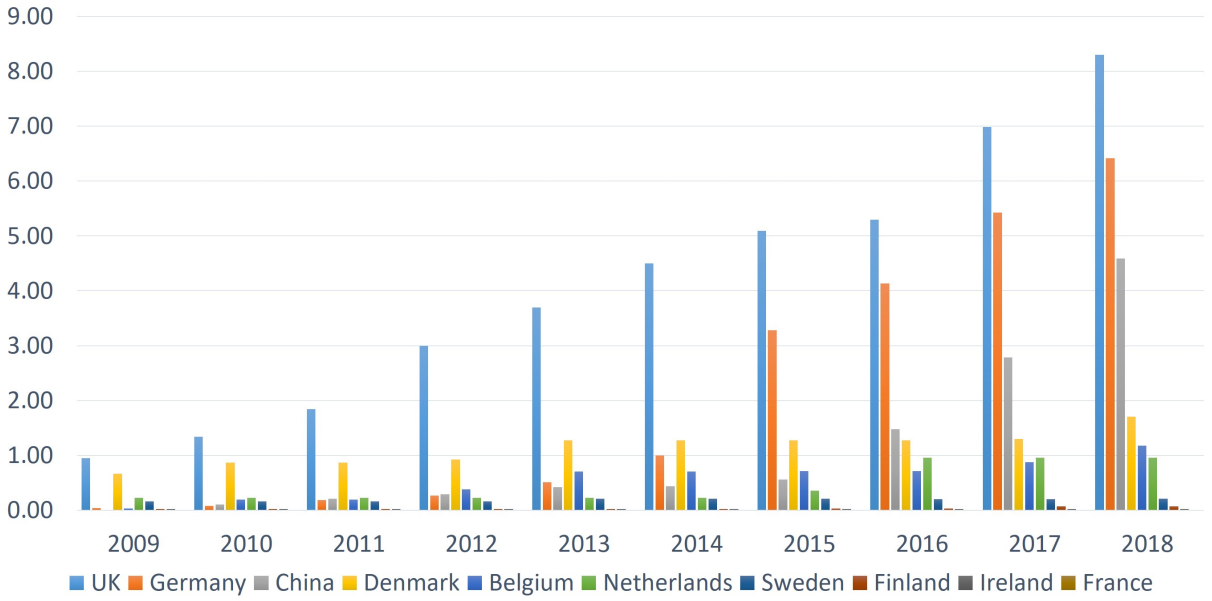

Figure 2: Croissance cumulative de la puissance installée (GW) éolienne offshore dans certains pays | source: IRENA [2]

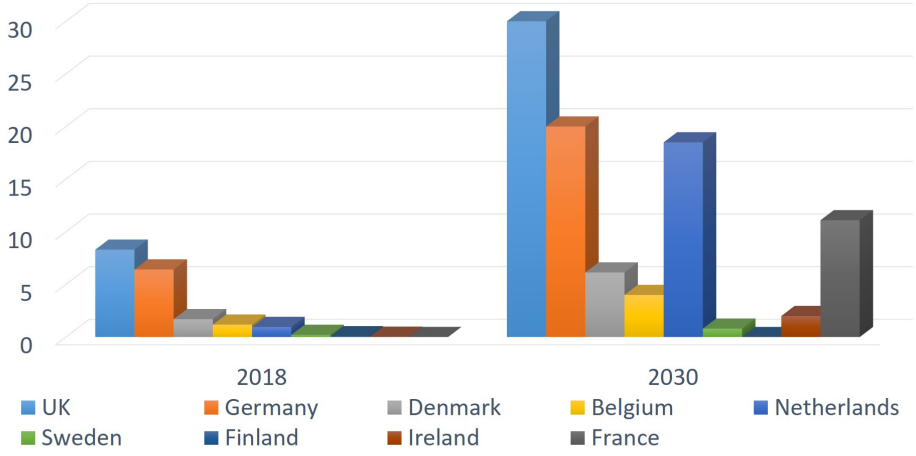

Figure 3: Capacité totale des centrales éoliennes offshore en Europe prévue pour 2030 selon [6]

gie dominante, avec ou sans des multiplicateurs. L'autre caractéristique importante parmi toutes les principales éoliennes est l'utilisation du convertisseur pleine échelle pour la connexion au réseau des PMSG et la tendance ne devrait que se poursuivre. Par exemple, aujourd'hui, la plus puissante des éoliennes - 12 MW et 260 m de hauteur - comme le montre le Tableau 1, se compose d'un PMSG couplé au réseau AC grâce à un FSC (convertisseur pleine échelle).

No	Turbine Manufacturer	Generator Type	Capacity (MW)	Rotor Diameter(m)
1	Siemens	DFIG	4	130
2	Alstom / GE	FSC-PMSG-DD	6	151
3	Siemens	FSC-PMSG-DD	6	154
4	Senvion	DFIG-GB	6.3	152
5	Siemens	FSC-PMSG-DD	8	154
6	MHI Vestas	FSC-PMSG-GB	8	164
7	MHI Vestas	FSC-PMSG - GB	9.5	164
8	Siemens	FSC-PMSG-DD	10	193
9	GE	FSC-PMSG-DD	12	220

Table 1: Liste des principales éoliennes disponibles sur le marché | DFIG- Doubly Fed Induction Generator, FSC- Full Scale Converter Coupled, PMSG - Permanent Magnet Synchronous Generator, DD - Direct Drive (Gearless), GB - (avec)Gear Box/Multiplicateur

Les sites potentiels pour le développement de l'énergie éolienne offshore en Europe, peuvent se situer à une distance de côtes allant jusqu'à 200 km [9]. Pendant le développement initial des OWPP (*Offshore Wind Power Plant*), les connexions en courant alternatif moyenne tension (MVAC) puis courant alternatif haute tension (HVAC) ont été utilisées pour l'intégration au réseau.

Pour les très grandes distances (typiquement au-delà de 80 km et selon les spécificités du projet), les connexions en courant continu haute tension (HVDC) présentent un avantage économique et technique, la technologie HVAC présentant des limites principalement liées à la consommation d'énergie réactive, à la chute de tension et à l'effet de peau [10]. Le convertisseur de source de tension (VSC) basé sur un convertisseur multiniveau modulaire (MMC) est la technologie de pointe utilisée aujourd'hui pour la conversion de la puissance AC en puissance HVDC dans la station offshore. Les coûts et l'empreinte au sol correspondants, bien qu'avantageux par rapport à la solution HVAC, sont néanmoins élevés. Ainsi l'exigence de réduire les subventions allouées à l'éolien offshore a poussé les efforts de recherche et d'innovation à réduire le coût de production de l'électricité (LCOE). Certains des éléments clés de ces efforts ont été l'augmentation de la taille des éoliennes, l'adoption du réseau de collecte MVAC 66 kV contre 33 kV auparavant et l'exploration de nouvelles topologies pour la transmission. L'une de ces innovations qui présente un immense potentiel économique est le remplacement de la station VSC offshore par un redresseur à diode (DR) passif.

La solution industrielle présentée dans [11] revendique une réduction de l'empreinte au sol, des pertes et des coûts (30% de réduction) et une augmentation de la fiabilité. La solution proposée est robuste, compte tenu de la nature passive du DR, avec la plupart des composants associés immergés dans un réservoir rempli d'huile, une exigence de maintenance des composants moindre par rapport à la technologie basée sur le convertisseur VSC. L'illustration de la topologie proposée est présentée dans la Figure 4. Un ajout important à l'architecture est le câble CA moyenne tension reliant directement le réseau terrestre au bus PCC offshore pour le démarrage du réseau offshore et ainsi éviter l'installation de grands générateurs diesel. Il est en effet nécessaire car la liaison HVDC n'est plus bidirectionnelle (comme dans le cas de la topologie VSC-HVDC). Le câble MVAC, avec le transformateur associé et la compensation de puissance réactive, est nommé ombilical. En plus de ce câble ombilical, des modifications du contrôle au niveau des éoliennes et la nécessité d'un convertisseur MMC full bridge pour la station terrestre s'ajoutent au compte du coût total du système.

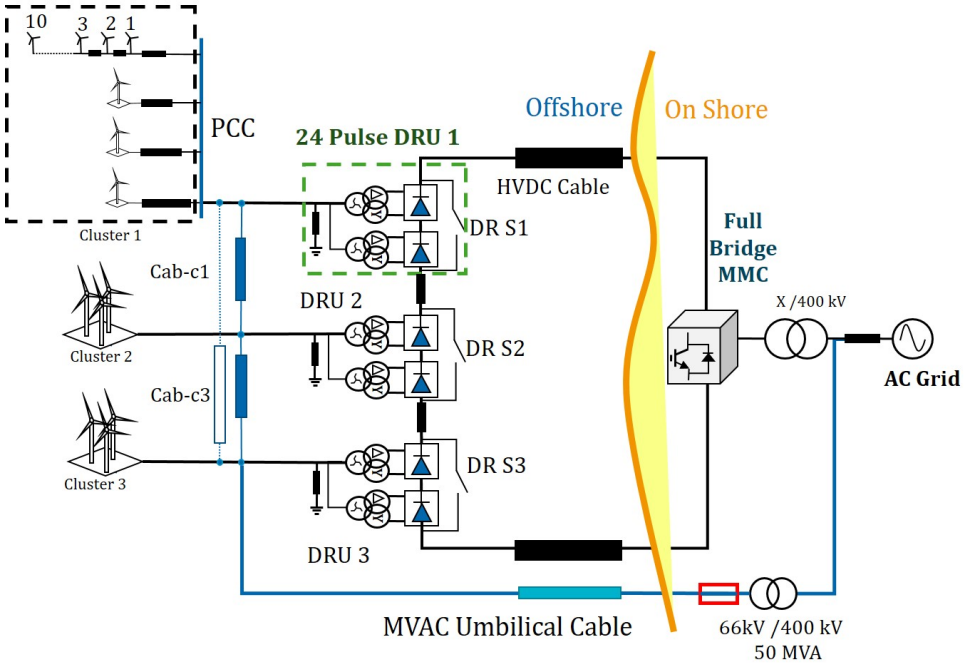

Figure 4: La solution industrielle - DR–HVDC [11]

Contexte et Motivation

Dans le scénario actuel, le développement rapide du secteur éolien offshore doit se poursuivre en Europe afin que les ressources qu'il présente participent aux efforts de décarbonisation du mix énergétique européen. La centrale éolienne offshore basée sur DR-HVDC est une avancée importante vers la réduction des coûts des grands parcs. Cependant, la solution industrielle actuelle

(bien sûr d'un seul fabricant) ne se révèle pas universelle, adaptée à tous les développeurs OWPP et fabricants connexes. En outre, aucun projet pilote n'a encore été mis en œuvre à la connaissance de l'auteur. Des efforts doivent donc être faits pour comprendre le fonctionnement de ce système, les défis liés à cette topologie et trouver des solutions adéquates aux différents défis pour permettre l'intégration de cet OWPP basé sur les DR-HVDC au réseau.

Cela nécessite également de prendre en compte deux tendances importantes des systèmes électriques en Europe aujourd'hui, résumées comme suit:

1. Aujourd'hui, les exigences de connexion au réseau évoluent pour les grandes centrales éoliennes offshore, en particulier celles connectées par transmission HVDC. Elles ont le potentiel de contribuer au bon fonctionnement du réseau AC, comme par exemple : aider à la restauration du système électrique (blackstart du réseau AC), fournir un support en fréquence [12], des services auxiliaires, etc., [13].
2. Le développement du réseau Multi Terminal DC (MTDC) en Europe nécessite une analyse des défis associés à l'intégration de cette topologie OWPP dans le futur réseau MTDC.

La motivation de cette thèse est fondée sur l'exploration d'alternatives à la solution industrielle actuelle, afin de faciliter la réduction des coûts, en évitant l'utilisation le câble ombilical, et en tenant compte des tendances mentionnées ci-dessus. Les défis à relever pour atteindre ces objectifs comprennent : le contrôle coordonné des éoliennes, la garantie d'une régulation stable de la tension et de la fréquence AC du réseau offshore (Grid Forming du réseau), le partage de la puissance réactive, la synchronisation des éoliennes, le démarrage système (alternative à l'ombilical), la gestion des modes de défaillance et l'intégration dans un réseau MTDC.

Contribution et Aperçu de la Thèse

Une approche en trois volets a été jugée nécessaire pour ce travail de thèse du fait de l'ampleur du sujet traité et de l'exigence de construire une base de connaissances sur celui-ci afin de permettre de futures innovations et projets.

- L'approche a d'abord impliqué une compréhension approfondie du fonctionnement et du contrôle des systèmes VSC-HVDC et DR-HVDC OWPP comme base de connaissances. Ce volet comprenait principalement une étude de la littérature et une analyse du système.
- Deuxièmement, des analogies ont été faites et des inspirations ont été tirées des systèmes d'alimentation comme le système d'alimentation AC traditionnel et les micro-réseaux alimentés principalement par des onduleurs. Ce processus de réexamen des solutions existantes dans d'autres systèmes électriques a été effectué pour traiter chacun des défis mentionnés et a également aidé à mieux comprendre le problème.
- La dernière composante de l'approche a consisté à relever ces défis dans un effort de fournir des nouvelles solutions et en s'appuyant fortement sur les deux premiers volets

ci-dessus.

Dans la perspective de relever certains de ces défis majeurs, les travaux suivants sont considérés comme les contributions majeures de cette thèse:

1. Modélisation dynamique, analyse du système DR-HVDC OWPP et proposition d'un schéma de contrôle du réseau offshore de façon distribuée par les éoliennes.
2. Etude et comparaison théoriques des solutions existantes pour cette topologie. Dans une autre étape, certaines des principales solutions de 'Grid Forming' (contrôle du réseau offshore) ont été évaluées en détail à l'aide de simulations dans le domaine temporel. L'analyse des coefficients de droop pour le partage effectif de la puissance réactive par les éoliennes a été effectuée pour l'une des solutions.
3. Revue de la littérature et analyse des différents types de défauts dans le réseau offshore. L'accent est mis sur compréhension des failles à travers les stratégies qui sont en place aujourd'hui pour les OWPP connectés au HVDC et analyse de l'extension des différentes approches pour le DR-HVDC Topologie.
4. Revue de la littérature et analyse préliminaire des défis liés à l'intégration du DR-HVDC OWPP dans un réseau MTDC.

Un bref aperçu des différents chapitres de thèse est présenté ici.

Le chapitre 2 fournit un contexte détaillé pour la thèse par l'examen de différents aspects technologiques liés à l'éolienne offshore. L'accent est mis sur la technologie WG, les topologies de système OWPP, les systèmes de contrôle et de protection OWPP, avec une section dédiée aux différents défis concernant l'intégration au réseau des OWPP basés sur DR-HVDC.

Le chapitre 3 traite la modélisation et l'analyse détaillée de la centrale éolienne offshore avec transmission DR-HVDC. Le système éolien offshore est analysé en utilisant les équations dynamiques développées en d-q pour les modes de fonctionnement tant insulaires que connectés (normaux). Cela permet d'établir les différentes exigences de contrôle pour les GT pour le démarrage et le fonctionnement stable dans les différents modes de fonctionnement.

Dans le chapitre 4, les différentes solutions de 'Grid Forming' et de gestion de l'alimentation pour le DR-HVDC OWPP basé sont examinées en détail. Une comparaison théorique est effectuée ayant pour but de mettre en évidence les similarités et différences entre solutions. Ceci est suivi d'une évaluation détaillée des solutions sélectionnées à l'aide d'un cas d'étude, qui est implémenté dans MATLAB Simulink. De plus, une des solutions est analysée de façon détaillée pour différents coefficients de droop afin de faire varier le rapport de partage de puissance réactive entre les éoliennes. Ces études permettent de bien comprendre les approches existantes de 'Grid Forming', ce qui peut aider dans les futures innovations ou améliorations de contrôle.

Le chapitre 5 présente le travail accompli pour comprendre le problème du démarrage et analyser les différentes alternatives. Celles-ci sont comparées en fonction de différents critères qualitatifs.

Le chapitre 6 tente de fournir une analyse préliminaire des différentes défaillances de la centrale éolienne offshore (OWPP) avec transmission DR-HVDC. Puis un aperçu des défis concernant l'intégration de cette topologie OWPP dans un réseau MTDC est présenté afin de mettre en évidence les problèmes potentiels au niveau du système tant pour le fonctionnement normal que pour les cas de défaut.

Contents

Abstract iii

Acknowledgment v

Résumé de la Thèse vii

List of figures xix

List of tables xxiii

1 General introduction 1

1.1 Energy Transition – The need of the hour . . . 2
1.2 Offshore Wind Energy – Current Context . . . 3
1.3 Context and Motivation . . . 5
1.4 Contributions and Thesis Outline . . . 7
1.5 List of Publications . . . 8

2 Offshore Wind Power Plants: An Overview 9

2.1 Chapter Introduction . . . 10
2.2 Background . . . 10
2.2.1 Basics on Wind Energy Conversion . . . 10
2.2.2 On the Maximum Power Point Tracking and Ideal Power Curves . . . 12
2.2.3 Operation Zones for a Wind Generator . . . 14
2.2.4 OWPP Architecture and Control Overview . . . 16
2.3 Wind Electric Generator Technologies . . . 18
2.3.1 Fixed Speed Wind Generators . . . 18
2.3.2 Limited Variable-speed Wind Generators . . . 19
2.3.3 Variable-speed Wind Generators with Partial–scale Converter . . . 20
2.3.4 Variable-speed Wind Generators with Full–scale Converter . . . 21
2.4 Offshore Wind Power Plant Topologies . . . 22

2.4.1 MVAC Collection with HVAC Transmission . . . 22
2.4.2 MVAC Collection with HVDC Transmission . . . 23
2.4.3 OWPP with DC Grids . . . 25
2.4.4 Other Innovative Topologies . . . 26
2.5 Offshore Wind Power Plant Control Principles . . . 28
2.5.1 General Description . . . 28
2.5.2 Wind Generator Control Capabilities . . . 29
2.5.3 Control Capabilities of the OWPPs from AC system perspective . . . 31
2.5.4 Control Overview of OWPP with VSC-HVDC transmission . . . 32
2.6 System Protection and Fault Ride Through . . . 33
2.6.1 Offshore Wind Power System Protection Layout . . . 33
2.6.2 Wind Generator Fault Ride Through Capabilities . . . 34
2.6.3 VSC-HVDC FRT Capabilities . . . 35
2.7 OWPP with DR–HVDC Transmission - Overview . . . 36
2.7.1 Interests in DR-HVDC Transmission . . . 36
2.7.2 Operation Characteristics of the Diode Rectifier . . . 37
2.7.3 Description of OWPP Topology . . . 40
2.7.4 OWPP Operation Overview . . . 43
2.7.5 Control Overview . . . 45
2.8 DR OWPP Grid Integration Challenges . . . 45
2.8.1 Overview of Challenges . . . 45
2.8.2 Grid Forming . . . 46
2.8.3 Black Start of the Offshore AC Grid . . . 48
2.8.4 Ensuring Safe operation during faults . . . 49
2.8.5 Integration into the MTDC Grid . . . 49
2.9 Chapter Conclusions . . . 50

3 Dynamic Modelling, Analysis and Control 53
3.1 Chapter Introduction . . . 54
3.2 Modelling of the Offshore Wind Power System . . . 54
3.2.1 Drive Train . . . 55
3.2.2 Permanent Magnet Synchronous Generator . . . 55
3.2.3 MSC and DC link . . . 56
3.2.4 Grid Side Converter and Filter . . . 57
3.2.5 Offshore Point of Common Coupling . . . 58
3.2.6 Diode Rectifier Model . . . 59
3.2.7 Simplified Model of the HVDC Link . . . 60
3.2.8 Onshore Converter Model . . . 61

3.3 Analysis of the Offshore Wind Power system . . . 62
3.3.1 Analysis of Islanded Mode of Operation . . . 63
3.3.2 Analysis of the Normal Mode of Operation . . . 69
3.3.3 Control Requirements for the Offshore Network . . . 75
3.4 Conclusion and Future Scope . . . 76
3.4.1 Chapter Summary . . . 76
3.4.2 Future Scope for the Grid Forming using WGs . . . 76

4 Grid Forming: Review and Assessment **79**
4.1 Introduction . . . 80
4.2 Review and Comparison . . . 80
4.2.1 Background . . . 80
4.2.2 Solution 1: Distributed Control of the PCC Voltage and grid Frequency 81
4.2.3 Solution 2: Fixref with an MVAC Umbilical Cable . . . 85
4.2.4 Solution 3: Distributed Control of the output Voltage and Frequency with a PLL based synchronization . . . 87
4.2.5 Solution 4: Decentralized frequency control with a secondary controller for frequency deviation . . . 89
4.2.6 Comparison of the Grid Forming Solutions . . . 91
4.3 Simulation Results and Assessment of Solutions . . . 93
4.3.1 Study Case Description . . . 93
4.3.2 Simulation and Analysis of Solution 1 . . . 94
4.3.3 Simulation and Analysis of Solution 2 . . . 95
4.3.4 Simulation and Analysis of Solution 3: Distributed voltage and frequency control with PLL based Synchronization . . . 99
4.4 Analysis and Discussion . . . 101
4.4.1 Solution 1 . . . 101
4.4.2 Solution 2 . . . 103
4.4.3 Solution 3 . . . 104
4.5 Conclusion . . . 105

5 On the Black Start of the Offshore AC Grid **107**
5.1 Chapter Introduction . . . 108
5.2 Overview of the Black Start Problem . . . 108
5.2.1 Black Start in the context of the traditional AC power system . . . 108
5.2.2 Black Start in the context of the Offshore Grid . . . 109
5.2.3 Black Start Capabilities of a WG . . . 110
5.2.4 Power Requirements of the OWPP system . . . 112
5.3 Assessment of Solutions for Black Start . . . 114

5.3.1 1a. VSC in series with the DR . . . 114
5.3.2 1b. Offshore VSC with a Centralized Energy Storage . . . 115
5.3.3 2a. Photo-Voltaic Panel installations on the Nacelle of WGs in addition to other energy source . . . 115
5.3.4 2b. Distributed Energy Storage at WG level . . . 116
5.3.5 Assessment and Comparison of Solutions . . . 117
5.4 Conclusion and Research Prospects . . . 119

6 On the Faults and MTDC Integration 121
6.1 Introduction . . . 122
6.2 OWPP Network Faults – Overview . . . 122
6.2.1 The fault response in traditional AC vs Inverter based Grids . . . 122
6.2.2 LVRT Requirements for Generators . . . 123
6.2.3 Fault Response of a Type 4 WG . . . 124
6.2.4 Faults in OWPP with DR HVDC Transmission . . . 126
6.2.5 Types of Faults and Failures . . . 126
6.3 Existing Fault Ride Through Strategies . . . 131
6.3.1 FRT at system level for Onshore AC grid Faults . . . 133
6.4 Integration into an MTDC Grid . . . 134
6.4.1 Overview of the MTDC Grid operation . . . 134
6.4.2 Operation of a Three Terminal MTDC Grid with DR-HVDC OWPP . . . 135
6.4.3 Faults and Failure Modes at System level . . . 137
6.5 Chapter Conclusion . . . 140

7 Conclusion 143
7.1 Summary and Major Conclusions . . . 144
7.2 Future Prospects for Research Work . . . 145

A MPPT Methods for Wind Generators 159

B MMC Converter Topology 161

C DC Voltage Control for Solution 1 165

D Aggregation of WGs and string impedances 167

List of figures

1 Capacité d'énergie renouvelable (GW) installée sur différents continents | source: base de données chez IRENA[2] . . . viii
2 Croissance cumulative de la puissance installée (GW) éolienne offshore dans certains pays | source: IRENA [2] . . . ix
3 Capacité totale des centrales éoliennes offshore en Europe prévue pour 2030 selon [6] . . . ix
4 La solution industrielle . . . xi

1.1 Installed Renewable Energy Capacity (GW) in Different Continents . . . 2
1.2 Offshore Wind Cumulative Installed Capacity Growth (GW) . . . 3
1.3 Capacity of total Offshore Wind in Europe projected for 2030 as per [6] . . . 4
1.4 Illustration of the industrial proposal . . . 6

2.1 Generic representation of a Wind Generator . . . 11
2.2 Variation of Power coefficient of the wind turbine with respect to β and λ . . . 13
2.3 Power output vs Generator speed for multiple wind speeds . . . 14
2.4 Ideal Operation Curves of a WG and the related Operation Zones . . . 15
2.5 Generic Architecture of an Offshore Wind Power Plant . . . 16
2.6 Hierarchical Control Architecture for an OWPP . . . 17
2.7 Fixed Speed Wind Generator . . . 19
2.8 Limited Variable Speed Generator . . . 19
2.9 Type 3 Wind Generator or the DFIG . . . 20
2.10 Type 4 or FSC Wind Generator . . . 21
2.11 MVAC topology with HVAC transmission . . . 23
2.12 MVAC Topology with a VSC-HVDC Transmission . . . 24
2.13 OWPP with MVDC-HVDC topology . . . 26
2.14 Hybrid DR-VSC Topology . . . 27
2.15 Control Capabilities of the Back to Back converter . . . 30
2.16 Block Diagram Representation of the PLL . . . 30

2.17 Control overview of the OWPP with VSC–HVDC transmission 32
2.18 Protection Layout for the OWPP AC Grid 34
2.19 Protection layout for WGs in a feeder for increased availability 34
2.20 VSC-HVDC system with crowbar at onshore VSC station 35
2.21 A Six Pulse Diode Bridge connected to a DC voltage source 37
2.22 Three Phase AC voltage and current at PCC and Six Pulse DC output 38
2.23 Characteristic harmonics of the six pulse DR (a) RMS AC voltage at DR input (b) RMS AC current at the DR input 39
2.24 AC Voltage (V_{gabc}) and Current (I_{abc}) in the DR input for (a) DCM (b) CCM1 (c) CCM2 41
2.25 OWPP with DR-HVDC Grid Integration 42
2.26 A single 12 pulse Diode Rectifier Unit, as illustrated in [58] 43
2.27 The various operating modes of the DR-HVDC OWPP 44
2.28 Control overview of the OWPP with DR-HVDC transmission 45
2.29 Illustration of a three terminal radial MTDC grid with DR-HVDC OWPP . . . 50

3.1 Overview of the Offshore Wind Power System 54
3.2 Wind Turbine Drive Train Model 55
3.3 Dynamic model of the PMSG (a) d–axis (b)q–axis 56
3.4 Machine Side Converter with DC link 57
3.5 Grid Side Converter with RL Filter 57
3.6 Grid Side Converter with LC Filter 58
3.7 Offshore PCC Terminal with aggregated Strings 59
3.8 DR and HVDC Link Model 59
3.9 Average Model of DR with Virtual impedance 60
3.10 T-Model of the HVDC link 61
3.11 Onshore VSC connection to the AC Grid 62
3.12 Equivalent Circuit of the OWPP in islanded mode 63
3.13 OWPP Island Network Analysis 67
3.14 Equivalent Circuit of the OWPP in Normal Operating Mode 69
3.15 Analysis of OWPP Connected Mode: dq currents injected by the GSCs 71
3.16 Analysis of OWPP Normal Operation 72

4.1 Aggregated model of multiple strings connected to the offshore PCC 82
4.2 Voltage and frequency control for a single aggregated GSC connected to the PCC 83
4.3 Distributed Control of offshore PCC voltage and frequency 84
4.4 DR-HVDC OWPP system with an MVAC cable and FIXREF system 85
4.5 Fixref Control scheme for Type 4 WG 86
4.6 Grid Forming with PLL based Synchronization 87

4.7 Grid Forming with PLL based Synchronization . . . 90
4.8 Study Case Network for Simulation Studies . . . 93
4.9 Simplified Models for the WG . . . 95
4.10 Simulation Results for Solution 1 . . . 96
4.11 Simulation Results for Solution 2 . . . 98
4.12 Simulation Results for Solution 2 - Droop Factor Variation . . . 100
4.13 Simulation Results for Solution 3 . . . 102
4.14 Differences between solutions 3 and 4 for frequency regulation . . . 104

5.1 Study Case Network for Black Start Analysis . . . 112
5.2 Illustration of Black Start Solutions possible for the OWPP system . . . 114
5.3 ESS integration at the AC side of the GSC . . . 116
5.4 ESS Integration in the DC bus of the GSC back to back converter system . . . 116

6.1 LVRT Requirements in Various Countries in and around Europe as illustrated in [103] . . . 123
6.2 Reactive Power Requirement in proportion to the decrease in AC voltage in a few European Countries [103] . . . 124
6.3 Typical Layout type 4 WG with Grid Following Scheme . . . 125
6.4 Various Faults and Failure cases in the DR–HVDC OWPP system . . . 127
6.5 Illustration for Fault case F1 (a) Fault Instance (b) Post Fault Condition / System Restoration . . . 128
6.6 Annual down time in days for different components of a WG. Courtesy: [115] . . . 131
6.7 Principle of VDCOL Strategy - Current Contribution vs Voltage Level . . . 132
6.8 FRT contribution based on Voltage Error, as per the strategy in [62] . . . 133
6.9 DC Voltage and Power Droop relationship Curve for a VSC station . . . 135
6.10 A Radial three terminal MTDC grid with DR-OWPP station . . . 136
6.11 Generic MTDC grid Droop Control scheme of the MMC stations . . . 136
6.12 FRT contribution based on Voltage Error, as per the strategy in [62] . . . 137
6.13 Illustration of faults in two inter-cluster cables in the Offshore AC grid . . . 139

B.1 Illustration of an MMC and a Half Bridge MMC Sub-module . . . 162
B.2 Illustration of a Full Bridge Sub-module . . . 162

C.1 Generic representation of a Wind Generator . . . 166

D.1 Study Case Network for Simulation Studies . . . 167

List of tables

1 Liste des principales éoliennes disponibles sur le marché x

1.1 List of major wind turbines available in the market 4

2.1 Control Strategies Possible for the Back to Back Converter System 30
2.2 Parameters for simulation of Six Pulse Diode Rectifier connected to a DC source 40

3.1 Network parameters for the analysis of the OWPP system 64

4.1 Comparison of the Different Grid forming Approaches 92
4.2 Network parameters for the Study case 94
4.3 Different droop settings for Fixref reactive power sharing 99

5.1 Network parameters for the Case Study 113
5.2 Comparison of the Different Black Start Solutions 118
5.3 Comparison of design requirements for solutions 1b and 2a for different cases . 119

1

General introduction

Contents

1.1 Energy Transition – The need of the hour 2
1.2 Offshore Wind Energy – Current Context 3
1.3 Context and Motivation 5
1.4 Contributions and Thesis Outline 7
1.5 List of Publications 8

1.1 Energy Transition – The need of the hour

Around the world, efforts were, are and will be made to address one of the most important challenge of our times – combating climate change. Multiple strategies are possible to reduce the green house gas emissions and promote sustainable development like energy conservation, increasing efficiency of systems, reducing fossil fuel consumption, carbon sequestration, to name a few. The development of renewable energy has been adopted as one of the prominent strategies towards decarbonization of the energy mix, by many countries across the world. This has evidently reflected in the cumulative renewable energy capacity in countries across the world as shown for different continents, in the Figure 1.1 (source: International Renewable Energy Agency - IRENA). In addition to reducing fossil fuel consumption, the development of renewable energy if planned well, can lead to socio-economic improvements (promote job growth, healthy environment and the economy), sustainable capacity addition, among other benefits [1].

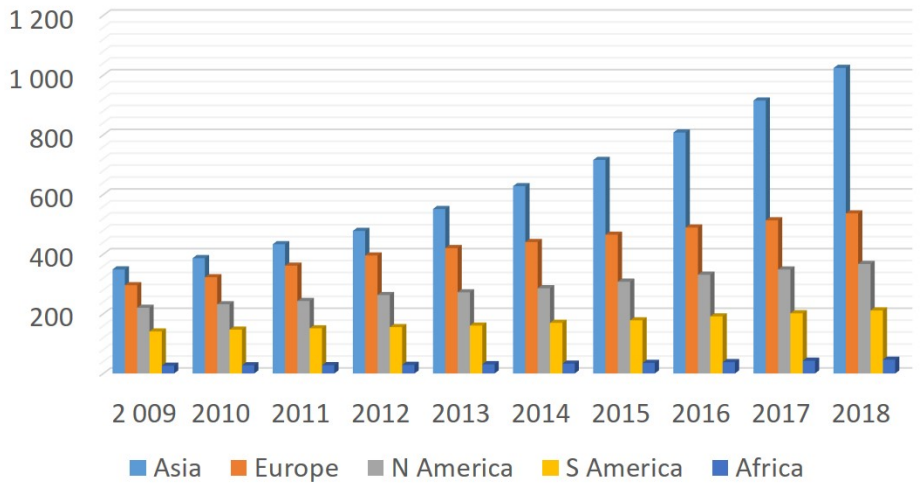

Figure 1.1: Installed Renewable Energy Capacity (GW) in Different Continents | source:IRENA database [2]

Especially in Europe, the energy provision from renewables has been set a target of 20% of the total energy needs, by the Renewable Energy Directive [3]. This resulted in the EU region, pumping in the highest new investments for renewable energy sector in the whole world during the period between 2005 and 2012 [4]. The renewable energy target has been recently increased to 30% of energy supply from renewables in the year 2030, since most of the countries are said to be on track and overall, the EU is expected to reach the goal of 20% RE supply.

1.2 Offshore Wind Energy – Current Context

One of the prominent industrial sectors which saw rapid growth due to the renewable energy directive in Europe is the Offshore Wind industry. As of today in Europe, the total installed capacity has crossed 20 GW (WindEurope). The development of offshore wind has been quite impressive (as in the Figure 1.2, sourced from [2]), as a consequence of innovations in turbines, foundations, transmission technologies among various other factors [5]. In addition to these efforts, the fact that the onshore wind power faces problems like high siting costs, higher public opposition stemming from various factors including visual aspects [5], has made offshore wind the cornerstone for many of the European countries in achieving the current goals and pursue future commitments. One report by WindEurope or formerly the European Wind Energy Association (EWEA) [6] projects the offshore wind capacity to be between 49 GW and 99 GW by 2030. The Figure 1.3 compares the cumulative capacity in 2018 for some of the European countries and the projection for 2030 as per [6], considering certain favorable factors. Some of the countries like France, for instance, is seen to rapidly develop and commission more offshore wind power plants in the coming years, including projects with floating wind turbines.

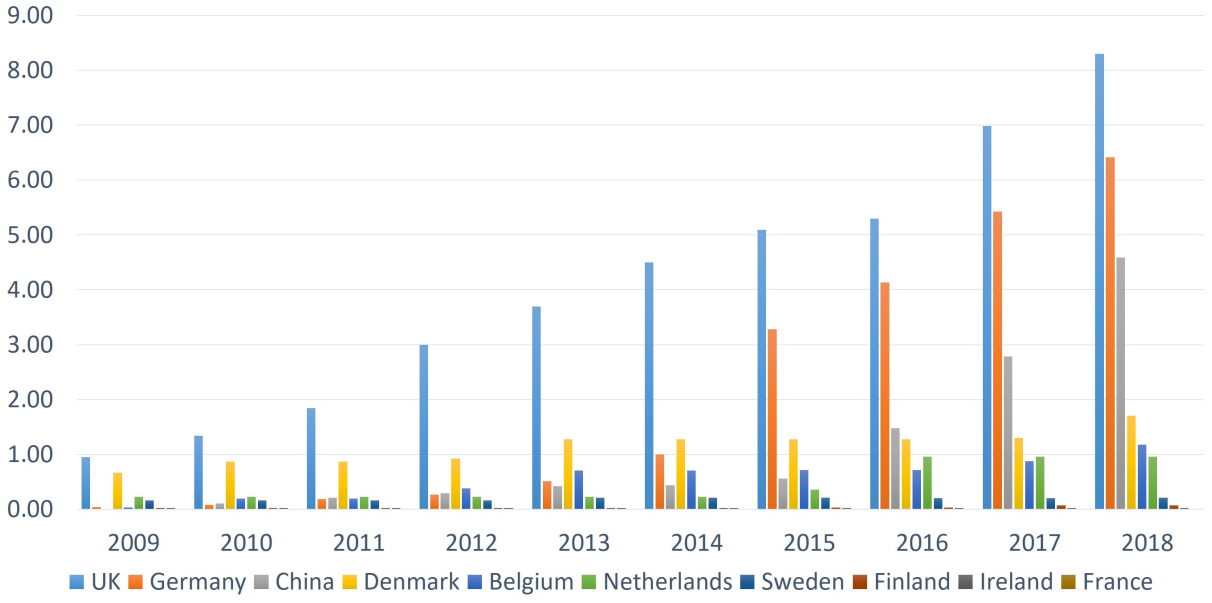

Figure 1.2: Offshore Wind Cumulative Installed Capacity Growth (GW) in selected countries | source: IRENA [2]

Outside Europe, the development of offshore wind has already been enormous or is gaining pace for sustained future developments. In China for instance (see Figure 1.2), the installed capacity of offshore wind has increased enormously and stands at 4.59 GW today. The US Offshore wind development, though seems to be lagging with only one offshore wind power plant installed as of today (the 30 MW Rhode Island), has a projected installed capacity of upto

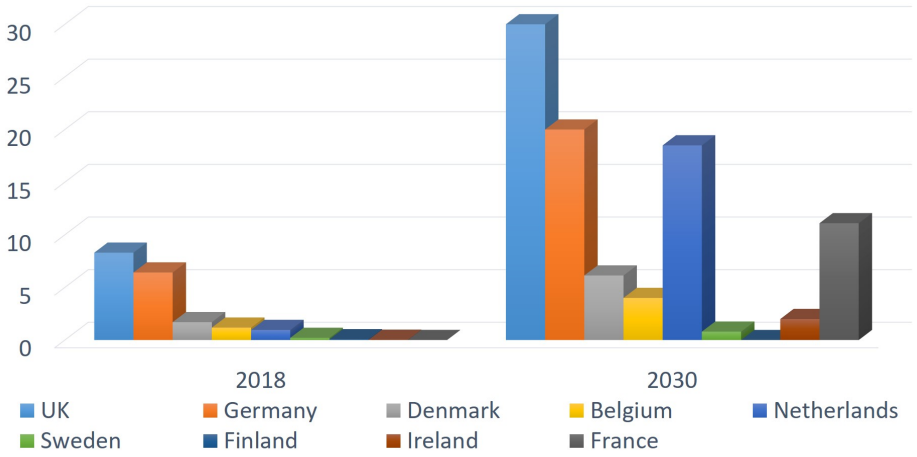

Figure 1.3: Capacity of total Offshore Wind in Europe projected for 2030 as per [6]

22 GW by 2030 [7].

According to recent statistics from WindEurope [8] the average size of an OWPP has increased beyond 500 MW and the average size of wind turbines installed in the year 2018 is 6.8 MW. The Table 1.1 shows the list of the largest wind turbines available today in the market, with the Permanent Magnet Synchronous Generator (PMSG) Type 4 as the prominent technology, with or without gear box. The other prominent feature among all the major wind turbines is the use of Full Scale Converter for grid connection of the PMSGs and the trend is only set to continue. For instance, today the largest wind turbine is a towering 12 MW, 260 m, as seen in the Table 1.1, consists of PMSG coupled with FSC (back to back converter) to the AC grid.

No	Turbine Manufacturer	Generator Type	Capacity (MW)	Rotor Diameter(m)
1	Siemens	DFIG	4	130
2	Alstom / GE	FSC-PMSG-DD	6	151
3	Siemens	FSC-PMSG-DD	6	154
4	Senvion	DFIG-GB	6.3	152
5	Siemens	FSC-PMSG-DD	8	154
6	MHI Vestas	FSC-PMSG-GB	8	164
7	MHI Vestas	FSC-PMSG - GB	9.5	164
8	Siemens	FSC-PMSG-DD	10	193
9	GE	FSC-PMSG-DD	12	220

Table 1.1: List of major wind turbines available in the market | DFIG- Doubly Fed Induction Generator, FSC- Full Scale Converter Coupled, PMSG - Permanent Magnet Synchronous Generator, DD - Direct Drive (Gearless), GB - (With)Gear Box

The potential sites for offshore wind power development around Europe, can be at a distance

of up-to 200 km [9]. During the initial development of OWPPs, MVAC and then High Voltage Alternative Current (HVAC) transmission connections have been used for grid integration.

For very large distances (80 km and beyond, but dependent on the project), High Voltage Direct Current (HVDC) transmission has economical advantage, due to limitations of the HVAC technology, mostly related to the reactive power consumption, voltage drop and skin effect [10]. The Modular Multilevel Converter (MMC) based Voltage Source Converter (VSC) is today's state of the art technology used for the AC to HVDC power conversion in the offshore station. The relevant costs and footprint, although advantageous compared to the HVAC solution, is by itself quite expensive. This, coupled with the requirement to reduce the Levelized Cost of Electricity (LCOE) and the subsidies for offshore wind, has pushed the research and innovation efforts on minimizing the former. Some of the key components of these cost reduction efforts have been the increase in the wind turbine size, adoption of 66 kV MVAC Collection network over 33 kV, exploration of new topologies for transmission, among others.

One such innovation that has an immense potential for cost savings is the replacement of the offshore VSC station with a passive Diode Rectifier. The industrial solution presented in [11] claims reduction in footprint, losses and costs (30% reduction) and an increase in reliability. The proposed solution is robust, given the passive nature of the DR, with most of the associated components immersed in an oil filed tank, with reduction in maintenance of components compared to the VSC based technology. The illustration of the proposed topology is shown in the Figure 1.4. An important addition to the architecture is the Medium Voltage AC cable connecting the onshore grid directly with the offshore PCC bus. It is required since the HVDC link is no longer bidirectional (as in the case of VSC-HVDC topology) and to avoid installation of large diesel generators for start-up purposes. The MVAC Cable, with the associated transformer and reactive power compensation is dubbed the umbilical. This and other features like grid forming WGs (of only one manufacturer), full bridge MMC for onshore station add up to the total cost of the entire system.

1.3 Context and Motivation

In current scenario, the fast offshore wind development will continue across countries to tap into their offshore resource potential in efforts to de-carbonize their energy mix. The DR-HVDC based Offshore Wind Power Plant is an important advancement towards the cost reduction of large OWPPs. However, the current industrial solution (of course from one single manufacturer) is not found to be universal, suitable for all OWPP developers and related manufacturers. Moreover, a Pilot project has not been yet implemented, according to the author's knowledge. Efforts need to be made to understand the operation of this system, challenges related to this topology and find solutions to the various challenges to enable seamless grid integration of this DR-HVDC based OWPP.

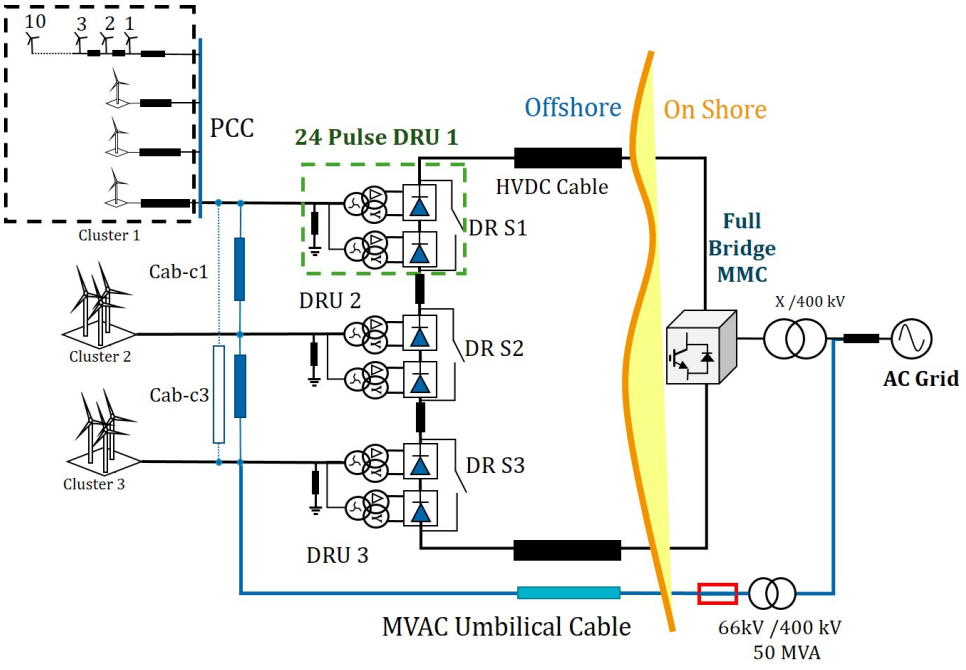

Figure 1.4: Illustration of the industrial proposal - DR–HVDC for Grid Integration of OWPP [11]

This also requires taking into account the two important trends in power systems in Europe today, highlighted as follows:

1. Today the grid connection requirements are evolving for large offshore wind power plants, especially connected by HVDC transmission. They can potentially contribute more towards the operation of the AC grid, for instance help in power system restoration (black start of AC grid), provide frequency support [12], ancillary services etc., [13].
2. The development of Multi Terminal DC (MTDC) grid in Europe requires analysis of challenges associated with the integration of this OWPP topology into the future MTDC grid.

The motivation for this thesis revolves around the exploration of alternatives to the current industrial solution, and facilitate a cost reduction, by avoiding the umbilical cable, with considerations of the above mentioned trends. Some of the challenges towards achieving these goals include, coordinated control of WGs, ensuring a stable AC voltage and frequency regulation of the offshore grid (grid forming), reactive power sharing, synchronization of WGs, black start of the system (alternative to the umbilical), fault studies, analysis of failure modes and integration into an MTDC grid .

1.4 Contributions and Thesis Outline

A three pronged approach was deemed necessary for this thesis work, partly because of its vastness and the requirement to build knowledge base of the subject to enable future innovations / projects.

- The approach first involved a deep understanding of operation and control of the VSC-HVDC and the DR–HVDC OWPP systems, which formed the knowledge base and comprised primarily of literature survey and system analysis.
- Secondly, analogies have been done and inspirations have been drawn from the existing power systems like both the traditional AC power system and the predominantly inverter fed micro-grids. This process of revisiting existing solutions in other power systems, has been done when tackling each challenge and it has also helped in the deeper understanding of the problem.
- The final component of the approach, is indeed, tackling the challenges, equipped with the above two components, in an attempt to provide novel solutions.

In the quest for addressing some of those major challenges, the following works are considered as major contributions of this thesis:

1. Dynamic modeling, analysis of the DR-HVDC OWPP system and proposal of a droop based distributed grid forming control scheme for the wind generators based on this understanding and the existing literature.
2. Review and theoretical comparison of existing solutions for this topology. As a further step, some of the major grid forming solutions have been assessed in detail by using time domain simulations. Analysis of droop coefficients for effective reactive power sharing by the WGs, has been done for one of the solutions.
3. Literature review and analysis of the various faults in the offshore system. Focus is on the understanding of the fault ride through strategies that are in place today for HVDC connected OWPPs and analysis of extension of the different approaches for the DR-HVDC OWPP topology.
4. Literature review and preliminary analysis of challenges related to integration of DR-HVDC OWPP into an MTDC grid.

A quick outline of the various thesis chapters is presented here.

Chapter 2 provides a detailed background for the thesis by the review of different aspects of the offshore wind technology. The focus is on the WG technology, OWPP system topologies, OWPP control and protection systems, with a dedicated section to discuss the various challenges regarding the grid integration of DR-HVDC based OWPPs.

Chapter 3 deals with the modeling and detailed analysis of the offshore wind power plant with DR-HVDC transmission. The offshore wind power system is analyzed by using the dynamic equations developed in an arbitrary d-q frame for both islanded and connected (normal) modes

of operation. This enables in establishing the various control requirements for the WGs to for the start-up and stable operation across the different modes.

In chapter 4, the various grid forming and power management solutions for the DR-HVDC based OWPP are reviewed in detail. Theoretical comparison is done between them to highlight how each approach is either similar or different or an evolution of another solution. This is followed by a detailed assessment of selected solutions using a study case, which is implemented in MATLAB Simulink. In addition, one of the solutions is analyzed further for different droop coefficients in order to vary the reactive power sharing ratio of the WGs. These studies provide a strong understanding of the existing grid forming approaches, which can help in future control innovations / enhancements.

Chapter 5 presents the work done towards the understanding the black start problem, the analysis of the various alternatives and determining the energy requirements for the black start operation.

Chapter 6 attempts at providing a preliminary analysis of the various faults in the Offshore Wind Power Plant (OWPP) with DR-HVDC transmission. Then, an overview of the challenges regarding the integration of this OWPP topology into an MTDC grid is also presented to highlight the potential issues at system level for both normal operation and fault cases.

1.5 List of Publications

1. R. Ramachandran, S. Poullain, A. Benchaib, S. Bacha, and B. Francois, "AC Grid Forming by Coordinated Control of Offshore Wind Farm connected to Diode Rectifier based HVDC Link - Review and Assessment of Solutions", 20th European Conference on Power Electronics and Applications (EPE'18 ECCE Europe), 2018, Riga, Latvia.
2. K. Shinoda, R. Ramachandran, A. Benchaib, J. Dai, B. Francois, S. Bacha, X. Guillaud, "Energy Control of Modular Multilevel Converters in MTDC Grids for Wind Power Integration ", 17th Wind Integration Workshop, Stockholm, Sweden, 2018.
3. R. Ramachandran, S. Poullain, A. Benchaib, S. Bacha, and B. Francois, "On the Black Start of Offshore Wind Power Plants with Diode Rectifier based HVDC Transmission", 21st European Conference on Power Electronics and Applications (EPE'18 ECCE Europe), Genoa, Italy, 2019.

2

Offshore Wind Power Plants: An Overview

Contents

2.1 Chapter Introduction 10
2.2 Background 10
2.3 Wind Electric Generator Technologies 18
2.4 Offshore Wind Power Plant Topologies 22
2.5 Offshore Wind Power Plant Control Principles 28
2.6 System Protection and Fault Ride Through 33
2.7 OWPP with DR–HVDC Transmission - Overview 36
2.8 DR OWPP Grid Integration Challenges 45
2.9 Chapter Conclusions 50

2.1 Chapter Introduction

Offshore Wind Technology has grown by leaps and bounds especially in the last two decades. Wind Power Plants (WPPs) have transcended from the onshore to the offshore environment and have continued to increase in terms of the distance from the shore, capacity of the wind power plant and the wind generator size itself. The offshore wind speeds are steadier and stronger and more predictable than the onshore ones . As a consequence, there is a huge advantage in terms of production and management facilities [14]. Initially, grid integration of Offshore Wind Power Plans (OWPPs) has been made with AC connections at various voltage levels and then eventually High Voltage AC (HVAC) connections. For potential sites at large distances from shore, the HVAC Transmission ceases to be economically and technically feasible and the alternative was the use of High Voltage DC (HVDC) transmission. Today, the HVDC transmission is the relevant grid integration method, for distances of around 50 km and beyond.

Apart from different transmission technologies currently available and under research, there are also different Wind Generator (WG) types. Indeed, there are many similarities in the control, operation and system protection aspects compared to an onshore wind power plant. The prominent differences are in the form of challenges due to the offshore environment and the high cost for installation and maintenance. However, the application of VSC-HVDC transmission technology is seen only for OWPP and is relatively new, compared to the traditional onshore wind power plants. Hence more focus in this chapter is on the review of different aspects of this technology, as it offers a background for understanding of the thesis subject.

Additionally, the background section serves in summarizing the basics of wind energy conversion and the evolution of WG types. This is followed by sections dedicated to OWPP system topology, control, protection and culminating with an overview of OWPP with Diode Rectifier based HVDC (DR-HVDC) transmission.

2.2 Background

2.2.1 Basics on Wind Energy Conversion

This section discusses some of the basic principles of wind energy conversion and an overview of the energy conversion chain.

The three blade Horizontal Axis Wind Turbine (HAWT) has been the primary type of wind turbine for large scale wind power extraction. A generic representation of a wind generator and its energy conversion system is shown in the Figure 2.1. It consists of a wind turbine to convert the wind energy into mechanical energy. Then one or more stages of gear box may be present and is designed to suit the generator speed and construction (number of pole pairs). The generator converts the mechanical energy into electrical energy, followed by a power electronic

conversion interface. This interface, can be as simple as a soft starter or as sophisticated as a back to back converter (B2B) based on VSCs with a partial or full decoupling from the grid. A transformer at the output of the WG performs the adaptation to the voltage level of the AC collection network / feeder. In case of a DC collection network, dedicated topology of power electronic converters must be considered.

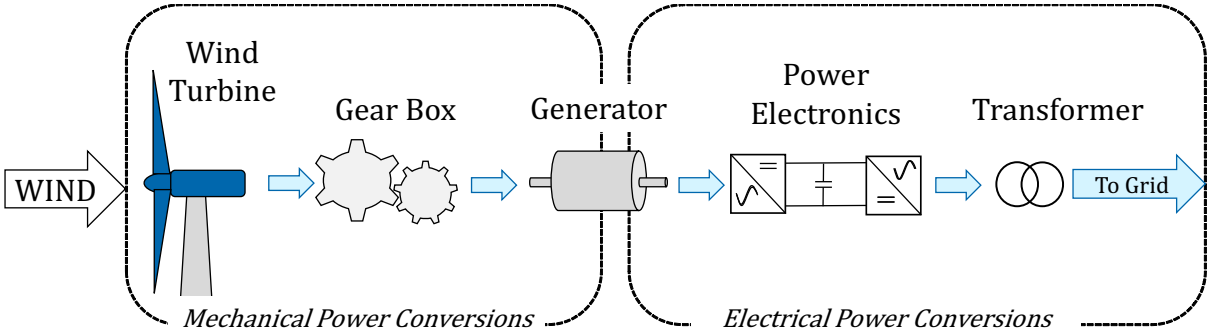

Figure 2.1: Generic representation of a Wind Generator

Conversion of Wind Energy

The inherent design of the wind turbine, is defined by an important physical characteristic, called the tip speed ratio (defined in equation (2.1)). It is defined as the ratio of the speed of the tip of the turbine blade to the wind speed. The value of the tip speed ratio at a given time, is used within the turbine characteristics, to determine the efficiency of power extraction.

$$\frac{\omega_m R_t}{v_w} \tag{2.1}$$

where

R_t - is the length of the wind turbine blade (m)

ω_m - is the angular speed of the rotor (rad/s)

v_w - is the wind speed (m/s)

The power extracted from the wind passing through the surface area swept by the turbine blades is given by the equation (2.2):

$$P_w = \frac{1}{2} C_p(\lambda_0, \beta) \rho \pi R_t^2 v_w^3 \tag{2.2}$$

where

P_w - is the power extracted by the wind turbine (W)

C_p - is the power coefficient, that corresponds to the wind power extracted by the wind turbine from the available wind resource

ρ - is the density of air ($\frac{kg}{m^3}$)

β - is the blade pitch angle ($degree$)

λ_0 - is the optimal tip speed ratio, defined later in the equation 2.4

The maximum power that can be extracted by the wind turbine is limited by the maximum value of this constant C_{pmax} called the Betz limit. Theoretical value of C_{pmax} is found to be 0.593, i.e. 59.3% of wind power can be extracted by the three bladed wind turbine, which directly translates as its maximum aerodynamic efficiency. While in practice, modern wind turbines can achieve an aerodynamic efficiency close upto 50%. This aerodynamic efficiency of the wind turbine depends primarily on the tip speed ratio and the blade pitch angle (β). For a given turbine, an approximate expression given by the equation (2.3) shows the dependence of C_p on the value of pitch angle and tip speed ratio.

$$C_p = 0.5176\left(\frac{116}{\lambda_0} - 0.4\beta - 5\right)\cdot e^{\frac{-21}{\lambda_0}} + 0.0068\lambda \tag{2.3}$$

where $\lambda 0$ is given by the following expression 2.4:

$$\frac{1}{\lambda_0} = \frac{1}{\lambda + 0.08\beta} - \frac{0.035}{\beta^3 + 1} \tag{2.4}$$

Similar to equation (2.2), the torque applied on the shaft is expressed as follows:

$$T_w = \frac{P_w}{\omega_m} = \frac{1}{2}C_T\rho\pi r^3 v_w^2 \tag{2.5}$$

where

T_w - is the torque acting on the wind turbine (W)

C_T - is the torque co-efficient

Thus, the relationship between torque and power coefficients is derived as below:

$$C_T\lambda = C_P \tag{2.6}$$

The equations (2.5,2.6), allow understanding the power conversion in both electrical and mechanical standpoints. The dependence of the power coefficient (C_p) on the pitch angle (β) and tip speed ratio (λ) is shown clearly in the Figure 2.2. Here the maximum value of power co-efficient corresponds to the minimum pitch angle (ideally zero) and an optimal tip speed ratio (λ_0).

2.2.2 On the Maximum Power Point Tracking and Ideal Power Curves

From the background on the wind energy conversion in the previous section, it is clear that the maximum power can be extracted when the optimal tip speed ratio is maintained, by variation of the shaft speed or the generator speed as the wind speed (v_w) varies. The Figure 2.3 shows the

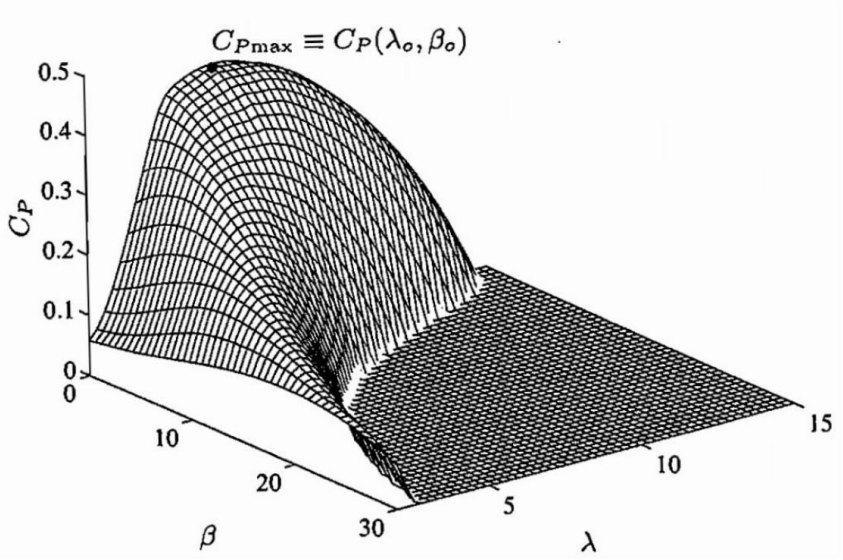

Figure 2.2: Variation of Power coefficient of the wind turbine with respect to β and λ

power curves for various rotor speeds, for different wind speeds. Each curve, corresponding to a particular wind speed, has a maximum available power. In order to extract this power, the rotor speed has to be changed while the pitch angle has to be kept at minimum. Thus a trace of ideal maximum power points is obtained (shown as a black trace in the Figure 2.3), corresponding to specific generator speeds for each wind speed. While actual MPPT implementation is such that power available is extracted but without exceeding generator speed limit. The design prevalent today for many of the offshore wind turbines is that the WG reaches nominal rotor speed before producing nominal power, in order to avoid any damages to the turbine [15].

This actual MPPT implementation is shown as a red trace along the black trace of theoretical MPPT but deviating for rated speed of the turbine. The cut-in wind speed v_0, is the speed after which the available wind speed can be extracted or in other words the wind is strong enough for the WG to produce power. The speed range of v_x to v_y is usually the nominal wind speed range for which the wind turbine is designed to operate at constant rotor speed, but the power increases for increasing wind speed.

There are various methods to implement MPPT [16], some of which are listed below. More details are provided on these methods in the appendix A

1. Optimal Tip Speed Ration
2. Optimal Torque Control
3. Power Signal Feedback Control
4. Perturb and Observe Method

Out of these methods, the Perturb and Observe Method is the most widely used method in the wind industry today.

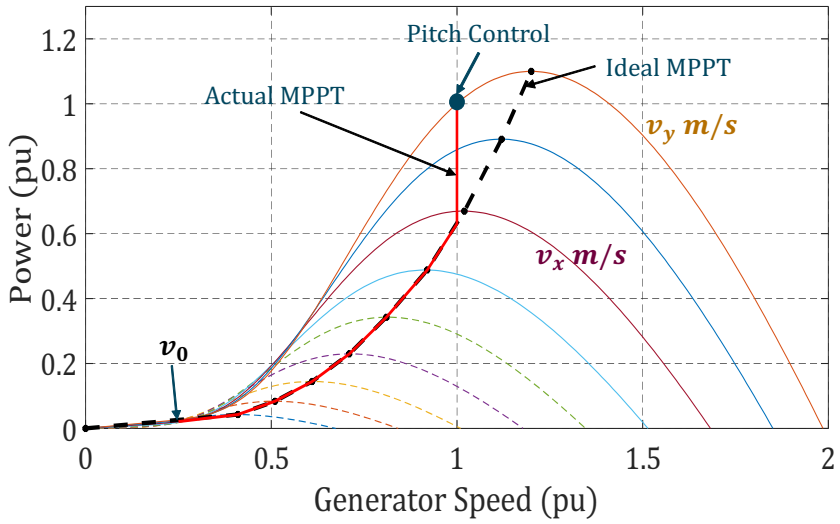

Figure 2.3: Power output vs Generator speed for multiple wind speeds

2.2.3 Operation Zones for a Wind Generator

The characteristic curves of the wind turbine, is used to implement an appropriate control of the generator speed and pitch angle. The WG can extract maximum power when feasible and limit power production and speed when desirable. The point highlighted in the Figure 2.3 at 1 pu power and 1 pu rotor speed is the point after which, for higher wind speeds, the pitch control is used to limit the rotor speed and ensure the power production at 1 pu. The desirable operating points (traced by the red curve in the Figure 2.3), provide a set of the well known ideal characteristics for a WG, shown in the Figure 2.4. There are four distinct zones of operation, based on the control of the pitch angle, rotor speed with respect to the wind speed.

- Zone 1 – the wind speed is lower than the cut–in wind speed (v_0) and the wind generators are not producing any power, that can be transmitted, as seen in Figure 2.4 (a).
- Zone 2 – this is the low wind speed zone, where MPPT operation is desirable. The pitch angle β is kept to a minimum value close to zero and rotor speed ω_m is varied so as to maintain optimal tip speed ratio. The corresponding power curve is of the form as seen in Figure 2.4 (b).
- Zone 3 – this is the transition zone, where the rated wind speed has been already reached and the increase of wind speed leads to an increase in the power extracted, with a minimum pitch angle (Figure 2.4 (a)). This corresponds to the region between the nominal wind speeds of the WG - v_x and v_y and this case is also illustrated in the Figure 2.3.
- Zone 4 – this is the zone where pitch angle control is used (as seen in Figure 2.4 (a)) to limit the rotor speed to the rated value, for high wind speeds, until the speed limit $v_{cut-out}$. After the cut–out limit, the wind speed is too high and the WG is usually stalled to avoid any damages.

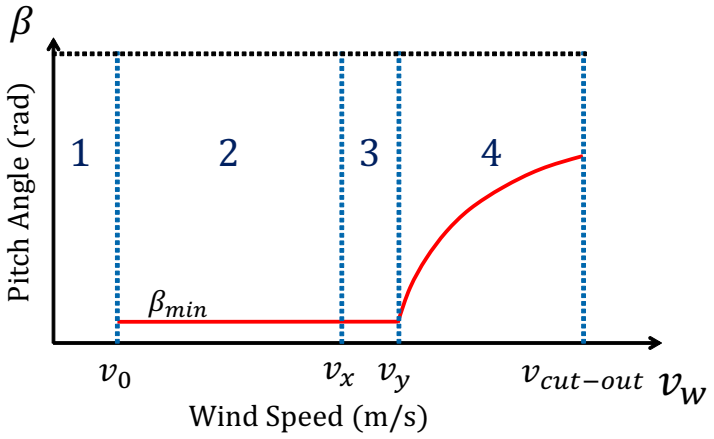

(a) Pitch angle vs Wind Speed

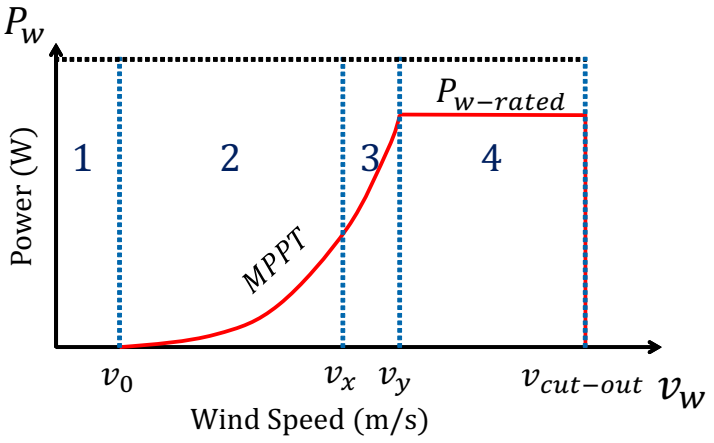

(b) Power vs Wind Speed

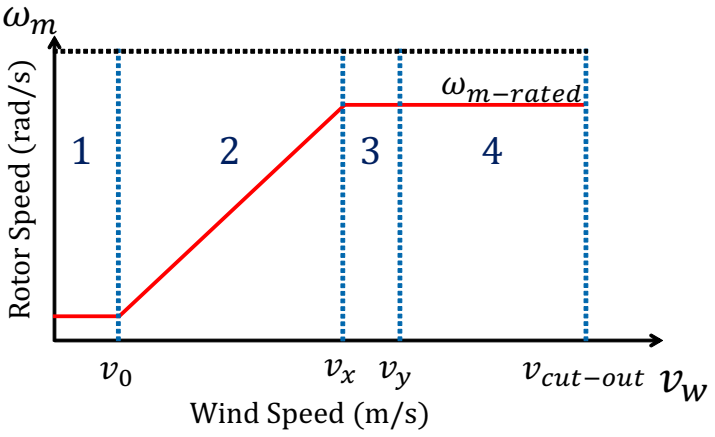

(c) Rotor Speed vs Wind Speed

Figure 2.4: Ideal Operation Curves of a WG and the related Operation Zones

2.2.4 OWPP Architecture and Control Overview

Generic Architecture of an Offshore Wind Power Plant

The offshore wind power plant has a general architecture that can be applied to every type of wind power plant topology that exists today and is being conceived. This architecture is shown in the Figure 2.5 and is a general extension of the architecture presented in [17]. It consists of the following components:

- a group of wind generators(WGs) connected to transformers to step-up the system voltage. This part of the system is called a collection network and the WGs could be connected in radial, ring or star configuration.
- an export network consisting of sub-marine cables connected to one or more export sub-stations to the main transmission terminal, from where the power is transmitted to the shore. Depending on the type of solution, the export network may be non-existent, as will be seen in one or more of the topologies described in the forthcoming sections.
- the offshore Point of Common Coupling (offshore PCC) consisting of a larger Collection Sub-station, encompassing a transformer to attain a suitable voltage for transmission – HVAC, AC-DC / DC-DC converter station (if applicable), other equipment for control, auxiliary supply, protection equipment etc.
- a transmission network at lower losses. At the onshore terminal, there is generally a sub-station with a converter (if applicable), along with the associated equipment (like switch-gear, transformers, Filter / capacitor banks etc.) and enables the integration to the onshore AC grid.

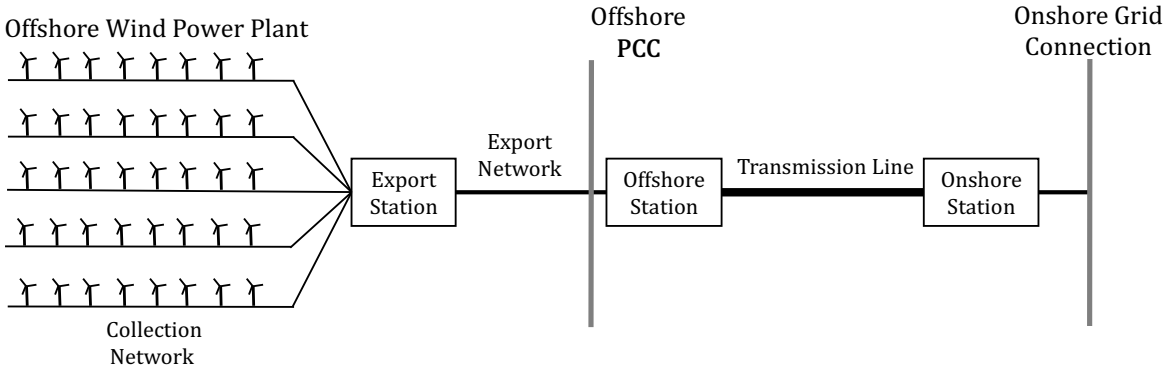

Figure 2.5: Generic Architecture of an Offshore Wind Power Plant

Offshore Wind Power Plant Control Overview

Similar to the onshore wind power plant, the control of OWPP is performed in a hierarchical manner as illustrated in Figure 2.6. This has been obtained by extending the control archi-

tectures presented in [18] for VSC-HVDC OWPP and for DR-HVDC OWPP [19]. Each WG consists of a controller for the entire WG system including the mechanical (pitch control for instance), electrical and other components. The control signals, for instance related to reactive power set points, may be distributed by the OWPP cluster controller. Multiple wind power plants (or clusters) could be grouped together and thus an OWPP central controller may be required. At the last level is the wind farm system operator, which controls and monitors the entire system and is in–turn is in coordination with the local AC grid operator. It can dispatch power references to each wind generator based on the requirements of the AC grid operator, if required. The structure on the right with the onshore and offshore VSC controllers are valid for HVDC transmissions and can vary or be absent according to the transmission solution. The double headed arrows (connecting each block to the other), indicate the presence of direct communication between the two blocks.

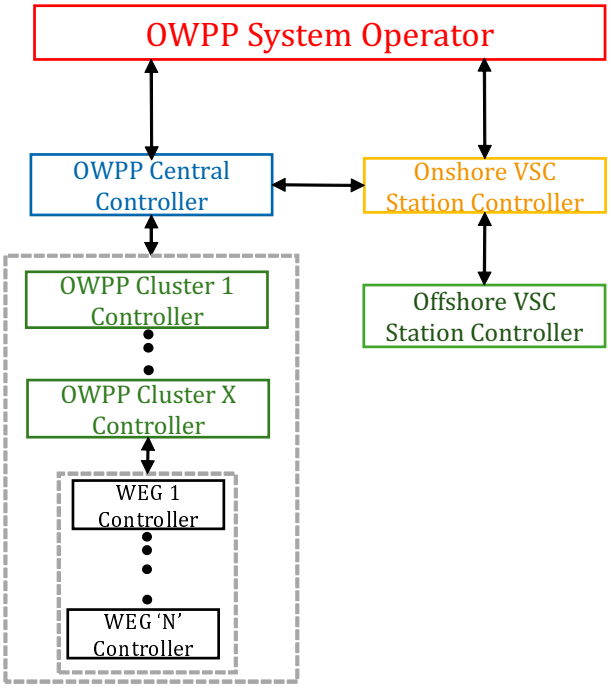

Figure 2.6: Hierarchical Control Architecture for an OWPP

Generally the control algorithms for the MPPT (or other control functions depending on the local measurements) are implemented at each WG level, with an option to over-ride the commands of the local controller(s) by a controller above in the hierarchy. This can be necessary in many cases, like power curtailment due to onshore transmission congestion, onshore Grid faults, power demand by the grid operator etc.

2.3 Wind Electric Generator Technologies

Modern wind generators, after the 1970s, consist of three blade, upwind, horizontal axis wind turbines equipped with the components illustrated in the Figure 2.1. Some of the components (for instance the gear box) may not exist according to the specific type of technology. Observing many of the illustrations by wind turbine manufacturers for offshore applications, it can be said that most (or all) of the components shown in the Figure 2.1 can be found located in the nacelle of the wind turbine.

The aerodynamic design of the wind turbines, itself enable a certain control of the generated power. For high wind speeds, the power can be limited by using passive stall, active stall or pitch control [20]. While in passive stall, the turbine blades are bolted to the hub, ensuring a fixed pitch angle, both pitch and active stall regulations involve the change of the pitch angle (in opposite directions). There are certain advantages associated with the pitch and stall regulated wind turbines. The combination of these two methods enables easy start–up and shut–down of the WGs. This said, in modern WGs (including offshore applications), due to slow response of the stall regulation, only pitch regulation is used for the power control above the rated wind speed [17]. Based on the electrical generator types and power electronic converters used, there are four principle types of wind electric generators. Their alternative or popular names are indicated as well.

1. Fixed Speed Wind Generators (Type1)
2. Limited Variable-speed Wind Generators (Type2)
3. Variable-speed Wind Generators with Partial–scale Converter (Type3 / DFIG)
4. Variable-speed Wind Generators with Full Scale Converter (Type4 / FSC)

2.3.1 Fixed Speed Wind Generators

Also known as the ‘Danish Concept‘, this WG consists of a Squirrel Cage Induction Generators (SCIG), a multi-stage gear box and capacitor bank, connected directly the AC grid using a transformer (see Figure 2.7). The SCIG always requires a certain amount of reactive power to magnetize the windings to operate slightly above the synchronous speed. Thus there is only one speed of operation, for all wind speeds. Some manufacturers used SCIG with two sets of windings, in order to achieve two speeds of operation, thus increasing the energy yield compared to one fixed speed of operation.

During operation, the WG operates at a single rotation speed and the wind speed thus needs to be high enough to enable its rotation around the synchronous speed. To avoid high transients during its connection to the grid, a thyristor based soft-starter is used to limit current inrush. The advantages of the Fixed speed WG comes from its simplicity in control and robust and cheap construction of the SCIG. The fixed speed operation, leads to several disadvantages like

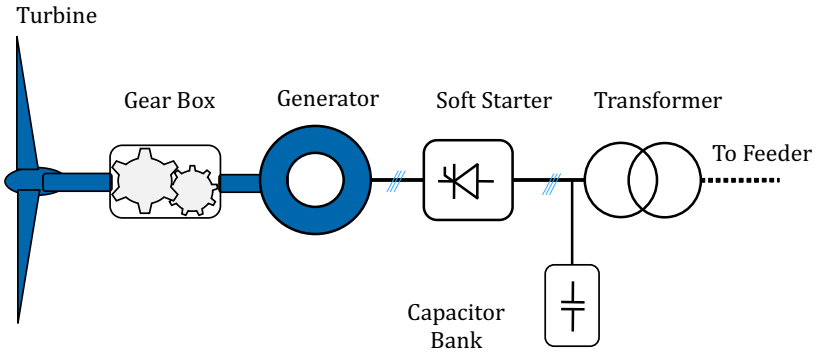

Figure 2.7: Fixed Speed Wind Generator

inability to extract maximum power from the wind, need to withstand high mechanical stress for various wind speeds and wind gusts etc, reactive power compensation and sensitivity to grid disturbances.

2.3.2 Limited Variable-speed Wind Generators

The next step in the evolution of WG technology was to operate in higher range of wind speeds to increase the energy yield. This resulted in the replacement of the SCIG by a Wound Rotor Induction Generator (WRIG), with variable rotor resistance. The variable resistance has been implemented by using power electronic devices as illustrated in the Figure 2.8. This allows a small speed variation (usually less than $\pm 10\%$), by using the change in slip, but at the cost of power loss in the rotor resistances. The use of additional equipment compared to the SCIG increases the maintenance requirement of the machine [20]. This technology is undeniably an important evolution in the application of power electronic devices to the wind generator.

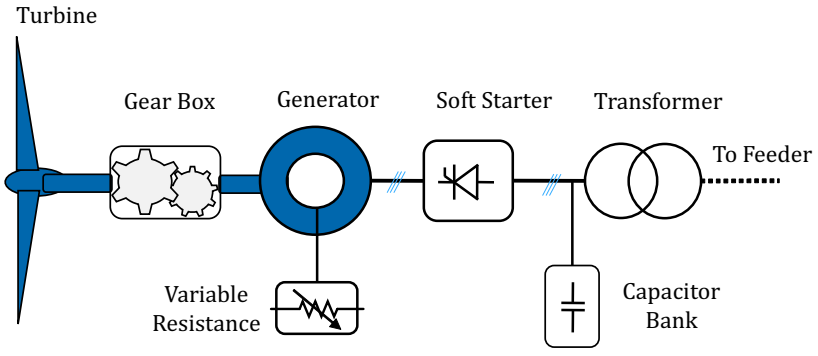

Figure 2.8: Limited Variable Speed Generator

The following types of generators are the most prevalent in the industry for both onshore and offshore applications today.

2.3.3 Variable-speed Wind Generators with Partial–scale Converter

This WG, also called the Type 3 as seen in the Figure 2.9, consists of a WRIG connected to the grid directly through its stator and its rotor connected to the grid (indirectly) through back to back converters (also dubbed as the partial–scale converter); hence the name Doubly Fed Induction Generator (DFIG). The variation of the rotor slip enables the variable speed operation.

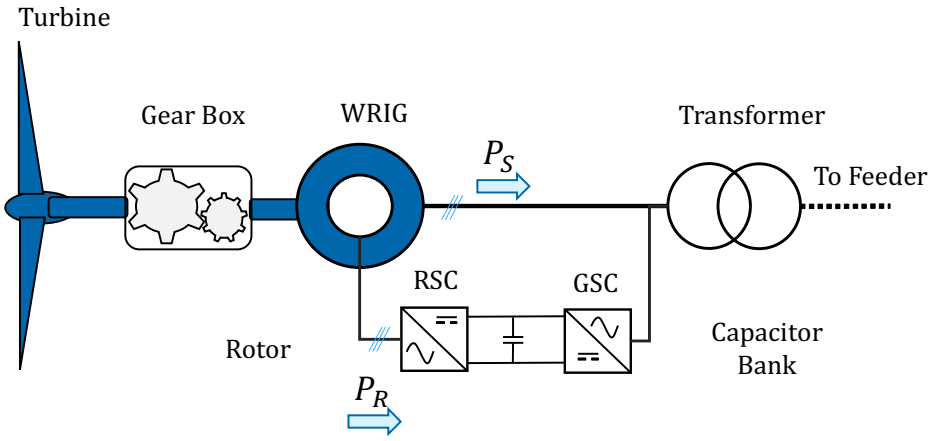

Figure 2.9: Type 3 Wind Generator or the DFIG

The equations that describe the power flow between the stator, rotor and the grid are given by the following equations:

$$P_R = s * P_S \tag{2.7}$$

$$P_{mech} = (1 - s) * P_S \tag{2.8}$$

where

P_S – is the power injected by the stator into the grid

P_R – is the power exchanged between the rotor and grid

P_{mech} – is the mechanical power extracted from the wind energy

s – is the slip in the rotor frequency

Thus to achieve a variable speed operation, the B2B converters extract active power from the rotor windings and inject it into the grid, when the rotor speed is over the synchronous speed and below it, absorb active power from the grid (or circulate injected power by stator into rotor). There are also specific control functions for each of the converters. The Rotor Side Converter (RSC) is connected to the rotor and enables the speed control, while the Grid Side Converter (GSC) can compensate for the DFIG reactive power demand at the grid connection point. The DC link voltage of the back to back converter is also controlled by the GSC. These converters are sized only for a fraction of the total power capacity of the machine, usually around 30% and

the total speed variation range around the synchronous speed is from -40% to +30%. The key advantages compared to Type 2, include:

1. Absence of a soft starter and capacitor banks for reactive power compensation.
2. Increased energy yield compared to WG Types 1 and 2, due to operation in higher wind speed range.
3. Additional control capabilities available as per grid operator's requirements (using the GSC).
4. Higher power quality is ensured.

However some drawbacks do exist: continued use of multi-stage gearbox, specific protection requirements for rotor faults, requirement of slip rings for rotor connection. Needless to say, this WG has dominated the onshore wind plant installations and the initial offshore installations.

2.3.4 Variable-speed Wind Generators with Full–scale Converter

The decoupling of the generator from the grid entirely by using a Full Scale Converter, enables the maximum power extraction from the wind and advanced control capabilities for the converters, especially at the grid connection point. The generator can be of SCIG or Wound Rotor Synchronous Generator (WRSG) type while many of the recent WGs for offshore applications have been employing Permanent Magnet Synchronous Generator (PMSGs), either driven directly by the turbine or using a gear box. Added advantages of using PMSG over a WRSG include higher power density, elimination of the excitation circuit for the rotor windings and lesser weight. While on the downside, the permanent magnets are difficult to handle during installation and also there is a requirement of flux weakening control to be implemented to avoid stator over-voltages. To prevent the over-voltages, a crowbar consisting of a DC chopper along with a resistor, is included in the DC link of the B2B converter for energy dissipation. A generic machine topology is shown in Figure 2.10.

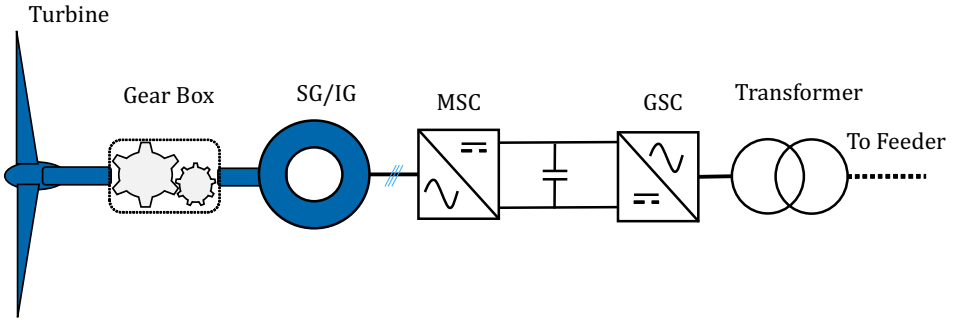

Figure 2.10: Type 4 or FSC Wind Generator

These WGs offer higher levels of control capabilities, like voltage and frequency support according to Transmission System Operator(TSO) connection requirements, fault ride through

and grid forming. It is the only type of WG among existing ones, that provides islanding capability for the wind power plant. As pointed out in Chapter 1, the Type 4 machine is dominating many of the current and future offshore wind installations. In the forthcoming chapters, WG with FSC will be the generator type considered for studies.

2.4 Offshore Wind Power Plant Topologies

The offshore wind power plant topology consists of two major sections, namely the collection network type and the transmission technology. The existence of the export sub-station or mid-level voltage conversions are not considered, for the preliminary classification.

For instance the collection network can be (but not limited to) one of the following types [17]:

1. Medium Voltage AC (MVAC).
2. Medium Voltage DC (MVDC).
3. Low Frequency AC (LFAC).

While the transmission technologies could be of the following types:

1. High Voltage AC (HVAC)
2. VSC based High Voltage DC (HVDC)
3. Diode Rectifier based HVDC (DR-HVDC)
4. MVDC-HVDC converter (obviously for DC collection)
5. Hybrid Converter Configurations (DR and VSC in series, for instance)

Although, various combinations of collection and transmission networks could be imagined, due to technical constraints and connection requirements, only a few such combinations are prevalent in the literature or implemented today. Currently, the most popular topologies in wind farms operating or constructed today [17] are

1. AC or High Voltage AC (HVAC) with MVAC Collection network
2. VSC based High Voltage DC (HVDC) with MVAC Collection network

While today, the DR-HVDC technology is a promising alternative to the VSC-HVDC technology and is a subject of research. Henceforth, the most important OWPP topologies are covered below and some additional innovative concepts are also mentioned.

2.4.1 MVAC Collection with HVAC Transmission

The choice of the HVAC transmission is a result of shorter distance of the wind farm site from the shore and in fact a very natural transition from the offshore wind power plants built very close to the shore. In fact before HVAC transmission, some of the earlier offshore wind power plants listed below were connected to the shore by using medium voltage string cables to the onshore AC grid, without the use of an offshore transformer / substation. Some of them include [17]:

1. Kentish Flats (90 MW and 8.5 km from shore)
2. Scraby Sands (60 MW and 2.5 km from shore)
3. Egmond aan Zee (108 MW)

The first project with the HVAC transmission cable (150 kV) and an offshore substation was the Horns Rev 1, off the coast of Denmark. Thus the architecture of a standard OWPP with MVAC collection network and HVAC transmission was adopted for further wind farm developments close to the shore. A generic topology of this type is represented in the Figure 2.11. The offshore network array or feeders are usually in the medium voltage level and these feeders are connected to an offshore sub-station, usually equipped with a step up transformer and reactive power compensations, filters, protection equipment. The MVAC collection system has been at 33 kV from the initial days, while 66 kV system is proposed due to its cost advantages [21]. Static VAr compensators may be used to provide the reactive power compensation, sometimes at both the ends of the cable in case of a longer transmission distance.

The HVAC transmission cable is submarine and the widely used one today is of type Cross-linked Poly Ethylene (XPLE). Compared to the overhead HVAC lines, the submarine HVAC cables have almost 20 times higher capacitance and thus require higher charging currents or reactive power compensation as the transmission distance increases [22].

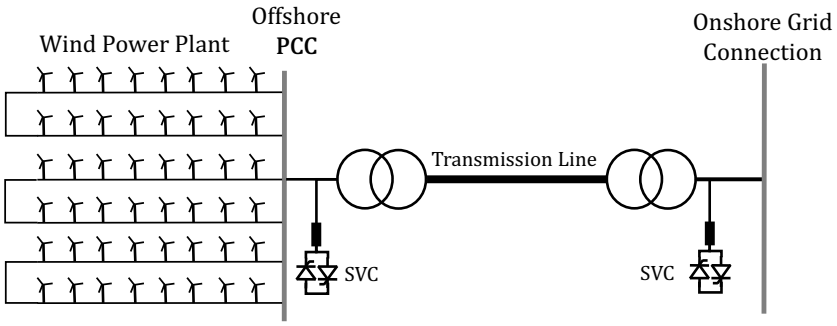

Figure 2.11: MVAC topology with HVAC transmission

Although relatively straightforward in terms of implementation, some of the drawbacks of the HVAC transmission technology are [23]:

1. Obviously, an increased reactive power compensation and losses with an increase of size of wind farm and distance from the shore.
2. Faults in the onshore AC grid have a direct consequence on or are propagated to the offshore wind power system and vice versa.

2.4.2 MVAC Collection with HVDC Transmission

As the distance of the wind power plant from the shore increases, a VSC based HVDC transmission gains advantages in terms of cost, losses and control capabilities, compared to HVAC.

The exact break-even distance to choose HVDC over HVAC could depend on multiple factors. However, analysis in [23] shows that for a 100 MW farm HVDC connection is cheaper than HVAC connection for a distance of 90 km and higher.

The MVAC-HVDC topology is illustrated in the Figure 2.12. It consists of multiple WGs connected at the medium AC voltage level (33 kV for instance). The MVAC collection network is connected to one (or a few) AC collector substation(s) with transformer(s) to step up the AC voltage, for connection to the export network. The typical value of export network voltage is greater than 100 kV (for instance, 132 kV or 150 kV). The export network cables are connected to the offshore VSC station, usually through another transformer, to attain suitable AC voltage for the HVDC converter. The AC collection substations may or may not be interlinked among each other. Such interlinking, for instance at the MVAC level is quite useful to avoid the lack of auxiliary supply to WGs when one of the main MVAC collection feeders are offline due to maintenance or fault events [24].

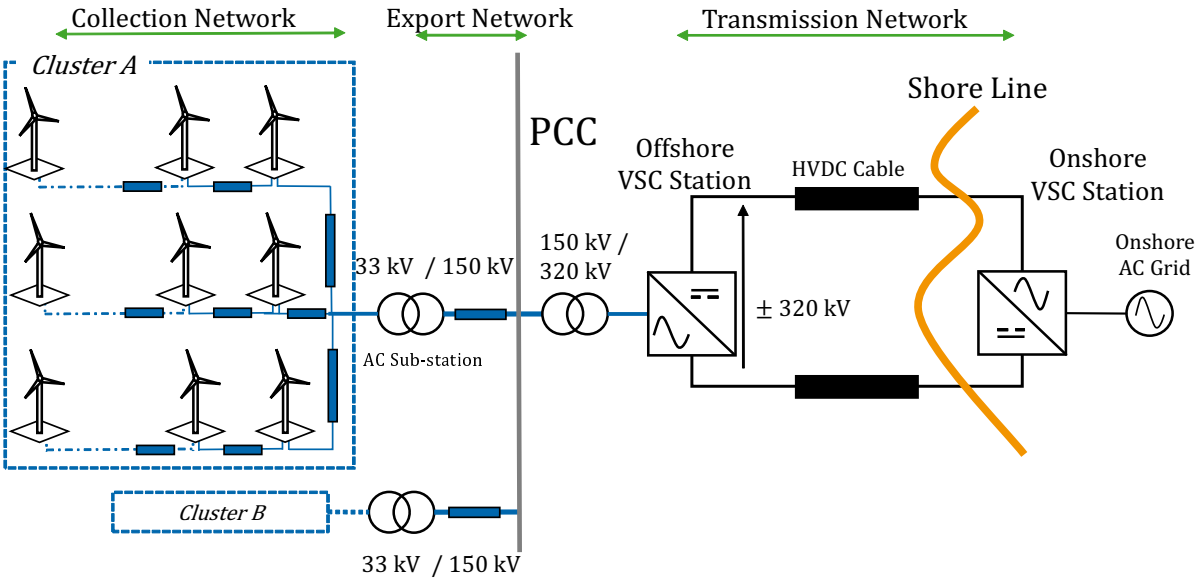

Figure 2.12: MVAC Topology with a VSC-HVDC Transmission

The other possible topology is to avoid the AC collection / export transformer stations and connect the MVAC feeders directly with the offshore converter platform (offshore Point of Common Coupling). This configuration has significant cost advantages, due to the elimination of the AC platform. This also implies a closer proximity between the offshore station to the wind power plant, to avoid transmission losses at the medium voltage level.

Overall, the VSC-HVDC system has multiple advantages compared to the HVAC, some of which are highlighted below [25]:

1. Decoupling by the HVDC link /grid means that offshore and onshore Grids are isolated from each other for AC faults.

2. Low or no reactive power compensation required.
3. Can be used to interconnect weak AC grids.
4. Can integrate offshore and onshore grids of different frequencies.

While the following benefits pit VSC-HVDC as a better alternative to the traditional Line Commutated Converter (LCC) based HVDC system:

1. Low footprint.
2. Black start capability.
3. Low or no reactive power compensation or STATCOM devices required for the offshore station.

The HVDC link configuration is generally bipolar and as of today, the maximum voltage capacity of a HVDC cable has been 320 kV. However, recently, a HVDC cable of 525 kV has been developed and may be used in future installations, as it has qualified the requirements of German TSOs [26].

The ability to connect distant offshore wind power plants through a HVDC transmission is largely attributed to the innovations in the converter technology. Thus, the basics of the Modular Multilevel Converter (MMC) are presented in the appendix B for a better understanding of the HVDC conversion capability.

2.4.3 OWPP with DC Grids

During the initial development of offshore wind power plants with a HVDC transmission, a scheme to use a DC collection network was proposed to eliminate the AC collection transformers, AC transformer at the output of the turbine among other benefits [27]. It is clear that a DC grid, avoids the need to synchronize or regulate the frequency and reactive power problem, when compared to an AC collection grid. Various topologies with DC collection grids are possible, as discussed in [27] and are further analyzed in [28] [15]. As is the trend today, Type 4-PMSG is the most prevalent type of WG manufactured for these offshore DC grids.

One such architecture [28] namely, the HVDC transmission system with MVDC collection network is presented in the Figure 2.13. The topology replaces the standard grid side converter (or rather inverter) of the type 4 wind generator with a DC-DC converter, connecting to an MVDC collection network, varying from 30 to 50 kV [29]. Then, the offshore station is used for conversion to a suitable higher DC voltage for transmission.

The onshore station is the standard VSC type and it controls the HVDC voltage (V_{HVDC}), similar to the previously discussed MVAC-HVDC topology. In the offshore network, the offshore DC DC station, controls the MVDC voltage (V_{D_GRID}). The DC-DC Grid Side Converter of the wind generator controls the DC link voltage (V_{dc1}) of its link to the Machine Side Converter (MSC). As usual, the MSC is performing the maximum power point tracking, and operating the generator at a variable frequency. Although there is no DC-DC topology solution commercially

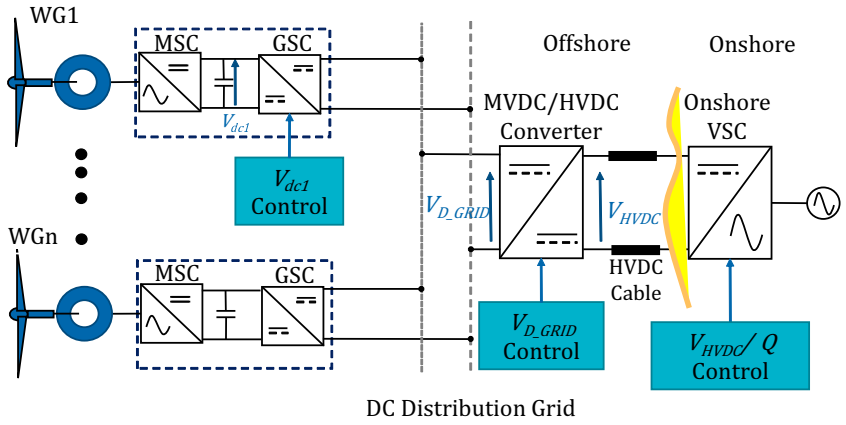

Figure 2.13: OWPP with MVDC-HVDC topology

available today for OWPPs, there might be an interest in the future, if its economical advantages are boosted with further research and development.

2.4.4 Other Innovative Topologies

The above concepts, are either industrially well established reference technologies or are in intense research and development phase. The same may not be stated for certain other topologies that are discussed in this part. They are in-fact derivatives or combinations of the above said concepts and have been analyzed well in the literature.

Hybrid VSC Configurations

A series connection of VSC with a diode rectifier (illustrated in Figure 2.14) has been presented in [30]. The initial analysis claims to have nearly a zero gain in terms of cost compared to the VSC HVDC station, despite the use of DRs. The cost offset is said be caused by the use of additional filters, transformers etc. In normal operation mode, the series connected offshore VSC, has grid forming capabilities and thus the conventional WEG controls can be retained, another distinct advantage over the DR-HVDC system. Moreover, active filtering is proposed to reduce filtering requirements of the DR station. However the analysis of black start of this offshore system has not been done.

An extension of [30] is the use of MMC in the place of the VSC [31]. The onshore station is a full bridge MMC, and this enables the reduced voltage operation of the HVDC link. This also allows the black start of the offshore AC grid by the offshore station, bypassing the diode rectifiers. The grid forming capability is retained and as an added advantage due to the MMC, a 30% reduction in the size of the DC inductance is claimed. These solutions are in the nascent phase of research and they keenly attempted to enable the DR-HVDC technology, modifying to

the very minimum, the WG control and (existing) offshore AC system.

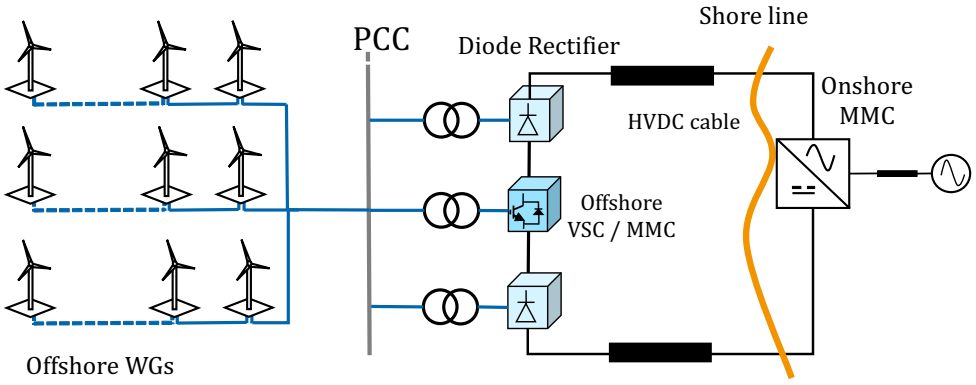

Figure 2.14: Hybrid DR-VSC Topology

Low Frequency AC Transmission

The Low Frequency AC transmission (LFAC) or Fractional Frequency Transmission System (FFTS) has been proposed first for offshore transmission applications in [32] as an economic alternative to the HVAC and the HVDC transmission scheme. The most important difference here (compared to the HVAC transmission) is the reduced cable inductance due to operation of the transmission line at a reduced frequency, thus increasing the power transmitted by the HVAC cable, with reduced reactive power compensation.

The overall topology is similar to the MVAC-HVAC topology shown in the Figure 2.11 and it consists of an OWPP AC collection network in low frequency AC, an offshore transformer, for HVAC transmission at desired voltage level and an onshore frequency converter which could be a cycloconverter or a Matrix converter or a special MMC based topology. The onshore converter enables the connection the AC grid at the desired frequency. Although the cost benefits are clear in terms of the transmission technology compared to HVAC and VSC-HVDC, the challenges of the system design that require further work are:

- Redesigning the wind generator output transformer for low frequency, which might result in larger structure
- Following the above requirement, the auxiliary supply of the wind generators also need to be appropriately designed.
- Relatively larger (and expensive) design of the offshore transformer for LFAC conversion (a frequency of 16.7 Hz increases the offshore transformer cost by three times).

2.5 Offshore Wind Power Plant Control Principles

2.5.1 General Description

As shown in the Figure 2.6, there are different levels in the control system for the OWPP. There are a set of control requirements at the (local) WG level and ultimately, there are control requirements for the entire wind power plant, as desired by the TSO or the OWPP operator. This section puts in perspective, the control capabilities or degrees of freedom available in a WG and also the requirements / capabilities of the entire OWPP as a whole. Such capabilities allow for a better grid integration of OWPPs and if possible provide additional services or functionalities to the AC grid. For instance, Tennet, one of the Dutch TSOs operating many OWPPs, has separate grid connection requirements for offshore wind.

The power electronic converters in the WG, are usually three-phase two-level VSCs. Vector control in a dq frame (or Synchronous Reference Frame), is a widely implemented control method for the converters of the WGs [33][34][35], while control in $\alpha - \beta$ frame (Stationary Reference Frame) could also be implemented in some cases. This control scheme [35] consists of an inner current control loop and outer voltage control or torque control loop with specific control functions (and slower dynamics). Pulse Width Modulation is the technique used to create the necessary three phase sinusoidal waveform, and RL or LC filter is used at the AC output of the VSC (or the Grid Side Converter) interfacing with the AC grid.

It is important to describe the major ways in which the VSC (of the HVDC transmission system or the Wind Energy Conversion System) can be controlled according to the capabilities of the VSC itself [36] [37].

1. **Grid Following / Grid Feeding** – In this operation, the AC voltage and frequency is maintained by the AC grid to which the VSC is connected [38]. The VSC is controlling the injected AC currents and the DC link voltage of the B2B converters. It uses a PLL for synchronization with the frequency imposed by the AC Grid. Such VSCs are called Grid Imposed frequency–VSC systems. In most cases, the GSCs of the wind generators and the onshore VSC station implement this Grid Following control strategy.
2. **Grid Forming** – the AC grid is non-existent or in some cases weak. The VSC in this situation, operates to regulate the AC voltage and frequency and thus 'forms'the AC voltage waveform in the grid [39]. In this case, more than one VSC could be involved in forming the AC voltage waveform. Such kind of VSC system is prevalent in distributed generation systems (microgrids), UPS systems and also relevant in islanded operation of WPPs. It is said to be a controlled frequency VSC system.
3. **Grid Supporting** – In this case the VSC is connected to a controlled AC grid (may be a weak AC grid) and it operates to participate in the regulation of voltage and frequency [38], by variation of its active or reactive power injection [37].

Having established the above terminologies, the control functions of the WG converters and the VSC stations are explained in a detailed manner.

2.5.2 Wind Generator Control Capabilities

The back to back converter (see Figure 2.15) is an integral part of the Type 4 WG due to the control capabilities it offers. In addition, Fault Ride Through (FRT) control can also be implemented, thanks to the crowbar. The use of a vector control is retained here after to describe the various control functions of the VSCs.

The overall control tasks of the back to back converter can be described as below.

1. **Control of the wind power extracted** – This includes, the MPPT, power curtailment or de–loading and power limitation for high wind speeds is implemented in coordination with the pitch control of the wind turbine.
2. **DC Voltage Control** – The dc link voltage of the converter system has to be regulated.
3. **Reactive Power contribution** – This is required at the grid connection point and is supposed to be provided by the GSC.
4. **Control to satisfy Generator Constraint** – This could manifest into different control objectives based on the requirement, for instance stator voltage control, unity power factor control etc.
5. **Grid Forming (optional)** – If necessary, the GSC can be involved in the AC grid voltage and frequency regulation.

This said, the exact control algorithms for the MSC or GSC are based on the choice to enhance fault ride through, for instance and sometimes by conditions imposed by the grid at the PCC. In general, the major control functions available for these converters are shown in the Figure 2.15. The Pitch Control is also used for power limitation control in coordination with the converter control, to achieve the desired operating point, in terms of generator speed and power production (red trace in Figure 2.3). This figure represents the two major control functions of the MSC and the GSC, without dwelling into the details of the exact control loop structures. Generally, one of the set of control algorithms (notably the MPPT for MSC and Grid Following mode control for GSC) is implemented commonly in the WGs operating today. The control mode switch S_{cm} symbolizes the capabilities of the two converters and its illustration does not infer that both the control strategies are implemented / available for use always in the WGs.

The choice of a particular control strategy for the combination of converters depends on the presence or absence of a stable AC grid for connection, need for the islanded mode, enhancing FRT capability etc. The control strategies applied for OWPP case are shown in the table 2.1.

The Grid following function is commonly implemented for the existing WGs connected to the VSC-HVDC system.

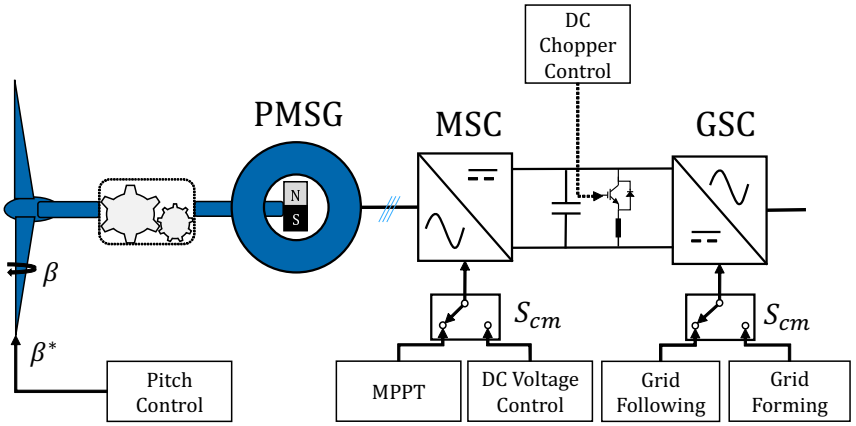

Figure 2.15: Control Capabilities of the Back to Back converter

Control Strategy	**MSC Control**	**GSC Control**
Grid Following	MPPT and Stator Voltage Control	DC link Voltage (or) MPPT and Q control
Grid Forming	DC link Voltage	V,f regulation and MPPT

Table 2.1: Control Strategies Possible for the Back to Back Converter System

WGs in Grid Following Control Mode

The Type 4 or the WG with FSC consists of a back to back converter to interconnect the generator to the collection network. For WGs connecting to an AC grid with imposed frequency, the Phase Locked Loop (PLL) is used as a method for synchronization with the grid, in case of vector control. A standard representation of the PLL [40] is shown in the Figure 2.16.

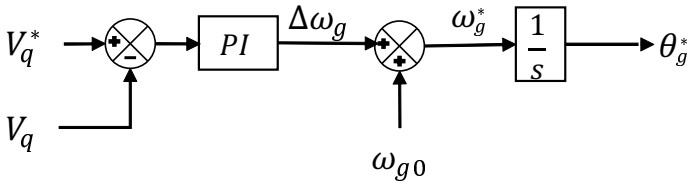

Figure 2.16: Block Diagram Representation of the PLL

In the grid following control scheme, the PLL ensures that the VSC is synchronized with the grid frequency, maintaining the Synchronous Reference Frame (SRF) or the rotating dq frame such that, the q-axis component of the voltage at the output filter terminal of GSC is maintained at zero ($V_q = 0$). Thus in the Grid following mode, the GSC independently controls the active and reactive power injected into the grid, as the AC voltage and frequency are set by the grid. The output power equations for the GSC are as follows:

$$P(t) = \frac{3}{2}(V_{fd}(t)i_d(t) + V_{fq}(t)i_q(t)) \tag{2.9}$$

$$Q(t) = \frac{3}{2}(-V_{fd}(t)i_q(t) + V_{fq}(t)i_d(t)) \tag{2.10}$$

Since the q-axis voltage component (V_q) is set to zero because of the PLL, independent active and reactive power control is possible by the VSC:

$$P(t) = \frac{3}{2}V_{fd}(t)i_d(t) \tag{2.11}$$

$$Q(t) = -\frac{3}{2}V_{fd}(t)i_q(t) \tag{2.12}$$

2.5.3 Control Capabilities of the OWPPs from AC system perspective

Regardless of the type of rectifier station offshore (i.e. DR or VSC), the onshore station of the MVAC-HVDC topology consists of a VSC based inverter, integrating the OWPP to the AC grid. Since it is the main component for the interconnection with the AC grid at certain voltage level, there are certain interconnection requirements to be met and it depends on the relevant TSO. The onshore wind power plants during the past decades, have been expected by the TSO to possess certain capabilities, some of which are highlighted below [17]:

- Reactive power control / contribution sometimes even during no-wind conditions.
- Voltage or power factor control at the interconnection point by using the wind generators or compensation devices (capacitor banks, Static VAr Compensators).
- Controlled reactive current provision during faults in the AC grid.
- Curtailment of wind power as per the signals from the concerned TSO or wind farm operator.

In case of OWPP, since a highly controllable VSC is used for onshore grid integration, certain additional requirements can be put forth

- Frequency support to the AC grid.
- Power Oscillation Damping which is possible by both active and reactive power contribution.
- Virtual Inertia support, in coordination with the WGs located offshore.
- Fault Ride Through (FRT) for onshore AC faults.
- Specifically, for the VSC-HVDC system, black start of the offshore AC grid, in coordination with the offshore VSC station.

Apart from the requirements, the major control function of the onshore VSC station is the control of the HVDC link voltage. Although, one or more of the above control possible capabilities, as a minimum, the onshore VSC contributes to the reactive power compensation at

its connection point. Below, the control overview of OWPP with VSC-HVDC transmission is provided.

2.5.4 Control Overview of OWPP with VSC-HVDC transmission

The overall control scheme, for WG converters and the VSC stations for a VSC-HVDC based OWPP topology, is shown in the Figure 2.17. Under normal operating condition, the HVDC voltage is regulated by the onshore VSC station (ONVSC).

The offshore VSC station (OFVSC) ensures the stable voltage and frequency in the offshore AC grid. The frequency reference is usually obtained from an internal oscillator. The WGs are in Grid following mode and inject active and reactive power, synchronizing to the AC grid by using PLL. The offshore VSC station acts as an ideal slack bus in normal operation mode, extracting all the available wind power and transmitting it to through HVDC link [41].

The black start / start up of the offshore AC grid, is the energization of the offshore AC network and also the supply of WG auxiliary equipment, enabling the WGs to produce power. This operation is performed either by the Diesel Generator and / or the Offshore VSC station due to its bidirectional operation. In the second case, the power (necessary for black start) is drawn from the onshore AC grid, by using the same control operations for the offshore and onshore VSC stations as in the Figure 2.17. In this case the offshore VSC is essentially a large uninterruptible power supply (UPS) [41], serving to provide energy, first for the offshore station equipment and then to the offshore network equipment, WG auxiliaries, until the OWPP is capable of producing power. Here, the offshore station is said to operate in 'phasor control mode'and it is analogous to an infinite voltage source energizing the offshore network loads.

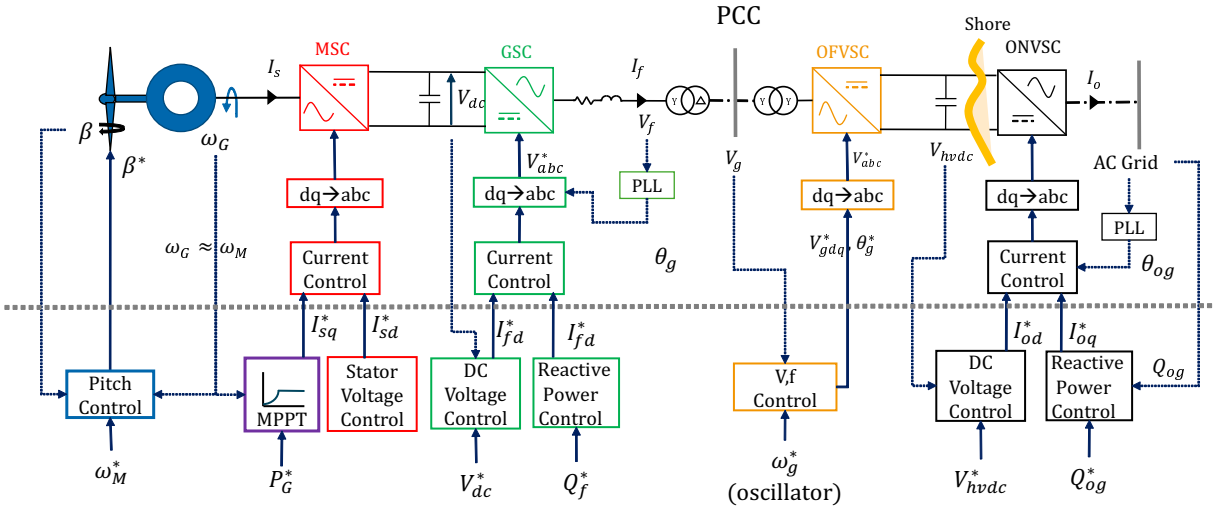

Figure 2.17: Control overview of the OWPP with VSC–HVDC transmission

2.6 System Protection and Fault Ride Through

The offshore wind power system has some similarities with the traditional wind power plants, in terms of system protection and fault ride through requirements. The grid code might enforce certain behavior from the WGs and a simple trip of the WGs during faults may no longer be an acceptable response [42]. Also with type 3 and type 4 WGs, there are advantages and limitations due to the presence of power electronic devices.

Some of the system protection requirements laid out in [18] that have to be met by HVDC connected OWPPs are:

- Provision of fault currents by the offshore VSC station and the WGs in case of offshore faults. This implies that the offshore VSC station and WGs need to inject currents to feed the AC grid fault, so that the offshore protection system can detect the fault condition and isolate the faulty section.
- Protection of faults on both offshore and onshore systems.
- Fault Ride Through for both offshore and onshore faults.

The term FRT means that the control functions have to be in place for the WGs and the offshore VSC station, so that the OWPP and/or the converter stations remain operational throughout the fault period. This makes the return to normal operation relatively easy, once the fault has been detected and cleared. The safe clearing of fault requires a reliable protection layout and relevant equipment (breakers, relays) in place in the offshore network and the WGs. This is described briefly in the following section. Also the control capabilities to ride through faults that are in place and also available in the literature are highlighted in the last part of this section.

2.6.1 Offshore Wind Power System Protection Layout

The Figure 2.18 shows a typical layout of protection devices in the offshore AC grid [18] [43]. The WG consists of breaker B_{wg1} and is usually protected by using an over-current protection strategy. This serves for WG protection against faults like generator and converter short circuits. The offshore PCC is connected to the transformer which could be a part of the collection station or the converter station. The layout also shows a single breaker per string to connect it to the PCC. Thus, in case of a fault in one of the string cables, the entire string is disconnected by the breaker (B_{S1}).

An alternative to this, is to connect the WG to the string with additional switches / circuit breakers [44] [45], as shown in the Figure 2.19. With such protection devices for each WG and also with the help of the ring configuration, a high availability is ensured so that when there is a fault in the string, only the faulty part of the string is isolated from the PCC and the WGs remain connected. The downside is, of course the additional cost associated with the extra switch gear and protection equipment. Careful choice must be made for the layout selection, for instance,

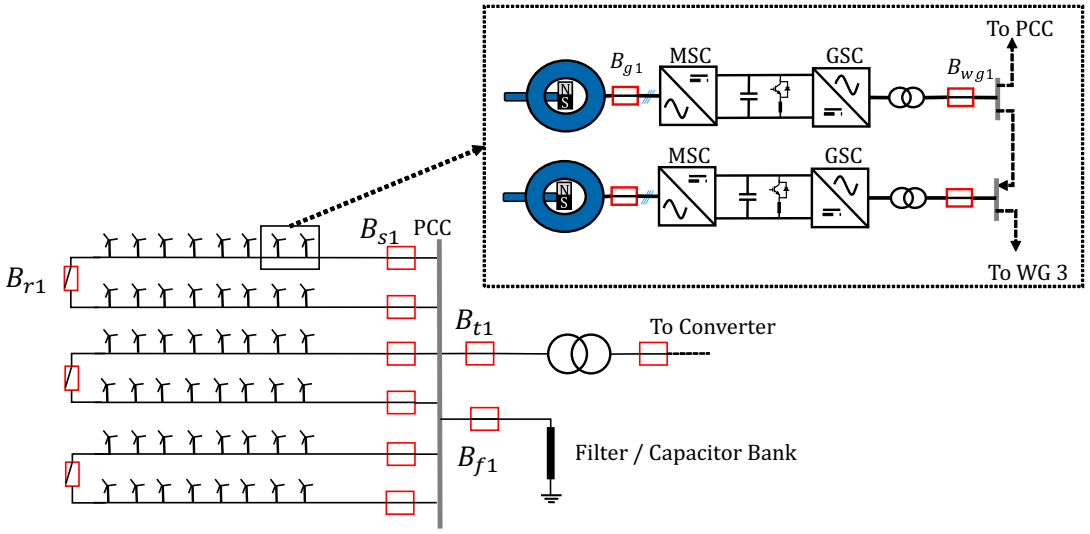

Figure 2.18: Protection Layout for the OWPP AC Grid

based on the historical data of failure rate of cables [46] and the corresponding Time to Repair and loss of energy per year.

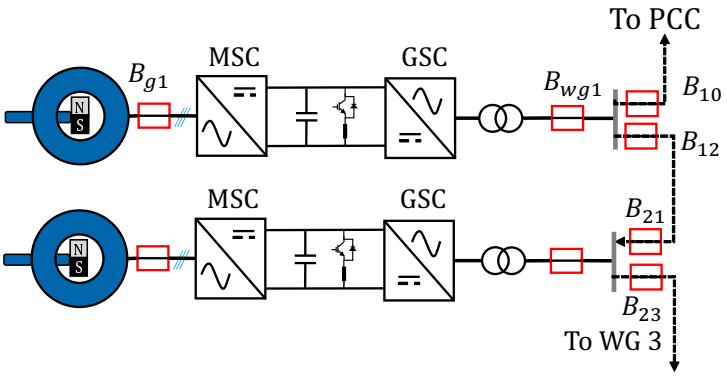

Figure 2.19: Protection layout for WGs in a feeder for increased availability

The primary and back up protection strategies can be of over–current (including directional over-current) or differential type [43]. This allows for interruption of most of the faults. The fault in the bus bar is considered to be the most critical and it has to be cleared as fast as possible. The protection strategy for the bus bar has to be designed suitably, while also avoiding its action for any fault in one of the feeders.

2.6.2 Wind Generator Fault Ride Through Capabilities

A typical type 4 WG has a crowbar (DC chopper + resistor) installed in the dc link of the B2B converter [47]. When a fault occurs for instance, in the offshore grid, the AC voltage

drops to a very low value. Thus the energy produced by the WGs can no longer be evacuated to the onshore grid and thus may lead to increase of the DC link voltage and acceleration of the turbines. It is paramount that these situations are avoided and thus the crowbar can be used to dissipate this energy during the fault.

A crowbar in simple terms (shown in Figure 2.15), is a resistor connected to a power electronic (PE) switch and is in parallel to the DC capacitance. Once a fault condition is detected, the PE switch is turned on and any excess energy that cannot be injected into the AC grid, is dissipated in this resistor. When the protection system of the OWPP clears the fault and restores the system, the WGs can resume operation in normal mode.

Fault current Provision by GSC

Another integral aspect of FRT by the Type 4 WG is the use of the Grid Side Converter to inject not active but reactive current contribution during a fault. The typical inverter (GSC) does not have a natural response to an AC fault, like a synchronous machine. The short circuit current capacity for an inverter is generally limited to 2 pu [48], to safeguard the power electronic switches from damage.

2.6.3 VSC-HVDC FRT Capabilities

The VSC-HVDC transmission (mostly made with MMC type converters today) has capabilities to provide fault current contribution to the offshore AC grid fault. Moreover, the system itself can be equipped with additional components and control algorithms to ride through faults in the onshore AC grid. The FRT capability is mainly required to continuously operate the DC system without over voltage due to the energy imbalance in the HVDC as a result of the wind power injection.

As pointed out in [42] [18], the fully rated crowbar can be used to dissipate the energy from the OWPP, in the event of the onshore AC grid fault (as in the Figure 2.20). This prevents the fast increase of the HVDC voltage and thus allows the OWPP to be unaffected, without the need to change the WG controls. A hysteresis controller can be used to trigger the crowbar as soon as an onshore AC fault is detected.

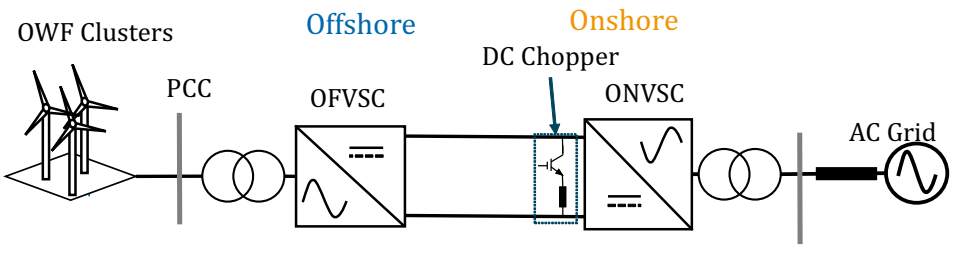

Figure 2.20: VSC-HVDC system with crowbar at onshore VSC station

Other alternatives to the crowbar have been explored in the work [42], some of which are briefly described below:

1. Setting a power reference (limitation) and frequency control mode for the offshore VSC station, with communication from the onshore VSC station.
2. Use WG control and crowbar to ride through, with communication from onshore VSC.
3. Reduce offshore AC voltage reference by using the offshore station, thus invoking the implemented FRT response of WGs.
4. Combination of two or more of the above methods to mitigate disadvantages involved in each individual approach.

It is observed in [49] that similar FRT response can be achieved by controlling the crowbars of all the WGs offshore and using only the DC crowbar of the onshore VSC station instead. However, in the former case, the triggering signals have to be communicated to the WGs and the associated time delay may lead to over–voltage in the HVDC link. And the latter case is a single entity, which is triggered by signal from the onshore station with local measurements. Thus, a crowbar at the onshore VSC station is more of a standard equipment and it can be used in combination with some of the above mentioned advanced strategies.

When considering the DR-HVDC system, the FRT becomes a more challenging task since there is no offshore active station to enforce any kind of fault response and the entire fault current contribution is coming from the WGs. The analysis of faults and means of ride through are the subject of discussion in Chapter 6.

2.7 OWPP with DR–HVDC Transmission - Overview

2.7.1 Interests in DR-HVDC Transmission

The DR–HVDC for OWPP continues to be a subject of research. As the potential OWPP sites get farther from the shore and as the WGs increase in size, the DR-HVDC becomes more interesting as an option for grid integration. It is clear that compared to the VSC-HVDC topology, the DR-HVDC topology, has some prominent advantages as listed below [50]:

1. The weight and volume of the rectifier platform is reduced drastically (industrial claims of 30 % cost savings overall).
2. There is no control needed and very less maintenance required for the offshore DR platform.
3. High reliability compared to the VSC-HVDC station.
4. Reduced conversion losses.
5. The MV–HV AC substations (export substations as seen in the Figure 2.12) are eliminated by directly connecting the 66 kV collection network to the DR platform.

A brief discussion on the characteristics of the DR is deemed necessary, before proceeding further with the description, control and operation modes of the DR-HVDC topology. The existence of different operation modes in the electrical system, due to the inherent nature of the DR and the conditions that ensure transition from one mode to the other are unique for DR-HVDC topology. The economic advantages and robustness of the DR-HVDC topology comes with some stark challenges related to grid integration, AC grid control and power management, among others and they would be briefly discussed in the last part of this chapter.

2.7.2 Operation Characteristics of the Diode Rectifier

The Diode Bridge

A three phase full bridge uncontrolled rectifier is shown in the Figure 2.21. For the study here, only a three phase AC voltage source is considered and this is connected to an inductance and then to the diode rectifier and the ideal DC voltage source. This electrical circuit is equivalent to the PCC of an OWPP connected to the DR by using a transformer. The DR has two cycles / phases during its rectification process namely – conduction and commutation cycles [51]. At a given instance, a pair of diodes conducts in the full bridge diode rectifier – one from the upper half of the bridge (i.e. D1,D3 or D5) and one from the lower half of the bridge (i.e. D2, D4 or D6). This is called the conduction cycle. Then as the three phase AC voltage waveform progresses, another pair of diodes (again one upper and one lower half of the bridge) conducts for 60°or one sixth of the time period of the AC wave. Six such possible diode pairs conducting at consecutive intervals for a full AC wave cycle are – D1D2, D2D3, D3D4, D4D5, D5D6 and D6D1.

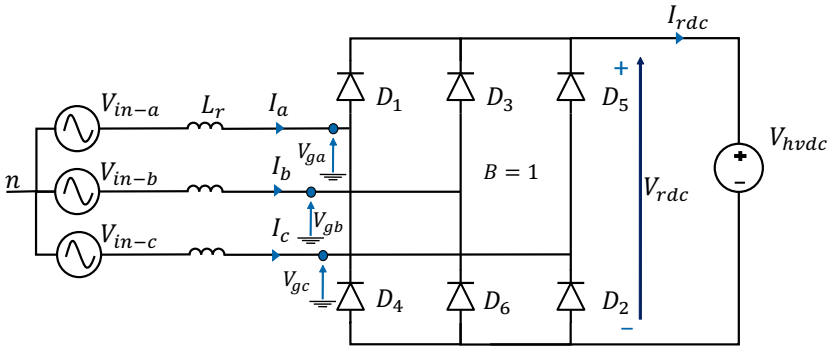

Figure 2.21: A Six Pulse Diode Bridge connected to a DC voltage source

The above mentioned six diode pairs conduct in an ideal situation where the switching between diodes is instantaneous. That means, to pass from one pair to another (for instance between the D1D2 pair to D2D3 pair, when D1 stops conducting and D3 starts conducting) there is no time delay. But in practice, such ideal commutation cannot occur, due to the presence an

inductance between the source and the converter, resisting the instantaneous change in current [52]. Thus, there may be a momentary overlapping of diode conduction when three (or more) diodes are conducting – i.e. more than one diode at the upper half or lower half of the bridge, at a given instance. This is called the commutation cycle and it is essentially a momentary short circuiting of the phases in the source. The corresponding angle during this period is called the commutation angle. Due to the connection to a DC voltage source, the DC current consists of six pulses (see Figure 2.22) for a period of an AC wave (20 ms) and thus it is called a six pulse diode bridge.

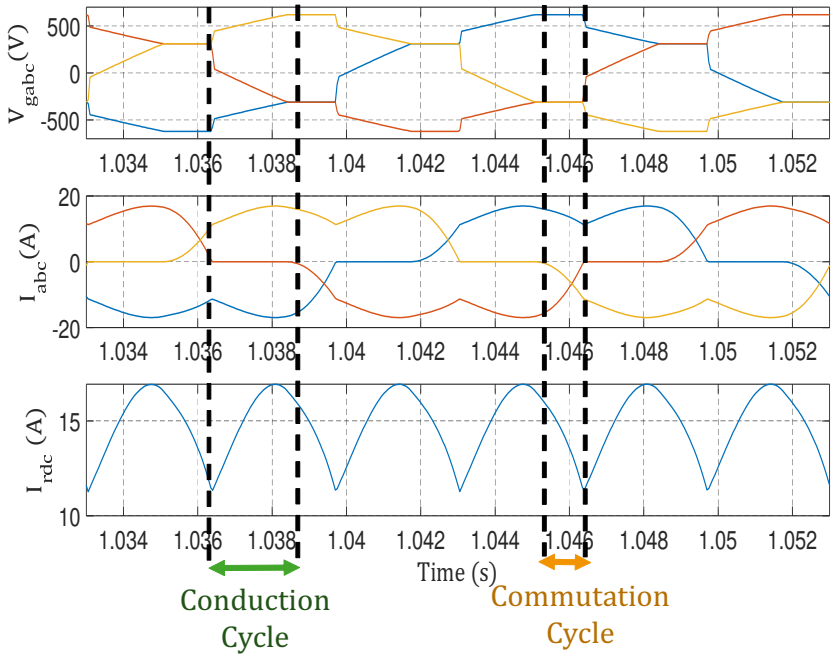

Figure 2.22: Three Phase AC voltage and current at PCC and Six Pulse DC output

Diode Rectifier with higher number of pulses per cycle of AC wave is also feasible. Just like LCC systems, the AC network can be connected to the DR with one or two separate transformers with star and delta secondary winding configurations, giving a natural phase shift of 30°. The secondary windings are connected to two separate six pulse bridges, which are connected in series on the DC side. This results in the so called 12 pulse bridge, given that there are 12 pulses in the DC current for an AC voltage cycle. As mentioned earlier, the industrial solution attains a 24 pulse configuration by using transformers with zig zag connections to create a phase shift of 15°on the primary side. The characteristic AC voltage and current harmonics, for a DR with B number of bridges are given by:

$$Harmonic\ Order = 6Bn \pm 1; n \in \{1,2,3,...\} \tag{2.13}$$

The advantage of connecting higher number of bridges in series with phase shifted configu-

rations is that harmonics are greatly reduced due to the cancellation of lower order harmonics, thus minimizing or eliminating the need for filters [53]. The distortion in voltage for different number of bridges in series, is shown in the Figure 2.23(a) and the corresponding distortions in current is shown in the Figure 2.23(b) for a particular operating condition of input voltage at 1.1 pu.

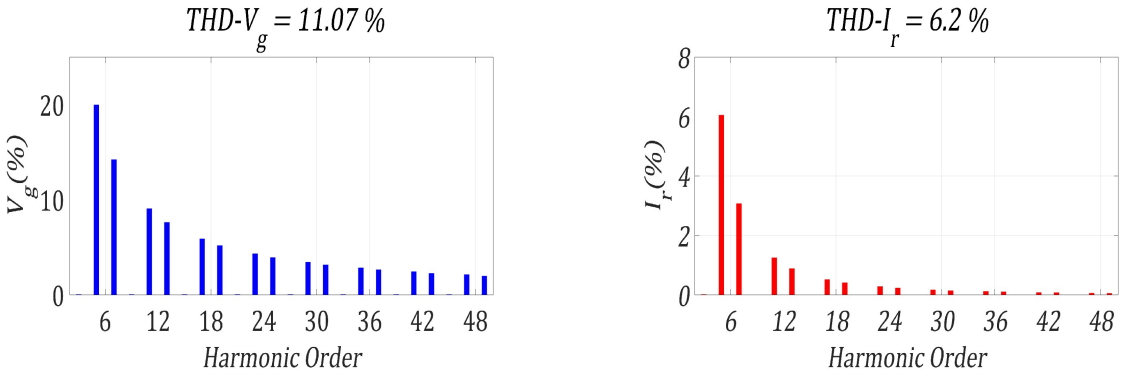

(a) (b)

Figure 2.23: Characteristic harmonics of the six pulse DR (a) RMS AC voltage at DR input (b) RMS AC current at the DR input

DR Conduction Modes

Before explaining the operating modes of the OWPP, it is necessary to describe the different conduction modes of the DR and later to find concurrence between these two sets of modes. The reference circuit to describe the modes is shown in Figure 2.21. The value of AC voltage applied at the input, determines which conduction mode prevails for the DR. The applied AC voltage must be such that, the rectifier DC output voltage is higher than the DC blocking voltage to allow the DR conduction. Once sufficient voltage level is reached, the AC voltage at the input of the DR is clamped to the DC voltage.

The following distinct conduction modes can be defined for the DR [51]:

1. **DCM** – Discontinuous Conduction Mode, when 1-2 diodes are conducting at any given time. It precedes the continuous conduction mode (CCM) of operation.
2. **CCM 1** – In this mode, 2 to 3 diodes conduct at any given time. Three diodes conduct during the commutation cycle. The commutation angle is less than 60°.
3. **CCM 2** – This occurs when the AC voltage is increased slightly beyond rated value of 690 V (RMS phase to phase value by up to 20 % - 30 %). For this mode the commutation angle is equal to 60°.
4. **CCM 3** – In this mode, there are three or four diodes conducting at the same time throughout the three phase AC cycle. It is observed when the AC voltage is beyond 30% of its

rated value. This is a permanent short circuit between AC phases and the corresponding commutation angle is between 60°and 120°.

The circuit in Figure 2.21 is simulated with the network parameters shown in the Table 2.2. The input AC voltage (V_{in-abc}) is ramped at 1 pu/s to illustrate the various conduction modes. It is clear that at the AC voltage of around 0.96 pu, the DR starts conducting and then the increase of input voltage leads to an increase in the DC current. The AC voltage measured at the input of the DR (V_g) becomes almost constant after the input voltage (V_{in}) reaches 1 pu. An important observation is that the increase of AC voltage (V_{in}) results in an increase of the DC current or power through the DR.

No	Parameter	Value
1	Base AC Voltage	690 V (line to line)
2	Base DC link Voltage	931.82 V
3	Base Power	50 kW
4	AC Inductance L_r	5.5 mH
5	Event	V_{in} ramp at 1 pu / s
6	Simulation Step	50 us

Table 2.2: Parameters for simulation of Six Pulse Diode Rectifier connected to a DC source

The DCM can be observed in the Figure 2.24(a) where the voltage V_g reaches close to 0.96 pu, just before CCM 1. Post conduction of DR, CCM 1 has the voltage and current waveforms at the input of the DR, as seen in the Figure 2.24(b). Then, with a higher input voltage beyond 1.2 pu, CCM 2 and eventually CCM 3 can be observed. The non conducting cycle ($V_g < 0.96$) and the CCM1 are the modes that are relevant to discuss the various operation modes of the OWPP.

2.7.3 Description of OWPP Topology

The power transmission for the OWPP system is predominantly unidirectional, except during specific cases like the OWPP black start (in the case of HVAC and VSC-HVDC topologies). Thus, the diode rectifier can be used as the offshore rectifier station and as explained before, there are drastic advantages compared to the VSC-HVDC system. This is already pitched as a commercial solution by Siemens, with additional innovations at the protection, wind generator control and the use of a full bridge MMC. Although this solution was first analyzed in [54] for grid integration of OWPP, one of the first mentions of the DR-HVDC for remote power transmission was made far back in 1980s in [55].

The DR-HVDC was considered more for the remote generation stations like hydro power plant initially, and regarded to be advantageous over the legacy LCC system due to reduced costs, higher reliability and harmonic stability [56]. Today, the advancements in DC breaker

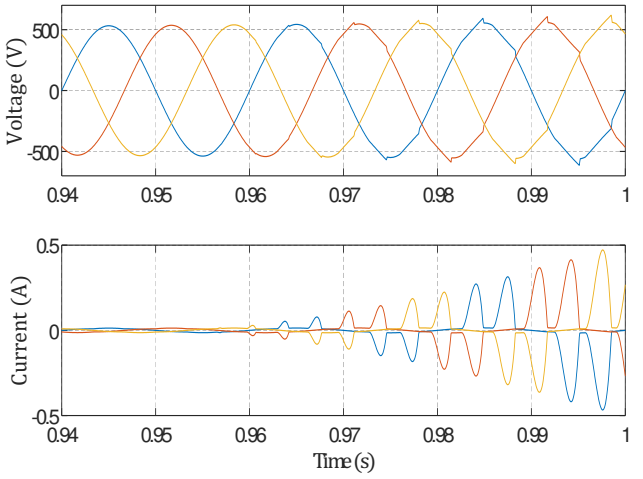

(a)

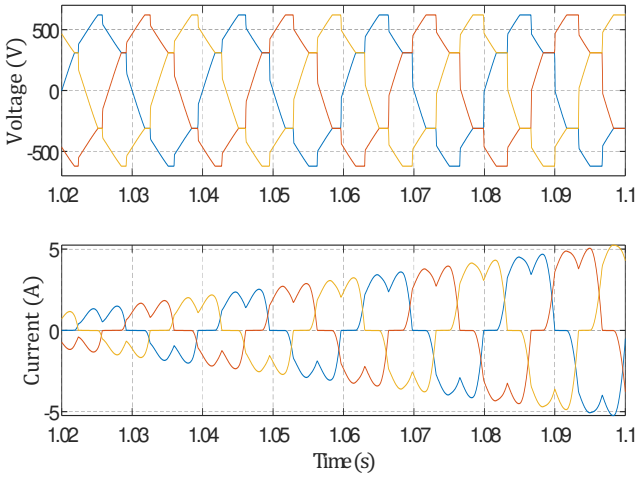

(b)

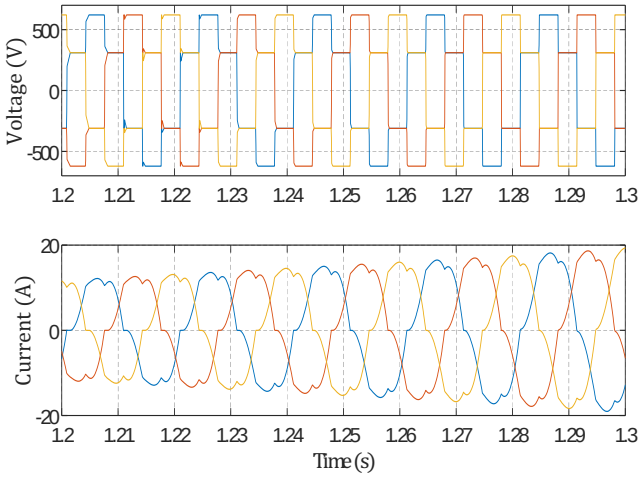

(c)

Figure 2.24: AC Voltage (V_{gabc}) and Current (I_{abc}) in the DR input for (a) DCM (b) CCM1 (c) CCM2

technology along with the existing HVDC converter technology of MMC have provided a great application case of the DR-HVDC system. Further, with potential wind farm sites moving farther from shore and the wind generator capacity increasing [57] , the high reliability and economic advantage of the Diode Rectifier Unit (DRU) could pay off as an interesting alternative to the VSC-HVDC in the near future.

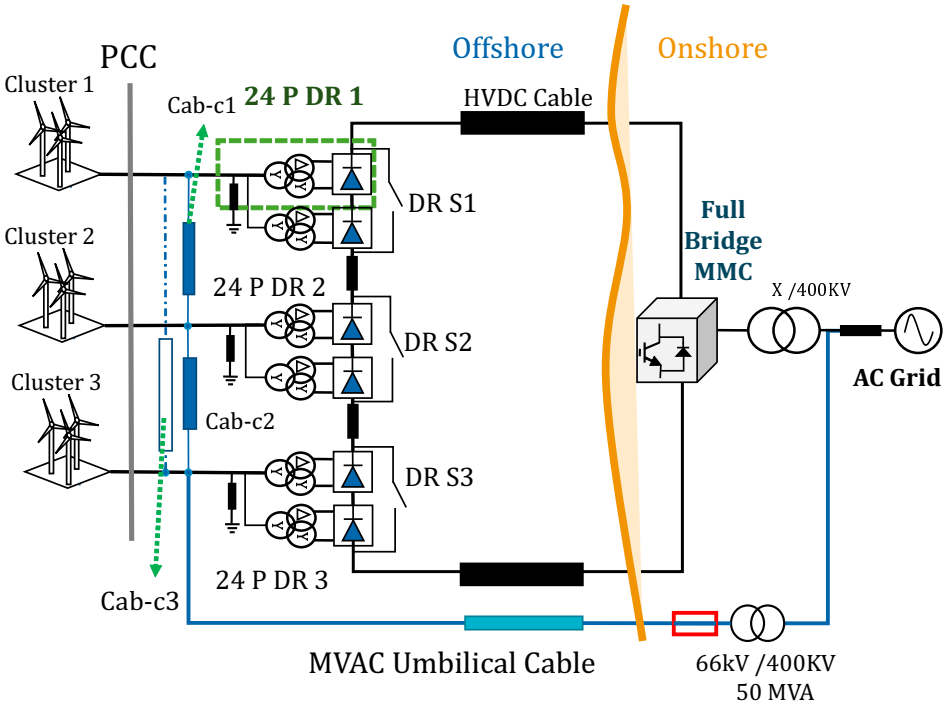

Figure 2.25: OWPP with DR-HVDC Grid Integration

An electrical scheme is shown in the Figure 2.25 for a large OWPP, with multiple clusters, separated by relatively larger distances. It is the illustration of the industrial solution [50], with two 12 pulse DRs connected using Zig-Zag connections on the primary sides of the transformers to achieve a phase shift of 15°among the four secondaries, for one 24 Pulse DR pair of stations. This 24 P DR (24 pulse DR 1), consists of two individual 12 pulse DRs. Each of these 12 pulse DRs is encapsulated into a single physical structure (as seen in the Figure 2.26), along with its transformer, filter and DC reactor, immersed in ester liquid with a specific cooling mechanism. The MVAC Umbilical Cable is used to enable the start-up of the offshore network, by energizing the offshore network components and supplying the WG auxiliaries initially. Moreover, the industrial solution proposes grid forming control of wind generator control [58], for regulation of offshore AC voltage and frequency.

The DR stations are located closer to the OWPPs, and so the export network and the associated transformer substation (as seen in Figure 2.12 for VSC-HVDC system) are eliminated. The MVAC collection network is directly connected to the DR stations and in-turn the DRs are connected in series on the DC side to achieve the desired HVDC transmission voltage. There

are also a parallel connection of AC side (Cab-c1, Cab-c2) by cluster interconnection cables, to ensure that equal power is transmitted by every DR station. A backup to the cluster interconnections is also provided in the form of Cab–c3 which is normally disconnected and used as back-up when, for instance when the cable Cab-c1 fails. In addition, by pass switches (DR S1,S2,S3) are provided for the DR stations, to allow power evacuation if one DR station fails.

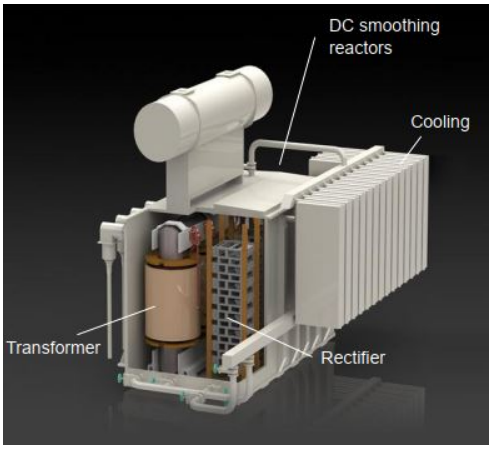

Figure 2.26: A single 12 pulse Diode Rectifier Unit, as illustrated in [58]

2.7.4 OWPP Operation Overview

The operational characteristics of the DR and the imposed HVDC voltage lead to the existence of different operating zones in an OWPP connected to the DR-HVDC transmission. In fact, they are related (but not entirely) to the DR conduction modes. It is necessary to understand these operating regions to effectively design the system and / or modify already existing WG control solutions. These zones were defined and explained in detail in the work [59] and form the basis for this subsection. The major zones of operation of the OWPP, which corresponds to the DR conduction operation are listed below (and shown in the Figure 2.27)

i. **The Islanded Mode** when the DR is not conducting. In this case the synchronous operation of the WGs must be ensured before moving to the normal mode.
ii. **The Transition** when the DR is about to start conduction or is conducting discontinuously. From the simulation studies done (as will be seen in the forthcoming chapters), the transition mode also includes the response time of the WG controllers or other equipment to increase the AC voltage sufficiently high (less than but close to 1 pu) so that conduction by the DR is forced.
iii. **The Normal or Connected Mode** when the DR is conducting current and, in turn, transmitting power into the HVDC link. The offshore PCC voltage is clamped to the HVDC voltage in this mode of operation.

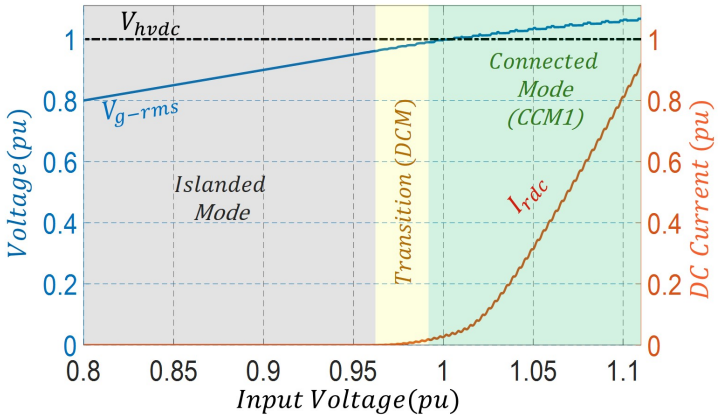

Figure 2.27: The various operating modes of the DR-HVDC OWPP

There is, in fact an inherent relationship between some of the conduction modes of the DR and the various operating regions for the OWPP listed above. It is very obvious that the non-conducting mode corresponds to the Island mode of the OWPP as in Figure 2.27. The Transition mode of the OWPP may contain the momentary DCM operation of the DR (seen in the Figure 2.24(a)).

Finally, in the normal operation mode of the OWPP, the desired operation mode for the DR is the Continuous Conduction Mode 1 (seen in the Figure 2.24(b)). As seen in further studies, this mode of operation is enabled by the control when the AC voltage reaches the rated rms value (corresponding to 1 pu) and the clamping of this voltage to the DC voltage is assured. But here, according to the parameters used for simulation, the rated current is achieved for 1.1 pu of the rms AC voltage at the input of the DR, as seen in the Figure 2.27. After conduction of the DR, the value of AC voltage slightly varies as a function of the injected DC current or in this case with increase in wind power, as observed from the equation (2.14) [59].

$$V_g = \frac{\pi}{3BN_T\sqrt{6}}V_{rdc} + \frac{L_r}{BN_T\sqrt{6}}\omega_g I_{rdc} \tag{2.14}$$

The various operation modes for the OWPP described here can pave the way to formalize the various requirements to ensure the stable operation in each of the modes and enable transition from one mode to another. These requirements can be in-turn used to devise the control scheme for the WGs, ensure a solution for start-up, tackle fault cases, among other issues during the OWPP operation in different modes. In the next section, a control overview for this OWPP topology is presented, highlighting the various control requirements and possible modifications to the conventional WG control.

2.7.5 Control Overview

The onshore station ensures stable HVDC voltage, as in previous case of the VSC-HVDC case. But in the offshore, the stable AC voltage and frequency control has to be ensured. Various approaches are possible in achieving this grid control, some of which are briefly pointed on in the section 2.8.2. A coordinated control among WGs is required, for the transition from the islanded mode to the connected mode (by forcing the DR conduction). A specific solution is also required for synchronization of the various WGs. Some of the recent WG control solutions, rely on WG control modification to achieve grid forming in the offshore AC grid. The general control overview of such schemes is shown in the Figure 2.28.

The major difference between this figure and the control of WGs in the VSC-HVDC OWPP topology (in the Figure 2.17) is the WG control algorithms are almost reversed. The MSC in the DR-HVDC topology, takes over the control of the DC bus voltage of the B2B converters in each WG as in the Figure 2.28. The GSC on the other hand, apart from performing MPPT, is also controlled for the grid forming of the offshore AC network. Apart from this general control scheme, there are other solutions that focus on (almost) retaining the WG grid following control scheme as in the Figure 2.17.

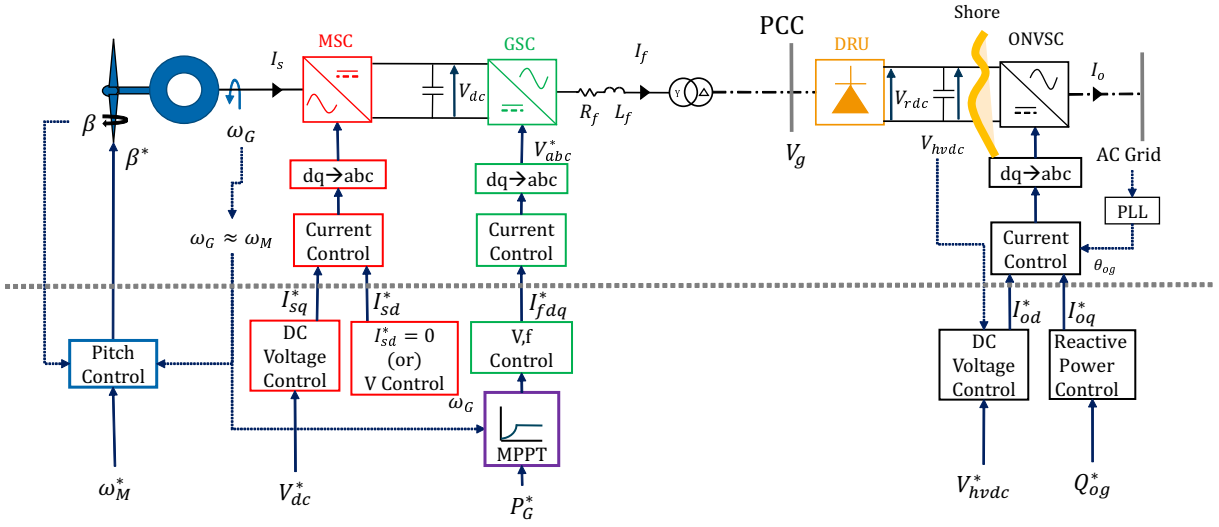

Figure 2.28: Control overview of the OWPP with DR-HVDC transmission

2.8 DR OWPP Grid Integration Challenges

2.8.1 Overview of Challenges

Having briefly described the various operation modes of the DR-HVDC connected OWPP, this section helps in establishing a background for this thesis. Certainly, the existence of an

industrial solution [58] has not encouraged an OWPP developer to implement it and also there are no pilot projects operating or planned today. Also the ongoing PROMOTioN Project [60] has one of its major working groups dedicated to enable and analyze this solution, with grid forming WGs. Literature survey and analysis during the period of the thesis did show that there are existing barriers that have not been addressed entirely in enabling the implementation of this technology.

The major challenges for grid integration of OWPPs with DR-HVDC transmission are described below:

1. **Grid Forming and Power Management** – The foremost challenge is how to ensure a stable voltage and frequency in the offshore grid. Moreover the WGs need to extract maximum wind power available or ensure te active power control and manage the reactive power flow in the offshore grid.
2. **Black Start Solution for the Offshore Grid** – The offshore AC grid equipment and the WG auxiliaries (in the worst case), need to be energized, to enable islanded mode and then the transition to the normal operation.
3. **Ensure safe operation during faults** – The lack of an active offshore (VSC) station means that the WGs need to ensure the safe operation during the various faults in offshore AC grid, the DC grid and the onshore AC grid. Also, once the fault is isolated, OWPP operation is restored, if necessary with a reduced power production.
4. **Integration into MTDC Network** – The existing and planned point to point HVDC links, may have to be connected by different means to form MTDC grids in the future. The integration of DR-OWPP to such an MTDC grid has to be analyzed and solutions need to be in place for the various system level challenges.

2.8.2 Grid Forming

The problem of grid forming can be broken down to essentially three major objectives, apart from ensuring a maximum wind power extraction.

i. **Voltage Regulation** – The AC Voltage level is crucial to maintain the islanded mode (prolonged if necessary) and then enable transition to the connected mode. Unless there exists an additional equipment for this purpose, the WGs have to perform this control in a distributed manner.
ii. **Frequency Regulation and Synchronization** – The frequency of the offshore grid has to be regulated by the WGs or by using other means. The WGs need to be synchronized with each other in order to allow a stable grid operation.
iii. **Reactive Power sharing** – The offshore grid reactive power demand has to be properly shared by the WGs, during different load conditions.

The grid forming capability can been provided to the OWPP system by using different solu-

tions. They can be classified into two groups:

- Solutions with major WG control modifications.
- Solutions with minor or no WG control modifications.

These two groups of solutions are briefly discussed below, while some of these are compared and assessed in detail in Chapter 4.

1. Solutions with Major Control modifications to WGs

This group of solutions have modified drastically the WG control functions. The resulting control scheme is of the form shown in the Figure 2.28.

The control of DR-HVDC OWPP system was first tackled in [54]. The work was presented in a more detailed manner in [59], where the dynamic modelling of the offshore wind power system was done and the analysis led to a distributed voltage and frequency control by the WGs. It was also stated that although certain grid forming schemes available in the microgrid literature could be extended, it was important to analyze the dynamics of the offshore system and propose a relevant control solution. Here the MSC of each WG has been used to control the DC link of the back to back converter (one of the degrees of freedom available as seen in the Figure 2.15). However there was no clear solution for the synchronization or black start.

The industrial solution described in [61] (illustration in the Figures 2.25 and 2.26) requires modifying the WG control scheme to render it as a grid forming unit, where the initial energization and frequency / voltage reference is provided by an umbilical cable connected directly to the onshore AC grid.

The solution proposed in [62], is an evolution of the approach presented in[54]. Moreover a solution using the PLL of the WGs is proposed for the synchronization among them, without using any high bandwidth communication. However the black start of the offshore system is assumed to be facilitated by the storage devices in the WGs but is not clearly demonstrated.

2. Solutions with Minor Control modifications to WGs

This group of solutions, argued that major control modifications are not required for the WGs and the stable grid forming and power management can be ensured with additional equipment or minor tweaks to the WG control.

One such approach in [63], focused on retaining the existing WG control scheme, and propose slight modifications to the architecture, by using high bandwidth communications to enable the synchronization. The presence of an AC umbilical is crucial for the start-up and provision of initial AC voltage reference. Frequency regulation and synchronization is implemented by using a GPS or radio based signal reference for all WGs from a central controller. This signal reference provides a fixed reference in dq frame, rotating at a fixed frequency, to all the WGs.

In [64] a compromise is found between changing completely the MSC and GSC control [59][62] and the retention of existing grid following control scheme [63]. In this work [64], the active power control or MPPT is kept at the MSC side and the GSC retains the DC link voltage control. The reactive current of the GSC is used for frequency regulation and synchronization with the AC grid by using a Q-f droop control. Deviations in frequency of the grid, is corrected by using a secondary control loop, while reactive power is shared by the WGs. Analysis is done in steady state and start-up and fault cases as well. But the exact solution and demonstration for black start hasn't been detailed.

2.8.3 Black Start of the Offshore AC Grid

Generally, the black start of any power system, is the process of providing power capacity and energy after a power system failure or a black out. The generator unit capable of providing this service or function is called a Black Start Unit (BSU). Such a Black start unit, may help in powering up larger generator units by supplying the required auxiliary power and energization requirements. Characteristics of such a unit includes fast response, very low self auxiliary supply, reliable in case of failures.

Moving onto the context of the OWPP, the black start of the offshore wind power system includes the following requirements:

i. Powering the WG auxiliaries in the worst case – loss of back-up power or long-term outages.
ii. Energization of the offshore equipment, submarine cables, WG transformers, offshore transformers etc, the loads, which are predominantly reactive.
iii. Energy for active power losses in the collection network and other equipment.

The existing industrial solution for black start of the offshore grid, as shown in the Figure 2.25, is an MVAC umbilical cable, which is sized to about 50 MVA for a 1200 MW farm i.e. around 4.2 % of the nameplate capacity of the farm, in real power. The exact black start sequence/strategy is unclear, but it is safe to assume that initially only a few WGs and a part of the OWPP grid are energized to allow the islanded operation, followed by the energization of the other WGs to enable the normal operation. When DR conducts, the MVAC cable is disconnected.

The tried and tested solution is the Diesel generator for black start and emergency purposes [17] for offshore platforms and the grid. But there are issues like environmental concerns, size of offshore platform and insurance costs [65]. Moreover, there is a question of maintenance and re-fueling, for a site which would be typically located at 100 km or more from the shore.

On the other hand the WGs of today do have certain self-start capabilities, as will be seen in the Chapter 5. Tapping into such existing features or modifying their design (addition of control or battery or other energy source) can avoid the installation of the MVAC umbilical

(the existing solution for black start). Other than modifying WG design itself, there could be many other solutions possible, with or without relying on the onshore AC grid to black start the offshore system. These solutions would be reviewed and compared in detail in the Chapter 5.

There is ongoing research to enable the OWPP (especially, connected through HVDC link) to provide black start services to the onshore AC grid [65]. In fact such features are put forth as grid connection requirements by ENTSO-E [66], and the black start service is an option that the concerned national TSO may request from a power plant. But, the topic of power system restoration for the onshore AC grid is beyond the scope of this thesis and thus is not reviewed in this section.

2.8.4 Ensuring Safe operation during faults

If type 4 WGs are considered, the offshore network is a 100% power electronics interfaced AC grid. As this OWPP configuration itself is new, dedicated WG control and protection strategies have to be in place to ensure Fault Ride Through capability and the restoration of power production, after the fault. Grid requirements have evolved such that a mere tripping of the WGs is no longer the means to respond to a fault, for instance in the onshore AC grid. The WGs and the OWPP as a whole need to be equipped with FRT capabilities, supported by dedicated protection strategies.

Compared to the VSC-HVDC topology, the DR-HVDC offshore wind power system clearly lacks the large offshore converter, regulating the grid frequency control and contributing to fault current in case of offshore faults. It is safe to assume that the protection system layout is similar in both offshore AC systems as shown in the Figure 2.18. Thus for faults in the offshore AC grid, the protection system has to rely upon the WG control alone to ensure safe operation and riding through the faults.

Certain failure modes are also supposed to be dealt with to ensure the availability of the remaining part of the OWPP network. Some of them include:

i. Failure of WGs due issues in power electronic system, control system, generator fault, other equipment.
ii. Failure of communication network between WGs and the main controller for instance.
iii. Failure of one of the DR stations (shown in the Figure 2.25) due to internal faults.

Detailed analysis of the various faults and failure modes and the fault ride through strategies are done in chapter 6.

2.8.5 Integration into the MTDC Grid

The Multi-terminal DC (MTDC) grid has been considered for the integration of multiple conventional AC grids [67] and VSC based OWPPs. The effective integration of such VSC-HVDC based OWPPs by using MTDC, is especially an interesting option for the European

Power system, to meet the energy transition targets [68]. Thus, any new configuration for OWPP power transmission in HVDC, like the DR-HVDC, has to be analyzed for its interoperability with an MTDC network.

The grid integration of remote generating plants (like hydro, nuclear etc.) with Diode Rectifier based HVDC was first considered in [55]. In fact, the analysis was also done on how series and parallel combinations of the DRs can be done to achieve the desirable voltage or network configuration. Here specifically, a radial MTDC network was considered with only DR stations. The advantages related to cost, reliability, maintenance were stated here, along with certain concerns related to the DC protection and unidirectional power flow.

In fact, one of the prominent analysis [69] of DR-HVDC integration into an MTDC grid has been done by the authors who proposed the grid forming solution in [54]. This work focussed on a VSC-based, three terminal, radially connected MTDC grid configuration, as in the Figure 2.29. However this work has only analyzed the feasibility and control of the grid, along with the fault case in the offshore grid.

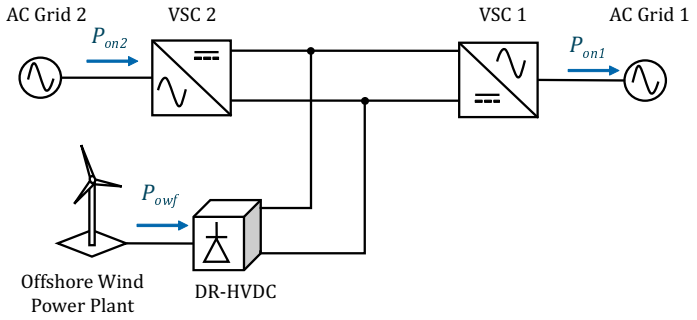

Figure 2.29: Illustration of a three terminal radial MTDC grid with DR-HVDC OWPP

Today, the literature is not sufficient regarding the integration of the DR-HVDC OWPP into an MTDC network. Thus, a system level analysis to understand the various faults and failure modes, integration issues etc., is deemed necessary to identify the technical barriers and propose solutions. This work is the last part of chapter 6.

2.9 Chapter Conclusions

In this chapter, an overview of Offshore Wind Power System has been established with a focus on the DR-HVDC OWPP. Beginning with a general overview on wind energy conversion, the different WGs and the offshore wind power topologies, focus has been on the MVAC-HVDC topology with Type 4 WGs. Today, the benchmark topology for reference is the VSC-HVDC based OWPP and it will be used to compare any new grid integration solutions for long distances of the future. With this in mind, the extended review of operation, control and protection of

OWPP with VSC-HVDC has been done, not only to draw parallels with the DR-HVDC system, but also to highlight the grid integration challenges of the latter.

Following this, the overview of the OWPP connected to DR-HVDC transmission is presented. A quick overview of the diode rectifier operation and its role in establishing distinct operation modes and constraints for the OWPP operation are highlighted. These are useful to understand the control requirements and the challenges for DR-HVDC OWPP grid integration, which are highlighted in the previous section.

Some of those challenges are tackled in this thesis and will be the subject of the forthcoming chapters. The next chapter will focus on the dynamic modelling and analysis of the DR-HVDC OWPP system for different modes of operation.

3

Dynamic Modelling, Analysis and Control of DR–HVDC OWPP

Contents

3.1 Chapter Introduction 54
3.2 Modelling of the Offshore Wind Power System 54
3.3 Analysis of the Offshore Wind Power system 62
3.4 Conclusion and Future Scope 76

3.1 Chapter Introduction

This chapter presents the modelling, analysis and control of an offshore wind power plant with DR-HVDC transmission. The offshore wind power system is analyzed by using the dynamic equations developed in an arbitrary $d-q$ frame. The existing literature on such studies is used to support the analysis. The dynamic model is also validated with circuit models in MATLAB Simulink environment. It is revealed from the analysis and also from the available literature on this OWPP topology that the active power and AC voltage ($P-V$) of the system are coupled, so are the reactive power balance and grid frequency ($Q-f$). Following this analysis and the conclusions made on the OWPP system dynamics, the control requirements for the offshore system are laid out for two different operation modes, namely the islanded mode and connected mode.

3.2 Modelling of the Offshore Wind Power System

The complete offshore wind power system is illustrated in the Figure 3.1. It consists of multiple strings of aggregated models forming a cluster. The collection network cable impedances are neglected to render easy, the modelling and dynamic analysis.

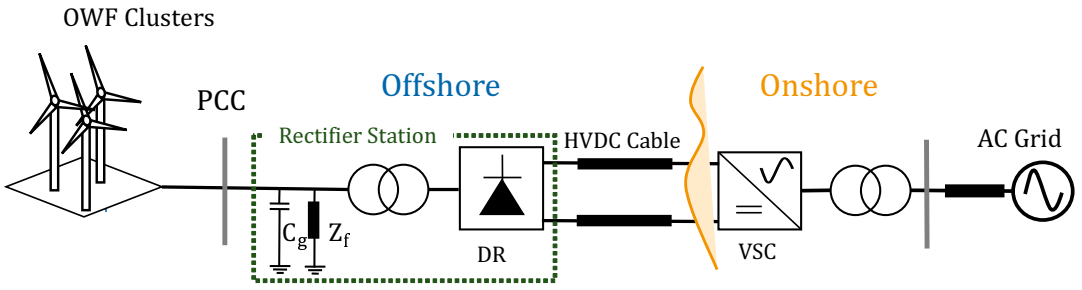

Figure 3.1: Overview of the Offshore Wind Power System

Emphasis is on the development of models for the dynamic analysis, while care has been taken to have a complete model of the system to allow its use in the further studies and also to understand the operation of the system (in the case of drive train model for instance). The models of the HVDC link and the onshore AC grid are simplified during the process of dynamic analysis, but they are defined with the vision for further analysis inside the thesis or beyond. Also since the aerodynamic model has already been presented in the section 2.2.1 of chapter 2, it has not been repeated here.

3.2.1 Drive Train

The two mass model shown in the Figure 3.2 of a wind turbine drive train is adopted, as in [59].

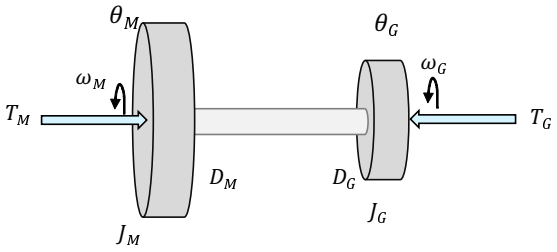

Figure 3.2: Wind Turbine Drive Train Model

The equations for the first rotating mass on the turbine side and the second mass on the generator are separately written.

$$T_M(t) - D_M \frac{d\theta_M(t)}{dt} - k(\theta_M(t) - \theta_G(t)) = J_M \frac{d^2\theta_M(t)}{dt^2} \tag{3.1}$$

$$T_G(t) - D_G \frac{d\theta_G(t)}{dt} + k(\theta_M(t) - \theta_G(t)) = J_G \frac{d^2\theta_G(t)}{dt^2} \tag{3.2}$$

where

T_M, T_G are the rotor and generator torques respectively (Nm)

D_M, D_G are the rotor and generator damping coefficients $(Nm/rad/s)$

$\theta_M \theta_G$ are the rotor and generator angles (rad/s)

k is the shaft stiffness factor (Nm/rad)

An important point to note here is the balance of the torque through the drive train. In steady state, the torque on the wind turbine is equal to that produced / extracted by the generator. To ensure operation at the reference / constant speed, the balance of power has to be ensured by control of the generator torque and the pitch of the wind turbine blades.

For the study and analysis of the offshore wind power system, it is assumed that the dynamics of the wind turbine mechanical system are slow enough to have a negligible impact on the system dynamics. This assumption is valid with the good performance of the pitch control and the control of the back to back conversion system (B2B).

3.2.2 Permanent Magnet Synchronous Generator

The model of PMSG is derived in a dq frame aligned with the rotor flux of the machine. The equivalent circuits in the dq frame are shown in Figure 3.3. Moreover the magnetic flux in the

air gap of the machine is assumed to be sinusoidal and the effects of saturation and damper winding are neglected.

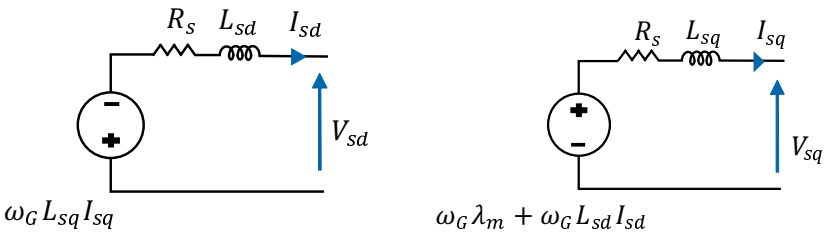

Figure 3.3: Dynamic model of the PMSG (a) d–axis (b)q–axis

$$V_{sd}(t) = -R_s I_{sd}(t) - L_{sd}\frac{dI_{sd}}{dt} - \omega_G L_{sq} I_{sq}(t) \tag{3.3}$$

$$V_{sq}(t) = -L_{sq} I_{sq}(t) - L_{sq}\frac{dI_{sq}}{dt} + \omega_G \lambda_m + \omega_G L_{sd} I_{sd}(t) \tag{3.4}$$

where V_{sd}, V_{sq} are the stator voltages of the PMSG in dq-frame (V)

I_{sd}, I_{sq} are the stator currents of the PMSG in dq-frame (A)

ω_G is the speed of the generator (rad/s). It is otherwise also the frequency of the stator voltages of the generator.

R_s is the stator resistance (Ω)

L_{sd} is the direct axis stator inductance (H)

L_{sq} is the quadrature axis stator inductance (H)

λ_m is the flux of the permanent magnet (Wb)

3.2.3 MSC and DC link

The PMSG is connected to the MSC, for the conversion of power from AC to DC (as shown in the Figure 3.4). The DC link is in–turn connected to the GSC. Here the power losses in conversion are neglected.

The Kirchoff's current equation for the DC link voltage calculation, gives the following equation:

$$\frac{dV_{dc}}{dt} = \frac{1}{C_{dc}} I_{dc1}(t) - \frac{1}{C_{dc}} I_{dc2}(t) \tag{3.5}$$

The equivalence of active power flow across the power conversion chain is represented by the following equation (should use a coefficient of $\frac{1}{2}$ instead of $\frac{3}{2}$ in case all quantities are represented in per unit).

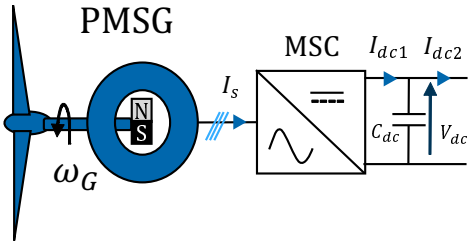

Figure 3.4: Machine Side Converter with DC link

$$V_{dc}(t)I_{dc1}(t) = \frac{3}{2} * \left(V_{sd}(t)I_{sd}(t) + V_{sq}(t)I_{sq}(t)\right) \tag{3.6}$$

3.2.4 Grid Side Converter and Filter

The grid side converter is connected to an RL filter and integrated to the offshore AC grid. An LC filter may also be used. In the former case, the RL filter and the transformer impedances are lumped together, scaled to the same per unit quantities and represented as in the Figure 3.5.

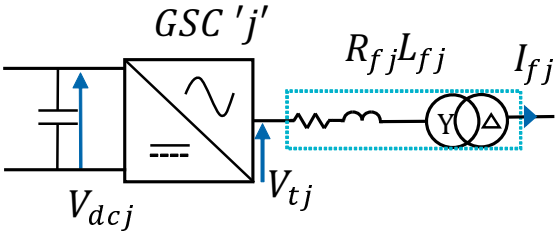

Figure 3.5: Grid Side Converter with RL Filter

For generalization, an aggregated model of a string 'j' is represented in this Figure 3.5. Aggregated strings are connected in parallel to the Point of Common Coupling (PCC). The dynamics of the currents injected by the GSC are given as follows:

$$\frac{dI_{fjd}}{dt} = \frac{V_{tjd}(t)}{L_{fj}} - \frac{R_{fj}}{L_{fj}}I_{fjd}(t) + \omega_g(t)I_{fjq}(t) - \frac{V_{gd}(t)}{L_{fj}} \tag{3.7}$$

$$\frac{dI_{fjq}}{dt} = \frac{V_{tjq}(t)}{L_{fj}} - \frac{R_{fj}}{L_{fj}}I_{fjq}(t) - \omega_g(t)I_{fdj}(t) - \frac{V_{gq}(t)}{L_{fj}} \tag{3.8}$$

During the literature review, it has been observed, for instance in [62] the use of LC filter at the output of the GSCs, for the design of a distributed voltage control scheme and also to enable the synchronization among the Wind Generators (WGs). The current dynamics are similar to the equations defined above (3.7, 3.8), with a small change in the voltage notation.

$$\frac{dI_{fjd}}{dt} = \frac{V_{tjd}(t)}{L_{fj}} - \frac{R_{fj}}{L_{fj}} I_{fjd}(t) + \omega_g(t) I_{fjq}(t) - \frac{V_{fjd}(t)}{L_{fj}} \tag{3.9}$$

$$\frac{dI_{fjq}}{dt} = \frac{V_{tjq}(t)}{L_{fj}} - \frac{R_{fj}}{L_{fj}} I_{fjq}(t) - \omega_g(t) I_{fdj}(t) - \frac{V_{fjq}(t)}{L_{fj}} \tag{3.10}$$

The dynamic equations for voltages at the capacitance terminal is written in an arbitrary $d-q$ reference frame as follows

$$\frac{dV_{fjd}}{dt} = \omega_g(t) V_{fjq}(t) - \frac{1}{C_{fj}} I_{tjd}(t) + \frac{1}{C_{fj}} I_{fjd}(t) \tag{3.11}$$

$$\frac{dV_{fjq}}{dt} = -\omega_g(t) V_{fjd}(t) - \frac{1}{C_{fj}} I_{tjq}(t) + \frac{1}{C_{fj}} I_{fjq}(t) \tag{3.12}$$

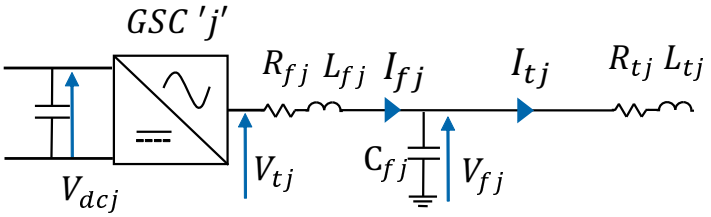

Figure 3.6: Grid Side Converter with LC Filter

3.2.5 Offshore Point of Common Coupling

The offshore PCC consists of a capacitance bus and possible filters for the reactive power compensation. This is connected to the voltage bus at which the DR transformer is connected. In the Figure 3.7 string wise aggregation is performed and J strings are connected to the PCC. Here simply an RL filter is considered for the output of each GSC, although the extension for the LCL filter case is straightforward.

The dynamic equations of voltages at this capacitance terminal is given as follows:

$$\frac{dV_{gd}}{dt} = \frac{1}{C_g} \sum_{j=1}^{m} I_{fdj}(t) - \frac{1}{C_g} I_{rd}(t) + \omega_g(t) V_{gq}(t) \tag{3.13}$$

$$\frac{dV_{gq}}{dt} = \frac{1}{C_g} \sum_{j=1}^{m} I_{fqj}(t) - \frac{1}{C_g} I_{rq}(t) - \omega_g(t) V_{gd}(t) \tag{3.14}$$

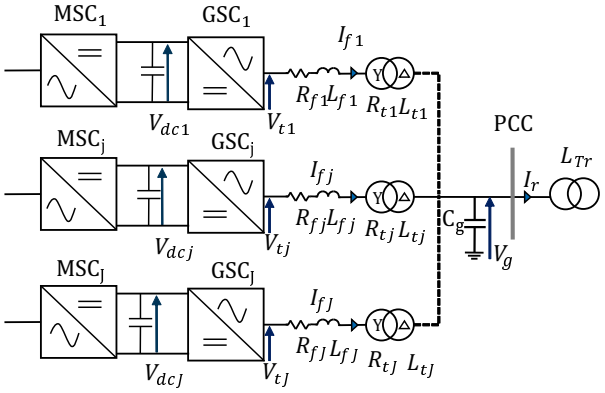

Figure 3.7: Offshore PCC Terminal with aggregated Strings

3.2.6 Diode Rectifier Model

The average value model of the DR is deemed sufficient to study the offshore network. This model has been adopted in the literature available for DR–HVDC OWPP system and the same approach is retained in this thesis. The PCC of the offshore system is connected through an AC filter to the DR, which is inturn connected to the DC link by using a DC filter, as shown in the Figure 3.8. This scheme is used for further dynamic analysis in the forthcoming sections.

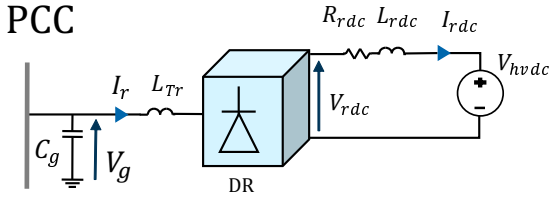

Figure 3.8: DR and HVDC Link Model

The following equations help represent the DR as an average model. The rms AC voltage at the PCC is given by the equation:

$$V_{grms} = \frac{1}{\sqrt{2}}\sqrt{V_{gd}^2 + V_{gq}^2} \tag{3.15}$$

The equation for the DC voltage at the output of the DR is given by:

$$V_{rdc} = \frac{3BN_T\sqrt{6}}{\pi}V_{grms} - \frac{3B}{\pi}\omega_g L_{Tr} I_{rdc} \tag{3.16}$$

where

V_{grms} – is the single phase RMS voltage at the PCC capacitance terminal

B – is the number of six pulse diode bridges connected in series on the DC side

V_{rdc} – is the voltage on the DC side of the DR

N_T – is the turns ratio of the transformer

ω_g – is the offshore AC grid frequency

L_{Tr} – is the inductance at the input of the DR

I_{rdc} – is the DC current

V_{gd}, V_{gq} – are the dq axis components of the offshore PCC voltage

I_{rd}, I_{rq} – are the dq axis current components at the input of the DR

The average value model described in [51] involves the use of a virtual impedance term to denote the effect of commutation of the diodes in the Full Bridge configuration, as in the Figure 3.9.

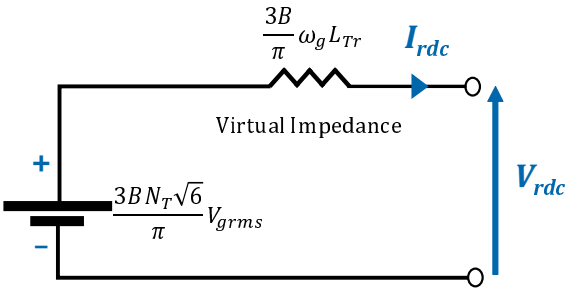

Figure 3.9: Average Model of DR with Virtual impedance

The active and reactive power at the input of the DR are given by the equations 3.17 and 3.19 [70]. The assumption is that the DR has negligible conduction losses. The expression for commutation angle μ [52] is used to represent the reactive power directly as a function of active power.

$$P_{rdc} = V_{rdc} I_{rdc} = \frac{3}{2}\left(V_{gd} I_{rd} + V_{gq} I_{rq}\right) \tag{3.17}$$

$$\mu = \cos^{-1}\left(1 - \frac{\sqrt{2}\omega_g L_{Tr} I_{rdc}}{\sqrt{3} V_{grms}}\right) \tag{3.18}$$

$$Q_{ac} = -P_{rdc} \cdot \frac{(2\mu - \sin(2\mu))}{(1 - \cos(2\mu))} \tag{3.19}$$

3.2.7 Simplified Model of the HVDC Link

The DR is connected to DC reactor/choke (L_{rdc}) and its losses are modeled by a resistor (R_{rdc}), as seen in the Figure 3.8. If a T-model for the HVDC link is considered, the above resistance and inductance can be used to denote the lumped model of the *RL* parameters of the HVDC link model. Similar to the DR model definition, the equation is written for a *B* number of

six pulse bridges connected in series. The dynamic equation of the DC current at the output of the DR (dropping the time varying notations for simplicity) is given by the following equation. Here the HVDC link voltage(V_{hvdc}) is assumed to be a constant value.

$$\frac{dI_{rdc}}{dt} = \frac{\frac{3B\sqrt{6}}{\pi}V_{grms} - \frac{3B}{\pi}\omega_g L_r I_{rdc} - R_{rdc}I_{rdc} - V_{hvdc}}{2L_r + L_{rdc}} \tag{3.20}$$

For the most part of the analysis done in this thesis, the HVDC voltage is considered to be well regulated by the onshore VSC and thus, it is assumed to be a constant. Moreover, the HVDC link impedances are neglected during the analysis in this chapter, for simplicity. Although not used in this chapter for analysis, the HVDC link model is defined for completeness and further analysis in the future chapters and research works. The simplest model that can be used is the T-model (Figure 3.10) (as is the case in [59]) and is adopted here for this thesis.

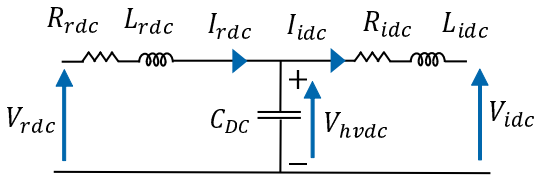

Figure 3.10: T-Model of the HVDC link

The dynamics associated with the rectified DC current I_{rdc} is given as follows:

$$\frac{d}{dt}I_{rdc} = -\frac{R_{rdc}}{L_{rdc}}I_{rdc}(t) + \frac{1}{L_{rdc}}V_{rdc}(t) - \frac{1}{L_{rdc}}V_{rdc}(t) \tag{3.21}$$

The dynamics for the inverter side DC current I_{idc} is given by:

$$\frac{d}{dt}I_{idc} = -\frac{R_{idc}}{L_{idc}}I_{idc}(t) - \frac{1}{L_{idc}}V_{idc}(t) + \frac{1}{L_{idc}}V_{hvdc}(t) \tag{3.22}$$

Finally, the dynamic equation associated with the HVDC link voltage V_{hvdc} is written as:

$$\frac{d}{dt}V_{hvdc} = \frac{1}{C_{DC}}I_{rdc}(t) - \frac{1}{C_{DC}}I_{idc}(t) \tag{3.23}$$

3.2.8 Onshore Converter Model

All of the OWPPs with HVDC transmission system operating currently (2018) have been built with the VSC based technology (two level or modular multilevel). Moreover, recent research works related specifically to DRU-based OWPPs [71] among others, have adopted the VSC based technology for modeling and analysis purposes. With these observations, the onshore converter is considered to be a VSC and specifically modeled by using an average value model of

a 2 level VSC. The onshore VSC is connected to the AC grid with an impedance that represents a filter.

The dynamics of the AC filter are written in the below equations, by using an average model for the onshore VSC. The PCC 2 here is the grid interconnection point of the onshore VSC with the AC grid as seen in the Figure 3.11

$$\frac{dI_{ocd}}{dt} = \frac{1}{L_{oc}}V_{ocd}(t) - \frac{R_{oc}}{L_{oc}}I_{ocd}(t) + \omega_{og}I_{ocq}(t) - \frac{1}{L_{foc}}V_{xd}(t) \tag{3.24}$$

$$\frac{dI_{ocq}}{dt} = \frac{1}{L_{oc}}V_{ocq}(t) - \frac{R_{oc}}{L_{oc}}I_{ocq}(t) - \omega_{og}I_{ocd}(t) - \frac{1}{L_{oc}}V_{xq}(t) \tag{3.25}$$

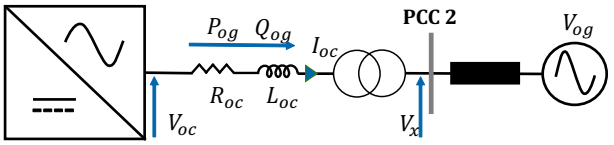

Figure 3.11: Onshore VSC connection to the AC Grid

3.3 Analysis of the Offshore Wind Power system

As explained in the section 2.7.4 of chapter 2, there are two major operating modes for the offshore wind power system:

- Islanded mode – It can last for a limited duration or may prolong based on the requirements / constraints. It is essential to ensure that all the WGs can operate and the offshore active and reactive power load is compensated. This mode requires the limiting power generated or de–loading the WGs to maintain constant power.
- Connected mode – This mode occurs when the DR is conducting and the WG can produce maximum power and all the generated power is transmitted to onshore.

Both modes are analyzed separately to observe the dynamics in the power system. Although this has been done in previous works, here the focus is to well establish the understanding of the system dynamics and highlight the couplings between the various electrical variables. A mathematical modelling of the offshore wind power system is done. The results of the dynamic modelling are compared with the circuit model in MATLAB Simulink for validation. This enables to lay down the control requirements, propose new control algorithms (in the later section of this Chapter) and also review existing control solutions (in Chapter 4).

3.3.1 Analysis of Islanded Mode of Operation

The offshore wind power system operating in islanded mode is considered here. This implies that the voltage is not high enough to force the DR to conduct. The WGs must maintain a minimum output power production, compensate for any local reactive power load in the offshore network and be synchronized with stable grid frequency and AC voltage.

Two aggregated WGs are modelled by using controlled current sources. The performance of each of the GSC's current control loop and the modulation control of the VSC is assumed to be satisfactory. Both the grid following and grid forming [72] [59] control solutions for WGs generally consist of a vector control structure, with a faster inner current control loop and a slower outer control loop(s). Thus, a controlled current source is considered here to represent the WG in totality.

The network used for the analysis is shown in the Figure 3.12. The capacitance at the output of each GSC, is part of the LC filter used for each inverter, for the grid connection. Then the LC filter of each GSC is connected to the WG transformer, here represented by impedances R_{ti}, L_{ti}, C_{fi}. The collection network impedances are neglected. Here, the transformer impedance is scaled by using per unit quantities to be represented along with the GSC and the PCC.

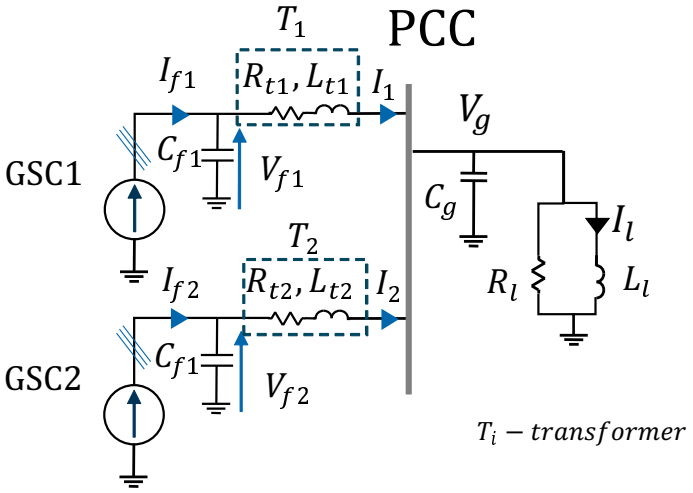

Figure 3.12: Equivalent Circuit of the OWPP in islanded mode

The parameters of the network components are shown in the table 3.1. It is applicable to both islanded and connected mode, except for the load parameters R_l, L_l, which is used only for the analysis of islanded mode. These load resistance and inductance may represent the active and reactive power loads respectively in the islanded offshore network. The dynamic model of the system is developed by using the equations in an arbitrary dq reference frame. Following this, the existing dynamics of the system will be studied by change of input currents of both VSCs. Simulations will also be performed by using a circuit model in MATLAB Simulink, to verify

this model.

Component	Parameter	Value
DR and HVDC link	Total Power Capacity	100 MW
	Base Voltage	66 kV
	DC Voltage	89.13 kV
	Offshore Capacitance C_g	2.5 μF
	Loads (R_l, L_l)	87.12 Ω, 370 mH
	Diode Rectifier Model	6 Pulse
GSCs	Power Capacity (VSC 1, 2)	50 MW, 50 MW
	C_{fi}, R_{ti}, L_{ti} (pu)	0.1, 0.036, 0.006
	Model Type	Controlled AC current source

Table 3.1: Network parameters for the analysis of the OWPP system

Dynamic equations of the system

The dynamic equations are written here to develop the complete model of the islanded OWPP system. It is assumed that an instantaneous synchronization exists for each WG (GSC of each WG) and the dynamic model is written by assuming that all the WGs are synchronized to the grid frequency ω_g. All equations are written in an arbitrary synchronous reference frame (dq frame) rotating at the frequency of ω_g. The notation for time dependency is omitted hereafter for simplicity, when representing the dynamic equations in dq frame.

Applying Kirchoff's current law for the capacitor terminal for GSC 1, gives the following equations in the natural (abc) reference frame.

$$\begin{pmatrix} I_{f1a} \\ I_{f1b} \\ I_{f1c} \end{pmatrix} = \begin{pmatrix} I_{1a} \\ I_{1b} \\ I_{1c} \end{pmatrix} + C_{f1} \cdot \frac{d}{dt} \cdot \begin{pmatrix} V_{f1a} \\ V_{f1b} \\ V_{f1c} \end{pmatrix} \tag{3.26}$$

For the first inverter GSC 1, the dynamic equations for voltage at the filter capacitance bus C_{f1} is derived as follows in an arbitrary dq reference frame, by the application of Park's transformation to the previous equation:

$$\frac{dV_{f1d}}{dt} = \frac{1}{C_{f1}} \left(I_{f1d} + \omega_g C_{f1} V_{f1q} - I_{1d} \right) \tag{3.27}$$

$$\frac{dV_{f1q}}{dt} = \frac{1}{C_{f1}} \left(I_{f1q} - \omega_g C_{f1} V_{f1d} - I_{1q} \right) \tag{3.28}$$

Just a change of notations or rather the suffixes gives directly the dynamic equations for the filter bus voltage V_{f2} for the second inverter GSC 2:

$$\frac{dV_{f2q}}{dt} = \frac{1}{C_{f2}}\left(I_{f2d} + C_{f2}\omega_g V_{f2q} - I_{2d}\right) \tag{3.29}$$

$$\frac{dV_{f2q}}{dt} = \frac{1}{C_{f2}}\left(I_{f2q} - C_{f2}\omega_g V_{f2d} - I_{2q}\right) \tag{3.30}$$

Applying Kirchoff's voltage law for the equivalent circuit between the GSC1 and PCC, the following equations are obtained:

$$\begin{pmatrix} V_{f1a}(t) \\ V_{f1b}(t) \\ V_{f1c}(t) \end{pmatrix} = R_{t1}. \begin{pmatrix} I_{1a}(t) \\ I_{1b}(t) \\ I_{1c}(t) \end{pmatrix} + L_{t1}.\frac{d}{dt}\cdot \begin{pmatrix} i_{1a}(t) \\ i_{1b}(t) \\ i_{1c}(t) \end{pmatrix} + \begin{pmatrix} V_{ga}(t) \\ V_{gb}(t) \\ V_{gc}(t) \end{pmatrix} \tag{3.31}$$

Thus dynamic equations for the current injected by the GSC 1 into the PCC through the *RL* filter are thus written in *dq* frame as follows:

$$\frac{dI_{1d}}{dt} = \frac{1}{L_{t1}}V_{f1d} - \frac{R_{t1}}{L_{t1}}I_{1d} + \omega_g I_{1q} - \frac{1}{L_{t1}}V_{gd} \tag{3.32}$$

$$\frac{dI_{1q}}{dt} = \frac{1}{L_{t1}}V_{f1q} - \frac{R_{t1}}{L_{t1}}I_{1q} - \omega_g I_{1d} - \frac{1}{L_{t1}}V_{gq} \tag{3.33}$$

For the GSC 2, the dynamic equations for the current injected into the PCC bus are directly written as follows:

$$\frac{dI_{2d}}{dt} = \frac{1}{L_{t2}}V_{f2d} - \frac{R_{t2}}{L_{t2}}I_{2d} + \omega_g I_{2q} - \frac{1}{L_{t2}}V_{gd} \tag{3.34}$$

$$\frac{dI_{2q}}{dt} = \frac{1}{L_{t2}}V_{f2q} - \frac{R_{t2}}{L_{t2}}I_{2q} - \omega_g I_{2d} - \frac{1}{L_{t2}}V_{gq} \tag{3.35}$$

Now, by applying Kirchoff's current law, the following equations for the PCC bus are written:

$$\begin{pmatrix} i_{1a}(t) \\ i_{1b}(t) \\ i_{1c}(t) \end{pmatrix} + \begin{pmatrix} i_{2a}(t) \\ i_{2b}(t) \\ i_{2c}(t) \end{pmatrix} = \begin{pmatrix} i_{la}(t) \\ i_{lb}(t) \\ i_{lc}(t) \end{pmatrix} + C_g \cdot \frac{d}{dt}\cdot \begin{pmatrix} V_{ga}(t) \\ V_{gb}(t) \\ V_{gc}(t) \end{pmatrix} + \frac{1}{R_l}\cdot \begin{pmatrix} V_{ga}(t) \\ V_{gb}(t) \\ V_{gc}(t) \end{pmatrix} \tag{3.36}$$

Applying the Park's transformation, as before, gives the voltage dynamics for the PCC voltage V_g:

$$\frac{dV_{gd}}{dt} = -\frac{V_{gd}}{C_g R_l} + \omega_g V_{gq} - \frac{I_{ld}}{C_g} + \frac{I_{1d}}{C_g} + \frac{I_{2d}}{C_g} \tag{3.37}$$

$$\frac{dV_{gq}}{dt} = -\frac{V_{gq}}{C_g R_l} - \omega_g V_{gd} - \frac{I_{lq}}{C_g} + \frac{I_{1q}}{C_g} + \frac{I_{2q}}{C_g} \tag{3.38}$$

By applying Kirchoff's voltage law for the voltage loop between the PCC and load, the following equation is obtained:

$$\begin{pmatrix} V_{ga}(t) \\ V_{gb}(t) \\ V_{gc}(t) \end{pmatrix} = L_l . \frac{d}{dt} \cdot \begin{pmatrix} I_{la}(t) \\ I_{lb}(t) \\ I_{lc}(t) \end{pmatrix} \tag{3.39}$$

Now the equations involving the load current dynamics at the PCC can be written in dq frame by applying Park's transformation to the above equation:

$$\frac{dI_{ld}}{dt} = \omega_g I_{lq} + \frac{V_{gd}}{L_l} \tag{3.40}$$

$$\frac{dI_{lq}}{dt} = -\omega_g I_{ld} + \frac{v_{gq}}{L_l} \tag{3.41}$$

Analysis of the dynamics through simulations

Step changes in the d and q axis components of the GSC 2 are applied to observe the changes. The results are plotted for both the dynamic model (non-linear) and also the circuit simulated by using MATLAB Simulink. It is worth recalling that all the GSCs are assumed to be synchronized to a common grid frequency ω_g. The results are shown in the Figure 3.13

In the arbitrary dq frame chosen, the d and q axis currents of the GSC 2 are varied each by 0.05 pu or 5% of the system base current value. The variations of the offshore network parameters are observed. At t = 0.25s the d-axis input current of the GSC 2 is varied and at t = 0.75 s the q–axis current of the same is varied.

It can be seen that for the increase of d-axis current by 5% of rated capacity of GSC 2, the PCC voltage increases by around 10%, as seen in the Figure 3.13(d). Indeed the terminal voltages of both the GSCs increase, as seen in the Figures 3.13(e) and (f). There is a small variation in the frequency as well, for the islanded network, around 2.1% to be precise.

Next, there is an increase of q-axis current by 5% of rated capacity of GSC 2 (or 0.025 pu for base current of the entire system). Now, stark behaviors are observed. The RMS AC voltage at the PCC and also the terminal voltages at the GSCs do not vary significantly and the variations are rather negligible. On the other hand the frequency of the network varies much more than the previous case. The variation in the input q-axis current results in a change of around 4.6%, more than twice, the variation for change in the input d-axis current.

As pointed out in [72], which has studied a similar system, there is a strong coupling between the d-axis current of the inverters and the AC voltage of the system. It is also observed in the results that the variation of the q-axis input current almost has a negligible impact on the system voltage. While for the frequency, the variation is twice higher for a change in the q-axis current than for the change in the d–axis current.

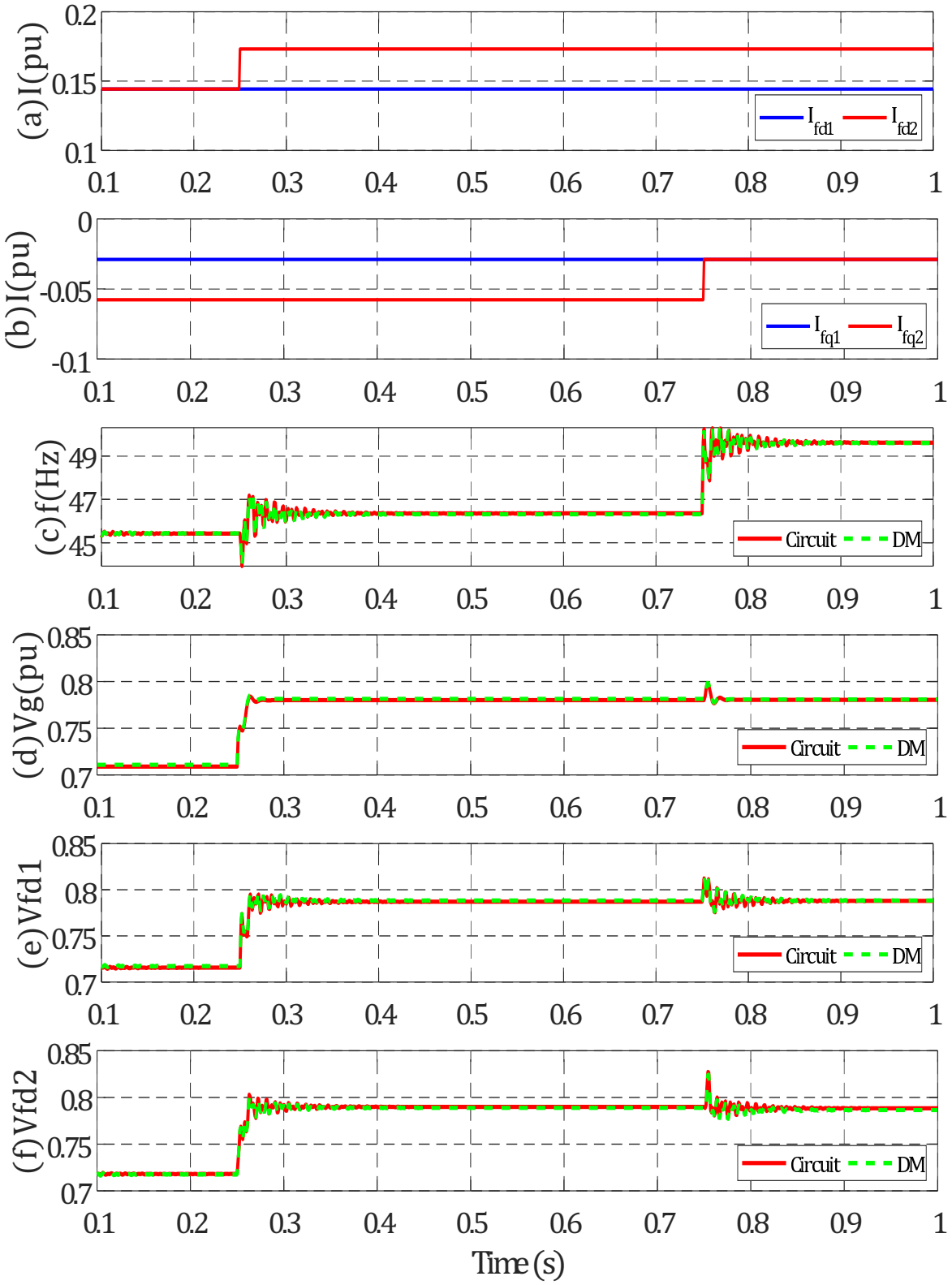

Figure 3.13: OWPP Island Network Analysis: Comparison of dynamic model and circuit models | (a)Input d-axis currents of GSCs (b) Input q-axis currents of the GSCs (c) Grid frequency (d)RMS AC voltage at the PCC (e) AC voltage component V_{fd1} for GSC 1(f) AC Voltage component V_{fd2} for GSC 2

It is worth mentioning that both the GSCs have their filter voltages along the arbitrary $d-q$ frame, i.e. $V_{fiq} = 0$ at their respective capacitance terminal. This leads to the decoupling of active and reactive power equations as follows:

$$P_{fi} = \frac{3}{2} V_{fid} I_{fid} \tag{3.42}$$

$$Q_{fi} = -\frac{3}{2} V_{fid} I_{fiq} \tag{3.43}$$

A change in the d-axis input current implies a change in the overall active power balance, which leads to a change in the AC voltage in the system. This shows the existence of a $P-V$ coupling. Also, the change in the q-axis current implies a change in the reactive power injection / balance in the network, which resulted in a strong change in the system frequency. This shows the existence of a $Q-f$ coupling. This has also been the conclusion of the analysis in [72] and specifically for DR-OWPP system in [59] and [54].

Analysis and Conclusion

The dynamic model for the islanded OWPP has been compared with the circuit simulation. The RL load is not mandatory and is used to represent central or aggregated load of the offshore system in islanded mode. The following observations can be made:

1. Thus coupling between the active power balance in the network and the AC voltage is confirmed.
2. Although it is obvious, the d-axis current injection by a GSC causes a prominent change in its local filter bus voltage and in–turn the PCC voltage as well. The increase of voltage at one terminal also causes a change in the AC voltage at the terminal of the second GSC.
3. The coupling between the reactive power balance and the frequency is also seen, although there is a weak coupling between the active power balance and frequency. This occurs because of the variations in the load currents. In other words, a change in the q-axis current injection by the GSC can effect a change in the system frequency, but has a negligible impact on the system voltage.
4. As pointed out in [72] [54], it is seen that the $P-V$ & $Q-f$ dynamics exist in the islanded offshore network. This is in stark contrast to the traditional droop relationships observed widely in power systems, with rotating machines and dominant inductive impedances, where the active power and frequency ($P-f$) are coupled and so are the reactive power and voltage ($Q-V$). Moreover, offshore power system dynamics is deemed different from the $P-V$ and $Q-f$ coupling found in the low voltage microgrids / power systems [73] where the cause for the opposite droop relationships is the resistive line impedance.

3.3.2 Analysis of the Normal Mode of Operation

The connected mode or normal mode of operation is the mode when the DR is conducting and the active power is transmitted through the HVDC link. The WGs are producing enough power and the PCC voltage is at a sufficient level to keep the DR in continuous conduction mode (as illustrated in the section 2.7.2, chapter 2).

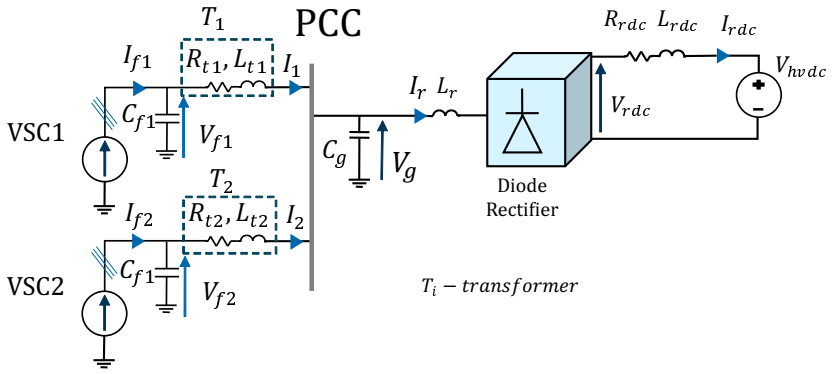

Figure 3.14: Equivalent Circuit of the OWPP in Normal Operating Mode

The model used for the islanded network, i.e. the GSCs with LC filters, is retained. The offshore load model is indeed, excluded. The network used for analyzing the normal mode of operation is shown in the Figure 3.14. The HVDC link is simplified by using an ideal voltage source (V_{hvdc}), assuming a good control of the DC voltage by the onshore VSC. The offshore filter is not modeled as well. A simple inductance (L_r) is used to connect the offshore PCC capacitance to the DR, which is usually representing a transformer connecting to the DR with high pulse number configuration. Any resistive losses for this inductance L_r is neglected. The DR is connected to the HVDC voltage source by using a reactor L_{rdc} with losses (reprented by R_{rdc}).

The DR is assumed to operate in the continuous conduction mode and especially in the Continuous Conduction Model 1 (CCM 1, as described in the section 2.7.2 of chapter 2). It is in this mode that the model and dynamic equations for the DR and the DC side are valid.

Dynamic Model of OWPP in the Connected Mode

The dynamic equations for the GSCs connected to the PCC have already been defined in the section 3.3.1. In addition to this, it is only required to recall the model for the DR, the connection to the DC link. The dynamic average value model for the DR connected to the DC link through a reactor as defined in [51] is presented below. The equation of the DC voltage is recalled from the subsection 3.2.6, but written specifically for a six pulse bridge, without any transformer.

$$V_{rdc} = \frac{3\sqrt{6}}{\pi} V_{grms} - \frac{3}{\pi} \omega_g L_r I_{rdc} \tag{3.44}$$

The RMS value of the voltage at PCC is written in terms of the d and q axis voltages.

$$V_{grms} = \frac{1}{\sqrt{2}} \sqrt{V_{gd}^2 + V_{gq}^2} \tag{3.45}$$

The dynamics of the DC current in the HVDC link, at the output of the DR has already been defined and recalled here:

$$\frac{dI_{rdc}}{dt} = \frac{\frac{3\sqrt{6}}{\pi} V_{grms} - \frac{3}{\pi} \omega_g L_r I_{rdc} - R_{rdc} I_{rdc} - V_{hvdc}}{2L_r + L_{rdc}} \tag{3.46}$$

The value of the commutation angle is useful in expressing dq axis input currents (I_{rdq}) at the DR terminal and also the reactive power consumption by the DR and the AC input inductance.

$$\mu = \cos^{-1}\left(1 - \frac{\sqrt{2}\omega_g L_r I_{rdc}}{\sqrt{3} V_{grms}}\right) \tag{3.47}$$

The effect of commutation of the DR has been added as a virtual impedance at the DC side of the DR, as illustrated in the Figure 3.9. The expressions for input AC currents at the DR terminal (I_{rdq}) have been written by using the DC current and other quantities. The expressions are derived by averaging the AC current values over both the conduction and commutation cycles, for one sixth of the total AC cycle (corresponding to 60°phase angle) [51] and expressed in a condensed form:

$$I_{rd} = \frac{2\sqrt{3}}{\pi} I_{rdc} * \cos(\mu) - \frac{3\sqrt{2} * V_{gd}}{\pi \omega_g L_r} (\cos(\mu) - 1) + \frac{3\sqrt{2} * V_{gd}}{4\pi \omega_g L_r} (\cos(2\mu) - 1) \tag{3.48}$$

$$I_{rq} = -\frac{2\sqrt{3}}{\pi} I_{rdc} \sin\mu + \frac{3\sqrt{2} * V_{gd}}{\pi \omega_g L_r} \sin(\mu) - \frac{3\sqrt{2} * V_{gd}}{4\pi \omega_g L_r} (\sin(2\mu) + 2\mu) \tag{3.49}$$

The dynamic equation related to the offshore PCC voltage are rewritten for this network, omitting the time dependence notation (t):

$$\frac{dV_{gd}}{dt} = \omega_g V_{gq} - \frac{1}{C_g} I_{rd} + \frac{1}{C_g} I_{1d} + \frac{1}{C_g} I_{2d} \tag{3.50}$$

$$\frac{dV_{gq}}{dt} = -\omega_g V_{gd} - \frac{1}{C_g} I_{rq} + \frac{I_{1q}}{C_g} + \frac{I_{2q}}{C_g} \tag{3.51}$$

Comparison of the dynamic model and Circuit Simulation

As done before for the study of the islanded mode, a circuit simulation is used for the comparison with the dynamic model and analyze the dynamics in the system. The network parameters are shown in the table 3.1 and the simulation is done in the MATLAB Simulink environment. The losses of the DR used in the circuit simulation, are considered to be negligible. The focus is to study the dynamics due to the variation in the injected currents.

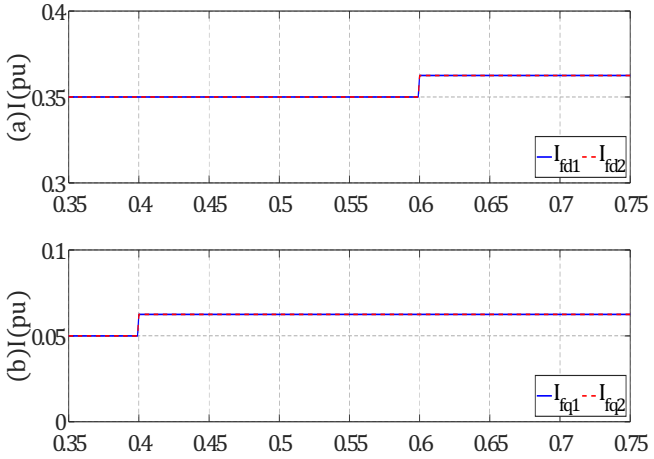

Figure 3.15: Analysis of OWPP Connected Mode: dq currents injected by the GSCs

The dq currents of GSCs 1 and 2 are both varied as shown in the Figure 3.15. A 2.5% variation in input currents is done for both the GSCs, first at $t = 0.4s$ for q–axis current and then, at $t = 6s$ for the d–axis currents. This corresponds to a total variation of 5% for the total input currents by the GSCs.

The circuit simulation revealed the presence of AC voltage and current harmonics (of orders $5, 7, 11, 13...$), due to the operation of the six pulse DR . Thus low pass filters were used for measuring the various electrical quantities which have been plotted in the Figure 3.16. The proposed dynamic model of the system is however valid only for the first order of the frequency component.

The increase of q-axis current at t=0.4s, causes a change in the frequency of the system. The frequency variation is around 9% for a 5% total variation in the input currents. Although there is a small change observed in the RMS voltage at the PCC, as well as the active power.

The increase of the d–axis input currents causes a change in both the voltage at the PCC and the system frequency. Although what is interesting to observe is the consequence: the increase of active power flow, roughly a 4.8% increase as shown in the Figure 3.16(a). There is also a sharp increase in the DC current as seen in the Figure 3.16(f). At the same time, as seen in the Figure 3.16(c), the variation of the frequency is not as prominent, around 6% for the change in the input d-axis current.

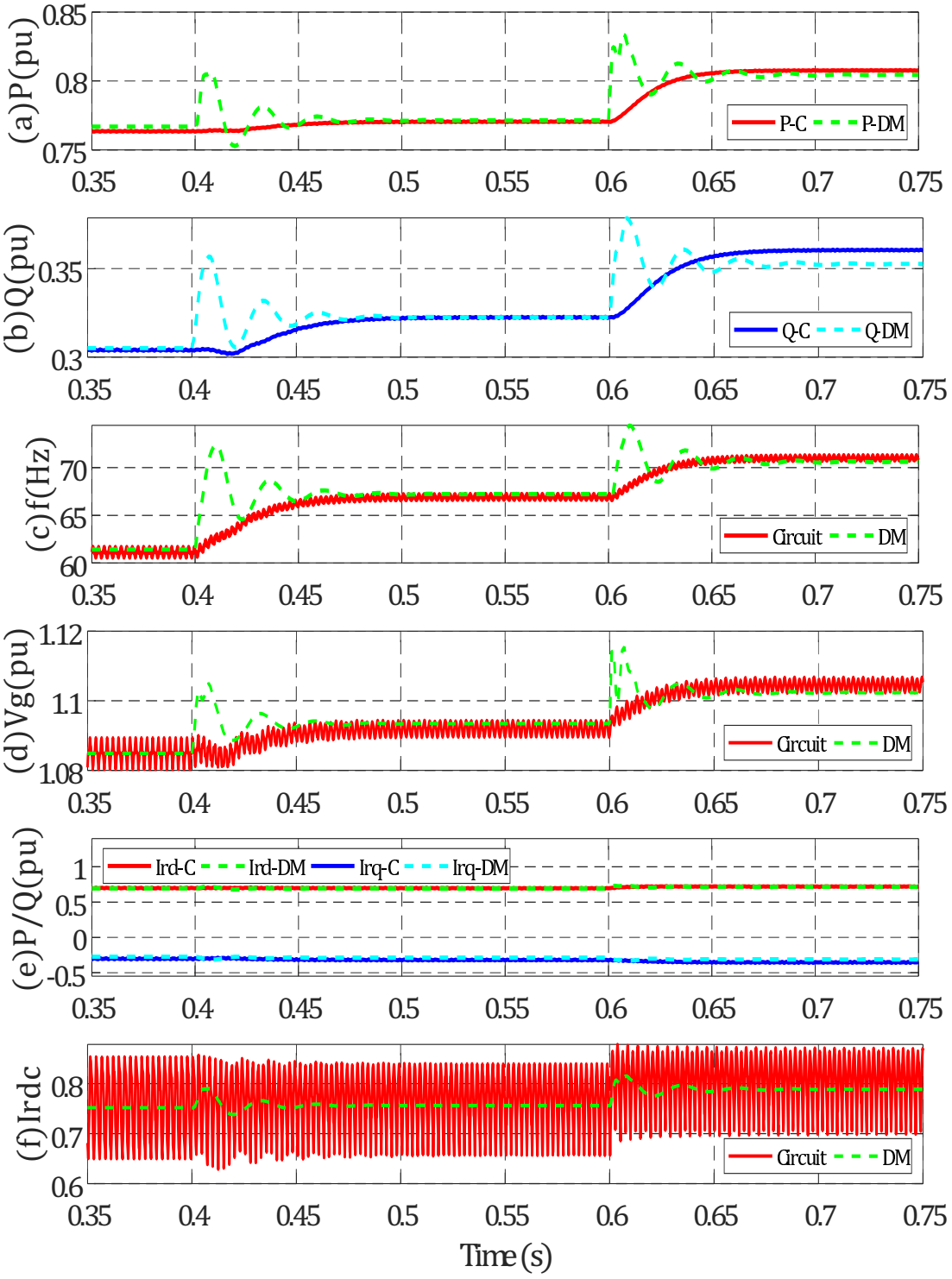

Figure 3.16: Analysis of OWPP Normal Operation: Comparison of Dynamic Model and Circuit Simulation | (a) Active power at the PCC terminal (b) Reactive power at the PCC terminal (c) Grid frequency (d) RMS AC voltage at the PCC (e) dq axis currents at the PCC (f) DC current I_{rdc}

Analysis and Conclusions

The analysis of the OWPP model and DR in the connected mode of operation is done in this section. Comparison with the behavior of the system in islanded mode also gives a general perspective. First up is the change of the PCC voltage for the increase in the d-axis current in islanded and connected mode of operation. This can be analyzed using the following expression in the steady state operation after the DR conduction (continuous conduction mode) begins. The static expression for the HVDC voltage is written from the equation 3.46, as follows:

$$\frac{3\sqrt{6}}{\pi}V_{grms} - \frac{3}{\pi}\omega_g L_r I_{rdc} - R_{rdc}I_{rdc} = V_{hvdc} \tag{3.52}$$

Since in the normal operation mode, the PCC voltage is clamped to the HVDC voltage, because of the DR conduction, the PCC voltage has the following expression [59]:

$$V_{grms} = \frac{\pi}{3\sqrt{6}}V_{hvdc} + \left(\frac{1}{\sqrt{6}}\omega_g L_r + \frac{\pi}{3\sqrt{6}}R_{rdc}\right) * I_{rdc} \tag{3.53}$$

From this, it is clear that there is a contribution of both the frequency and the dc current. In the offshore power system, the operation at or close to a certain value of frequency is desirable. This leaves - the DC current injected into the DC link as the only factor influencing the offshore PCC voltage. Thus if the operating frequency of the grid is relatively constant, (assuming a control scheme to ensure its regulation) the coupling between the active power and the AC voltage in the OWPP system is ensured by this expression. This observation is in line with the analysis presented in [59] [62], some of the relevant works related to DR-HVDC OWPP.

The islanded and connected modes of operation, including the transition between the modes, rely on the value of the PCC voltage. While in islanded mode, the voltage regulation is rather a mandatory requirement, in connected mode, the AC voltage is ensured by the minimum power availability, once the AC voltage is increased to 1 pu (or slightly above). Due to the $P-V$, coupling, the transition to the connected mode is ensured by the availability of active power, setting up the AC voltage (and compensating all the losses in the offshore network).

But in the connected mode, provided sufficient wind power production (relatively higher than the active power loads and losses in the system), the AC voltage is determined by the HVDC link voltage. Slight variations are a consequence of higher active power injection (as seen by comparing the figures 3.16 (a) and (d). This is valid as long as the frequency is regulated to a relatively constant value, as is the case with the control solutions proposed today.

Recalling the equation 3.54 again, the variation in the offshore PCC voltage occurs as a result of the frequency variation, due to the increase in the q-axis current injection. According to this expression, the frequency component can also effect a slight change in the offshore voltage, as observed. The terminal voltages of the WGs have to increase because of the above said constraint of the offshore network. Since the dq input currents are controlled, naturally

the output d-axis voltages of each GSCs increase, thus they provide a higher active power, maintaining the P–V balance, eventhough the cause was a change in the frequency.

In a real environment, the WG's objective is usually power control according to MPPT or other algorithms. Thus changes in the frequency cannot cause change in the output power but will only result in a decrease of overall d–axis current injection by the WG (by means of a closed loop control) to maintain the same power reference, for the increase in the AC voltage. This is because of the assumption that the $V_{fiq} = 0$ as a result of synchronization. The active power injections are of the form:

$$P_1 = \frac{3}{2}.V_{f1d}I_{f1d};\ \ P_2 = \frac{3}{2}.V_{f2d}I_{f2d} \tag{3.54}$$

To conclude, the active power balance or reference power production for a WG is maintained by the regulation of its d–axis current. Slight changes in frequency is a consequence as well, so is the change in the AC Voltage across the network, because it is dictated by the PCC voltage depending on HVDC voltage and power injection (or dc current).

Grid Frequency

Generally by considering just the offshore system in islanded mode, the capacitive impedance is the dominant source of reactive power injected, due to the submarine cables in the collection network. But in the connected mode, the reactive power requirement for the offshore inductance and DR operation is crucial and it increases with the increase in power injection (or rather current through the DR). The expression of reactive power as a function of active power is recalled here (assuming negligible power losses in the DR) [70].

$$Q_{ac} = -P_{rdc}\frac{(2\mu - \sin(2\mu))}{(1-\cos(2\mu))} \tag{3.55}$$

A quick calculation is done by using the limits of power production, assuming constant frequency during operation, using the above expression for per unit quantities. For the AC voltage variation between 1 pu and 1.2 pu, the offshore reactive load varies between 0.115 pu for 10% active power production to 0.381 pu for 100% power production. The reactive power in the offshore network has to be compensated by the WG current injection. And the reactive power balance is ensured by the injection of q-axis current at the GSC terminal, since the injection of d–axis current is used to set the active power reference, as elaborated previously. If the WGs try to control rigidly the output reactive power, due to the absence of a slack bus (like the offshore VSC in the case of the VSC–HVDC OWPP), the required reactive power is not compensated. This could lead to reactive power circulation and possible instabilities in cases of insufficient reactive power. This said, there is a coupling between frequency and reactive power coupling, as observed in the network simulation and also concluded by related research works.

3.3.3 Control Requirements for the Offshore Network

It is important to understand the control requirements for the OWPP from the power system perspective. The requirements are laid out for islanded mode and connected mode of operations separately, but have to be considered together, while designing the control of WGs. It is also recalled that the WG inverters themselves are to be used for the black start, islanded mode and connected mode of operations. No additional equipment, like the AC uambilical is used initially for the black start or the islanding operation.

The WGs may contain additional equipment, like local storage, designed for backup as well as black start purposes. This aspect is entirely another topic of discussion and dealt in detail in chapter 5. But here, for the purpose of devising the control for the OWPP, the following assumptions are made:

i. It is assumed that the WGs have a black start capability (energy source and control strategy) and they are readily available for the grid forming of the offshore network.
ii. Enough wind power is assumed during the activation of the grid forming control.
iii. The WGs are equipped with sufficient capability to ensure de-rated power production, with negligible impacts of the mechanical drive train and on the offshore system dynamics.
iv. the DC voltage of the back to back converter system in each WG is regulated with sufficient performance by the Machine Side Converter (MSC).

For the islanded mode, the OWPP system has the following control requirements

i. regulation of AC voltage of the offshore system and the frequency. Since the level of voltage determines the operation zone of the OWPP, sufficient voltage regulation performance is crucial.
ii. The local offshore active power losses and other loads have to be supplied by the WGs. This includes resistive components of collection network, transformers and any auxiliary loads. The loads are supposed to be proportionally shared, to avoid any one or few WGs attempting to compensate most or all of the loads. In this case the GSC control will indirectly load its respective wind turbine to compensate the active power requirement. For this purpose, the MPPT cannot be done by the WGs, at least throughout the islanded mode, as the active power loads are quite low.
iii. The reactive power load of the system – due to the collection network impedances, transformers etc., have to be shared proportionally by the WGs.
iv. Synchronous operation of WGs –There is a need to ensure that each GSC maintains its dq reference frame along the capacitive filter (C_{fi}) bus voltage. i.e. $V_{fiq} = 0$, for each GSC. This ensures that all WGs are synchronized to the same reference frame in dq, at their terminals.

For connected or normal mode of operation, most of the control requirements from the is-

landed mode remain:

i. The AC voltage control function becomes irrelevant in this mode, because of the DR conduction. Thus there is no need for a specific voltage control function for the WGs.
ii. The minimum AC voltage to ensure DR conduction, is guaranteed by sufficient wind power production (sufficiently more than the losses and offshore loads, let's say 10% of the rated capacity). Thus the important control objective is MPPT or power control of WGs by their respective GSCs.
iii. As in islanded mode, the frequency has to be regulated and synchronization among WGs has to be ensured.
iv. Indeed the reactive power load, which varies according to the power production, has to be compensated by the WGs and possibly by use of passive filters at the offshore terminal.

The developed grid forming strategy for the control of the OWPP is not presented here due to confidentiality reasons.

3.4 Conclusion and Future Scope

3.4.1 Chapter Summary

This chapter began with the aim to study the offshore wind power system dynamics and propose a grid forming control scheme following the detailed analysis. With regards to this, the offshore system dynamics were studied for islanded and connected modes of operation separately. For the islanded mode, the dynamic coupling between the $P-V$ and $Q-f$ was shown, as described in the literature and also concluded by many research works related to the offshore wind power system. For the connected mode, after a detailed analysis, the same coupling is found to be valid. The value of AC voltage at the WG terminal and in-turn the PCC is an important criteria to ensure a stable operation in one mode or the other. So is the synchronization between WGs to maintain a common grid frequency. Thus, based on the analysis and also the available literature, the control requirements were laid out. Following this, a grid forming control scheme has been proposed for the GSCs.

3.4.2 Future Scope for the Grid Forming using WGs

The control scheme validity can be supported by detailed stability studies for real issues and transients in the offshore wind power systems. Also, such analysis of the system can shed light on possible resonances between the control schemes and the offshore system components, as an extension of studies about the resonances of control scheme with the HVDC cable presented in [74].

The real time implementation and analysis of the grid forming control for WGs, or any grid forming control scheme for that matter is indeed not commonly observed in the literature (exceptions could be found in the case of microgrids). Future work can be directed towards further analysis and implementation of the grid forming scheme in real time simulation platforms. With the rise of research aimed at advanced control functionalities for the OWPPs, like enabling the black start to the onshore AC grid, such control scheme validations would aid in designing reliable solutions.

4

Grid Forming: Review and Assessment of Solutions

Contents

4.1 Introduction 80
4.2 Review and Comparison 80
4.3 Simulation Results and Assessment of Solutions 93
4.4 Analysis and Discussion 101
4.5 Conclusion 105

4.1 Introduction

In section 2.8.2 of chapter 2, the various solutions for grid forming were briefly mentioned and have been classified according to the level of modification of the conventional WG control scheme. Chapter 3 dealt with the dynamic modelling and analysis of the offshore wind power system with a DR-HVDC transmission.

In this chapter, the various grid forming and power management solutions are reviewed in detail in the section 4.2. A theoretical comparison is done between them to highlight how each approach is either similar or different or an evolution of another solution. This is done without dwelling into the comparison of costs or resources to implement these solutions, i.e. it is a comparison of technical aspects.

Following the theoretical comparison, some of the approaches deemed quite distinct from each other, are analyzed in detail by using a study case network. The Electromagnetic Transient (EMT) simulation studies in MATLAB Simulink® attempt at backing up the theoretical comparison and also highlight specific features and drawbacks of each solution. The goal has been to establish a thorough knowledge of the existing grid forming approaches, establish a detailed understanding of the different approaches by using the assessment and to help in future control innovation or enhancements.

4.2 Review and Comparison of Grid Forming Solutions

4.2.1 Background

As described in detail in the section 2.7.4 of chapter 2, the DR-HVDC OWPP has distinct operation characteristics that dictate the control solution to a large extent. Moreover, there exist distinct control requirements for both the islanded and the connected modes. Thus, a grid forming control has been designed, in chapter 3, with the analysis of the operation modes and constraints posed by the Offshore AC network and the DR characteristics.

In this section some of the prominent grid forming and power management control schemes are reviewed. Some of the features or criteria for comparison, include but are not limited to, the following:

i. WG control modification.
ii. Additional equipment in OWPP topology.
iii. Requirement of high band width communication.
iv. Black start approach
v. Synchronization approach.
vi. Prolonged Islanding Capability.

The industrial solution [61] is called as the 'advanced network bridge control'. This has not been elaborately discussed in this chapter, partly because the available literature is limited and also because it is a patented grid forming approach [75].

It is worth noting that, certain solutions rely on modification of the OWPP topology by using additional equipment, which are necessary to achieve the control objectives. Others solutions rely on the use of WGs to enable this function, with minimal additional equipment to the existing offshore network. The economic aspect of either the control modifications or the topology modifications are not discussed in detail, as this is not the focus of this research work. The islanding capability during any unforeseen events in the offshore / onshore is an important issue to be addressed by these solutions (or their extensions), as highlighted in [31] [65] [76] for the OWPPs.

4.2.2 Solution 1: Distributed Control of the PCC Voltage and grid Frequency

This was one of the first solutions proposed for the control of DR-HVDC OWPP topology. This solution [54][59] was initially proposed with LCC based HVDC converter onshore and it was an extension of the approach presented in [77]. A later work showed a successful implementation by using a VSC HVDC converter model onshore [71]. The approach argues, that instead of extending any of the available grid control solutions from the Microgrid literature, the grid forming solution has to be derived for the considered offshore network, as the network characteristics are well known [54]. A $P-V$ and $Q-\omega$ droop based control with enhancements to share the reactive power load and improve the accuracy of the voltage and power control by WGs, has been presented in [78].

As revealed in chapter 3, the work points out that the presence of strong capacitive compensation in the network, can lead to a strong coupling between the grid voltage and active power and between grid frequency and reactive power. This is in stark contrast to the classical droop scheme that is used to control inverter based Microgrids with inductive filters [79]. Such classical scheme is based on $P-\omega$ and $Q-V$ based droop relationships, for grid forming VSCs.

Being one of the first to take up the DR-HVDC topology grid forming problem, many simplifications or assumptions were made for the analysis and conception of this control solution. Some of the major ones are listed below:

- The collection network impedance has been neglected for simplicity.
- The WGs are assumed to have a self start capability and help in the black start of the offshore network.
- Shunt impedances of transformers are negligible.
- The WG converter losses are negligible.

The significant change to enable the grid forming capability to the GSC, is by providing the

dc voltage control function to the MSC. The conception of the DC voltage control scheme by this solution 1, is elaborated in the appendix C for clarity. Henceforth, the grid forming control approach of the solution 1 is discussed.

Grid Forming Control Scheme

The synthesis of the grid forming control is elaborated by using the dynamic equations for the aggregated string models of the offshore wind power system. Consider the model shown in the Figure 4.1. Here multiple WGs in a string, are aggregated into a single model and 'J' strings are connected to the PCC. As mentioned before, the collection network cable impedances are neglected [77].

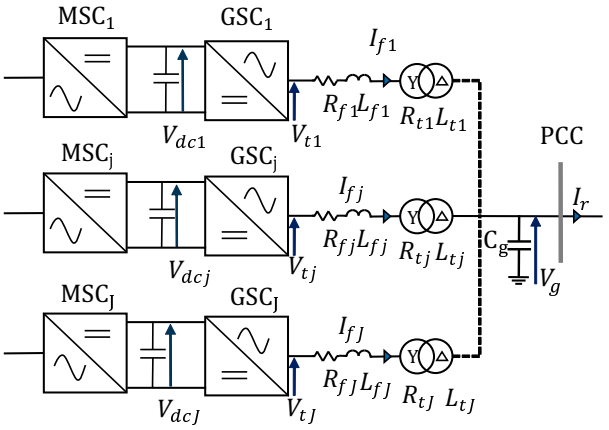

Figure 4.1: Aggregated model of multiple strings connected to the offshore PCC

An important point to note here is that the WGs do not have a capacitor filter at their output terminal. The WGs use only an RL filter at their output, for connecting with the offshore AC grid. The capacitance terminal C_g is located at the PCC and the voltage at this terminal 'V_g'will be regulated by all the WGs. All the dynamic equations are developed by considering that the synchronous reference frame (dq frame) is rotating with a frequency of ω_g and oriented along the capacitance bus voltage V_g, i.e., the q component of the capacitance voltage is null ($V_{gq} = 0$). The dynamic equations for the generalized current term I_{fj}, for any string 'j', neglecting notations for time dependency, are given by:

$$\frac{dI_{fdj}}{dt} = \frac{V_{tdj}}{L_{fj}} - \frac{R_{fj}}{L_{fj}} I_{fdj} + \omega_g I_{fqj} - \frac{V_{gd}}{L_{fj}} \tag{4.1}$$

$$\frac{dI_{fqj}}{dt} = \frac{V_{tqj}}{L_{fj}} - \frac{R_{fj}}{L_{fj}} I_{fqj} - \omega_g I_{fdj} \tag{4.2}$$

The voltage dynamics at the offshore capacitance bus result in the following eqauations. Here, the AC voltage value at the PCC is dependent on the d-axis current and the frequency

is dependent on the q-axis currents injected by the WGs. The overall control scheme for one such aggregated WG is shown in the Figure 4.2.

$$\frac{dV_{gd}}{dt} = \frac{1}{C_g}\sum_{j=1}^{J} I_{fdj} - \frac{1}{C_g} I_{rd} \tag{4.3}$$

$$\omega_g V_{gd} = \frac{1}{C_g}\sum_{j=1}^{J} I_{fqj} - \frac{1}{C_g} I_{rq} \tag{4.4}$$

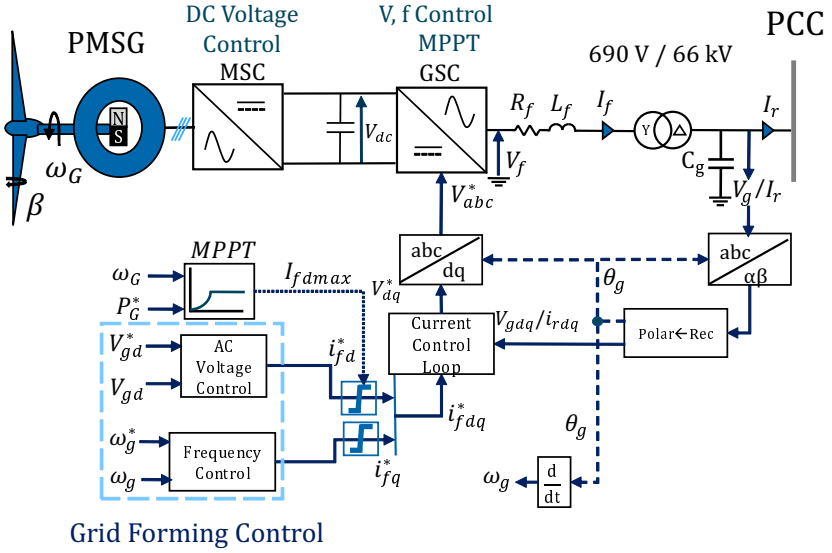

Figure 4.2: Voltage and frequency control for a single aggregated GSC connected to the PCC

With the above equations, a distributed control droop control scheme for PCC voltage and frequency is proposed, where the system frequency and PCC voltage are regulated by all the WGs. This type of control is a direct extension of the control scheme presented in [72] for islanded microgrids, with current controlled VSCs and a prominent capacitance bank at the PCC. In order to share the grid forming control, a droop parameter k_{gj} is used and distributed equally for all the WGs, such that:

$$k_{gj} = \frac{\text{Rated power of the generator } j}{\text{Total power capacity of OWPP}} \tag{4.5}$$

$$\sum_{j=1}^{J} k_{gj} = 1 \tag{4.6}$$

The error in AC voltage is eliminated by using a single centralized integrator, that feeds all the distributed proportional voltage controllers. These two control schemes are shown in detail in the Figure 4.3.

Implementation of Power Control

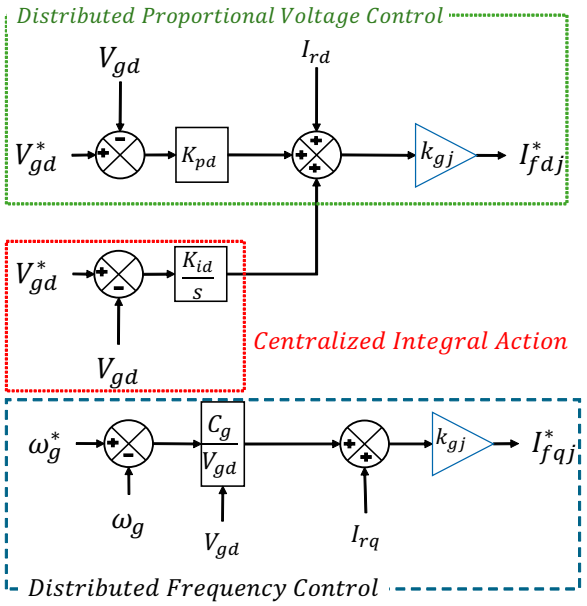

Figure 4.3: Distributed Control of offshore PCC voltage and frequency

During the islanded mode, the power control is rather indirect, i.e. the WG is loaded indirectly by the GSC to maintain the desired AC voltage value in the offshore grid and also controls the AC voltage to reach connected mode (i.e. after DR conduction). Thus, the distributed proportional action for voltage control ensures that the active power load in the offshore network (for instance the losses in the transformers in this network) is shared by the WGs.

The implementation of the MPPT is done by directly overriding the output of the voltage controller during DR conduction mode of operation. After the DR conduction, the voltage control loop saturates (in the Figure 4.2), providing a value of d-axis current I_{fd}^* greater than 1 pu. This is because, the PCC voltage during the normal system operation / DR conduction, is clamped to the HVDC voltage. Any arbitrary reference greater than the actual AC voltage (clamped to HVDC voltage), implies that the error in voltage continuously increases and the integral part of the controller saturates.

Thus, the voltage control loop action is rather irrelevant, once normal mode of operation for the OWPP is reached. The dynamic upper limit for I_{fd} indicated as I_{fdmax} sets the power to be drawn from the wind turbine (see Figure 4.3). This I_{fdmax} is set dynamically in accordance with the MPPT curve, implemented for instance by using a look-up table.

The control implementation is such that, if the power production is not high enough for transmission (low wind speeds and power not sufficient to even supply the offshore auxiliary load), the offshore network AC voltage reference can be decreased to maintain a prolonged islanded mode, subject to the presence of wind power. In the absence of any wind power, prolonged islanded mode is difficult to maintain. This solution only relies on the wind power for the OWPP operation and control. The absence of wind power and the loss of backup power

implies that the WGs may no longer stay in operation and lose communication with the OWPP operator.

4.2.3 Solution 2: Fixref with an MVAC Umbilical Cable

This solution has been proposed initially to interconnect the WGs with the VSC- HVDC topology, stating the possible stability limits of the PLL, for a large OWPP [80]. Naturally it was extended to the DR-HVDC OWPP [81], to provide a black start and grid forming capability to the system.

The major motivation behind the proposal of the solution [81] was to avoid drastic WG converter control changes and to retain as much as possible, the conventional Grid Following control scheme. This solution clearly decouples the grid forming challenge into two parts:

1. The start-up or black start problem, which requires the supply of the WG auxiliaries, the energization of the offshore network equipment. A stable AC voltage source is required for this purpose.
2. Synchronization and frequency control of the offshore grid, without relying on the PLL.

The offshore grid architecture is altered, by introducing a Medium Voltage AC (MVAC) cable from onshore AC grid, connected to the PCC directly, by using an AC/AC power electronic converter as in the Figure 4.4. It supplies the active and reactive power demand for the offshore grid equipment, including the WG auxiliaries.

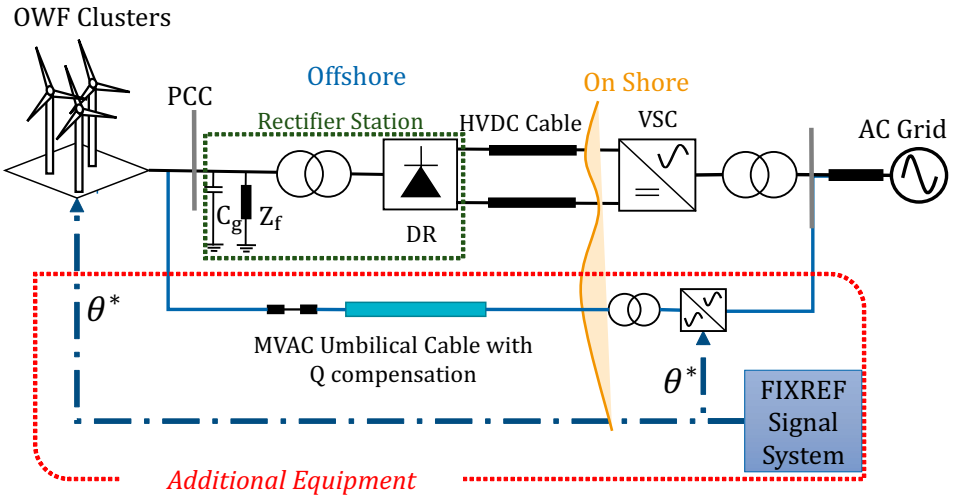

Figure 4.4: DR-HVDC OWPP system with an MVAC cable and FIXREF system

The WGs have to operate with a common AC grid frequency, synchronized to each other during the various operation modes of the OWPP. This requirement is fulfilled by using a fixed reference frame (FIXREF) in dq for the control of all the inverters. The instantaneous values of the phase angle and frequency are transmitted by using a GPS or a radio communication system

to all the GSCs and also to the onshore AC/AC converter. Hence, the frequency regulation and synchronization are made up of an open loop control system, unlike the PLL and thus frequency stability problem is theoretically non existent [81]. Thus the Fixref system along with the black start and voltage support from the umbilical cable, provide the grid forming capability to the offshore system. The overall control scheme for a single WG is shown in the Figure 4.5.

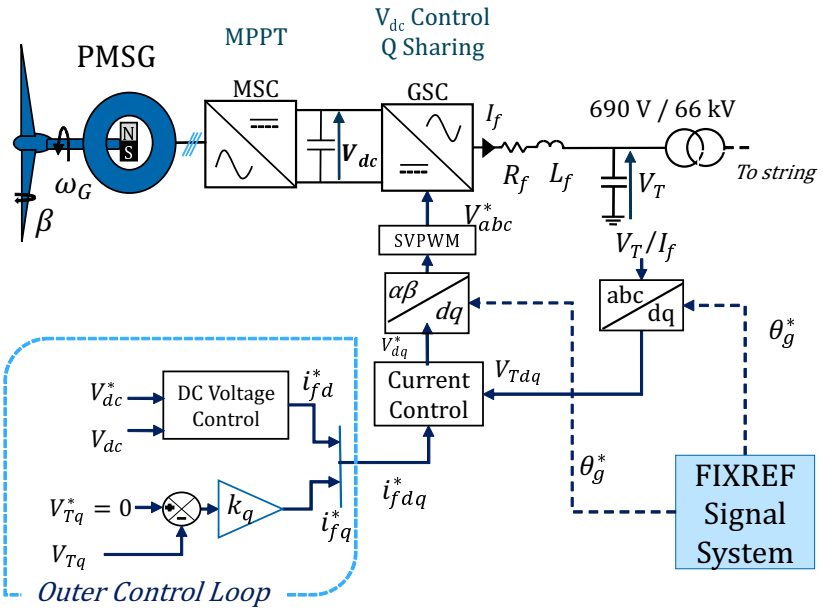

Figure 4.5: Fixref Control scheme for Type 4 WG

Sharing of reactive power

The reactive power sharing among WGs is achieved by using a closed loop control of the q-axis component of the local AC voltage (V_{Tq}). A droop factor k_q is used to share the reactive power production among various WGs. This factor k_q can be adjusted during OWPP operation, to ensure that the WG(s) with the lowest active power injection can participate the most in reactive power compensation (by setting higher k_q) of the offshore collection network and also to prevent overloading the GSCs injecting higher/rated active power (by setting lower k_q). The regulation of V_{Tq} to zero by using the droop factor ensures that V_{Td} is in line with the FIXREF frame d-axis [81]. This synchronized power injection means that unwanted circulation of reactive power would be minimized.

The use of a signal system like GPS along with communication protocols, has been proposed for inverter based microgrids, for power–angle droop control [82]. The same work also points out issues that can occur due to the loss of the communication network. This solution has not discussed the alternative measures for a failure or inaccurate timing signal. But, this solution nearly succeeds in maintaining the grid following scheme while using the MVAC Umbilical

cable for start–up.

4.2.4 Solution 3: Distributed Control of the output Voltage and Frequency with a PLL based synchronization

In [62] a distributed control of voltage and frequency, is proposed. The synchronization among the WGs is facilitated by appropriately setting GSC q–axis current component along with the use of a PLL, to orient the local filter capacitor bus voltage (V_{fd}) along an arbitrary dq reference frame. Notable differences from the solutions 1 and 2 are listed below:

i. This solution is different from that presented in section 4.2.2 [54] in that the control of the terminal voltage of each GSC is done instead of the control of the unique PCC voltage. As a consequence of the distributed AC voltage control actions at each WG terminal, the PCC voltage is built-up, eventually leading to the DR conduction.

ii. It is different from the Fixref Solution [81] (section 4.2.3) because it avoids the use of a GPS signal system, or any high bandwidth communication network. The PLL (commonly available in today's WGs) is used with additional control modifications for the GSC to regulate the frequency and enable the synchronization.

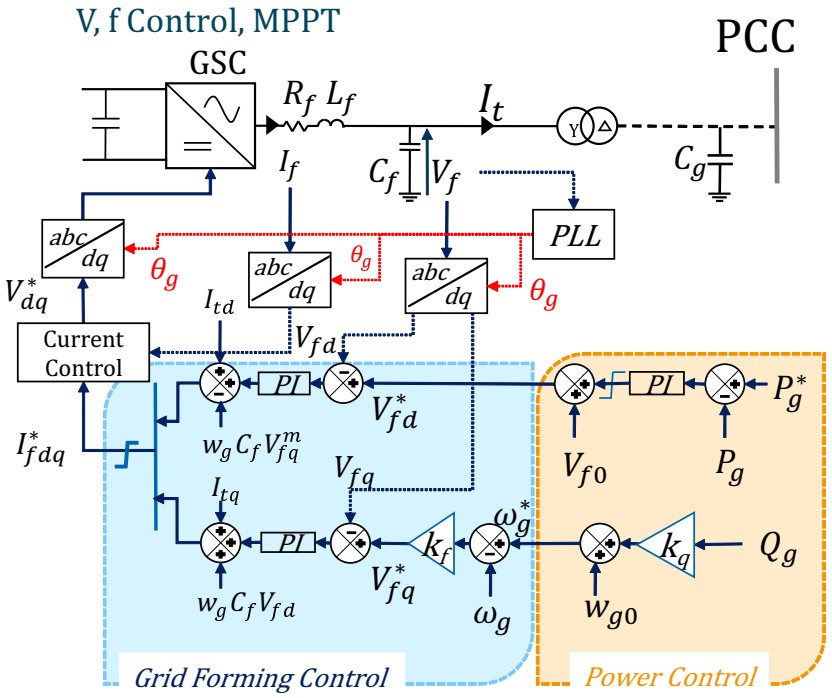

Figure 4.6: Grid Forming with PLL based Synchronization

A major assumption done is that the WGs in the farm have a self-start capability with the help of energy storage devices. The overall control scheme is shown in the Figure 4.6. The LC filter enables the generation of controlled three phase AC voltages at each WG terminal. The voltage

references (V_{fd}^*, V_{fq}^*) are derived by the two outer loops and enable the control of active power and the sharing of reactive load respectively (shown as power control loop in the Figure 4.6). The different aspects of this control scheme are elaborated below.

Active Power and Voltage Control

From the analysis of the system dynamics in chapter 3, it is clear that there is a coupling between the offshore AC voltage and the active power or d-axis current reference of the GSC. This dynamic relationship is exploited by using a droop control scheme for the control of voltage and sharing of the active power load in islanded mode (active power losses in the offshore network, for instance). Such a scheme is also useful during prolonged islanded mode, after faults or other such unexpected events onshore. The scheme enables the uniform sharing of the offshore active power load, indirectly loading the wind turbines to provide this necessary active power demand.

This approach is an evolution from the solution 1 presented in the section 4.2.2. The differences include (see Figures 4.2 and 4.6):

- The presence of a power control loop in addition to the voltage control loop.
- Instead of the PCC voltage control, the voltage at each WG filter terminal (LC) is regulated.
- The $P-V$ droop is used for load sharing in islanded mode (as shown in the equation 4.7) and PI controller for power control or MPPT in the connected mode are proposed here. Whereas, in the solution 1, a PI loop saturation of the voltage control and d-axis current limit (in the Figure 4.3) is used the for active power control in connected mode.

$$V_{fd}^* = (k_{pp})\left(P_g^* - P_g\right) + V_{fd0} \tag{4.7}$$

In the connected mode (DR is conducting), the PI controller is useful to track accurately, the reference for P_g^* as dictated by the MPPT algorithm (see Figure 4.6).

Reactive Power sharing and Synchronization

The reactive power sharing by the use of $Q-\omega$ droop, is in line with the relationship observed between the output q-axis current of the GSC and the offshore network frequency, in chapter 3. The reference frequency (ω_g^*) is derived by using a droop coefficient shown in the Figure 4.6, as follows:

$$\omega_g^* = k_q Q_g + \omega_{g0} \tag{4.8}$$

where

ω_{g0} is the nominal frequency of the offshore network,

Q_g is the reactive power measured at the WG terminal,

k_q is the reactive power sharing coefficient.

The problem of synchronization is solved by setting the V_{fq}^* according to the frequency reference (ω_g^*) derived from the above equation. The droop function for the frequency regulation, is implemented in a uniform manner across all the WGs (same PLL and droop constants k_q, k_f) and is expressed as follows:

$$V_{fq}^* = k_f \left(\omega_g^* - \omega_g\right) \tag{4.9}$$

where

ω_g^* is the reference frequency derived from the equation 4.8,

k_f is the droop coefficient,

ω_g is the frequency as measured by the PLL.

Thus, every time the droop function generates a new frequency reference to share the change in reactive power load (from previous equation 4.8), it results in an increase in the reference voltage V_{fq}^*. According to the following representation (for output frequency measured by the PLL) this leads to a change in the measured / sensed frequency, by the PLL [62]:

$$\omega_g = k_{lp} V_{fq} + k_{li} \int V_{fq} dt + \omega_0 \tag{4.10}$$

where

k_{lp} is the proportional gain of the PI controller in the PLL,

k_{li} is the integral gain of PI controller in the PLL,

ω_0 is the nominal grid frequency (50 Hz).

The consequence is that all the WGs synchronize to this newly computed reference grid frequency. Eventually the $d-q$ reference frame is re-oriented such that $V_{fq}^* = 0$ at the capacitor filter terminal of each WG, and the entire OWPP synchronizes to a common frequency. The frequency may slightly around the nominal value, as observed in the simulation results [62].

4.2.5 Solution 4: Decentralized frequency control with a secondary controller for frequency deviation

In [64] a similar approach is used (as in the previously described solution [62]), for using a $Q-f$ droop for reactive power sharing and synchronization purpose. As an extended functionality, the frequency deviation (in the offshore grid) due to the droop based primary control by the WGs, is compensated by using a secondary frequency controller.

Regarding the control of active power, the authors point out that the clamping of the AC voltage to the HVDC voltage, means that there is no requirement to control the AC voltage by the WGs during connected mode of operation. With sufficient wind power available, the DR

conduction can be forced by increasing the WG output power.

The d-axis current reference, no longer needs to be set for AC voltage control and power control, as in the solution 3 [62]. This allows the GSC of each WG to retain the DC link voltage control action (of the B2B converters), and the MSC performs MPPT (almost similar to a grid following control scheme), while the q-axis current reference is set for synchronization. This turns out to be a hybrid approach between the complete grid forming approach presented in [62] and the Fixref based scheme for WGs presented in section 4.2.3 [81]. The overall control scheme for the GSC with only the decentralized frequency control scheme is shown in the Figure 4.7.

The d-axis current reference is set for the dc link voltage control, while the control action on the q–axis current is set to ensure $V^*_{fq} = 0$. This scheme ensures synchronization i.e. aligning the voltage V_{fd} along the output capacitance filter (C_f) voltage. Along side this scheme is the now known $Q - f$ droop scheme generating the frequency reference and the required phase angle for the GSC, directly, without the use of an external frequency source or the PLL.

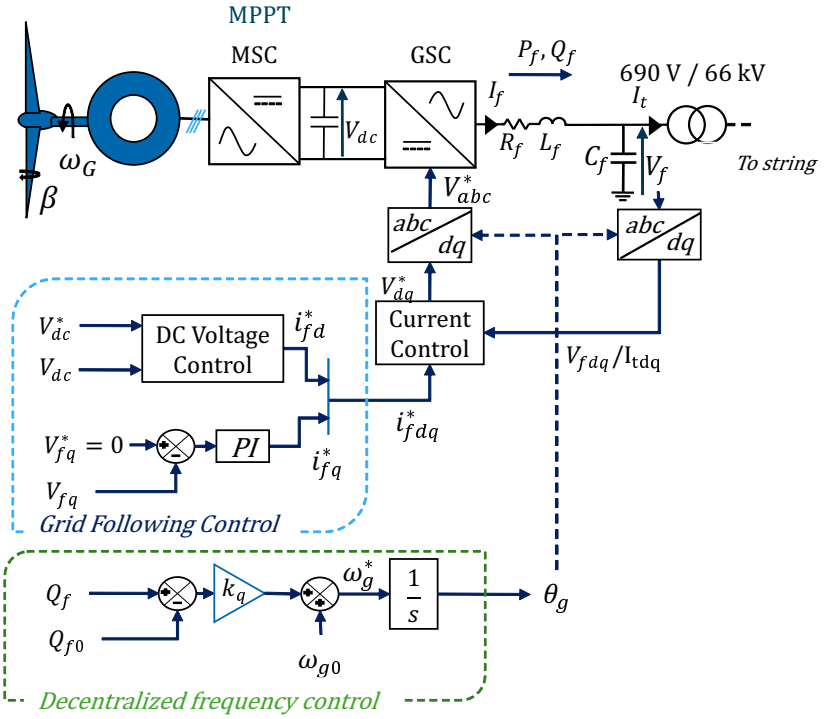

Figure 4.7: Grid Forming with PLL based Synchronization

This work [64] demonstrates the start-up, normal operation and control of the WGs during a fault condition in the offshore system. However the exact approach for the black start operation is not discussed and moreover, the prolonged islanded capability has not been demonstrated. Since the GSCs do not regulate the RMS voltage of their respective LC filter terminals by using a specific control scheme, a prolonged islanded capability does not seem feasible, unless an

additional physical equipment is used for this purpose (like the MVAC umbilical).

4.2.6 Comparison of the Grid Forming Solutions

A comprehensive comparison is attempted of the above grid forming solutions, by considering different aspects of approaches, in the table 4.1. It might seem unfair to compare, for instance, one of the first solutions, laying the foundations for this research topic, with the latest publication. But the goal is, to highlight the evolution and similarities of approaches on one hand and the drastic differences on the other.

All of the solutions reviewed, have common features and also drastic differences between them. It is seen that the Solutions 3 and 4 have almost identical approach for the synchronization and frequency control. And all three solutions 1, 2 and 4 focus on exploiting the Q-f relationship for sharing the reactive power load of the grid. Solutions 2 and 4 succeed in retaining the MSC control function just as in a conventional Type 4 WG (i.e. MPPT or power control). While solution 2 explicitly mentions the use of an MVAC umbilical (an industrial approach), the other solutions either assume certain new capabilities of the WG or additional storage in performing the black start of the offshore grid. They have not clearly demonstrated the use of a particular approach and strategy.

There is also a clear evolution seen, in the later approaches. The importance of solution 1 is that it lays down the offshore network dynamics and the theoretical analysis for grid control. The solution 2 is rather an industrial approach to the issues related to start up and grid forming. The solution 3, though seems like an iteration of solution 2, succeeds in demonstrating the grid forming with complete network impedances like sub–marine cables and solves synchronization among WGs, by using the PLL. Moreover, this solution has analyzed the various faults in the offshore, DC and onshore AC grid. System protection solution and WG control solutions to provide FRT capabilities [48][83] were also performed.

Characteristics	**Solution 1**	**Solution 2**	**Solution 3**	**Solution 4**
Approach	Distributed V,f control	Fixref	Distributed PLL based Grid Forming	Decentralized, with secondary frequency control
GSC Control Variables	PCC V,f and MPPT	DC voltage and Q	Distributed V,f and MPPT	DC voltage and frequency
Synchronization	Problem not addressed	Using GPS / Radio communication	PLL–based & Q-f droop	Q-f droop without PLL
MSC Major Control	DC link voltage control	MPPT	DC link voltage control	MPPT
High bandwidth communication	Yes, PCC voltage measurement	Yes, dq FIXREF signal	Not required	Yes, for secondary frequency control
Black start of offshore grid	By WGs	By AC Umbilical + Fixref	By additional storage in WGs	By WGs
Prolonged Islanding Capability	Subject to wind power availability	Onshore AC Power + Fixref	Using Control and WG local storage	Not dealt with, Voltage Control solution not implemented

Table 4.1: Comparison of the Different Grid forming Approaches

4.3 Simulation Results and Assessment of Solutions

In this section, the first three grid forming solutions reviewed above, are simulated in MATLAB Simulink® and analyzed further. A single study case is used to assess these control solutions, which can enable an easy comparison between the control implementations. The objectives to perform these studies are three fold:

I. to enhance further the knowledge of the DR-OWPP operation and control,
II. to establish the methods to compare any future grid forming solutions,
III. to aid in future control proposals/enhancements based on this work.

4.3.1 Study Case Description

The study case network used for simulation studies is shown in the Figure 4.8. The parameters for simulations are indicated in the table 4.2. The OWPP network consists of three aggregated WG strings of capacities 80 MW, 72 MW and 96 MW. The aggregation of the string cable parameters is done according to the methods described extensively in [84] and presented with more details in the appendix D.

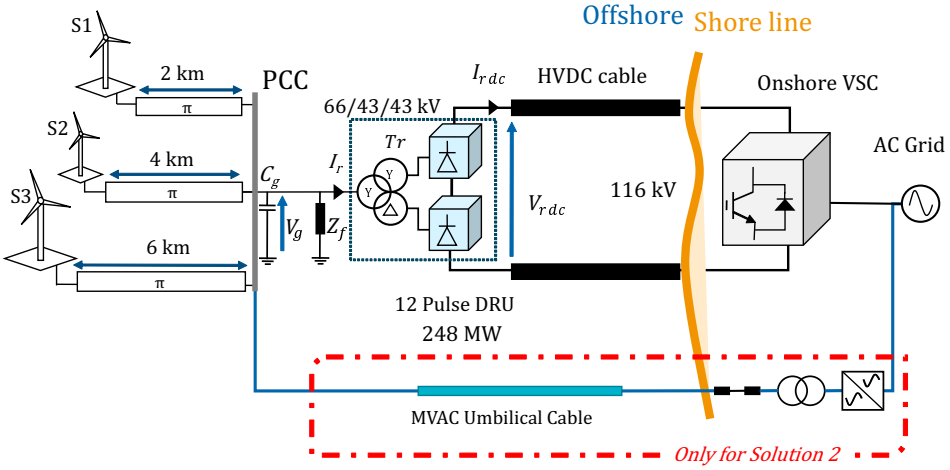

Figure 4.8: Study Case Network for Simulation Studies

Assumptions and Simplifications in the Modelling

Some of the assumptions made for the modelling are listed out below:

i. The dynamics related to the mechanical characteristics of the wind turbine, are considered to be slower than the AC network dynamics and thus neglected. This is relatively a valid assumption, considering very large inertia of the rotating system.
ii. The collection network is assumed to be of radial configuration.

Component	Parameter	Value
DR and HVDC link	Total Power Capacity	248 MW
	Transformer Voltage	66/ 43/43 kV
	DC Voltage	110 kV
	Transformer Impedance	R = 0.002 pu ; X = 0.18 pu
	Offshore CapacitanceC_g	2.4 μF
	Diode Rectifier Model	Switched Model
	Offshore Filter (Z_f)	49.6 MVAr
Collection Network	RLC Parameters(per km)	0.1 Ω;0.366 mH;0.224 μF
	Distance from PCC (S1, S2, S3)	2 km, 4 km, 6 km
	String S2 interarray Cables	Radial, 1km each
WG Strings	Rated Power unit WG(S2)	8 MW
	Power Capacity (S1,S2,S3)	80 MW, 72 MW, 96 MW
	Transformer voltage	690 V / 66 kV
	Filter Resistance	0.0012 pu
	Filter Inductance	0.3 pu
	Filter Capacitance	0.1 pu
	VSC Model Type	Average Value Model

Table 4.2: Network parameters for the Study case

iii. The onshore VSC performs a good regulation of HVDC voltage.
iv. The DC reactor and the HVDC transmission cables are neglected.

The resulting simplifications are listed out below:

i. Due to assumption (i), for solutions 1 and 3 the WG model is simplified as shown in the Figure 4.9(a), consisting of a DC voltage source connected to the GSC.
ii. Similarly for solution 2, the simplified WG model, consists of a DC current source with a capacitor connected to the GSC, as in the Figure 4.9(a).
iii. due to assumptions (iii),(iv), the DC link and VSC are together simplified by a single constant DC voltage source.
iv. the MVAC umbilical is represented by using a simple VSC (Figure 4.9(b)), regulating voltage and frequency of the AC network. This is done because, the requirement for solution 2 is a stable AC voltage source, during the start-up and possibly during a prolonged islanded mode.

4.3.2 Simulation and Analysis of Solution 1

The solution 1 [54] has been simulated by using the study case architecture in the Figure 4.8, consisting of three strings of aggregated WG models. The impedance of the collection network cables are neglected in the model (as done in the concerned work as well). The simulation

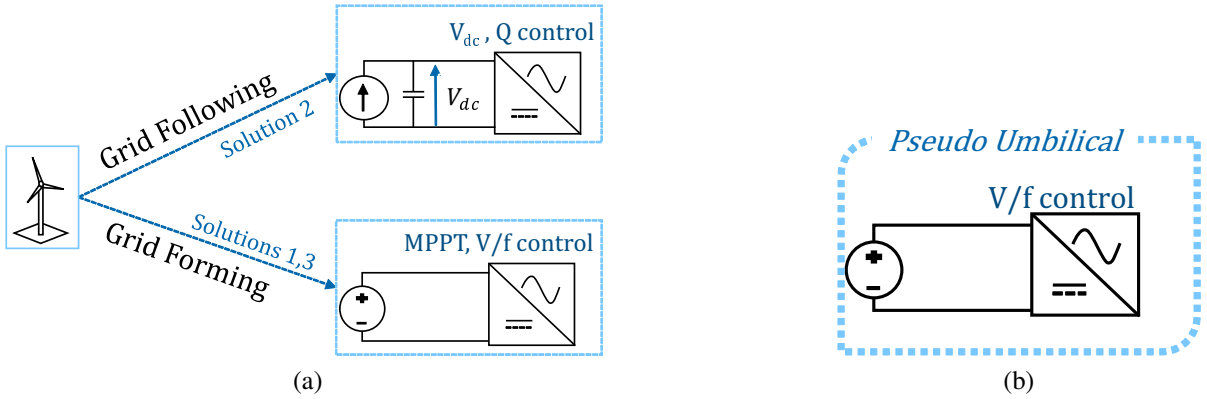

Figure 4.9: Simplified Models (a) Pseudo Umbilical represented with a VSC and DC voltage source (b) Simplification of the WG model based on implemented control

results are presented in the Figure 4.10.

Initially, the WGs ramp up the voltage at the PCC, by equally sharing the voltage control. The frequency of the grid is fixed and all the WGs are synchronized to a common arbitrary reference frame. At $t = 0.96s$ the PCC voltage is high enough, to allow the DR (continuous) conduction. Once the DR conduction begins, as explained before, the voltage control loop saturates and the value of d-axis current is directly controlled by the upper limit. This upper saturation limit for the $d-axis$ current is directly varied to change the active power outputs of the WG strings 1,2,3 at time $t = 3$, $t = 4$ and $t = 5s$ respectively (Figure 4.10(a), (b)). The droop constants are set as per the equation 4.5 for droop proposed by this solution. As the active power production varies, each increases its reactive power contribution, due to an equal distribution of this control function. Thus at $t = 3s$ for instance, the increase of power output from S1 forces all the WGs to share the reactive power load.

The PCC voltage increases, slightly for every change in the active power injection by the WGs. For a step of the active power reference from 30 % to 90 % for each WG (between $t = 3s$ and $t = 6s$), the PCC voltage increases slightly, from 1 pu to eventually 1.08 pu (seen in the Figure 4.10(c)). The AC Voltage reference for WGs, is set slightly higher than the actual PCC voltage that will be attained during normal operation for 100 % power production. This is to ensure the DR conduction and the saturation of the AC voltage controller.

4.3.3 Simulation and Analysis of Solution 2

The Fixref[81] solution is studied in this section by using simulation of the study case network presented. The collection network cables are included in the model. To mock the behavior of the AC umbilical cable, an inverter connected to the ideal DC voltage source, is used. The Umbilical cable is simplified as an energy source providing the start-up and initial voltage build-up for the offshore grid. In fact, it could be any device other than an umbilical cable (offshore storage

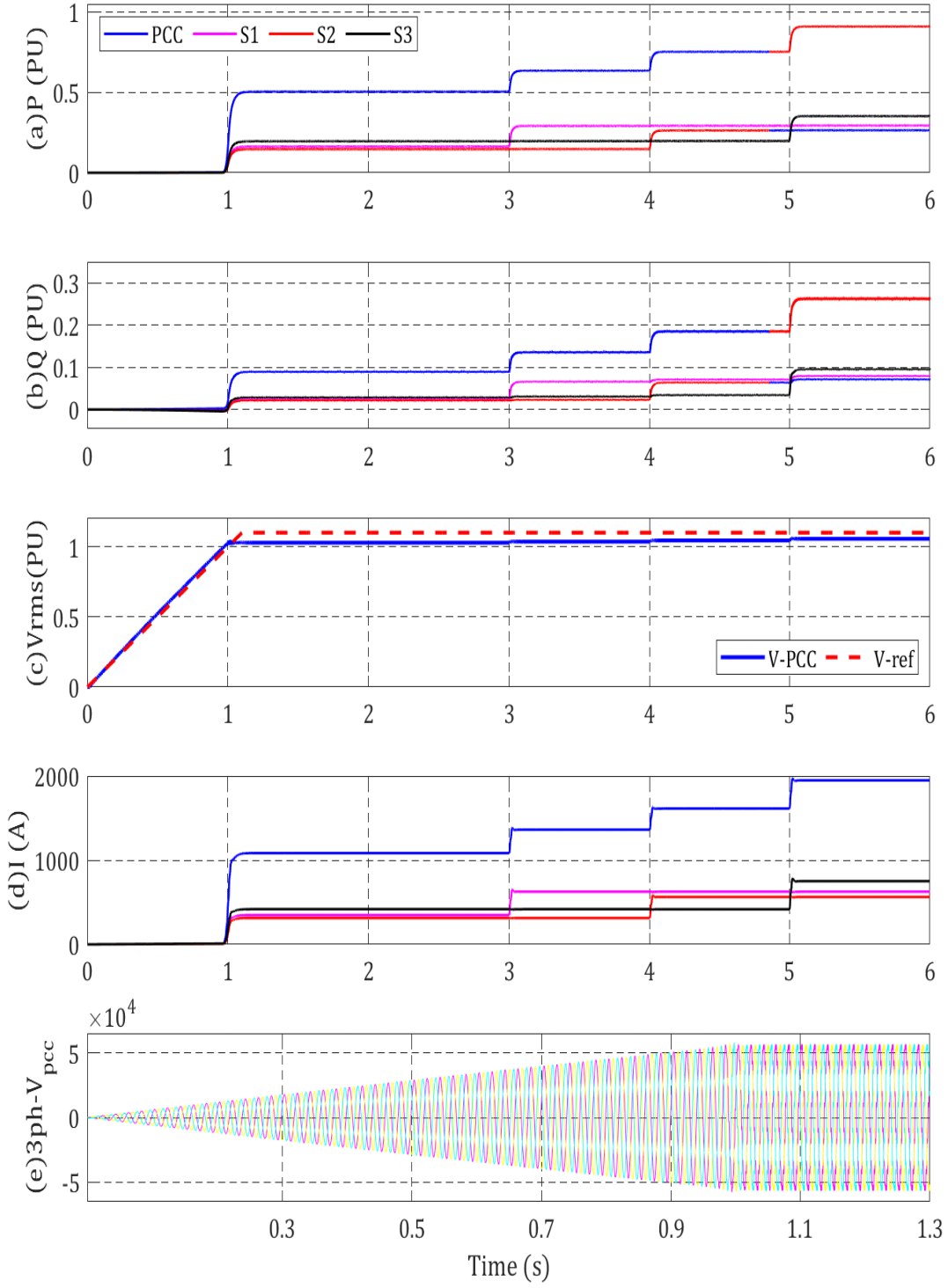

Figure 4.10: Simulation Results for Solution 1 | (a) Active Power (b) Reactive Power (c) RMS AC voltage at PCC vs reference value (d) RMS AC Currents (e) Three phase AC voltages at the PCC

platform, Diesel generator, closest VSC station etc.). The 'Pseudo umbilical cable' and all the GSCs are provided with the same reference signal for the dq frame, rotating synchronously at the same frequency.

Initially, the pseudo umbilical cable is connected to the network and it compensates for the active power losses in the network and the reactive power requirement of the collection network (Figure 4.11(a)). The AC voltage is controlled at 0.9 pu at the PCC (Figure 4.11(c)). In reality, it is important that all the WGs are connected to the AC network and DC voltage of each GSC is regulated in a stable manner. Then, the MSC (along with Pitch control) can be controlled to set the desired power reference / enable the MPPT for the WG.

At $t = 3s$, the WGs start producing active power, and this naturally leads to an increase in the PCC voltage, until the DR is forced to conduct. During the evolution of the PCC voltage, the pseudo umbilical system is disconnected automatically, once the PCC voltage reaches a higher value than the set point assigned for the islanded mode (0.9 pu in this case). This is shown by the active and reactive power outputs of the umbilical system in the Figure 4.11 (a) reaching zero. It is pointed out that the prolonged islanded mode can be maintained here, if required, due to onshore fault events or low wind conditions, due to the reliability of the umbilical cable. After $t = 3s$ the power set points for the WGs are varied and finally all of the set points reach 80 % for each WG at $t = 7 - 8s$. Following this, the power production by each WG decreases gradually. This variation in active power production is done to show the AC voltage changes (shown in the Figure 4.11(c),(d)) and the reactive power sharing among the WGs (Figure 4.11(c)).

It is seen that the reactive power is shared among WGs such that the WG with the highest active power production compensates a higher proportion of the total reactive power load. The Figure 4.11(c) shows for instance, from $t = 6 - 8s$, the circulation of reactive power. This is undesirable for the optimal operation of the wind power plant and it is important that the WG string / cluster with the highest active power production should be alleviated from the supplying higher reactive power. This type of compensation risks the WG current references to reach their limits. Thus, a droop control is essential to share the reactive power load in an orderly fashion.

Impact of the droop coefficients

The aggregated WGs when injecting unequal power, lead to the reactive power circulation between WGs, as observed in the simulation results in [81] and also in the previous simulation case.

The solution in the original work [81] is to set droop coefficients so that WGs with higher active power production compensate less reactive power load. This seems to suggest real time calculation and distribution of droop coefficients based on the measurement of the active power production. This is feasible, for instance using the central OWPP controller and it relies on the active communication between this controller and the WGs. However, the recalculation and re-distribution of droop coefficients could be avoided by using alternate methods. For instance the

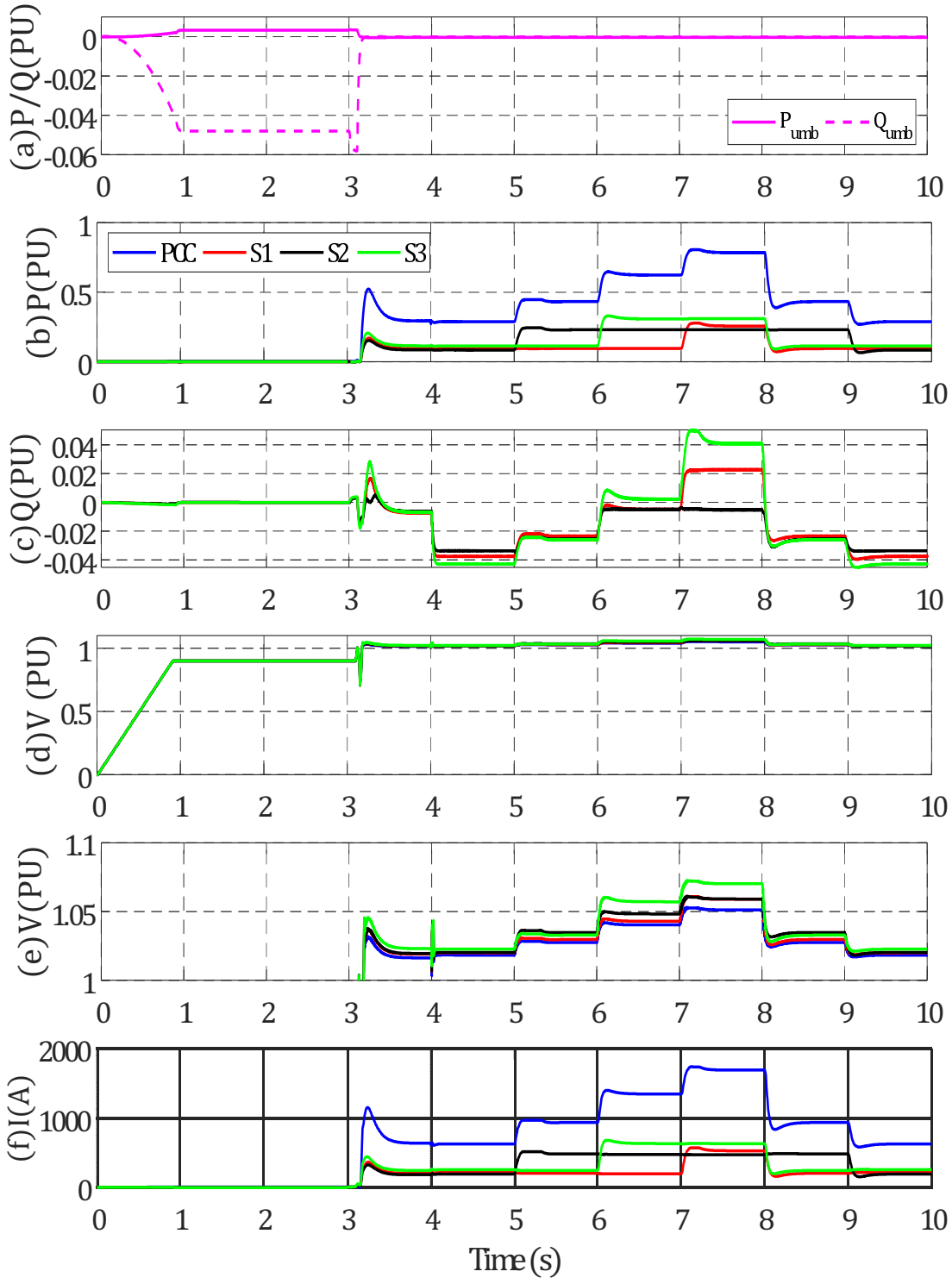

Figure 4.11: Simulation Results for Solution 2: (a) P,Q measured at the Pseudo Umbilical (b) Active Power – WG strings and PCC (c) Reactive Power – WG strings and PCC (d) RMS AC voltage (e) Zoom of AC voltages at WG strings and PCC (f) RMS AC Currents

use of fixed droop coefficients as proposed in the previously reviewed work [54] is independent of any communications from central controller and relies on local measurements only.

Thus a quick analysis is done for the setting of droop coefficients from the known approaches and also the approach suggested in this work. The reactive power injections are compared for the same active power production events of the WGs. The table 4.3 shows the various droop setting cases (based on the previous proposals and also as proposed in the Fixref solution).

Case	Droop Coefficients			Comments
	k_{q1}	k_{q2}	k_{q3}	
1	1	1	1	No droop coefficients
2	0.333	0.333	0.333	Equal droop coefficients
3	0.3226	0.2903	0.3871	Droop according to WG capacity
4	0.3871	0.2903	0.3226	Arbitrary droop settings
5	0.407	0.1046	0.4884	Droop setting by FIXREF

Table 4.3: Different droop settings for Fixref reactive power sharing

The simulation results are shown in the Figure 4.12, for different cases of droop settings. It is worth pointing out, that the voltage values were affected only by the active power injection, and they were the same for all reactive power droop settings. It is seen that case 2 and case 3 in the Figure 4.12(b)(c), already alleviate the circulation problem and excessive loading of the WG producing higher active power. This sharing of reactive power is similar to the results for the previous grid forming solution shown in the Figure 4.10.

The droop settings for the cases 4 and 5, gives reactive power sharing specific to particular cases of active power injection.

- Case 4: The droop constants of S1 and S3 are reversed, so that S1 has slightly higher reactive power sharing, even if it has lower capacity than S3. The impact can be seen by comparing Figures 4.12(c) and (d), for the time interval t= 4–5s.
- Case 5: Here the goal was to fix droop co-efficients for a particular time interval t = 5–6s where S2 is producing higher power than S1 and S3. The droop coefficients are set such that strings S1 and S3 alleviate S2 from compensating for the reactive power load. Comparing the Figures 4.12(c) and (e) for the time interval between t = 5–6s, it is clear that S1 and S3 have shared higher reactive power load, compared to S2. Such droop settings can be set as required, according to the real power production.

4.3.4 Simulation and Analysis of Solution 3: Distributed voltage and frequency control with PLL based Synchronization

For this solution, the string 2 is modeled by using individual WG models instead of a single aggregated model. The offshore reactive power compensation is at 49.6 MVAr. The aggregation

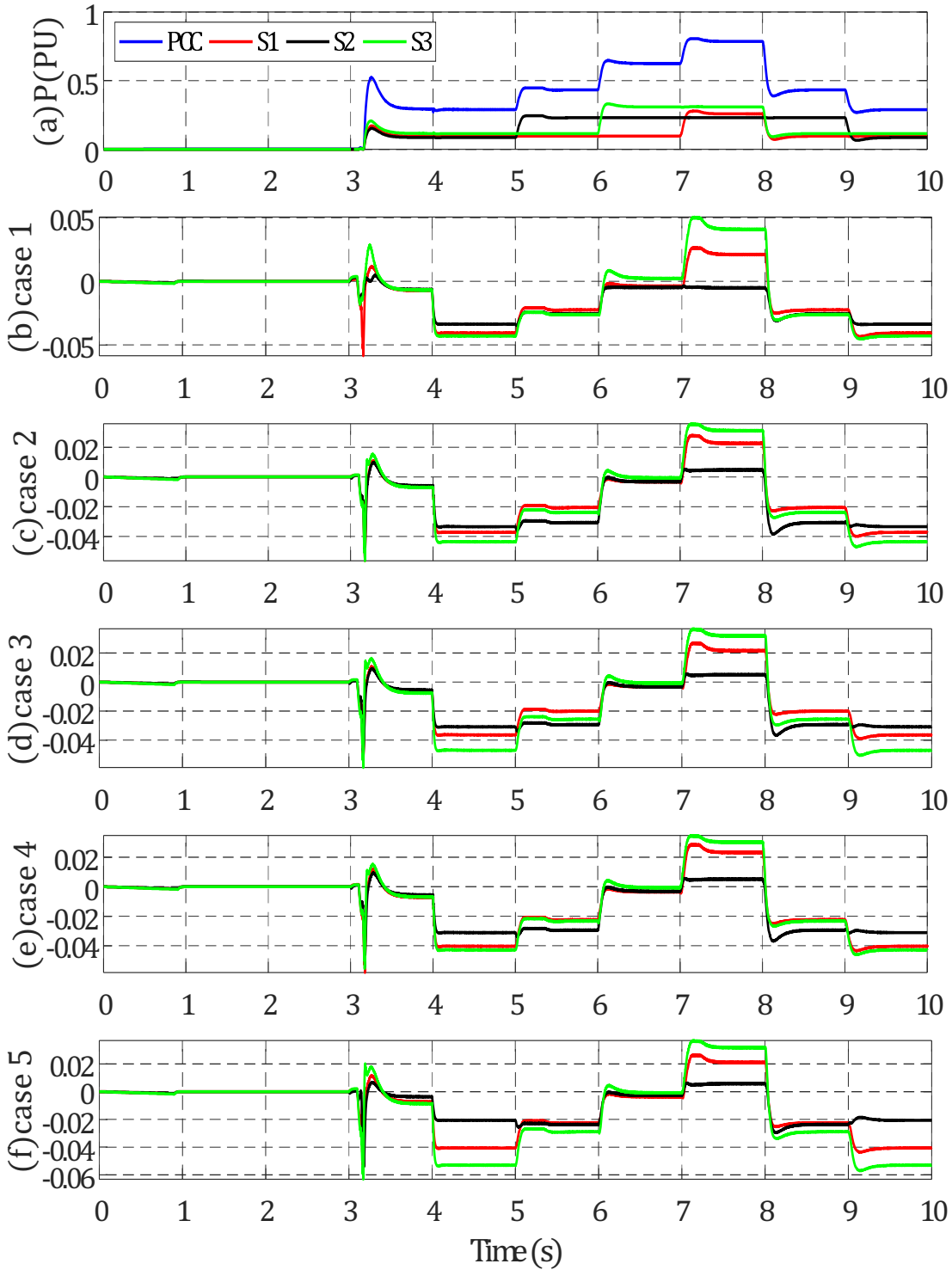

Figure 4.12: Simulation Results for Solution 2: Reactive power sharing for different cases of droop setting

approach justifies the use of mixed modelling techniques to analyze the following:

- The dynamics inside the string – notably the synchronization, reactive power sharing and voltage build–up.
- The dynamics at the PCC and OWPP level by using aggregated string models.

The initial start-up sequence, comprising the energization of WG auxiliaries and control of the MSC DC voltage are not demonstrated, due to the simplified nature of the models. The islanded operation within the string S2 is shown in the Figure 4.13(c), when each WG connecting the string, regulates the voltage, by using the P-V droop scheme.

The connection of String S2 to the islanded AC network at t = 7.5s, is seen as a sharp transient in the AC voltage value, which is almost non existent in the case of the connections of S1 and S3. The reactive power compensation of the string S2 cables, is done only by the WG 2 (Figure 4.13(f)) from time t = 2–2.5s. Gradually, as other WGs are connected to the string, the reactive power load of the array cables inside string S2, is equally shared by the connected WGs. This evolution of equal reactive power sharing by the connecting WGs in string S2, is seen clearly in the (Figure 4.13(f)) and also as gradual change in frequency in the Figure 4.13(c).

A sharp change in the reactive power load is seen, changing from positive (inductive) to negative (capacitive) at $t = 8.5s$ when the offshore filter is connected to the network. For low active power production, the reactive load for the offshore network is more capacitive, since the DR and offshore transformer have higher reactive power consumption, for higher power production. It is decided to connect the offshore filter after the conduction of the DR, to highlight the variations in load for the WGs and the grid frequency.

The frequency measured at WG 2 is shown in the Figure 4.13 (d) while it is verified that all the WGs synchronize to this common grid frequency, by equal sharing of this reactive power load. The change from zero power in islanded mode to almost 100 % power production in connected mode, has resulted in relatively smaller changes in the network frequency.

4.4 Analysis and Discussion

Three of the grid forming solutions reviewed in the section 4.2 are assessed by using simulation studies. This enables a deeper understanding of the control implementation and also provides the extension of the comparison in this section.

4.4.1 Solution 1

The solution 1, has neglected the collection network cables in the dynamic models, being one of the first, to propose a grid forming control scheme. Including these cables may require further tuning of the controllers, and this can become complicated with multiple WGs in a large wind farm.

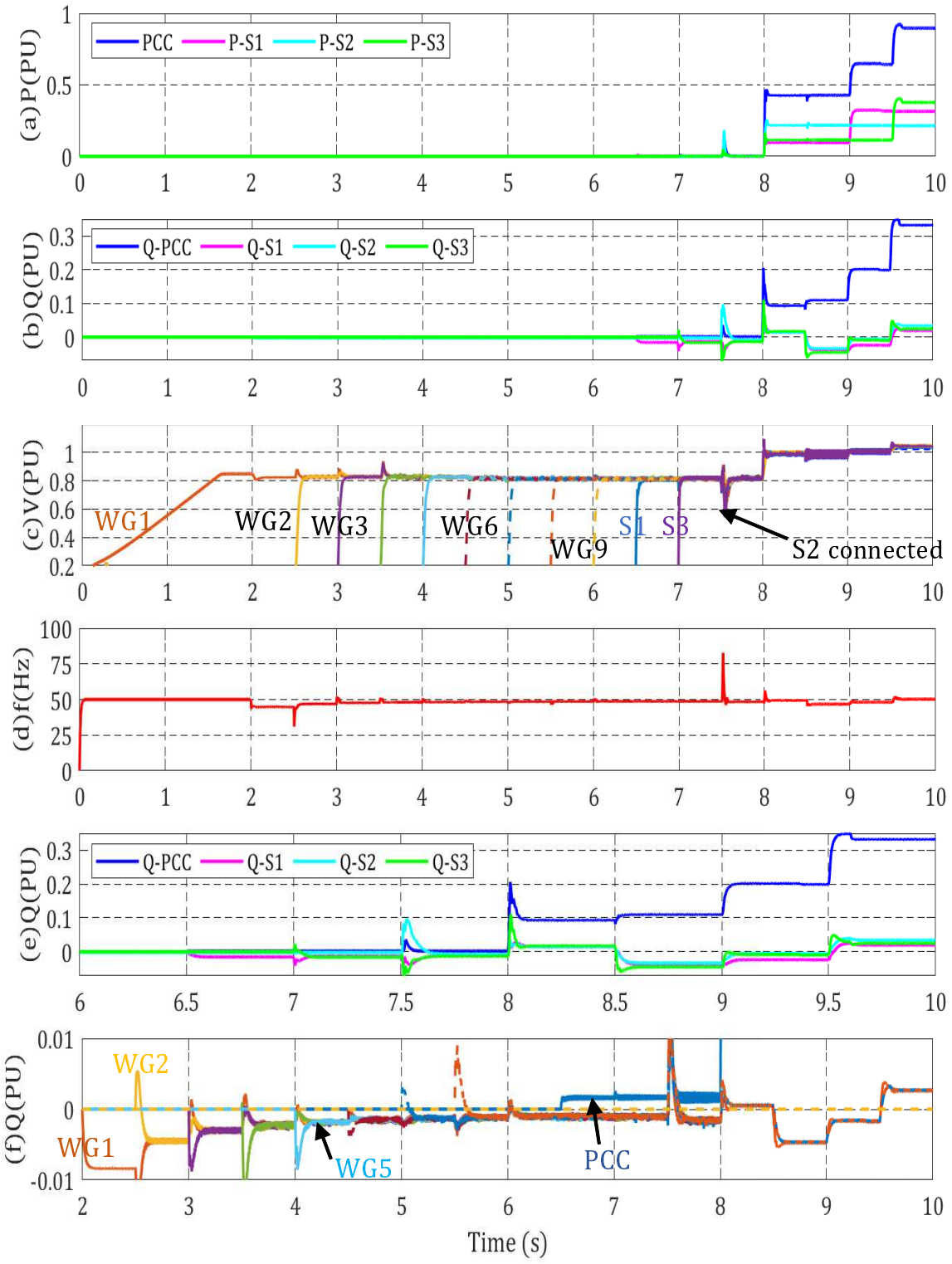

Figure 4.13: Simulation Results for Solution 3 | (a) Active power of Strings and PCC (b) Reactive Power (c) RMS AC Voltage at various terminals (d) Frequency of the AC grid (e) Reactive Power contribution of strings (f) Reactive power of individual WGs in string 2

The control of a remote AC bus voltage by using the WGs connected by array of cables, is rather not straightforward, since the equivalent impedance seen by each WG can vary. Real time communication of the PCC voltage measurement to all the WGs, is required, for the distributed voltage control. On the other hand, the use of reactive power droop coefficients, enabled an automatic sharing of the reactive power load. The WGs were able to share the reactive power according to their own rated capacity. However, it is seen that the synchronization of the WGs to a common grid frequency is not clearly dealt by this solution.

4.4.2 Solution 2

In the simulation studies in the section 4.3.3, the initial voltage control is straightforward and provided by the MVAC umbilical cable. The connected/normal mode is smoothly reached by increasing the OWPP power production. As power production evolves, so does the offshore PCC voltage and eventually, the clamping of the DR is achieved. Sensing the increase of PCC voltage due to active power increase, the umbilical cable is disconnected from the offshore AC grid.

Analysis on the impact of droop coefficients, in the section 4.3.3 shows that, the Q–sharing concept according to the active power capacity of each WG (in Solution 1), is deemed sufficient, for the given network. It can be chosen to dispatch computed coefficients, as proposed in this solution, if an inverter (GSC) overloading situation is foreseen, or if it could occur in a specific offshore AC network. A possible case is when one of the WGs in a string produces rated active power while most other WGs produce low power.

The prolonged islanded mode can only be maintained if a stable AC voltage source is connected to the offshore network. The MVAC umbilical cable relies on a stable onshore AC grid to supply the auxiliaries and ensure the islanded mode of the OWPP. In case of an event like a fault in the onshore AC grid, if the outage exists for a relatively long duration, the prolonged islanded may not be feasible. The WGs would have to rely on internal back up supplies to remain operational. Thus the MVAC umbilical cable, has to be backed up, by other sources of energy, local or centralized, to ensure that the WGs are functional during such events.

Availability of the Timing Source

The solution 2, enables the WGs to operate in a fixed frequency and the synchronization by using the FIXREF signal system, providing fixed reference in an arbitrary dq frame. A robust communication network is a must and the solution proposes the use of radio based or GPS system to ensure this. As a failsafe mechanism, additional timing sources could be used. It is unclear if the receivers of the GPS / timing signals in the OWPP system are compatible with other Global Navigation Satellite Systems (GNSS) like the GALILEO (European) etc. The work [85] is based on the use of synchrophasors for the American power system and it

suggests that the receivers (existing today) are mostly compatible with at least two of the existing GNSS systems. It is also indicated that the receivers in a general power system have to be compatible with multiple GNSSs to increase availability, when one of the systems fails. Thus the FIXREF systems could be designed to be interoperable with multiple GNSSs and / or other timing sources.

4.4.3 Solution 3

In solution 3, the islanded operation and the synchronization of each WG is seamless using the PLL, with minor transients observed, as in the Figure 4.13. As they are connected to the string, they automatically share active and reactive power load, maintaining the reference voltage. This is in stark contrast with solution 2, which has suggested manipulation of droop constants, during the operation. Here in solution 3, the WGs have similar parameters for droop control schemes and they automatically share the loads of the offshore network. They only require proper references from the central controller during start up and islanded mode, until the transition to the connected mode. Transients are observed in the frequency and AC voltage, for instance, during switching of the WG terminals to the network. But soon after a WG or a string is connected to the network, it shares the loads of the offshore grid. All the WGs then synchronize to a slightly different grid frequency, as observed in the Figure 4.13.

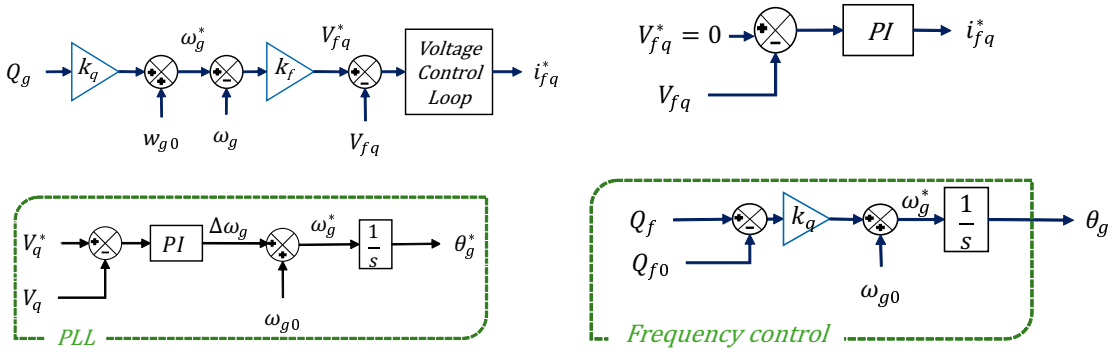

(a) (b)

Figure 4.14: Differences between solutions for frequency regulation / synchronization (a) Solution 3 uses the PLL (b) Solution 4 obtains phase angle directly

The start–up or the black start is conveniently assumed to be enabled by local storage devices. But the problem of the black start operation, the optimal design of the system and such other integral requirements have not been discussed in this work. Also the stability problems that are related to the PLL for OWPP systems, as analyzed in [80], may occur in such a large system, relying on the PLL to perform a part of the grid forming function.

Regarding the frequency control, the Solution 4 reviewed in the section 4.2.5, demonstrates that the PLL is not required to synchronize the inverters to a common grid frequency. The

solutions 3 and 4 seem to use almost the same approach to achieve the synchronization, since the V_{fq} component eventually reaches zero as revealed in [62][64], presenting these two solutions. The part of the control scheme showing the generation of the phase angle and the q-axis current refrence for the solutions 3 and 4 are compared in the Figure 4.14. However, the analysis here, shows that initially a V,f control is deemed necessary for one or a few WGs, so that in the worst case, they remain in self sustained mode, with an internal oscillator frequency / phase reference.

The solution 3 is chosen for further studies in the forthcoming chapter 5, due to the following reasons:

I. From the literature review, this solution seems to be the reference for grid forming control of the DR-HVDC OWPP system today, as it addresses most of the issues related to the OWPP operation, control and fault ride through.

II. The solution assumes that the energy storage (installed in the WGs) provide the black start capability for the OWPP. This is especially advantageous, to avoid additional installations like the umbilical and enhance the already existing storage systems in the WGs. This type of analysis is the main objective of chapter 5, on the black start of the offshore AC grid.

4.5 Conclusion

This chapter reviewed some of the major solutions for the grid forming of the DR-HVDC OWPP and attempted a theoretical comparison. The comparison has revealed important features and the presence or absence of essential requirements for the DR-HVDC OWPP system. Moreover, selected solutions have been studied further by using EMT simulations, in a study case network.

Through simulation studies, the various features of the selected solutions were analyzed in detail. Especially for solutions 2, the impact of different droop coefficients on the reactive power sharing has been analyzed. In solution 3, the transition from the islanded to the connected mode and the grid forming by individual WGs are analyzed by using individual (simplified) WG models in one of the strings. Similarities between solutions 3 and 4 regarding frequency regulation and synchronization are also highlighted.

It is shown that the availability of solution 2 can be increased by relying on multiple GNSSs or time sources, from the available literature. The analysis of solution 3 provides further understanding of the different operation modes, the transients involved during offshore grid voltage build–up, and eventually the transition between the different modes. Equal reactive power load sharing seems to be a better approach, rather than controlled sharing, unless otherwise required.

The comparison and detailed analysis, has been done to attempt a deeper understanding of the existing grid forming solutions. Future control proposals can be compared in a more intensive manner, citing advantages and drawbacks. This helps in choosing a grid forming solution to use in the analysis of the OWPP systems for other related research and innovation. In addition, the

analysis performed in this chapter, can provide a certain technical benchmark, to work towards new grid forming control schemes and / or work on enhancements of an available solution. However, the real decision making process to select a particular solution (including the physical equipment involved) is dependent on both the technical and economic comparison.

This chapter does not conclude that one of the solutions is the best. But, for convenience, the solution 3 is chosen to analyze the problem of black start operation of the offshore grid in the chapter 5 of this thesis.

5

On the Black Start of the Offshore AC Grid

Contents

5.1 Chapter Introduction 108
5.2 Overview of the Black Start Problem 108
5.3 Assessment of Solutions for Black Start 114
5.4 Conclusion and Research Prospects 119

5.1 Chapter Introduction

In chapter 2, the black start of the Offshore Wind Power Plant (OWPP) with DR–HVDC transmission has been introduced as one of the grid integration challenges. Exploring for alternatives to the existing black start solutions (Diesel Generators or Medium Voltage AC Umbilical Cable) could lead to a solution that is economically beneficial. Also the alternative could enable the OWPP to provide a black start service to the onshore AC Grid, as foreseen today based on the guidelines by ENTSO–E and the studies presented in [76] , [65]. The foreseen capability of OWPP services to the onshore AC grid, is however not in the scope of this thesis.

This chapter presents the work done towards understanding the problem of black start, analyzing the various alternative solutions and proposing a black start strategy. First, an overview is provided on the requirements of the OWPP for black start, existing capabilities of the WGs to help in the process and the power requirements.

Following this, various alternatives are analyzed for the black start of the offshore AC grid, and compared by using important qualitative criteria. The idea here is to highlight the various potential advantages and drawbacks in terms of operation and also certain strong indications for added costs at the system level, for each solution. Further analysis is done to compare two of the solutions – one involving a centralized Energy Storage System (ESS) and the other, with a distributed ESS across multiple WGs in a plant.

5.2 Overview of the Black Start Problem

5.2.1 Black Start in the context of the traditional AC power system

European Network of Transmission System Operators for Electricity (ENTSO-E) describes black start as the process of restarting a grid after a black out [86]. In traditional AC power systems, a Black Start Unit (BSU) is a generator unit capable of starting by itself without much or no external power supply. The BSUs are dedicated units to support other larger generator units to restart them after a black out. This enables establishing stable grid voltage and frequency, a subsequent connection of local loads and eventually synchronization of multiple generation units in the larger power system in consideration.

Black start in the classical AC network is performed by power plants with a low start up time and a high reliability like diesel plants, gas turbines or hydroelectric generators. According to a survey by the ENTSO-E [87], most of the TSOs in the European countries have the above mentioned generators for black start, while additional types of sources like nuclear plants (RTE, France), pumped storage plants (EliaGrid) are also observed. In case of a large scale black out, when none of the neighboring AC grids can help in the restoration, these designated generators or the BSUs are used to begin the power system restoration process. This is otherwise called

the bottom up approach [88], starting from a single generating unit and progressing forward (or rather upwards in the power system hierarchy) by connecting the loads and other larger generating units. Multiple generation units can be used simultaneously to create multiple islands in a given power system. Eventually, the synchronization is achieved among them in a sequential manner and finally, the entire AC grid (for instance in a region of a country) is fully functional.

5.2.2 Black Start in the context of the Offshore Grid

Generally for an OWPP with Voltage Source Converter (VSC) based HVDC transmission, the start-up of the offshore grid is performed by a diesel generator [18] located at the offshore platform and/or by using the offshore VSC by drawing required energy from the onshore grid through the HVDC link [18][41]. It is clear that the latter solution relies on the stability and reliability of the onshore AC grid, which is usually a large AC power system, known for the aforementioned characteristics.

But, in the case of the DR-HVDC based OWPP, the bidirectional capability of the offshore converter station is rather non-existent. This forces the system to rely upon a different source of black start. Examining the offshore wind power system, the energy requirements for black start can be designated as twofold:

I. The power requirement of the auxiliaries of the WGs, which includes the pitch and yaw drives, cooling systems, nacelle / tower lights and control systems among other equipment. Although there could be a small amount of reactive power requirement involved, these loads are deemed predominantly active.
II. The reactive power load of the AC sub–marine cables (with predominant capacitive impedance), offshore transformer(s), WG transformers along with resistive power losses (i.e. small active power load).

The auxiliaries of the WGs could be modeled as constant power loads, by assuming that the variations corresponding to the use of pitch or yaw operations are minimum. The requirements are elaborated further to sum–up the challenges that are involved in enabling the black start of a DR–HVDC OWPP.

i. Power supply of the WG auxiliary equipment with a reduced power production by the WGs. This active power requirement is estimated to be 1-5 % [65] of the WG capacity and the pitch and the yaw motors require a fraction of this power to enable the controlled extraction of wind power. Two different operating cases are identified regarding the control of power output
    - Low or medium wind condition where the power set point can be altered with the control of electromagnetic torque and the use of pitch angle control of the turbine blades.

- Wind speeds above rated speed where pitch control has to be employed (sometimes excessively) to reduce power production.

ii. The offshore network equipment like the submarine cables and the WG transformers and the offshore transformer(s) have to be energized. Especially, for the offshore collection network, the total active power losses are relatively less compared to the reactive power demand. The WG inverters or the black start source should be able to support the inrush current of transformers among other losses and compensate the reactive power due to the submarine cables.

iii. Once individual WGs are self-sustaining and the network equipment are energized, the offshore grid has to be maintained in islanded mode, with a synchronous operation of WGs with controlled AC voltage and frequency.

iv. Since the HVDC voltage is already set to its rated value by the onshore VSC, the offshore AC voltage has to be regulated in a coordinated manner, to a sufficient value to enable the DR conduction and wind power extraction. Islanding capability is also necessary in cases of faults in the HVDC link or the onshore AC grid.

5.2.3 Black Start Capabilities of a WG

In [65] many inventions and research works that ensure black start or self-start capability of the wind generators in general have been reviewed. Although the focus in [65] and [76] has been the restoration of the onshore grid by the OWPPs, they provide a valuable insight on existing technologies and research. Some of the major energy sources (used for self-starting or self–sustaining the wind generators) are listed below:

i. Diesel generator, which is a tried and tested solution.
ii. Battery storage, already part of the wind generator system or designed for the purpose.
iii. Using the wind energy itself (with support from energy source 1 or 2) to power neighboring wind generators and in some cases perform voltage and frequency regulation.
iv. Other sources like a stable AC grid, neighboring VSC Station etc.

Another important aspect of the WG physical characteristics is the intermittent nature of the energy source- i.e. the wind. On this regard, if the wind energy participates in the black start procedure, the output power has to be controlled with the use of both the pitch angle and electromagnetic torque loading (converter control). This can be achieved for instance by a look–up table implementation for desired power set point operations or by calculations for de–loading of the generator [89] [90].

A brief review of the existing literature and industrial inventions is done to identify the existing approaches for self-starting and independent operation of the WGs.

Review of industrial inventions

It has been observed from the existing inventions, that maintaining the WG in operation, is a significant requirement, especially for remote and offshore environments. Some minimal functions to ensure the operational status of WG include health monitoring of the various components, prevention of rotor or blades getting locked due to harsh conditions etc.

The work in [91] indicates that the black start could be performed by using the wind power itself. Also it is stated that diesel generator and battery storage could be used in order to help in the process. The initial charging of the DC link capacitance is done through a simple diode rectifier, by using the AC power supply.

In the invention [92], a method for islanding a WPP is described where a WG (by using wind power) can provide the auxiliary supply to a group of wind turbines and thus maintain the islanded operation. It seems that only the Uninterrupted Power Supply (UPS) unit is involved but not necessarily any additional storage equipment. The *Pilot* wind turbine is used to supply the auxiliary equipment of other wind turbines, which perform the connection to the local AC grid by using switches. This work also highlights disadvantages of using diesel generators for the auxiliary supply, like the need for maintenance and refueling. Also ,wind is pitched as a better auxiliary power source (for the local grid and other wind turbines) than batteries because of the monitoring, maintenance activities involved with the latter.

In [93] it is indicated that supplying the pitch motors is enough to start the wind turbine operation. Although, the need to yaw the turbine nacelle against the apt wind direction has not been mentioned, as pointed out by the work [65]. The work [59] seems to suggest that the wind turbine itself has a self-start capability and that the wind availability is enough for the black start and grid forming functions. But initial power requirement for the control systems, and other equipment (especially the pitch and the yaw motors) is not discussed.

In the invention [94] the WG is connected to an auxiliary energy storage unit thorough an auxiliary converter. The advantage of providing the supply to the WG auxiliaries by using this storage and an auxiliary converter during the absence of the AC grid is highlighted. Once the WG is functional, the energy is drawn to recharge the storage system by the auxiliary converter. The converter operation models and relevant control schemes are however not discussed here.

The work in [95] mentions the use of a wind turbine itself or an energy storage system to produce power for the auxiliaries in which case the inverters associated to the ESS or the wind turbine operate in grid forming or V/f control mode, deemed as the first energy source. The second energy source (connected to an inverter) which is not performing the V/f control (either the ESS inverter or the WG inverter) will participate in the power control for balancing the required auxiliary load that cannot be supplied entirely by the chosen first source. The grid forming is performed by using a traditional droop (P-f, Q-V droop) control scheme. Also the smoothness of wind variations is measured to decide whether to use the wind generator or

the ESS to power the auxiliaries. It is claimed that the transient stability of the voltage and frequency is increased due to the participation of the second energy source in power control.

The above said inventions indicate different approaches to provide the self start capability to the WG and to operate in isolated condition. There are also indications of using the WGs to power neighboring WG auxiliaries, leading to the question, if the black start sequence and control strategy have been explored for the Offshore Wind Power System. It is seen that such sophisticated and detailed strategies have either not been designed or are not public knowledge. Moreover for the OWPP system with DR–HVDC transmission, the problem has not been posed and treated in detail.

In the next section, the energization and control requirements of the offshore grid are discussed. Then, some of the solutions feasible for the black start of the DR-HVDC OWPP topology are presented with the relevant criteria for comparison.

5.2.4 Power Requirements of the OWPP system

The energy requirements for the black start of the OWPP system is calculated here by using a study case network (shown in the Figure 5.1). This network is retained for all the future analysis and simulation studies. Both the calculations and simple grid forming simulations are used to obtain the exact requirements and / or validate against the simulations.

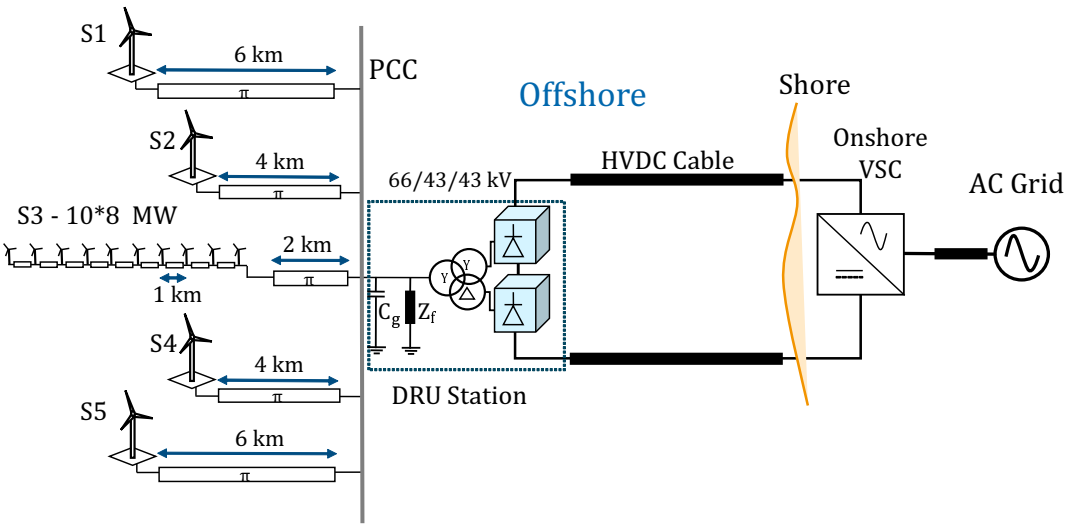

Figure 5.1: Study Case Network for Black Start Analysis

It is important to note that the inrush currents related to the transformers, the mechanical effects on the WG drive train are not analyzed in this work. The power requirements presented are the load requirements in the steady state, islanded mode and are shown in the last column of the table 5.1. Clearly, the power requirement for a string is dominantly reactive, with a reactive power injection of 2 MVAr by the submarine cables, for an AC voltage value of 0.8 pu.

Roughly, the offshore islanded network has an apparent power requirement of 23.7 MVA, which is around 6 % of the OWPP rated capacity. For comparison, the sizing of the AC Umbilical transformer for the DR–HVDC industrial solution is at 4.2% [58]. The above two power requirement figures are comparable, with an assumption for the size of WG auxiliaries in this work (3% of WG capacity in the study case used). The 23.7 MVA sizing is useful for deciding the minimum dimensions of the centralized black start source, for instance or can be broken down into detailed ratings per string / WG. Corresponding to the chosen solution, a specific black start strategy can be designed. Another additional problem that remains to be solved is the duration of this power requirement, which induces the energy rating of the black start source in terms of Wh capacity. However, this sizing problem can be done according to the exact requirements of the wind power plant, duration of black start, OWPP operation data etc., and are not dealt with in this chapter.

Component	**Parameter**	**Value**
DR and HVDC link	Total Power Capacity	400 MW (base Power)
	Transformer (3 Winding) Voltage	66/43/43 kV
	Base Voltage	66 kV
	HVDC Voltage	110 kV
	Transformer Impedance	R = 0.002 pu ; X = 0.18 pu
	Offshore Capacitance C_g	2.5 μF
	Diode Rectifier Model	Switched Model(12 Pulse DR)
	Offshore Q Compensation Z_f	49.6 MVAr
Collection Network	RLC Parameters(per km)	0.1 Ω;0.224 μF;0.366 mH
	Distance from PCC (S1, S2, S3, S4, S5)	6 km, 4 km, 2 km, 4 km, 6 km
WG Strings	Rated Power of unit WG«i»(S2)	10 MW
	Power Capacity (S«j»)	80 MW
	Transformer voltage	690 V / 66 kV
	Filter Resistance	0.0012 pu
	Filter Inductance	0.3 pu
	Filter Capacitance	0.1 pu
	VSC Model Type	Average Value Model
PQ Requirement	String level – S3	$P \sim= 0.6\ kW$; $Q = -2.16\ MVAr$
	Offshore Island Network	$P \sim= 0.8\ MW$; $Q = -14.12\ MVAr$
	Auxiliaries of WG in a String	$2.4\ MW; 1.16\ MVar(pf = 0.9)$
	Auxiliary supply for all WGs	$12\ MW; 5.82\ MVar(pf = 0.9)$
	Total Power Requirement	$23.69\ MVA$

Table 5.1: Network parameters for the Case Study

5.3 Assessment of Solutions for Black Start

In this section the various solutions feasible for black start of the offshore wind power system are discussed and elaborated briefly. Technical feasibility and some relevant criteria are used for comparison of the various features and to provide the challenges involved as well. Detailed cost analysis and comparison by using cost models are not the intention here. However, any cost indications and features suggesting that one solution may be cheaper or expensive than the other, have been highlighted.

The numbered grouping (1,2,3) for the solutions is done to categorize the type of solution based on the following description.

i. Additional VSC based solution either in series or in parallel with the DR HVDC system.
ii. Use of additional energy source, preferable avoiding the diesel generator.
iii. Using the tried and tested diesel generator – centralized or distributed.

The illustration of all the solutions is shown in the Figure 5.2

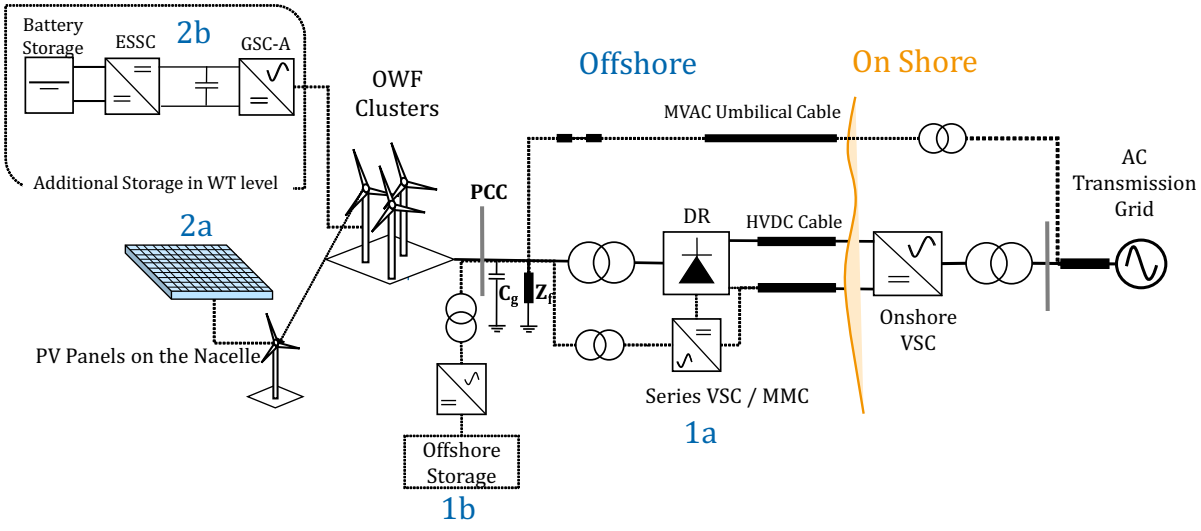

Figure 5.2: Illustration of Black Start Solutions possible for the OWPP system

5.3.1 1a. VSC in series with the DR

Solution 1a as indicated in Figure 5.2 is the use of a VSC or a Modular Multilevel Converter (MMC) in series with the DR. Such configuration is analyzed in [30], [31] in a detailed manner related to system design, control schemes and cost indications. Due to the bidirectional power transfer capability, the offshore VSC can now perform the black start by drawing power from onshore grid for the offshore loads and auxiliaries. In this case, the onshore MMC has to be of full bridge type so that the DR can be bypassed to connect the offshore MMC /VSC at a

reduced HVDC Voltage. The WGs may retain the grid following control scheme, because the offshore VSC is capable of regulating the voltage and frequency of the offshore AC grid. In [30], a Full Bridge (FB) MMC (in series with the DR) is designed to a third of the total OWPP power capacity. This significantly reduces the cost advantage of the DR-HVDC due to the cost and footprint involved with the installation of the MMC in the offshore platform. However, the added advantages of retaining WG control and active filtering by the VSC do exist in this configuration.

5.3.2 1b. Offshore VSC with a Centralized Energy Storage

In [96] an offshore storage platform with a VSC to ensure the islanded operation is proposed. This configuration can also be extended to perform the black start of the offshore grid for the DR-HVDC OWPP, either completely or partially. The VSC could be used also to ensure grid forming of the offshore network, providing the possibility for the WGs to retain their grid following control scheme, as in a conventional VSC-HVDC connected OWPP. The energy storage system (ESS) used here can also be considered for multiple purposes apart from the black start of OWPP, such as time shifting, power smoothing etc.

Investigations need to be made if a small sized VSC can regulate the voltage and frequency in a stable manner. It remains to be verified, if for a large OWPP, the use of PLLs in the grid following WGs, would be stable, with only one VSC in the entire offshore network regulating the frequency. There could be alternate solutions to this, for instance slight modification of the WG control to help in the frequency support or regulation.

5.3.3 2a. Photo-Voltaic Panel installations on the Nacelle of WGs in addition to other energy source

Another interesting proposition can be the use of Photovoltaic (PV) panels to provide a part of the required auxiliary power. In this case, no additional changes to the wind turbine structure is made to install the solar panels and only the surface area available on the WG Nacelle is used for the initial power estimation.

For machines with gear box between the PMSG and the turbine like the V164-9.5 MW [97], the available nacelle surface is approximately 192 m^2. Considering the installations like the heli-hoist platforms for WG service needs, it is safe to assume that only half of the surface area could be available, i.e. 96 m^2 for PV installations. By assuming a power density of 175 Wp/m^2 [98] for the PV panel, this available area can have an installation of 17.28 kW peak capacity. The factors like angle of inclination of the panel, the solar irradiance etc. and their effects on power production are not analyzed in detail at this point. But WG active power load is relatively larger compared to this capacity of PV panels that can be installed on the Nacelle surface. Assuming a 3% constant auxiliary requirement as nominal for the 10 MW WG, the power requirement

for self-sufficient operation is around 300 kW of constant load. Thus, alternate energy source / wind power has to be used during the black start, with the PV panels playing a minor role in the auxiliary supply (possible assistance in pitch or yaw actions).

5.3.4 2b. Distributed Energy Storage at WG level

As pointed out, dedicated UPS systems exist at WG level to provide the standby power. Additional battery storage could be required to maintain the WGs in operation beyond a certain duration. Thus, it could be a good approach to design additional energy storage system to ensure the black start operation at WG level. Two different configurations of energy storage integration can be used for this purpose, as shown in the Figure 5.3 and Figure 5.4, based on the review of existing solutions.

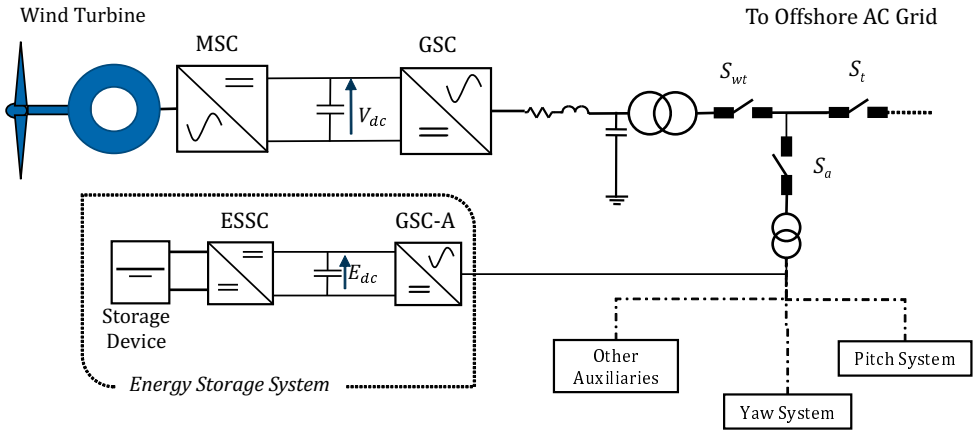

Figure 5.3: ESS integration at the AC side of the GSC

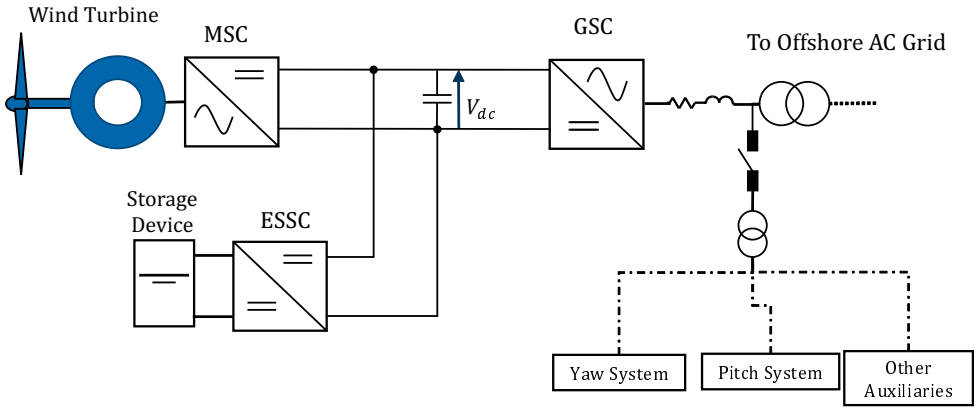

Figure 5.4: ESS Integration in the DC bus of the GSC back to back converter system

In the Figure 5.3, the storage device is connected to a DC–DC converter, indicated as the Energy Storage Side Converter (ESSC) and the auxiliaries can be powered through the Grid

Side Converter for Auxiliaries (GSC-A). In this case the DC link can be energized, for instance by the antiparallel diodes of the IGBTs in the GSC or by controlling the main GSC for DC voltage control function. Once the DC link is charged, the MSC can regulate this DC bus voltage. In Figure 5.4, the ESSC is connected directly to the DC link and the auxiliaries are supported by using a GSC-A connected to the storage device.

In both cases of ESS integration, the additional capacity could offer services like smoothing of wind power production, storage of surplus during low demand etc., for better usage of the capacity [99]. The choice of a particular configuration can be based on cost considerations, sizing capabilities of existing storage systems for a given WG manufacturer, available space in the WG platform, among others.

5.3.5 Assessment and Comparison of Solutions

A quick comparison is made of all the solutions discussed above in the Table 5.2. They are mainly compared on technical grounds. As it can be seen, the use of a VSC platform in the solutions 1a and 1b, provide for grid forming control in the offshore AC grid.

Although the detailed cost modeling and estimations are not done in this work, this qualitative assessment does highlight potential cost barriers involved due to certain features of the solutions. For instance, the use of additional PV panels, needs to be revisited by considering the available space, environment and maintenance issues. And also the use of an additional offshore VSC platform is known to be disadvantageous in terms of cost and it needs to be analyzed in detail for sizing. Based on a qualitative comparison, it is found interesting to compare the solutions with ESS, namely 1b (Centralized VSC + ESS) and 2a (ESS distributed in WGs) with regards to the sizing aspects.

No	Type	Energy Source	Comments	Control of WG Converters	Advantages	Drawbacks / Potential Issue
1a	Series VSC + DRU	Onshore Grid (through HVDC link)	Specifically Sized VSC	Grid Following Mode	Active filtering and Grid Forming by VSC.	Sizing of the VSC, and cost / footprint of VSC substation
1b	VSC offshore platform + Batteries	Dedicated VSC with battery as a separate platform	Active filtering and Grid Forming by VSC (feasible)	Grid Following Mode	Must Ensure charge of Storage. Additional platform. Investigation for stability with Grid Following WGs	
2a	Additional energy storage	Batteries	Additional Battery at WG level	Grid Forming Mode	Energy Storage exist at WG level, only question of upsizing and design	Coordinated Control among WGs, sizing / space requirements
2b	PV Panels + Battery	Photo Voltaic Panels in addition to Storage	In addition to minimum battery, use PV on Nacelle top of WGs	Grid Forming Mode	Use of hybrid Renewable Energy systems	Small Capacity on Nacelle Top and Maintenance of PV
3	Diesel Station / Mobile Unit	Diesel Fuel	Use Diesel fuel at WG level or additional station.	Grid Forming Mode.	Familiar Technology and years of working experience	High Insurance costs for Diesel, Maintenance issues.

Table 5.2: Comparison of the Different Black Start Solutions

Comparison of Centralized VSC and ESS vs Distributed ESS

In the section 5.2.4, the offshore auxiliary power requirement is calculated by assuming a constant auxiliary power requirement for the WGs, calculations using the network impedances and finally with support from simulations. The capacity of the additional storage to power both the WG auxiliaries and the offshore components is estimated at 24 MVA (approx). There is also a question of energy requirement itself, i.e. required energy consumption by the auxiliaries during the worst cases / for the duration of black start or the MWh sizing problem. This sizing entirely depends on the duration of black start and also the duration to ensure the energization of the offshore system either for WG health or for prolonged islanding. This indeed can be done with operation data of existing offshore wind farms, coupled with data of wind measurements and forecasts. As an example, the estimate in [31] puts the number of occurrences of wind speeds less than cut-in speed, for a duration greater than 3 days, at less than 10 times in the years between 1955-2000. These figures, are not useful for the precise design/sizing of the black start solution. However, they help in arguing that there are chances where the backup systems for the WGs, designed for a maximum of 24-36 hours, may fail to keep them in operation at all times during the lifetime of the OWPP.

In case of availability of the UPS backup systems, it is possible that they can also power the auxiliaries in their respective WGs. This reduces the power requirement / load on the black start source (battery storage, because for reactive power requirement it is necessary only to dimension the inverter). The table 5.3 highlights the requirement breakdown and the case where the UPS system is able to or not able to power the auxiliaries. In any case, the minimum design for the VSC station is for the total capacity of 24 MVA.

Offshore Load Types	**1b (with UPS)**	**1b (UPS failed)**	**2a (with UPS)**	**2a (UPS failed)**
WG Auxiliaries (12 MW; 5.82 MVar)	UPS	Additional VSC - ESS	UPS	Additional ESS
Offshore Transformer (0.8 MW)	VSC - ESS	VSC - ESS	WG	WG
Collection Network (-14.12 MVAr)	VSC - ESS	VSC - ESS	WG	WG

Table 5.3: Comparison of design requirements for solutions 1b and 2a for different cases

5.4 Conclusion and Research Prospects

In this chapter, the black start problem of the DR–HVDC based offshore wind power plant has been tackled. In the beginning the black start problem is clearly defined for the OWPP

system case. The relevant challenges and power / control requirements are laid out, with support from the existing literature. The existing solutions for black start - i.e. the MVAC umbilical cable or the diesel generator, prove to be disadvantageous. By using the existing literature and further analysis, the alternatives to black start solutions have been examined and compared with various qualitative criteria. The developed black start approach as part of this thesis work is not presented because of confidentiality reasons.

The possible extensions that form part of the future scope include

- Consideration for optimal placement and sizing of the energy storage, to minimize costs.
- Consideration of the cost models of the various black start solutions for a better comparison and analysis.
- Including the effects of wake, wind variations and other such variables, for better decision making when executing the black start sequence.
- Extension of the black start capability towards providing the restoration service to the onshore AC grid, as foreseen in the future for the OWPPs.

6

On the Faults and MTDC Integration of DR–HVDC OWPP

Contents

6.1 Introduction 122
6.2 OWPP Network Faults – Overview 122
6.3 Existing Fault Ride Through Strategies 131
6.4 Integration into an MTDC Grid 134
6.5 Chapter Conclusion 140

6.1 Introduction

This chapter attempts at providing a preliminary analysis of the possible faults in the Offshore Wind Power Plant (OWPP) with a DR-HVDC transmission. The available literature on Fault Ride Through (FRT) Strategies are discussed by considering the WG and the electrical network points of view. The different types of faults and possible ride through strategies are also suggested for the DR–HVDC OWPP topology, with support from the available literature.

An overview of the challenges regarding the integration (of this OWPP topology) into an MTDC grid, is also presented towards the end of this chapter. The focus here is to highlight the potential issues at the electrical system level for both normal condition and operation during possible faults / failures. This acts as a basic foundation for any future research works on the topic, as the solution to integrate this (or any) OWPP topology is significant for the future development of MTDC grids that would integrate huge capacities of offshore wind.

6.2 OWPP Network Faults – Overview

6.2.1 The fault response in traditional AC vs Inverter based Grids

The offshore WGs have gradually increased in size and of course in capacity. The predominant WG technology of today is the Type 4 WG, given the complete fleet of WGs by most of the manufacturers are of Type 4, above the 6 MW capacity is of this type. Grid integration with a HVDC transmission system, is a specific case, since the offshore AC grid, is decoupled from the main AC grid. If type 4 WGs are used, again, the mechanical rotating machine is decoupled from the offshore AC grid, due to the use of back to back (B2B) power converters in the WGs. Thus the offshore AC grid is fully an inverter based AC grid.

Traditionally AC power system faults, the associated responses and protection algorithms, rely largely on the operation and fault current provisions of the rotating synchronous machines. Such a rotating AC Generator can provide fault currents of up to six times the rated value for the first few cycles of AC wave during a fault, before reaching a steady state contribution of 2 pu [100]. The characteristic sub–transient, transient and synchronous reactance values (that change because of the winding temperature), influence the machine's natural response characteristics.

On the other hand, the offshore AC grid, being a 100% inverter (power electronic converter) based grid, the response of such a system during any fault, is largely dependent on the control system employed for the Grid Side Converter of each WG and the offshore VSC station [101] [102]. This also differentiates the fault responses of an onshore AC grid connected wind power plant from a HVDC connected OWPP. The common knowledge of fault protection methods in an onshore WPP, cannot be applied for the Offshore WPP. Thus, effort is made to understand the fault characteristics in the OWPP by using the available literature, first for a VSC-HVDC

connected system and then, for a DR–HVDC connected system.

6.2.2 LVRT Requirements for Generators

The Low Voltage Ride Through (LVRT) or FRT requirements are imposed by the Grid Codes of the concerned TSOs. In principle, it requires the OWPP to stay connected with the grid for a specific amount of time, as defined by the voltage versus time profile, and also during frequency variations. The LVRT requirement for the various European countries is shown in the Figure 6.1, as of 2013 [103]. Moreover, some of the European countries define the reactive power requirement to ensure an AC voltage support in the local region, as illustrated in the Figure 6.2. It is important to note that these requirements are imposed by considering different types of WGs and also for both onshore and offshore wind power plants. In the context of the OWPPs, all these above requirements must be applied at the point of coupling (at the onshore station) with the classical AC grid.

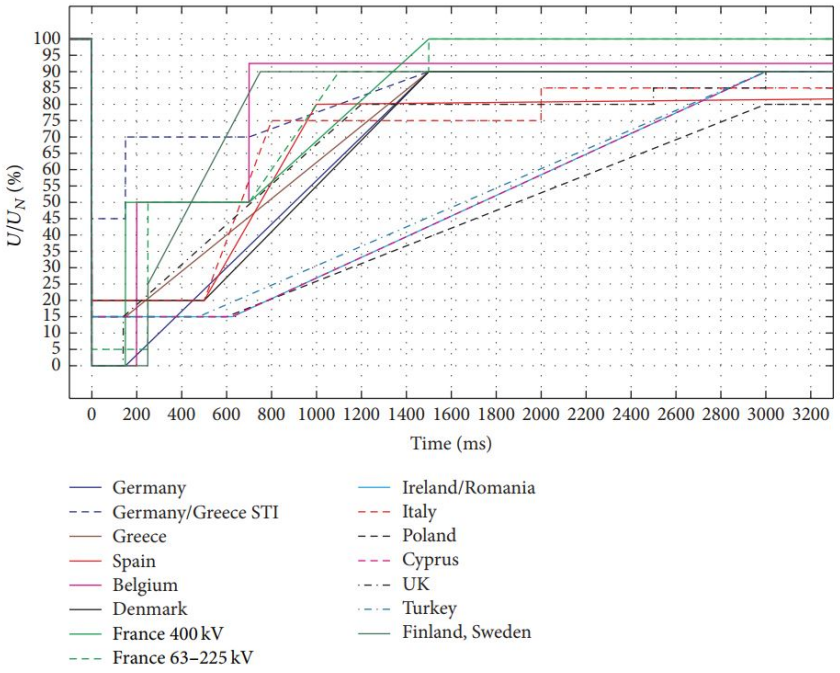

Figure 6.1: LVRT Requirements in Various Countries in and around Europe as illustrated in [103]

But, for the offshore AC grid in an OWPP with HVDC transmission, there are no fixed grid codes to be respected. The related literature focus on fast provision of fault currents by the WGs, and assume almost traditional protection strategies (overcurrent or differential) as in the case of an onshore wind farm network. They seem to suggest that a tuning of these protection devices coupled with a fault current provision by the WGs are the sufficient steps towards ensuring FRT of offshore faults [104][48][105]. This philosophy is retained in the following sections as well.

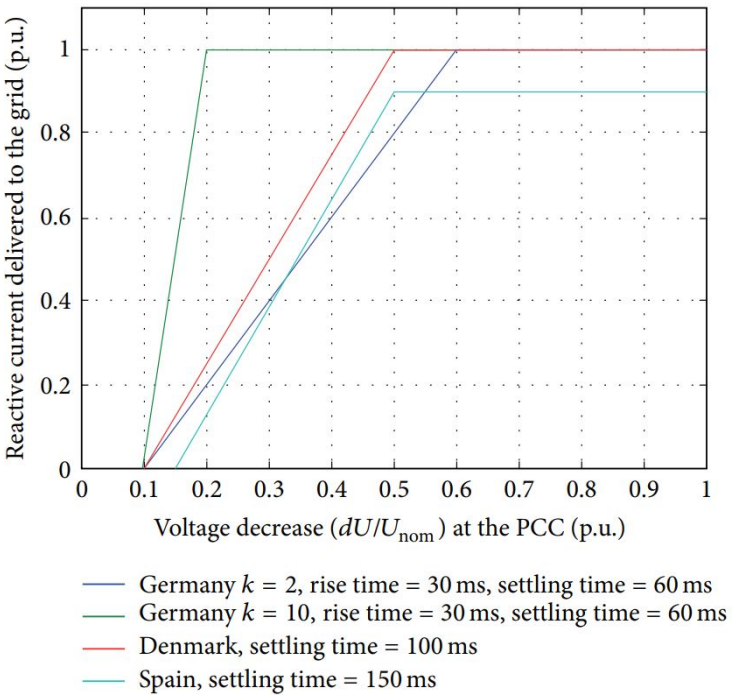

Figure 6.2: Reactive Power Requirement in proportion to the decrease in AC voltage in a few European Countries [103]

6.2.3 Fault Response of a Type 4 WG

The fault response of the type 4 WG is described in this section using the available literature. Generally, the fault response is dependent on the GSC controller, more specifically the setting of the current limit, Phase Locked Loop (PLL) response etc. The natural response related to the rotating machine (wind turbine generator) is non–existent due to the decoupling of the mechanical systems and offshore AC network by the B2B power electronic converters. Physical constraints require the current be limited at 2 pu, the limit at which the IGBT needs to be blocked [48]. However during faults the range of maximum current contribution is anywhere between 1.1 to 1.5 [104].

During a fault in the AC network to which the WG is connected, with a conventional grid following scheme in place (see Figure 6.3), the DC link voltage of the B2B increases quickly, since the active power is not evacuated. To avoid this, generally the excess energy is dissipated in a resistance with a DC chopper / crowbar in the DC link, once the over voltage in the DC link of the B2B converters is detected [106][107][108]. Along with this dynamic braking action, the pitch control of the turbine and power control for the converter may also be required to reduce the output power and avoid a mismatch between the power extracted and the output power of the generator [109].

For the Grid Side Converter (GSC), the general approach is to reduce the active current (d-axis component) contribution to almost zero and provide the maximum reactive current (q-axis

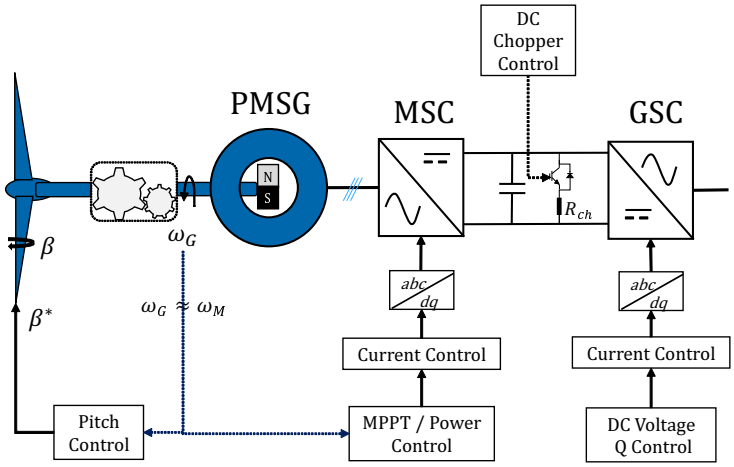

Figure 6.3: Typical Layout type 4 WG with Grid Following Scheme

component), when either in onshore WPP or in a HVAC connected OWPP [106]. Alternative proposals or modifications to the grid following WG control have been attempted for a better FRT response in the literature. In [110], it has been suggested to use the Machine Side Converter (MSC) to control the DC bus voltage of the B2B system while the Maximum Power Point Tracking (MPPT) or Power Control is done by the GSC. It argues that this change in the control functions of MSC and GSC ensures that no other additional measure is required for FRT. Thus DC chopper, used in the previous control strategy (see Figure 6.3), can be avoided with this approach. Additionally the torsional oscillations in the drive train are damped by using a specially designed damping controller. But here, the WG continues to inject a reduced active power to the AC grid and the AC voltage is maintained with the help of an AC voltage control by the GSC. This type of AC voltage control scheme is valid in the AC grid with dominant inductive impedance, where a prominent coupling between reactive power and AC voltage exists.

In [111] an extension of the abovesaid approach, the use of MSC for DC link voltage of the B2B power converters, is presented. The control scheme has been designed by using a feedback linearization technique. Also, experimental results for a PMSG of a few kW capacity has been presented in [111]. In [112] an Energy Storage System (ESS) is integrated in the DC link of the B2B power converters, to enhance the LVRT response. The MSC controls the active power flow and the GSC controls the DC link voltage in this configuration, as is the traditional scheme for WGs. During faults, the ESS takes over the control of the DC link voltage of the B2B converters, relieving the GSC of this control function. The GSC is operated like a Statcom, to provide reactive power to the AC grid according to the Grid code requirements.

All the above said FRT enhancements and control schemes for the WGs are valid to a large extent for the onshore AC grid requirements. For the offshore environment, especially for the HVDC integrated OWPPs, it is necessary that the WGs provide fault current contributions. The FRT capabilities of both the offshore VSC station and the WGs in a VSC–HVDC OWPP, have

been briefly mentioned in the section 2.5 of chapter 2 and are not revisited in detail here. The focus in the next section is to discuss the faults and failures related to the DR–HVDC OWPP system.

6.2.4 Faults in OWPP with DR HVDC Transmission

Some of the distinct characteristics of the DR–HVDC topology compared to the traditional AC power system and also the VSC–HVDC based OWPP topologies are highlighted below, for different faults in the system

1. For the faults in the offshore AC grid, compared to the VSC-HVDC topology, the DR-HVDC topology lacks the largest contributor to the offshore AC grid faults, the VSC transmission station, in the former. In this case, the most suitable protection strategy for the breakers is the differential scheme, combined with a coordinated over current protection scheme, as proposed for the offshore system in general [105].
2. For a fault in the bus bar at the PCC for instance, it is necessary to use a differential protection scheme [105], to provide selectivity and avoid its activation for faults in any of the string cables.
3. For DC grid faults, due to the passive nature of the DR, there is a continued injection of the current into the fault, until the DC protection system isolates the faulty DC link, while the WGs are commanded to reduce/stop power production.
4. For any asymmetric faults in the offshore AC grid, it is necessary to design control loops for both positive and negative sequence currents for the GSCs, as demonstrated in [48] [104].

6.2.5 Types of Faults and Failures

The different faults / failures in the DR-HVDC OWPP system are illustrated in the Figure 6.4. They are described briefly below:

i. **F1** is the fault at any of the cables inside the string including the cable connecting the WG with the offshore AC bus.
ii. **F2** is characterized as the failure of one of the DRUs in the offshore system. The 1200 MW OWPP system proposed by the industrial solution, consists of 6 individual DRU tanks connected in series on the DC side, with dedicated filters, breakers, etc. The failure F2 is the failure of one of these six units. Failure of two DRUs at the same time is not discussed as a failure case in this analysis.
iii. **F3** is a fault in any one of the cables interconnecting different clusters. One extra cable is also available in ring configuration (cab3 in the Figure 6.4).
iv. **F4** is a symmetric or asymmetric fault in the Onshore AC grid.
v. **F5** is a DC link Pole to Pole fault.

vi. **F6** is the internal fault of the VSC due to which an open circuit can occurs.

vii. **F7** is a failure or issue in any one of the WGs. The general procedure is to disconnect it from the offshore AC grid network and perform repairs.

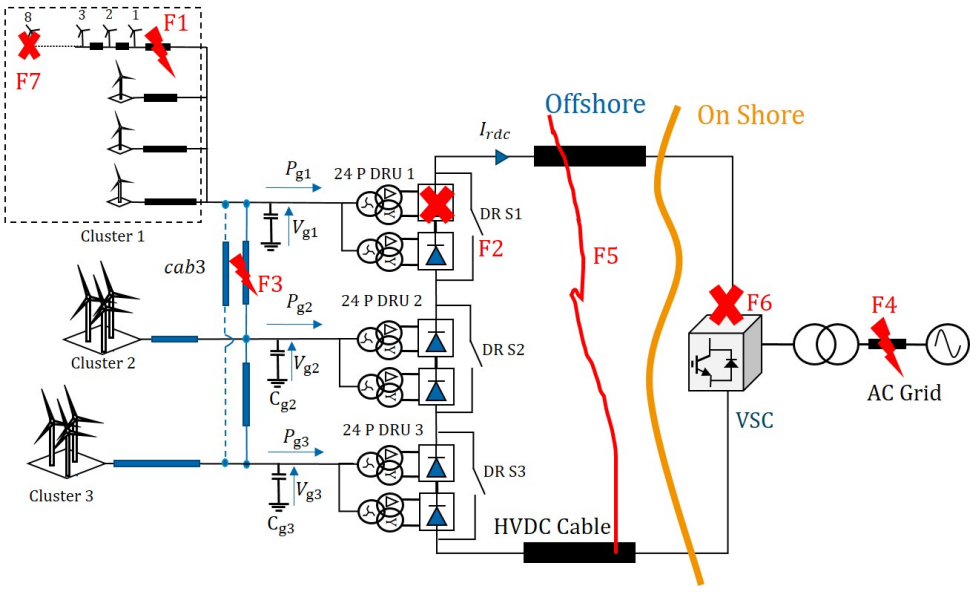

Figure 6.4: Various Faults and Failure cases in the DR–HVDC OWPP system

F1 – collection network cable fault

A symmetrical fault in one of the offshore string cables leads to the drop in voltage to zero, in the offshore AC grid. The presence of the DR ensures a natural blocking of the HVDC link contribution to any offshore AC grid fault. Thus, all of the WGs would feed into this fault as illustrated in the Figure 6.5 (a). For a symmetrical fault, the active power component of the current is decreased, detecting the drop in AC voltage below the nominal. Only the reactive current is fed in order to trigger the over-current/differential protection systems [59][48].

In case of an asymmetric fault in the offshore system, the negative sequence current injections of the GSC also need to be controlled, to avoid power oscillations and instability that may result during the restoration. However this also depends on the type of control scheme implemented, and any new control solutions for the grid forming have to analyzed in detail, as done in [48] for instance. This work proposes the control of positive and negative sequence currents in an arbitrary synchronous (dq) reference frame, suppressing completely the negative sequence currents.

Once the faulty part of the string is isolated (by the breakers $BG1$ and $BS1$ as seen in the Figure 6.5 (b)), to ensure maximum power transfer, all the upstream WGs need to be reconnected to the PCC. If the string consists of a ring configuration, the power production of all the WGs

can be resumed as illustrated in the Figure 6.5 (b). while in case of a radial configuration, these WGs have to power down and await the repair / re-installation of this AC cable section.

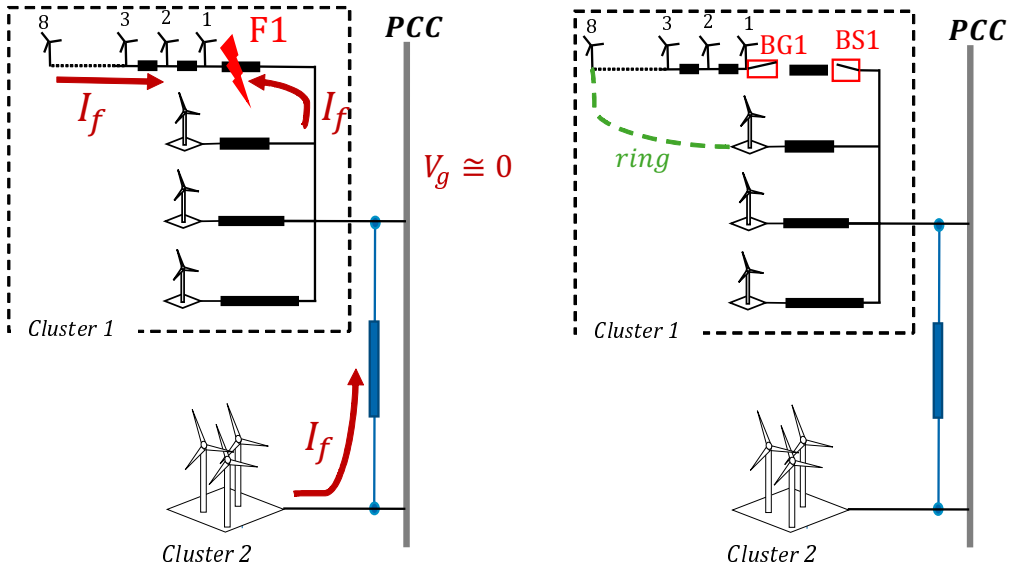

Figure 6.5: Illustration for Fault case F1 (a) Fault Instance (b) Post Fault Condition / System Restoration

F2 –Failure of a Diode Rectifier Unit

The diode rectifier platforms are connected in series to enable the evacuation of more power evacuation from the OWPP and build the rated voltage to any designated HVDC voltage (for instance, 640 kV DC). Here, three 24 pulse DRs are used and the configuration is achieved by using zig zag primary windings in all of the transformers to have a phase shift of 15° between each secondary winding of the transformers [11]. Thus, the failure of one of the DR stations leads to the drop in the HVDC voltage capacity of the DRs by a third. Two of the possible solutions are:

1. The need for a full bridge MMC (illustration in the appendix B) station on shore, so that the DC voltage can be reduced to two thirds of the rated value.
2. The use of hybrid half bridge–full bridge as suggested in [113], to have a trade-off for cost and power losses between the use of half bridge and full bridge MMCs.
3. If a half bridge MMC is used for the onshore station, then, the failure of one DR station leads to the loss of the entire offshore wind capacity. To reach the HVDC voltage level, it is not an option to operate the entire offshore AC grid at a higher voltage as it would turn out an expensive investment (sizing up all the equipment like submarine cables, WG transformers etc). Alternatively, the following solutions are possible:

(a) The over sizing of one or more of the DRU stations and provision of tap changers for its transformers to enable a higher HVDC voltage capacity.
(b) The installation of tap changers in the onshore transformer (connected to the onshore inverter station), so that the available AC voltage at the MMC station can be reduced and finally, the HVDC link can be operated at a reduced voltage.

The option 1 is proposed in today's literature and also in the industrial solution. The main issues with alternatives 3(a) and (b) are additional costs, the slow operation of tap changers and also a need to analyse their dynamic performance.

Considering the availability of a full bridge MMC, once the DR failure is detected, it is tripped from the network, and the ring network enables the alternative path to the AC power from different clusters. If the DRs and the transformers are not over-sized, the power production may have to be reduced in case of high wind availability. The central OWPP commands the override of local MPPT implementations, and the new power limit is communicated to all the clusters and the individual WGs.

F3 – Fault in cables interconnecting clusters

The inter-cluster cable connection, is to uniformly distribute the power transmitted by each of the DR stations. If all the three clusters have equal power production, these cables transmit very less active power, apart from reactive power for compensation. Thus, a differential protection scheme for relays connected is the best fault detection scheme for this cable. This is because a fault in the inter-cluster cable (F3) leads to the feeding of fault currents by the WGs. The offshore AC grid voltage drops to zero. The GSCs are controlled such that the active power injection is immediately reduced to zero and the reactive currents are provided to trigger the differential protection scheme.

In case of loss of one of the inter-cluster cables, power production can be resumed by isolating the faulty cable and the inter-cluster cable cab3 (normally disconnected) is included in the network. This provides a backup in case of failure of one of the inter-cluster cable.

F4 – Fault in the onshore AC grid

A fault (F4) in the onshore AC grid leads to the AC grid voltage at the connection terminal to reach almost 0 pu and the wind power extraction by the onshore station is not possible. But the OWPP, due to the grid forming control, maintains the voltage and continues to inject active power through the HVDC link. There is a need to rapidly communicate the rise in the HVDC link voltage to the OWPP controller so that all the WGs are controlled to operate accordingly (for instance by a form of implementation as in [114] for a fast de-loading of the turbines based on HVDC voltage measurement). As this is detected, the AC voltage reference is immediately set to a limit (say 1 pu) for all the GSCs and the active power limit is also set, to maintain the

wind farm in island mode. During the complete reduction of power, the dc chopper may have to be used at each WG level, to dissipate the wind power that cannot be exported through the HVDC link.

Alternatively a crowbar (DC chopper connected to a resistor) can be installed at the onshore station, and it can be used to dissipate the power injected by the OWPP, without any additional communication signals and control operations at the WG side. Of course there is an additional cost for this crowbar rating [49], compared to the crowbars at the WG level.

F5 – Fault in the HVDC link

A pole to pole fault in the HVDC link (indicated as F5) is a rare event, if the two poles of the HVDC cables are laid separately with some distance between them. However, it is the most severe of the DC faults. Generally, a contribution to this fault, is the continuous injection of current by the generators into the fault in the DC link, once the fault occurs. The difference between this fault and the onshore AC grid fault (F4) is that the WGs do not naturally feed into the fault in the latter, while in the former, there is natural contribution to the fault because of the DR. If full bridge MMC is used in the onshore station, the converter does not need to be blocked and can continue to provide reactive power to the onshore AC grid[83].

Once the fault occurs, the HVDC link voltage drops to zero. The offshore AC voltage also drops, since it is clamped to the HVDC link voltage (DR operation characteristics). But, the value may not be zero, since the WEGs are in grid forming mode and feeding the fault. The dc current may have oscillations due to the passive components of the DC link [83]. The control requirements include:

1. The decrease of the active power to zero in the WGs. If not, the power imbalance between generation and extraction may lead to acceleration of the their turbines or an overvoltage in their B2B converters, depending on the duration of the fault.
2. The provision of reactive current by the inverters, so that the protection system trips the offshore AC network from the DC grid.
3. The onshore MMC has to control the DC current, which is feeding the fault to zero, since a high current contribution through the MMC station can damage the power electronic components [83].
4. The WGs, could be operated in islanded mode and the offshore PCC is disconnected from the DR station, until the HVDC system is restored for power transmission.

F7 – Wind Turbine Failure

A wind generator failure can arise due to many reasons. The gear box, generator, pitch / yaw drives, turbine blade related issues, bearings for the various equipment, power electronic devices are some of the major equipment susceptible to a failure. Although, the cost for each

failure can vary, the repair usually requires a visit to the wind turbine site – either by boat, or if possible by air. The nacelles of the new wind turbine designs consist of a Heli-hoist platform to enable access for maintenance and repairs by a helicopter. Thus, the cost and the repair time of the failed equipment are important in deciding which failure is more crucial.

The annual downtime in days is presented for a WG in the Figure 6.6, sourced from [115]. The failure of a WG due to any of its components is considered as a tripping event, as the breaker of the WG is used to disconnect it from the offshore network. It is seen that electrical components lead to slightly higher downtime. The trend for wind turbines has been to perform condition monitoring and fault diagnosis [116] in general and it has continued for offshore wind farms as well [115]. Such approach is especially useful for the Operation and Maintenance (O&M) aspect of the OWPP, to estimate remaining lifetime of a component in a particular WG and plan in advance maintenance activity [115]. Increasing the efficiency of the O&M activities has the potential to contribute towards decreasing the Levelized Cost of Electricity (LCOE) of future OWPP projects [117].

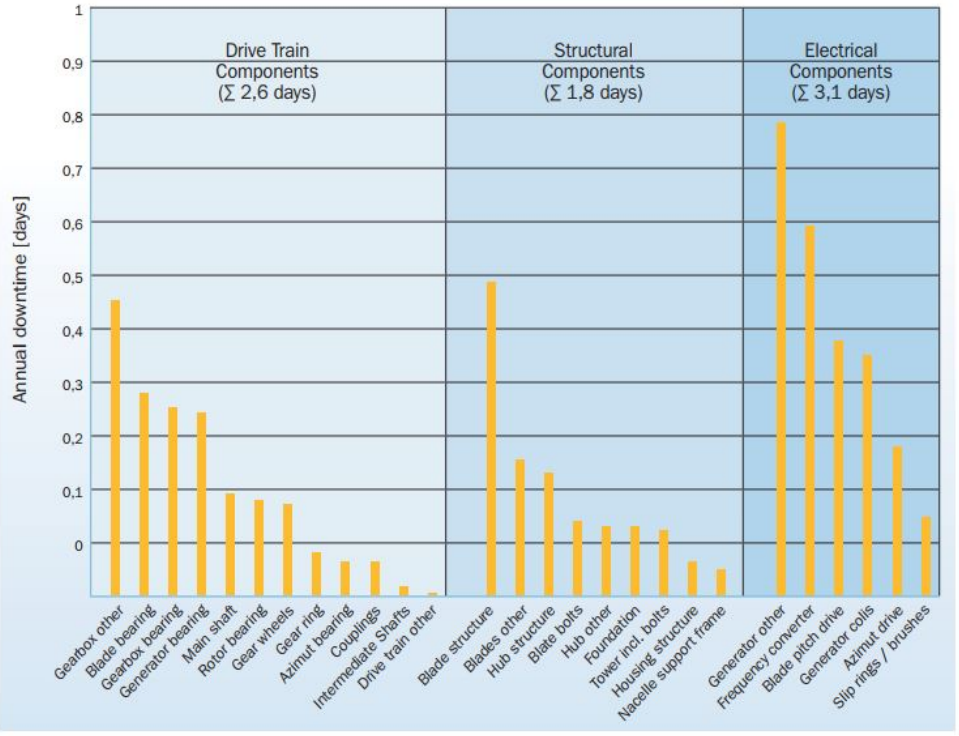

Figure 6.6: Annual down time in days for different components of a WG. Courtesy: [115]

6.3 Existing Fault Ride Through Strategies

The control solution implemented for the WG for this DR-HVDC topology, dictates the responses during the various faults and thus, a detailed analysis has to be done with a given

control solution. Also, additional FRT strategies have to be implemented and validated for the fault cases. In case of grid forming WGs, it is important that they are capable of maintaining the frequency relatively constant during faults and ensure fault current contribution, without causing adverse mechanical impacts to the turbine.

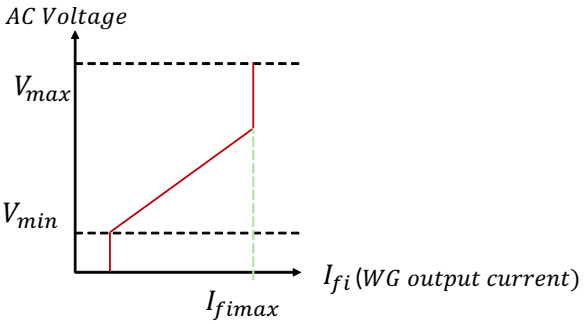

Figure 6.7: Principle of VDCOL Strategy - Current Contribution vs Voltage Level

The existing FRT strategies for the WGs in the literature, particularly those implementing the grid forming control scheme are discussed here. One of the first analysis and FRT schemes for DR-HVDC based OWPP has been presented in [118]. Grid Forming WGs have been used and the FRT strategy termed Voltage Dependent Current Order Limit (VDCOL) was used to provide the maximum reactive current contribution during faults. The crowbar (DC chopper with resistor) have to be used in the WGs, for the dissipation of excess energy, during the fault in the offshore grid. The principle of VDCOL is to inject q-axis current contribution according to the voltage measured at the input (illustration in the Figure 6.7). Thus the WG suppresses d-axis current and injects q-axis current, according to the measured voltage level measured, as per the following equations.

$$I_{fiq} = \left|I_{fi}\right|_{\max} \tag{6.1}$$

$$I_{fid} = 0 \tag{6.2}$$

where

$\left|I_{fi}\right|_{\max}$ is the maximum current limit for the GSC,

I_{fid} is the d-axis current contribution of the GSC,

I_{fiq} is the q-axis current contribution of the GSC.

In [48] a similar strategy has been implemented for the grid forming control designed previously in [62], with a detailed analysis of the protection strategies to be used for offshore AC grid faults. Here the principle is to increase q–axis current contribution, according to the error between the voltage set point and the measured voltage, as illustrated in the Figure 6.8. The d-axis current contribution is suppressed.

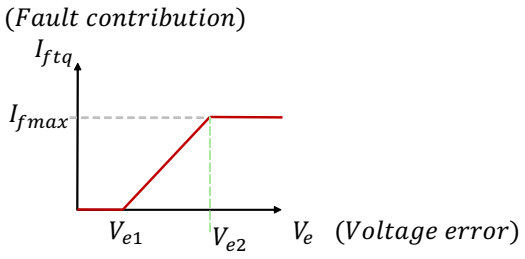

Figure 6.8: FRT contribution based on Voltage Error, as per the strategy in [62]

The current contributions are calculated as shown in the following equations:

$$I_{ftq} = 0 \text{ if } \left(V_{fd}^{*} - V_{fd}\right) \leq V_{e1} \tag{6.3}$$

$$I_{ftq} = \frac{I_{f\max}}{V_{e2} - V_{e1}} \left\{ \left(V_{fd}^{*} - V_{fd}\right) - V_{e1} \right\} \text{ if } V_{e1} < \left(V_{fd}^{*} - V_{fd}\right) \leq V_{e2} \tag{6.4}$$

$$I_{ftq} = I_{f\max} \text{ if } \left(V_{fd}^{*} - V_{fd}\right) > V_{e2} \tag{6.5}$$

where

I_{ftq} is the fault current component to be added to the q-axis current reference,

V_{e1} and V_{e2} are voltage error thresholds for the minimum and maximum fault current contributions,

$I_{f\max}$ is the maximum current limit of the inverter.

6.3.1 FRT at system level for Onshore AC grid Faults

The VSC-HVDC system presented an interesting alternative to ride through the onshore AC grid faults. The offshore VSC station, may be controlled in such a manner (AC voltage reduction, frequency variation) that the onshore AC fault condition is indirectly communicated to the WGs [42]. But, in the DR-HVDC topology, there is no such possibility. Thus some of the ride through measures feasible (in case of onshore AC grid faults) include:

- A DC chopper controlled resistor or crowbar [49] at the onshore station (which may be present as a backup measure) to reduce power transmission to the onshore grid. Here the WGs may operate without any additional control actions.
- Fast communication of the fault information to the Offshore cluster controller, to reduce and activate safety measures in each of the WGs. This usually involves decrease of the power set point at the WG converter level. It may be required to activate the crowbar in each WG, to dissipate the excess energy from the wind turbine during the fault.

In case of a fault in the HVDC network, the DC protection systems have to be in place to isolate the faulty network. Considering that the HVDC link is unavailable post after the fault, the offshore AC grid have to be operated in the islanded mode, awaiting further control command from the OWPP operator.

6.4 Integration into an MTDC Grid

Today, there are quite a few of Multi Terminal DC Grids considered for development (with a few already existing), that use VSC based converters [119]. Especially in Europe, such grids are proposed in order to reinforce the existing AC grids system, to provide mode flexibility in transmission and most importantly, to integrate large renewable energy plants like OWPPs [120]. Given the large economic advantages provided by the DR-HVDC OWPP topology and the importance of the MTDC grid, a thorough analysis of the various operational aspects of integration of the former into the latter is deemed necessary towards future power system planning and development.

This section gives an overview of the challenges concerning the integrating a DR–HVDC based OWPP into an MTDC grid. The theoretical analysis, includes the issues related to the normal operation and also in case of faults and failures. The characteristics of faults are defined along with certain failure cases and the possible solutions are explored.

6.4.1 Overview of the MTDC Grid operation

Different architectures of MTDC grids are feasible, namely radial, meshed or series connected. For simplicity, a radial configuration is considered for analysis in this section. There are two major approaches in literature towards the control of an MTDC grid – namely the Master-Slave (or slack bus based) control and the droop control [121]. In the former, a single VSC station in the MTDC Grid is in charge of controlling the DC voltage and is termed the slack bus while the remaining stations control the power flowing into and out of the HVDC grid. This method needs no external communication, and requires sufficient power reserve at the slack bus station to maintain the DC link voltage. Moreover, this type of control implementation is also a single point of failure for the entire MTDC grid. Alternative to a single slack bus, is the implementation of the back-up slack bus (or Master) [122], increasing the system level reliability.

However, such additional backup slack buses continue to inherit the constraints associated with the Master-Slave approach. The problems can be exacerbated by factors like coping up with the loss of a converter station (N-1 contingency problem), the physical locations of the slack buses, physical size of the MTDC grid and capacity of associated AC grids in each stations [122]. Thus, the droop control of MTDC grids is the preferred method [123], which is

classified into two types, namely - the Voltage–Current droop and the Voltage–Power Droop. The Voltage–Power droop adopted in [124] is considered for discussions here. Moreover, similar to the classical AC grid, the future MTDC grids may need to have a hierarchical control structure with primary, secondary and higher levels of control loops for dedicated control actions. The generalized $V_{DC} - P$ droop relationship is illustrated in the Figure 6.9. The power reference for a given VSC station is derived as follows:

$$P_{ac} = P^* - g\,(V_{dc} - V_{dc}^*) \tag{6.6}$$

where

– P_{ac} is the active power set point for a given MTDC station, negative value implies that the station is extracting power from the MTDC grid (inverter operation), with inclusion of the droop control contribution (MW),

– P^* is the actual active power set point of the station (MW),

– V_{dc} is the HVDC link voltage, a common value across the stations (kV),

– g is the droop constant for the contribution by a given station (MW/kV),

– V_{dc}^* is the reference for the HVDC voltage (kV),

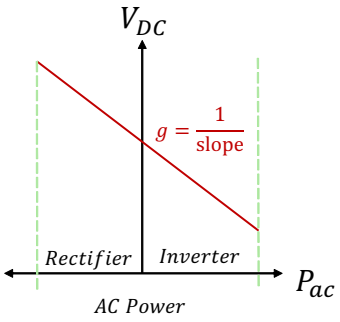

Figure 6.9: DC Voltage and Power Droop relationship Curve for a VSC station

6.4.2 Operation of a Three Terminal MTDC Grid with DR-HVDC OWPP

A simple configuration of MTDC Network is considered for analysis and discussion in section. A radial connection of three converter stations with one DR-HVDC station, is shown in the Figure 6.10. A preliminary analysis on the operational characteristics and the possible approaches towards control and power management of the entire system are performed in this section.

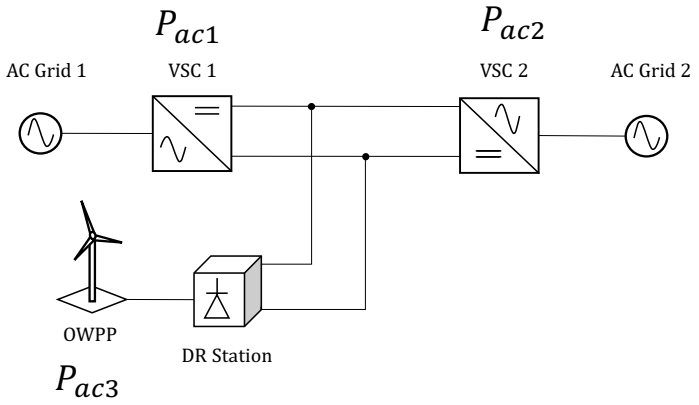

Figure 6.10: A Radial three terminal MTDC grid with DR-OWPP station

Use of Half bridge or Full bridge MMCs

Regarding the VSC stations, the use of MMC full bridge converters may not be feasible or practical for all cases. For instance, situations like integrating the DR-HVDC OWPP into an existing point to point HVDC link, cost factors among others, may lead to the assumption that only half bridge MMC technology is being used for all the VSC stations. Thus, as in the case of the VSC–HVDC based OWPP, the failure of one DR station among multiple series connected stations for the OWPP, leads to the loss of the entire OWPP.

Control of the MTDC Grid

In [69] such a network was chosen to implement a Master–Slave based control of the DC grid. Considering the three terminal MTDC in the Figure 6.10, one of the stations is an uncontrollable DR station. Owing to the above said shortcomings of such a Master - Slave control scheme and to the future development / extension of the three terminal connection, a droop based control approach is suggested. The droop based scheme is said to enhance the dynamic behavior of the MTDC grid, as demonstrated in [123], which analyzed a DC grid with VSC-HVDC based OWPP. A typical Voltage–Power droop control scheme is shown in the Figure 6.11.

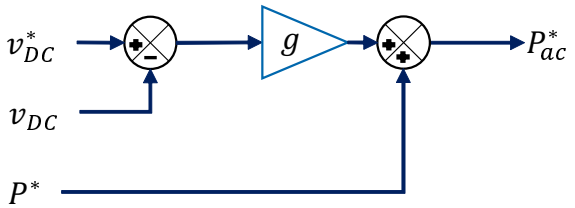

Figure 6.11: Generic MTDC grid Droop Control scheme of the MMC stations

Based on the droop relationships illustrated in the Figure 6.9 and elaborated previously by

using the equation 6.6, the power references are set for each of the stations as follows:

$$P_{ac1} = P_1^* - g_1 \left(V_{dc} - v_{dc}^*\right) \tag{6.7}$$

$$P_{ac2} = P_2^* - g_2 \left(V_{dc} - v_{dc}^*\right) \tag{6.8}$$

$$P_{ac3} = P_{owpp} \tag{6.9}$$

Further analysis remains to be done on the development of MTDC models and integration of the droop control schemes for the VSC stations and the grid forming control scheme for the WGs in the OWPP. This can be a subject of future work.

6.4.3 Faults and Failure Modes at System level

Some of the major faults possible in the MTDC network with DR–HVDC OWPP terminal are indicated in the Figure 6.12. This is more of an extension of the Figure 6.4 and the related offshore AC grid faults are not represented in detail. As pointed out in the literature, the loss of one of the stations causes a huge impact in the operation of the MTDC grid. The VSC stations and the concerned AC grid should be capable of coping with this event.

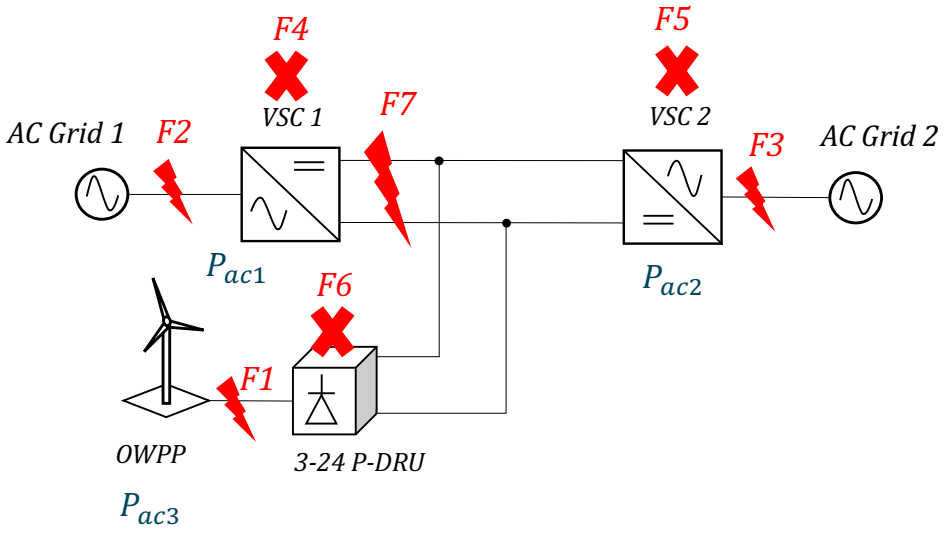

Figure 6.12: FRT contribution based on Voltage Error, as per the strategy in [62]

A brief analysis is made on the type of faults and the required control actions. Important failure modes and the possible solutions to some of them are highlighted as well. It is assumed that both stations are evacuating power from the MTDC grid, at the instance of the fault. The fault types and failures to be briefly analyzed in the following sections include:

1. F1 is a fault of any kind in the offshore AC grid - for instance a string cable failure, inter-cluster cable failure. It excludes the failure of a single or few WGs as its impact is

considered to be negligible, at the MTDC grid level.

2. F2 and F3 are the faults in the AC grids 1 and 2 respectively and they may be of symmetric or asymmetric in nature.
3. F4 and F5 denote the failures of the VSC stations 1 and 2 respectively.
4. F6 is the failure of one of the DR stations (out of multiple DR platforms connected in series, as illustrated in the Figure 6.4)

The fault F7, which is associated to the DC link, is not analyzed here, because the MTDC grid protection is in itself a vast topic.

Faults in offshore AC grid in OWPP

Based on the FRT implementations discussed for a grid forming WG, as in [48], the control implementation immediately decreases the active current contribution and increases the reactive current contribution, in the event of a fault F1. The DR is no longer in conduction mode and at the MTDC level, this is seen as the loss of a converter station during the fault duration. For the AC grids 1 and 2, if the surplus of power is exported from the OWPP, they both experience a loss in the active power availability. These stations have to act based on the available power reserve to regulate HVDC voltage, based on the implemented droop scheme. Key takeaways here are:

1. Fast recovery from the fault and restoration has to be enabled by reliable WG control implementations and the offshore protection system.
2. Duration for repairing the faulty part and scale of the fault is also important. The fault in a single string or array cable, which requires a cable replacement, still can allow the OWPP to continue operation. Here the loss of power is not significant.
3. In case of faults in two inter-cluster cables (as illustrated in the Figure 6.13), only the backup inter-cluster connection is available for use i.e. *Cab*3, which is connected between Clusters 1 and 3. In this case if the recovery takes longer due to permanent faults, it is necessary that all the clusters should be operated with almost same power production, for a smooth operation of the system. This requires additional commands and control efforts at the OWPP controller level.

Faults in one of the AC grids 1 or 2

A fault in one of the onshore AC grids (1 or 2), leads to a power imbalance in the MTDC grid, as power from the OWPP cannot be evacuated by the station which is connected to the AC grid exposed to the fault. Thus the result is a fast increase of the HVDC voltage. It is necessary that the onshore MMC station associated with the fault reduces the active current injection and operates as a statcom, providing fault current contribution to the AC grid. Possible measures to tackle a fast increase of the HVDC voltage include:

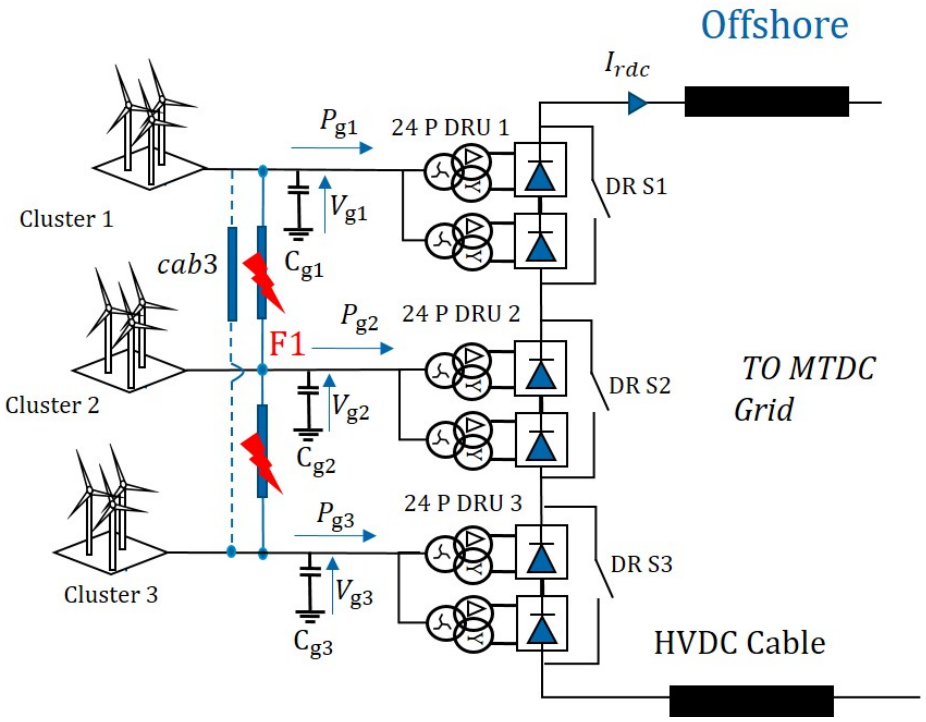

Figure 6.13: Illustration of faults in two inter-cluster cables in the Offshore AC grid

1. Detection of the HVDC voltage rise and using the signal to decrease the wind power production and if required activate reactive current injection by the WGs in order to disconnect them from the station.
2. Detection of the HVDC voltage rise and command the use crowbars at each WGs.
3. Use the HVDC chopper at the onshore station associated with the AC grid fault, to prevent active power injection into the fault. Is is pointed out in [125] that DC chopper can slightly compliment droop control actions of MMC stations, if there is a lack of power reserve, for an onshore AC grid fault.

Failures of the VSC stations 1 or 2

A failure of one of the VSC stations causes a lack of the power transmission capacity from the MTDC perspective. If the failure extends for a relatively long duration, the associated onshore AC grid suffers a deficit in active power. Also the OWPP cannot produce at full capacity, if its production exceeds the transmission capacity of the MTDC grid. It is recalled that both the VSC stations 1 and 2 are exporting wind power injected into the MTDC grid i.e., they are operated in inverter mode.

If the healthy station has not enough power reserve, the maximum power limit for generation ($P_{ac3}(max)$) value is reset for the OWPP controller. The OWPP cannot operate in MPPT mode at all times and is subject to this maximum limit $P_{ac3}(max)$. At the instance when the failure of

the VSC station occurs, the burden of DC voltage control falls on the other VSC station. Rapid power reduction can be done either by reducing production at the WGs or use of DC chopper at the VSC station suffering failure. Once the failed station is disconnected from the MTDC grid, it becomes a point to point HVDC link, extracting wind power with a certain limit on the power production, depending on the available power reserve at the healthy station.

Failures of one of the DR stations

If the failure F6 occurs, i.e. failure of one of the DR stations, there is a fall in the total voltage built by the remaining DR stations connected in series. Two cases are possible with respect to the MTDC design:

1. If all the stations consist of Full Bridge MMCs or Hybrid Half Bridge-Full Bridge MMCs, they can be coordinated to reduce the HVDC voltage, so that the switch DR S1 (as seen in the Figure 6.13, for the failure of the DRU station 1) is bypassed to connect the OWPP to the MTDC grid. Although the availability of the OWPP is increased, there is an additional cost due to the use of Full Bridge MMCs.
2. If all the VSC stations employ half bridge MMCs, the HVDC voltage cannot be reduced. Thus the entire OWPP has to be powered down and the production can be resumed once the failure is repaired. Thus the installation of the bypass switches DR S1/S2/S3 (in the Figure 6.13) can also be avoided

6.5 Chapter Conclusion

This chapter has presented an extended literature and preliminary analysis on the various faults in the offshore wind power system with a DR–HVDC transmission. A literature survey is done on the existing fault ride through strategies for the various faults both from the WG and the HVDC converter perspective, focusing especially on type 4 WGs and VSC-HVDC OWPP topology. The existing literature for DR-HVDC OWPP topology are rather only handful and the approaches adopted in these works are presented, especially for grid forming WGs.

Following this, an extended literature survey is made on the general operation and control of MTDC grids. The challenges related to the integration of DR-HVDC based offshore wind power plant into a three terminal MTDC grid are highlighted, with brief discussions on various faults and failures at the system level. Possible ride through measures and impacts on the system serve as the foundation for future research on this subject.

Future works possible based on the existing literature and the preliminary analysis done here include:

1. Dynamic modeling and analysis of the OWPP with DR–HVDC integrated into the MTDC grid, with droop control implementations for the VSC stations.

2. Detailed analysis of all the faults and failure modes by using the models and EMT simulations for the DR–HVDC based OWPP integrated into the MTDC Grid. The studies can be extended using benchmark models or possible future MTDC grid configurations.
3. Investigate any degrees of freedom available at the OWPP level, to allow better dynamic behavior of the MTDC system during the various faults.

7

Conclusion

Contents

7.1 Summary and Major Conclusions 144

7.2 Future Prospects for Research Work 145

7.1 Summary and Major Conclusions

Combating climate change and promoting sustainable growth is the need of the hour for the world. The decarbonization of the energy mix by renewable energy (RE) development facilitates the reduction of green house gas emissions, apart from providing supplementary benefits like socio-economic growth. The European Union has been setting and revising ambitious targets for renewable energy capacity in the total energy mix and has made fast progress. The development of offshore wind serves as one of the important contributors to the increase of renewable energy capacity, especially in many of the European countries.

But it is a necessity that the Levelized Cost of Electricity (LCOE) of offshore wind energy be competitive with the onshore wind and in turn with the conventional sources of energy. Constant research and innovation efforts have been directed towards the rapid development of the integral aspects of offshore wind such as wind turbine technology, transmission solutions, collection network solutions, turbine foundations etc. In line with these efforts, alternative topologies are also explored for grid integration of large OWPPs. The DR–HVDC transmission, which consists of a point to point HVDC link with a diode rectifier based station to evacuate all the offshore wind, is seen as a promising solution to drastically reduce the cost, footprint, losses and increase reliability compared to the VSC–HVDC transmission solution prevalent today.

But the industrial solution of today relies on specific innovations related to the WGs and the use of an AC umbilical cable for start–up and the full bridge MMC. It is deemed necessary to understand the DR–HVDC topology in a detailed manner to see if further cost reductions are feasible and also if the current and future power grid requirements for OWPP grid integration are respected. Some major challenges that have been identified for successful grid integration of the DR-HVDC OWPP include offshore AC grid control, grid forming, reactive power sharing among the wind generators, black start alternatives to the AC umbilical cable, fault studies and ride through strategies and finally, the integration into an Multi Terminal DC Network (MTDC Network). This thesis attempted at tackling some of the above challenges in an elaborate manner, while the remaining issues have been discussed with the support of existing literature and preliminary analysis.

Chapter 2 attempts at providing an overview of the offshore wind power system and its various aspects, establishing a solid background for the thesis work. In addition to this, the DR-HVDC system operational characteristics are briefly presented, following which the various challenges for grid integration related to this topology are presented.

Following this overview, in chapter 3, the dynamic modeling of the offshore wind power system is presented. With regards to this, the offshore system dynamics were studied for different modes of operation separately. It was revealed that, dynamic couplings of P–V (active power and AC Voltage) and Q–f (reactive power and grid frequency) exist, for both island and connected modes of operation.

The different grid forming solutions available in the literature are reviewed in detail in chapter 4. Focus is on the comprehensive theoretical comparison to highlight the different features of each solution and evolution of the various approaches. As a step further to this review and comparison, the assessment of selected solutions is done by using a study case OWPP model and time domain simulations. One of the solutions is analyzed for varying the reactive power contributions by the WGs for different droop coefficients and in fact, a similar approach can be extended for any of the solutions. Also, if a solution to synchronize the WGs is enabled by an external signal source (like Radio / GPS), additional timing sources (for instance, GALILEO) can be used to increase the reliability and avoid a single point of failure. The comparison and assessment performed in this chapter can serve in establishing a strong knowledge base and help in future research works towards enhanced control implementations.

Chapter 5 tackles the challenge of offshore AC grid black start. Based on the existing literature and further analysis, the alternatives to black start solutions have been examined and compared with various qualitative criteria.

Chapter 6 presents an extended literature and preliminary analysis on the various faults in the offshore wind power system with DR-HVDC transmission. The focus is on the Fault Ride Through (FRT) strategy implemented for the control solutions for both grid following and grid forming WGs. Then, one of the approaches is implemented in the droop based Grid Forming control scheme (devised in chapter 3). The FRT implementation is validated by using time domain simulations in a selected study case, for a three phase fault in one of the string cables in the offshore AC grid. The WGs activate the FRT logic after the fault occurs and succeed in providing maximum reactive current contribution and decreasing the active current components.

In the final part of the chapter, an extended literature survey is made on the general operation and control of MTDC grids. The challenges related to the integration of DR-HVDC based offshore wind power plant into a three terminal MTDC grid are highlighted. The importance of voltage droop control (DC Voltage-Active Power droop) implementation for the two MMC based terminals in the MTDC grid is highlighted and future studies should be focused on the analysis of such implementations while integrating a DR-HVDC terminal. A brief analysis is performed on the various faults and failures and possible ride through measures for the above-said the terminal network.

7.2 Future Prospects for Research Work

The following prospects are proposed for future research works. These are proposed, based on the progress of the thesis work as well as the current and future requirements for the grid integration of offshore wind energy.

I. A framework has to be devised to compare the various black start solutions in terms of cost and overall advantages, considering different case studies.

II. Explore the extension of a given offshore black start solution to provide the system restoration services to the onshore AC grid.
III. Further studies and analysis on the asymmetric faults in the offshore system and ride through strategies by using grid forming WGs.
IV. Progress on modeling, analysis and control of an MTDC grid with DR-HVDC OWPP for different operation modes and fault cases, using suitable models of the grid and power converters. These studies can pave the way for the successful integration of the DR-HVDC OWPP into the MTDC grid in the future.

Bibliography

[1] IPCC, "IPCC Special Report on Renewable Energy Sources and Climate Change Mitigation", Abu Dhabi, United Arab Emirates, Summary of Policy Makers, May 2011.

[2] (2019). IRENA Data & Statistics, [Online]. Available: https://www.irena.org/statistics (visited on 11/01/2019).

[3] (Jul. 2014). Renewable energy directive, [Online]. Available: https://ec.europa.eu/energy/en/topics/renewable-energy/renewable-energy-directive/overview (visited on 10/16/2019).

[4] C. Conti, M. L. Mancusi, F. Sanna-Randaccio, R. Sestini, and E. Verdolini, "Transition Towards a Green Economy in Europe: Innovation and Knowledge Integration in the Renewable Energy Sector", *Research Policy*, vol. 47, no. 10, pp. 1996–2009, 2018.

[5] P. Enevoldsen, F.-H. Permien, I. Bakhtaoui, A.-K. v. Krauland, M. Z. Jacobson, G. Xydis, B. K. Sovacool, S. V. Valentine, D. Luecht, and G. Oxley, "How much wind power potential does europe have? Examining european wind power potential with an enhanced socio-technical atlas", *Energy Policy*, vol. 132, pp. 1092–1100, Sep. 2019.

[6] Wind Europe, "Wind energy in Europe Scenarios for 2030", WIndEurope, Tech. Rep., Sep. 2017.

[7] AWEA. (2018). US Offshore Wind Industry Status Update 2018, [Online]. Available: https://www.awea.org/Awea/media/About-AWEA/U-S-Offshore-Wind-Fact-Sheet-September-2018_2.pdf (visited on 10/15/2019).

[8] WindEurope, "Offshore Wind in Europe - Key trends and statistics 2018", Annual Statistics Report, Feb. 2019.

[9] Hundleby, G and Freeman, K, "Unleashing Europe's offshore wind potential - A new resource assessment", Tech. Rep., Jun. 2017.

[10] K. Meah and S. Ula, "Comparative Evaluation of HVDC and HVAC Transmission Systems", in *2007 IEEE Power Engineering Society General Meeting*, Jun. 2007, pp. 1–5.

[11] T. Hammer, S. Seman, and P. Menke, "Diode-Rectifier HVDC link to onshore power systems: Dynamic performance of wind turbine generators and Reliability of liquid immersed HVDC Diode Rectifier Units", *CIGRE 2016*, vol. B4-121, 2016.

[12] B. Silva, C. Moreira, L. Seca, Y. Phulpin, and J. P. Lopes, "Provision of Inertial and Primary Frequency Control Services using Offshore Multi-terminal HVDC Networks", *IEEE Transactions on Sustainable Energy*, vol. 3, pp. 800–808, 2012.

[13] J. N. Sakamuri, M. Altin, and Z. H. Rather, "Coordinated Control Scheme for Ancillary Services from Offshore Wind Power Plants to AC and DC Grids", in *2016 IEEE Power and Energy Society General Meeting (PESGM)*, 2016, pp. 1–5.

[14] R. Green and N. Vasilakos, "The economics of offshore wind", *Energy Policy*, vol. 39, no. 2, pp. 496–502, Feb. 2011.

[15] H. Zhang, "Series Parallel Offshore Wind Farm", PhD thesis, Université de Lille, Lille, 2017.

[16] M. A. Abdullah, A. H. M. Yatim, C. W. Tan, and R. Saidur, "A review of maximum power point tracking algorithms for wind energy systems", *Renewable and Sustainable Energy Reviews*, vol. 16, no. 5, pp. 3220–3227, Jun. 2012.

[17] T. Ackermann, Ed., *Wind power in power systems*, 2. ed. Chichester: Wiley, 2012, OCLC: 794590486.

[18] S. Bolik et al, "HVDC connection of offshore wind power plants", English, CIGRE, Paris, Tech. Rep., 2015, OCLC: 920034203.

[19] PROMOTioN Project, "Deliverable 3.2 - Specifications of the control strategies and the simulation test cases.", Project PROMOTioN, European Project Deliverable, Mar. 2017.

[20] Z. Chen, S. Member, J. M. Guerrero, S. Member, and F. Blaabjerg, "A review of the state of the art of power electronics for wind turbines", *Chalmers University of Technology*, pp. 1859–1875, 2009.

[21] A. Ferguson, P. de Villiers, B. Fitzgerald, and J. Matthiesen, "Benefits in moving the intra-array voltage from 33 kV to 66 kV AC for large offshore wind farms", in *European Wind Energy Conf.*, Copenhagen, Denmark, 2012, p. 7.

[22] D. Van Hertem, O. Gomis-Bellmunt, and J. Liang, Eds., *HVDC grids: for offshore and supergrid of the future*, ser. IEEE Press series on power engineering 51. Hoboken, New Jersey: John Wiley & Sons, 2016.

[23] P. Bresesti, W. L. Kling, R. L. Hendriks, and R. Vailati, "HVDC Connection of Offshore Wind Farms to the Transmission System", *IEEE Trans. on Energy Conversion*, vol. 22, no. 1, pp. 37–43, Mar. 2007.

[24] Cigre Working Group, *Special considerations for AC collector systems and substations associated with HVDC-connected wind power plants: B3.36.* English. Paris: CIGRÉ, 2015, OCLC: 919034774.

[25] J. Glasdam, J. Hjerrild, Ł. H. Kocewiak, and C. L. Bak, "Review on multi-level voltage source converter based HVDC technologies for grid connection of large offshore wind farms", in *2012 IEEE International Conference on Power System Technology (POWERCON)*, Oct. 2012.

[26] (Nov. 2018). Nexans successfully qualifies a 525 kV HVDC underground cable system to German TSO standards, [Online]. Available: https://www.nexans.com/news/nexans-com/2018/11/Nexans-successfully-qualifies-a-525-kV-HVDC-underground-cable-system-to-German-TSO-standards.html (visited on 06/22/2019).

[27] C. Meyer, M. Hoing, A. Peterson, and R. W. De Doncker, "Control and Design of DC Grids for Offshore Wind Farms", *IEEE Trans. on Ind. Applicat.*, vol. 43, no. 6, pp. 1475–1482, 2007.

[28] P. Monjean, "Optimisation de l'architecture et des flux énergétiques de centrales à énergies renouvelables offshore et onshore équipées de liaisons en continu", PhD thesis, Arts et Métiers ParisTech, Sep. 2012.

[29] W. Chen, A. Q. Huang, C. Li, G. Wang, and W. Gu, "Analysis and Comparison of Medium Voltage High Power DC/DC Converters for Offshore Wind Energy Systems", *IEEE Transactions on Power Electronics*, vol. 28, no. 4, pp. 2014–2023, Apr. 2013.

[30] T. H. Nguyen, D. C. Lee, and C. K. Kim, "A Series-Connected Topology of a Diode Rectifier and a Voltage-Source Converter for an HVDC Transmission System", *IEEE Transactions on Power Electronics*, vol. 29, no. 4, pp. 1579–1584, Apr. 2014.

[31] M. Von Hofen, D. Karwatzki, L. Baruschka, and A. Mertens, "Hybrid offshore HVDC converter with diode rectifier and Modular Multilevel Converter", in *2016 IEEE 7th International Symposium on Power Electronics for Distributed Generation Systems (PEDG)*, Jun. 2016, pp. 1–7.

[32] N. Qin, S. You, Z. Xu, and V. Akhmatov, "Offshore wind farm connection with low frequency AC transmission technology", in *2009 IEEE Power & Energy Society General Meeting*, Calgary, Canada: IEEE, Jul. 2009.

[33] A. Teninge, "Participation aux Services Système de Parcs Eoliens Mixtes : Application en Milieu Insulaire", PhD Thesis, Grenoble INP, 2009.

[34] S. E. Aimani, "Modèlisation de différentes technologies d'éoliennes", PhD Thesis, Ecole Centrale de Lille, 2004.

[35] S. Li, T. A. Haskew, and L. Xu, "Conventional and novel control designs for direct driven PMSG wind turbines", *Electric Power Systems Research*, vol. 80, no. 3, pp. 328–338, Mar. 2010.

[36] F. Katiraei, R. Iravani, N. Hatziargyriou, and A. Dimeas, "Microgrids management", *IEEE Power and Energy Magazine*, vol. 6, no. 3, pp. 54–65, May 2008.

[37] J. Rocabert, A. Luna, F. Blaabjerg, and P. Rodríguez, "Control of Power Converters in AC Microgrids", *IEEE Trans. Power Electron.*, vol. 27, no. 11, pp. 4734–4749, Nov. 2012.

[38] T. Zhou, "Control and Energy Management of a Hybrid Active Wind Generator including Energy Storage System with Super-capacitors and Hydrogen technologies for Microgrid Application", PhD Thesis, Ecole Centrale de Lille, 2009.

[39] D. Lu, "Conception et contrôle d'un générateur PV actif à stockage intégré Application à l'agrégation de producteurs-consommateurs dans le cadre d'un micro réseau intelligent urbain", PhD Thesis, Ecole Centrale de Lille, 2010.

[40] P. Rault, "Dynamic Modeling and Control of Multi-Terminal HVDC Grids", PhD Thesis, Centrale Lille, Lille, 2014.

[41] M. Bahrman and P.-E. Bjorklund, "The New Black Start: System Restoration with Help from Voltage-Sourced Converters", *IEEE Power and Energy Mag.*, vol. 12, no. 1, pp. 44–53, Jan. 2014.

[42] C. Feltes, H. Wrede, F. W. Koch, and I. Erlich, "Enhanced Fault Ride-Through Method for Wind Farms Connected to the Grid Through VSC-Based HVDC Transmission", *IEEE Transactions on Power Systems*, vol. 24, no. 3, pp. 1537–1546, Aug. 2009.

[43] Anaya-Lara, Olimpo, Campos-Gaona, David, Moreno-Goytia, Edgar, and Adam, Grain, *Offshore Wind Energy Generation*. John Wiley \& Sons, 2014.

[44] J. Schachner, "Power connections for offshore wind farms", Diploma Thesis, Delft University of Technology, Jan. 2004.

[45] ABB. (2014). Technical note ABB medium voltage wind turbine converters enable island mode operation, [Online]. Available: https://library.e.abb.com/public/dee1542f16c66b39c1257d2d00284d9a/PCS6000%20technical%20note_island%20mode_lowres.pdf.

[46] P. Gardner, L. M. Craig, G. J. Smith, and G. Hassan, "Electrical Systems for Offshore Wind Farms", in *Proceedings of the 20th British Wind Energy Association Conference, Cardiff, UK*, Cardiff, 1998.

[47] L. Peng, "Reconfiguration du dispositif de commande d'une éolienne en cas de creux de tension", PhD Thesis, Centrale Lille, Lille, 2010.

[48] R. Li, L. Yu, and L. Xu, "Offshore AC Fault Protection of Diode Rectifier Unit Based HVDC System for Wind Energy Transmission", *IEEE Transactions on Industrial Electronics*, vol. 2, no. 7, pp. 5289–5299, 2018.

[49] S. K. Chaudhary, R. Teodorescu, P. Rodriguez, and P. C. Kjar, "Chopper controlled resistors in VSC-HVDC transmission for WPP with full-scale converters", in *2009 IEEE PES/IAS Conference on Sustainable Alternative Energy (SAE)*, Valencia, Spain: IEEE, Sep. 2009, pp. 1–8.

[50] P. Menke, "New grid access solutions for offshore wind farms", in *EWEA Offshore, 2015*, 2015.

[51] S. Chiniforoosh, H. Atighechi, A. Davoudi, J. Jatskevich, A. Yazdani, S. Filizadeh, M. Saeedifard, J. A. Martinez, V. Sood, K. Strunz, J. Mahseredjian, and V. Dinavahi, "Dynamic Average Modeling of Front-End Diode Rectifier Loads Considering Discontinuous Conduction Mode and Unbalanced Operation", *IEEE Transactions on Power Delivery*, vol. 27, no. 1, pp. 421–429, Jan. 2012.

[52] Krause, Paul C, Wasynczuk, Oleg, Sudhoff, Scott D, and Pekarek, Steven, *Analysis of Electric Machinery and Drive Systems, 3rd Edition*, 3rd ed. Wiley Online Library, 2002, vol. 2.

[53] S. Añó-Villalba, S. Bernal-Perez, R. Pena, R. Vidal-Albalate, E. Belenguer, N. Aparicio, and R. Blasco-Gimenez, "24-Pulse rectifier for harmonic management in HVDC diode rectifier wind power plants", in *12th IET International Conference on AC and DC Power Transmission (ACDC 2016)*, May 2016, pp. 1–6.

[54] R. Blasco-Gimenez, S. Añó-Villalba, J. Rodríguez-D'Derlée, F. Morant, and S. Bernal-Perez, "Distributed Voltage and Frequency Control of Offshore Wind Farms Connected With a Diode-Based HVdc Link", *IEEE Transactions on Power Electronics*, vol. 25, no. 12, pp. 3095–3105, Dec. 2010.

[55] J. P. Bowles, "Multiterminal HVDC Transmission Systems Incorporating Diode Rectifier Stations", *IEEE Transactions on Power Apparatus and Systems*, vol. PAS-100, no. 4, pp. 1674–1678, Apr. 1981.

[56] T. Machida, I. Ishikawa, E. Okada, and E. Karasawa, "Control and protection of HVDC systems with diode valve converter", *Elect. Eng. Jpn.*, vol. 98, no. 1, pp. 62–70, Jan. 1978.

[57] Walsh, Colin, "Offshore wind in Europe: Key Trends and Statistics 2018", Wind Europe, Tech. Rep., Feb. 2019.

[58] T. Hammer, S. Seman, and P. Menke, "Diode-Rectifier HVDC link to onshore power systems: Dynamic performance of wind turbine generators and Reliability of liquid immersed HVDC Diode Rectifier Units", *CIGRE 2016*, vol. B4-121, 2016.

[59] J. J. R. D'derlée, "Control strategies for offshore wind farms based on PMSG wind turbines and HVdc connection with uncontrolled rectifier", PhD thesis, Polytechnic University of Valencia, Dec. 2013.

[60] (2019). PROMOTioN - Work Packages Structure, [Online]. Available: https://www.promotion-offshore.net/about_promotion/work_packages_structure/ (visited on 10/24/2019).

[61] S. Seman, R. Zurowski, and C. Taratoris, "Interconnection of advanced Type 4 WTGs with Diode Rectifier based HVDC solution and weak AC grids", in *Proceedings of the 14th Wind Integration Workshop*, 2015.

[62] L. Yu, R. Li, and L. Xu, "Distributed PLL-Based Control of Offshore Wind Turbines Connected With Diode-Rectifier-Based HVDC Systems", *IEEE Transactions on Power Delivery*, vol. 33, no. 3, pp. 1328–1336, Jun. 2018.

[63] C. Prignitz, H. G. Eckel, and A. Rafoth, "FixReF sinusoidal control in line side converters for offshore wind power generation", in *2015 IEEE 6th International Symposium on Power Electronics for Distributed Generation Systems (PEDG)*, Jun. 2015, pp. 1–5.

[64] M. Á. Cardiel-Álvarez, S. Arnaltes, J. L. Rodriguez-Amenedo, and A. Nami, "Decentralized Control of Offshore Wind Farms Connected to Diode-Based HVdc Links", *IEEE Transactions on Energy Conversion*, vol. 33, no. 3, pp. 1233–1241, Sep. 2018.

[65] Ö. Göksu, O. Saborío-Romano, N. A. Cutululis, and P. Sørensen, "Black Start and Island Operation Capabilities of Wind Power Plants", in *16th Wind Integration Workshop*, Berlin, Germany, Oct. 2017.

[66] ENTSO-E, "ENTSO-E Network Code for Requirements for Grid Connection Applicable to all Generators", Tech. Rep., Aug. 2013.

[67] L. Xu, B. W. Williams, and L. Yao, "Multi-terminal DC transmission systems for connecting large offshore wind farms", in *2008 IEEE Power and Energy Society General Meeting - Conversion and Delivery of Electrical Energy in the 21st Century*, Jul. 2008, pp. 1–7.

[68] K. Bell, D. Cirio, A. M. Denis, L. He, C. C. Liu, G. Migliavacca, C. Moreira, and P. Panciatici, "Economic and technical criteria for designing future off-shore HVDC grids", in *2010 IEEE PES Innovative Smart Grid Technologies Conference Europe (ISGT Europe)*, Gothenburg, Sweden: IEEE, Oct. 2010.

[69] S. Bernal-Perez, S. Añó-Villalba, R. Blasco-Gimenez, and N. Aparicio, "Connection of off-shore wind power plants to VSC-MTdc networks using HVdc diode-rectifiers", in *2013 IEEE International Symposium on Industrial Electronics (ISIE)*, May 2013, pp. 1–6.

[70] R. Li, L. Yu, and L. Xu, "Hierarchical control of offshore wind farm connected by parallel diode-rectifier based HVDC and HVAC links", *IET Renewable Power Generation*, vol. 13, no. 9, Mar. 2019.

[71] S. Bernal-Perez, S. Ano-Villalba, R. Blasco-Gimenez, and J. Rodriguez-D'Derlee, "Offshore wind farm grid connection using a novel diode-rectifier and VSC-inverter based HVDC transmission link", in *IECON 2011-37th Annual Conference on IEEE Industrial Electronics Society*, IEEE, 2011, pp. 3186–3191.

[72] C. K. Sao and P. W. Lehn, "Intentional islanded operation of converter fed microgrids", in *2006 IEEE Power Engineering Society General Meeting*, 2006.

[73] H. Han, X. Hou, J. Yang, J. Wu, M. Su, and J. M. Guerrero, "Review of Power Sharing Control Strategies for Islanding Operation of AC Microgrids", *IEEE Transactions on Smart Grid*, vol. 7, no. 1, pp. 200–215, Jan. 2016.

[74] M. Amin, M. Molinas, and J. Lyu, "Oscillatory phenomena between wind farms and HVDC systems: The impact of control", in *2015 IEEE 16th Workshop on Control and Modeling for Power Electronics (COMPEL)*, Jul. 2015, pp. 1–8.

[75] T. Christ, S. Seman, and R. Zurowski, "Verfahren zur regelung eines selbstgeführten umrichters, selbstgeführter umrichter sowie anordnung zur übertragung elektrischer leistung", EP3311481A1, Apr. 2018.

[76] A. Jain and K. Das, "Control Solutions for Blackstart Capability and Islanding Operation of Offshore Wind Power Plants", in *17th Wind Integration Workshop*, Stockholm, Sweden, Oct. 2018, pp. 1–7.

[77] R. Blasco-Gimenez, S. Ano-Villalba, J. Rodriguez, V. Aldana, A. Correcher, F. Morant, and E. Quiles, "Variable voltage off-shore distribution network for wind farms based on synchronous generators", in *20th International Conference and Exhibition on Electricity Distribution - Part 1, 2009. CIRED 2009*, Jun. 2009, pp. 1–4.

[78] A. I. Andrade, R. Blasco-Gimenez, and G. R. Pena, "Distributed control strategy for a wind generation systems based on PMSG with uncontrolled rectifier HVDC connection", in *2015 IEEE International Conference on Industrial Technology (ICIT)*, Seville: IEEE, Mar. 2015, pp. 982–986.

[79] J. M. Guerrero, J. C. Vasquez, J. Matas, L. G. d. Vicuna, and M. Castilla, "Hierarchical Control of Droop-Controlled AC and DC Microgrids - A General Approach Toward Standardization", *IEEE Transactions on Industrial Electronics*, vol. 58, no. 1, pp. 158–172, Jan. 2011.

[80] M. Gierschner, H. J. Knaak, and H. G. Eckel, "Fixed-reference-frame-control: A novel robust control concept for grid side inverters in HVDC connected weak offshore grids", in *2014 16th European Conference on Power Electronics and Applications (EPE'14-ECCE Europe)*, Aug. 2014, pp. 1–7.

[81] C. Prignitz, H. G. Eckel, S. Achenbach, F. Augsburger, and A. Schön, "FixReF: A control strategy for offshore wind farms with different wind turbine types and diode rectifier HVDC transmission", in *2016 IEEE 7th International Symposium on Power Electronics for Distributed Generation Systems (PEDG)*, Jun. 2016.

[82] J. M. Guerrero, M. Chandorkar, T.-L. Lee, and P. C. Loh, "Advanced Control Architectures for Intelligent Microgrids—Part I: Decentralized and Hierarchical Control", *IEEE Trans. Ind. Electron.*, vol. 60, no. 4, pp. 1254–1262, Apr. 2013.

[83] R. Li, L. Yu, L. Xu, and G. P. Adam, "DC Fault Protection of Diode Rectifier Unit Based HVDC System Connecting Offshore Wind Farms", in *2018 IEEE Power Energy Society General Meeting (PESGM)*, 2018.

[84] E. Muljadi, C. P. Butterfield, A. Ellis, J. Mechenbier, J. Hochheimer, R. Young, N. Miller, R. Delmerico, R. Zavadil, and J. C. Smith, "Equivalencing the collector system of a large wind power plant", in *2006 IEEE Power Engineering Society General Meeting*, 2006, pp. 1–9.

[85] A. Silverstein, "Time Synchronization in the Electric Power System", North American SynchroPhasor Initiative, Technical Report, Mar. 2017, p. 59.

[86] (2018). ENTSO-E - Market Committee. en-us, [Online]. Available: https://www.entsoe.eu/about/market/ (visited on 09/25/2018).

[87] ENTSO-E. (Oct. 2017). Survey on Ancillary Services Procurement, Balancing Market Design 2016, [Online]. Available: https://docstore.entsoe.eu/Documents/Publications/Market%20Committee%20publications/WGAS_Survey_final_10.03.2017.pdf (visited on 07/03/2018).

[88] J. W. Feltes and C. Grande-Moran, "Black start studies for system restoration", in *2008 IEEE Power and Energy Society General Meeting - Conversion and Delivery of Electrical Energy in the 21st Century*, Jul. 2008.

[89] J. L. Rodriguez-Amenedo, S. Arnalte, and J. C. Burgos, "Automatic generation control of a wind farm with variable speed wind turbines", *IEEE Transactions on Energy Conversion*, vol. 17, no. 2, pp. 279–284, Jun. 2002.

[90] R. deAlmeida, E. Castronuovo, and J. Pecas Lopes, "Optimum Generation Control in Wind Parks When Carrying Out System Operator Requests", *IEEE Trans. Power Syst.*, vol. 21, no. 2, pp. 718–725, May 2006.

[91] R. Teichmann, L. Li, C. Wang, and W. Yang, "Method, apparatus and computer program product for wind turbine start-up and operation without grid power", US7394166B2, Jul. 2008.

[92] F. J. Bodewes and F. L. H. Strik, "Wind farm island operation", EP2236821A1, Oct. 2010.

[93] T. Edenfeld, "Use of pitch battery power to start wind turbine during grid loss/black start capability", US20100013224A1, Jan. 2010.

[94] M. Schult, D. Flum, P. Weisenberger, and T. Harder, "Method for operating an energy installation, and an energy system comprising such energy installations", WO2014082757A1, Jun. 2014.

[95] X. Huang and Y. Chen, "Method for black starting wind turbine, wind farm, and restoring wind farm and wind turbine, wind farm using the same", US20170074244A1, Mar. 2017.

[96] N. Kouassi and B. Francois, "AC offshore grid forming of a collection network for wind park by considering storage and hybrid power electronic systems", in *2016 International Conference on Electrical Sciences and Technologies in Maghreb (CISTEM)*, Oct. 2016.

[97] (2017). Inching toward 10 MHI Vestas unwraps a 9.5-MW design, [Online]. Available: https://www.windpowerengineering.com/design/inching-toward-10-mhi-vestas-unwraps-9-5-mw-design/ (visited on 10/01/2018).

[98] N. T. Ave. (2019). Datasheet for Panasonic HIT Power 220a, [Online]. Available: http://www.panasonic.com/business/pesna/includes/pdf/eco-construction-solution/HIT_Power_220A_Datasheet.pdf.

[99] H. Zhao, Q. Wu, S. Hu, H. Xu, and C. N. Rasmussen, "Review of energy storage system for wind power integration support", *Applied Energy*, vol. 137, pp. 545–553, Jan. 2015.

[100] J. Keller and B. Kroposki, "Understanding Fault Characteristics of Inverter-Based Distributed Energy Resources", Tech. Rep. NREL/TP-550-46698, 971441, Jan. 2010.

[101] C. A. Plet, M. Brucoli, J. D. F. McDonald, and T. C. Green, "Fault models of inverter-interfaced distributed generators: Experimental verification and application to fault analysis", in *2011 IEEE Power and Energy Society General Meeting*, Jul. 2011, pp. 1–8.

[102] C. A. Plet, M. Graovac, R. Iravani, and T. C. Green, "Fault Response of Grid-Connected Inverter Dominated Networks", in *IEEE PES General Meeting*, 2010, pp. 1–8.

[103] C. Sourkounis and P. Tourou, "Grid Code Requirements for Wind Power Integration in Europe", *Conference Papers in Energy*, vol. 2013, 2013.

[104] S. K. Chaudhary, "Control and protection of wind power plants with VSC-HVDC connection", OCLC: 831214051, PhD Thesis, Department of Energy Technology, Aalborg University, Aalborg, 2011.

[105] O. Anaya-Lara, D. Campos-Gaona, E. Moreno-Goytia, and A. Grain, "OFfshore Wind Farm Protection", in *Offshore wind energy generation: control, protection, and integration to electrical systems*, John Wiley & Sons, 2014.

[106] G. Ramtharan, A. Arulampalam, J. Ekanayake, F. Hughes, and N. Jenkins, "Fault ride through of fully rated converter wind turbines with AC and DC transmission systems", *IET Renew. Power Gener.*, vol. 3, no. 4, p. 426, 2009.

[107] A. Teninge, D. Roye, S. Bacha, and J. Duval, "Low voltage ride-through capabilities of wind plant combining different turbine technologies", 2009.

[108] L. Peng, "Research on Graphical Modeling and Low Voltage Ride-Through Control Strategies of Doubly Fed Induction Wind Generator System", PhD Thesis, Ecole Centrale de Lille, 2010.

[109] V. Gevorgian and E. Muljadi, "Wind Power Plant Short Circuit Current Contribution for Different Fault and Wind Turbine Topologies: Preprint", Quebec, Canada, Oct. 2010.

[110] A. Hansen and G. Michalke, "Multi-pole permanent magnet synchronous generator wind turbines' grid support capability in uninterrupted operation during grid faults", *IET Renew. Power Gener.*, vol. 3, no. 3, p. 333, 2009.

[111] K.-H. Kim, Y.-C. Jeung, D.-C. Lee, and H.-G. Kim, "LVRT Scheme of PMSG Wind Power Systems Based on Feedback Linearization", *IEEE Trans. Power Electron.*, vol. 27, no. 5, pp. 2376–2384, May 2012.

[112] T. H. Nguyen and D. Lee, "Advanced Fault Ride-Through Technique for PMSG Wind Turbine Systems Using Line-Side Converter as STATCOM", *IEEE Transactions on Industrial Electronics*, vol. 60, no. 7, pp. 2842–2850, Jul. 2013.

[113] R. Vidal-Albalate, R. Pena, S. Añó-Villalba, E. Belenguer, and R. Blasco-Gimenez, "Hybrid full bridge-half bridge MML power converter for HVDC diode rectifier connection of large off-shore wind farms", in *2018 IEEE International Conference on Industrial Technology (ICIT)*, IEEE, 2018, pp. 994–999.

[114] G. Ramtharan, A. Arulampalam, J. B. Ekanayake, F. M. Hughes, and N. Jenkins, "Fault ride through of fully rated converter wind turbines with AC and DC transmission", *IET Renewable Power Generation*, vol. 3, no. 4, pp. 426–438, Dec. 2009.

[115] UpWInd Project, "Design Limits and Solutions for Very Large Wind Turbines", Tech. Rep., Mar. 2011.

[116] Y. Amirat, M. Benbouzid, B. Bensaker, and R. Wamkeue, "Condition Monitoring and Fault Diagnosis in Wind Energy Conversion Systems: A Review", in *IEEE IEMDC'07*, vol. 2, Antalya, Turkey, May 2007, pp. 1434–1439.

[117] M. Martinez-Luengo, A. Kolios, and L. Wang, "Structural health monitoring of offshore wind turbines: A review through the Statistical Pattern Recognition Paradigm", *Renewable and Sustainable Energy Reviews*, vol. 64, pp. 91–105, Oct. 2016.

[118] S. Bernal-Perez, S. Ano-Villalba, R. Blasco-Gimenez, and J. Rodriguez-D'Derlee, "Efficiency and Fault Ride-Through Performance of a Diode-Rectifier- and VSC-Inverter-Based HVDC Link for Offshore Wind Farms", *IEEE Transactions on Industrial Electronics*, vol. 60, no. 6, pp. 2401–2409, Jun. 2013.

[119] G. Buigues, V. Valverde, A. Etxegarai, P. Eguía, and E. Torres, "Present and future multiterminal HVDC systems: current status and forthcoming", *REPQJ*, vol. 1, no. 15, pp. 83–88, Apr. 2017.

[120] K. Shinoda, A. Benchaib, J. Dai, and X. Guillaud, "DC voltage control of MMC-based HVDC grid with Virtual Capacitor Control", in *2017 19th European Conference on Power Electronics and Applications (EPE'17 ECCE Europe)*, Warsaw: IEEE, Sep. 2017.

[121] C. E. Spallarossa, T. C. Green, C. Lin, and X. Wu, "A DC voltage control strategy for MMC MTDC grids incorporating multiple master stations", in *2014 IEEE PES T&D Conference and Exposition*, Chicago, IL, USA: IEEE, Apr. 2014.

[122] J. Beerten, D. Van Hertem, and R. Belmans, "VSC MTDC systems with a distributed DC voltage control - A power flow approach", in *2011 IEEE Trondheim PowerTech*, Trondheim: IEEE, Jun. 2011.

[123] O. Marjanovic, M. Barnes, and W. Wang, "Droop control modelling and analysis of multi-terminal HVDC for offshore wind farms", in *10th IET International Conference on AC and DC Power Transmission (ACDC 2012)*, Birmingham, UK: Institution of Engineering and Technology, 2012.

[124] K. Shinoda, "Control and Energy Management of MMC-based Multi-Terminal HVDC Grids", PhD Thesis, Centrale Lille, 2017.

[125] C. Nentwig, J. Haubrock, R. H. Renner, and D. Van Hertem, "Application of DC choppers in HVDC grids", in *2016 IEEE International Energy Conference (ENERGYCON)*, Leuven, Belgium: IEEE, Apr. 2016.

[126] A. Zama, S. A. Mansour, D. Frey, A. Benchaib, S. Bacha, and B. Luscan, "A comparative assessment of different balancing control algorithms for modular multilevel converter (MMC)", in *2016 18th European Conference on Power Electronics and Applications (EPE'16 ECCE Europe)*, Karlsruhe: IEEE, Sep. 2016.

[127] Lin, Weixing, Jovcic, Dragan, Nguefeu, Samuel, and Saad, Hani, "Full Bridge MMC Converter Optimal Design to HVDC operational Requirements.pdf", *IEEE Transactions on Power Delivery*, vol. 31, no. 3, pp. 1342–1350, 2015.

[128] A. Hansen and G. Michalke, "Multi-pole permanent magnet synchronous generator wind turbines' grid support capability in uninterrupted operation during grid faults", *IET Renew. Power Gener.*, vol. 3, no. 3, 2009.

A

MPPT Methods for Wind Generators

1. Optimal Tip Speed Ratio

This is a straight-forward implementation of MPPT through maintaining the optimal tip speed ratio. It is worth noting that there is a need for precise wind speed measurements to have an accurate MPPT and thus is more complicated and costly to implement.

2. Optimal Torque Control

Using the equations (2.1, 2.2), the power extracted by the wind turbine can be rewritten, with substitution for the term wind speed (v_w)

$$P_w = \frac{1}{2}\rho\pi R_t^5 \frac{\omega_m^3}{\lambda^3} C_P \tag{A.1}$$

The above equation A.1 is re-written for the optimal values of the tip speed ratio ($\lambda = \lambda_0$) and ($C_P = C_{Pmax}$). Thus, the maximum power extracted from the wind can be obtained as follows:

$$P_{\max} = \frac{1}{2}\rho\pi R^5 \frac{C_{P\max}}{\lambda_0^3}\omega_m^3 = K_{\mathrm{p-opt}}\omega_m^3 \tag{A.2}$$

Finally, the optimal torque equation can be written as follows:

$$T_{\mathrm{opt}} = \frac{1}{2}\rho\pi R^5 \frac{C_{P\max}}{\lambda_0^3}\omega_m^2 = K_{\mathrm{opt}}\omega_m^2 \tag{A.3}$$

Here, the optimal torque constant K_{opt} is invariant and can be directly used to track the maximum power point. It is considered to be a simple and fast method, while the drawback could be that the lack of wind measurement, prevents the impact of fast wind speed changes on the reference signal.

3. Power Signal Feedback Control

The above method involved the implementation of an optimal torque control, by using a constant reference of K_{opt}. But in this MPPT method, a look up table is constructed using the experimental results of the wind turbine operation. A measurement of the rotor speed is used to directly fetch the optimal power set point value, with also a power signal feedback for the controller.

4. Perturb and Observe Method

Otherwise called the Hill Climb Search method, the Perturb and Observe method is a mathematical optimization algorithm to locate the maximum point in a curve for a given wind speed. Here, the perturbed variable is the rotor speed or the generator voltage and the observed quantity is the mechanical or electrical power, respectively. The biggest advantage of this method is that all the required measurements to implement the control are generally local and thus it is fast and efficient. Also the method can be implemented with little or no knowledge of the wind turbine characteristics, since it is a mathematical optimization approach. Certain problems do exist related to a smaller or a bigger step size for perturbation, wrong perturbation due to sudden change of wind speed etc. However, it is worth pointing out that a lot of research studies have been done to tackle such problems.

B

MMC Converter Topology

MMC converter topology

The first offshore wind power plant with HVDC connection (BorWin 1), used a 2 level VSC configuration. It is worth highlighting that after this installation, all the future VSC projects for offshore wind, used or will use a more advanced VSC converter type called the MMC [25]. As the name suggests, the MMC consists of multiple identical units made up of switches and capacitors, forming a basic unit called the sub-module. Then, the required converter is designed by cascading the sub–modules.

There are different technologies commercially available today but they share similar advantages compared to the two level VSC such as modular design, scalability, elimination of DC filters and DC Capacitor, lower switching losses among others. The general topology [126] with half bridge sub modules, is illustrated in the Figure B.1. The MMC consists of multiple sub–modules connected in series per phase to form a phase arm. The two arms per phase form a phase leg. The half bridge sub module consists of two IGBTs and anti-parallel diodes connected to a capacitance. There are three major switching states based on the gating pulses to the IGBTs:

1. ON state - is when S_1 is on and S_2 is off, allowing SM voltage equal to the capacitor voltage
2. OFF state - is when S_1 is off and S_2 is on, bypassing the capacitor and thus the voltage across the capacitor is zero.

3. BLOCKED state - is when both S_1 and S_2 are off, allowing current to pass through the freewheeling diodes

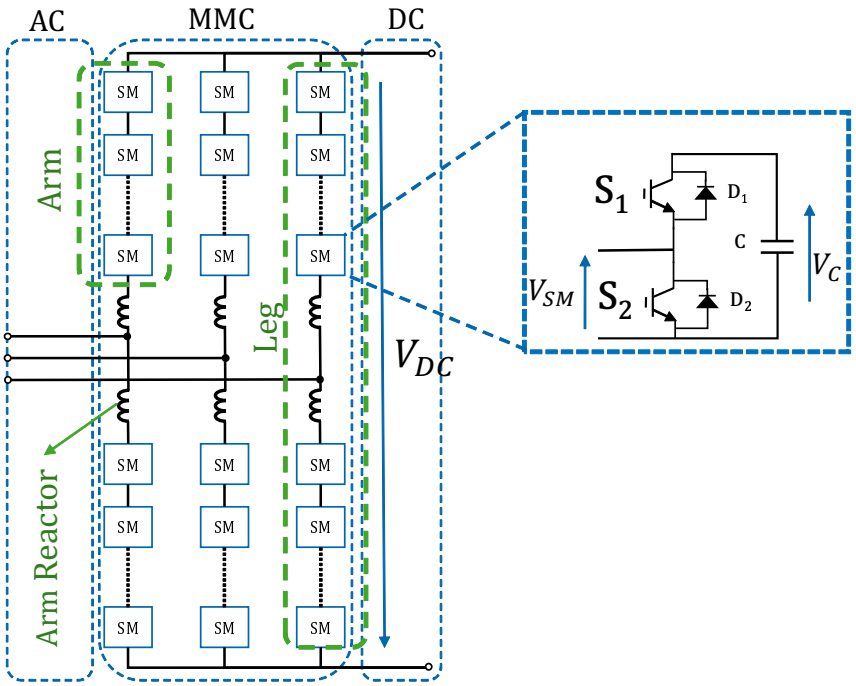

Figure B.1: Illustration of an MMC and a Half Bridge MMC Sub-module

By appropriately switching the sub–modules, desired AC voltage can be obtained in the three phases. The reactances in each phase are used to limit the balancing current between the three legs, since they do not exactly generate the same voltage. This reactance also limits the DC fault current, permitting safe blocking of the IGBTs before high levels of fault currents are achieved. The complex configuration of the MMC results in certain additional control requirements compared to the classical two level VSC system. Notable requirements for instance are the control of the circulating currents between the MMC arms and also the balancing control for the SM capacitor voltages [126].

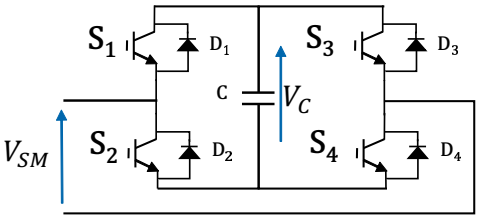

Figure B.2: Illustration of a Full Bridge Sub-module

The MMC converter modules could also be of Full bridge (H bridge) – in which there are two additional IGBT switchtes per sub–module, as shown in the Figure B.2. The Full Bridge MMC has certain clear advantages over the half bridge MMC [127], like, the ability to suppress

DC fault currents, the operation at reduced HVDC voltage etc. But using additional switches induces twice the losses and higher cost, compared to the half bridge configuration. d. Here, the perturbed variable is the rotor speed or the generator voltage and the observed quantity is the mechanical or electrical power, respectively. The biggest advantage of this method is that all the required measurements to implement the control are generally local and thus it is fast and efficient. Also the method can be implemented with little or no knowledge of the wind turbine characteristics, since it is a mathematical optimization approach. Certain problems do exist related to a smaller or a bigger step size for perturbation, wrong perturbation due to sudden change of wind speed etc. However, it is worth pointing out that a lot of research studies have been done to tackle such problems.

C

DC Voltage Control for Solution 1

The control of DC voltage (of the back to back converter) by the MSC has been suggested, to enhance their fault ride through capability. In case of a fault in the feeder or the AC grid, the control of the DC link of the B2B converter is not lost and so a better fault ride through is achieved [128]. The GSC, directly connected to the AC grid, can reduce the power production when it detects a fault condition.

The solution 1 [54] adopted this approach, so that the GSC can participate in grid forming function. The dc voltage control scheme is of the form as shown in the Figure C.1. Recalling the dynamic equation, in time domain, for the DC link from chapter 3 for the back to back converter:

$$\frac{dV_{dc}}{dt} = \frac{1}{C_{dc}} I_{dc1}(t) - \frac{1}{C_{dc}} I_{dc2}(t) \tag{C.1}$$

The AC power on the Machine side and the DC power are assumed to be equal, without any power losses. And given that an arbitrary reference frame in dq is aligned along the stator voltage (V_{sd}=0), the following equation is written:

$$V_{dc} C_{dc} \frac{dV_{dc}}{dt} + V_{dc} I_{dc2} = \frac{3}{2}(V_{sq} I_{sq}) \tag{C.2}$$

Multiplying by 2 on both side and rearranging the above equation, gives the following form:

$$2V_{dc}C_{dc}\frac{dV_{dc}}{dt} = 3\left(V_{sq}I_{sq}\right) - 2V_{dc}I_{dc2} \tag{C.3}$$

In fact the term $2V_{dc}C_{dc}\frac{dV_{dc}}{dt}$ can be expressed as the double derivative of V_{dc} and thus:

$$\frac{dV_{dc}^2}{dt} = \frac{3}{C_{dc}}\left(V_{sq}I_{sq}\right) - \frac{2}{C_{dc}}V_{dc}I_{dc2} \tag{C.4}$$

A decoupling term U_{dc} is introduced in order to derive the control scheme for the DC voltage V_{dc}, as follows:

$$\frac{dV_{dc}^2}{dt} = U_{dc} \tag{C.5}$$

$$U_{dc} = \frac{3}{C_{dc}}\left(V_{sq}I_{sq}\right) - \frac{2}{C_{dc}}V_{dc}I_{dc2} \tag{C.6}$$

The reference current of the stator, I_{sq}^* can now be directly derived, since the inner current loop is assumed to be faster than the outer (DC) voltage control loop:

$$I_{sq}^* = \frac{C_{de}}{3V_{sq}}U_{vdc} + \frac{2}{3V_{sq}}\cdot V_{d\varepsilon}I_{dc2} \tag{C.7}$$

The final control scheme for the DC voltage control in the Figure C.1, is obtained by using the following form of the above equation:

$$I_{\mathrm{sq}}^* = \frac{1}{3V_{\mathrm{sq}}}\left(C_{\mathrm{de}}U_{\mathrm{Vde}} + 2V_{dc}I_{\mathrm{dc2}}\right) \tag{C.8}$$

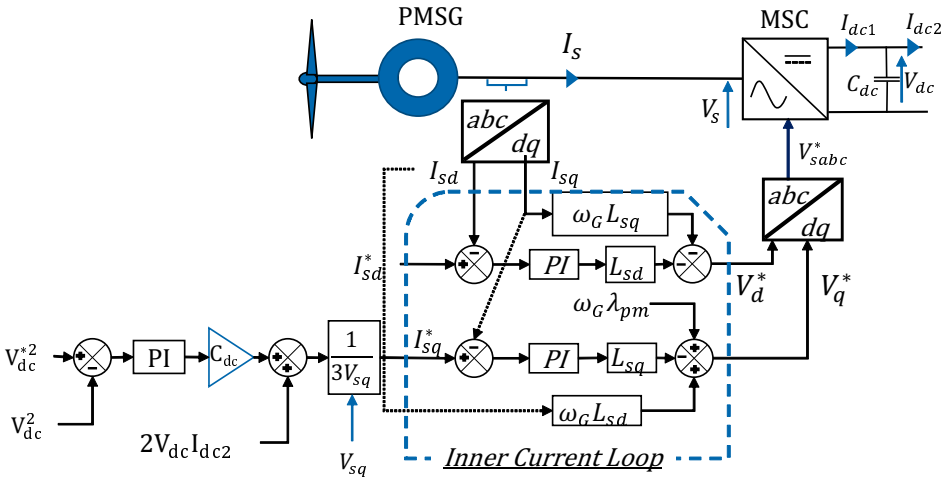

Figure C.1: Generic representation of a Wind Generator

D

Aggregation of WGs and string impedances

The aggregated model for a string can be obtained by sizing up the capacity (in current) for a single WG, while also sizing the transformers and filters accordingly. For the submarine cables, the series and shunt impedances are aggregated according to the approach presented in [84].

Consider a string connected in a radial fashion as in the Figure D.1. The string is assumed to have the same cable parameters for all the sections i.e. it does not vary according to the current capacity. This is not the case in reality, since the cable section closest to the PCC will have the largest current capacity. Due to radial connection, the current in each cable increases from the cable farthest (cable 1) from the PCC to the cable closest (cable n).

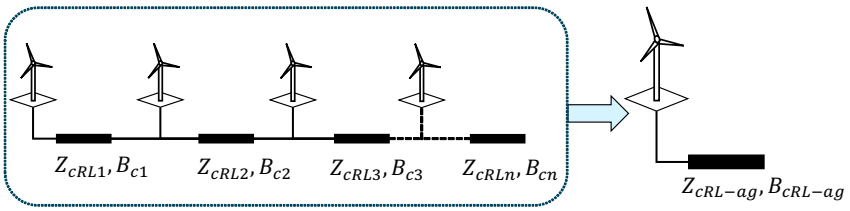

Figure D.1: Study Case Network for Simulation Studies

Thus, the following equations are valid and used to simplify the aggregation process.

$$Z_{cRL1} = Z_{cRL2} = ... = Z_{cRLn} \quad and \quad B_{c1} = B_{c2} = ... = B_{cn} \tag{D.1}$$

This allows a simplified formula for series impedance aggregation, as shown in the equation D.2. For shunt capacitance, the sum of all the shunt impedances is suggested by [84] and validated by using study cases.

$$Z_{\text{cRL-ag}} = Z_{cRL} \frac{(n_c + 1)(2n_c + 1)}{6n_c} \tag{D.2}$$

$$B_{\text{c-ag}} = \sum_{i=1}^{n_c} B_{ci} \tag{D.3}$$

Gestion des Flux Energétiques d'une Ferme Eolienne en Mer connectée à un Système HVDC au travers d'un Redresseur à Diodes

Résumé: La transition énergétique pour un monde plus durable est désormais la priorité de nombreux pays. Dans cet objectif, notamment en Europe, le développement de l'énergie éolienne en mer (offshore) a été rapide. Le transport de l'électricité en Courant Continu Haute Tension (HVDC) basé sur un convertisseur électronique à source de tension (VSC) est la solution de transport aujourd'hui, pour les fermes éoliennes en mer éloignées de plus de 50 km de la côte. La solution d'un redresseur à diodes dans les stations de conversion en mer est plus compacte, plus robuste et moins chère. Cette thèse porte sur les divers problèmes technologiques et scientifiques liés au contrôle du réseau alternatif isolé en mer permettant le raccordement des fermes éoliennes. Ces verrous sont d'abord examinés en détail dans l'état de l'art. Ensuite, le système éolien offshore est analysé en utilisant les équations dynamiques développées en d-q pour les modes de fonctionnement tant insulaires que connectés (normaux). Certaines des solutions de contrôle en Grid Forming sont comparées et évaluées à l'aide de simulations dans le domaine temporel, pour un cas d'étude donné. Puis, les différentes solutions de démarrage du réseau offshore (dit Black Start) sont identifiées dans la littérature et comparées, avec plusieurs critères qualitatifs. Ensuite, les différents types de défauts du système sont analysés à l'aide de la littérature. Enfin, une brève analyse est faite sur les défis pour l'intégration de ce type de ferme au réseau MTDC.

Mots-clefs: ferme éolienne offshore, contrôle du réseau, contrôle de la tension, gestion de la ferme, démarrage, courant continu haute tension

Control and Power Management of an Offshore Wind Power Plant with a Diode Rectifier based HVDC Transmission.

Abstract: Energy Transition for a more sustainable world is now the priority in societies. Towards this objective, especially in Europe, the offshore wind energy development has been fast. For Offshore Wind Power Plants (OWPP) farther from the shore (50 km and beyond) Voltage Source Converter (VSC) based High Voltage DC (HVDC) Transmission has become the prominent solution. Replacement of offshore VSC station by multiple Diode Rectifier Units (DRUs) led to a cheaper, more compact and robust solution. This thesis focuses on various technological and scientific problems involved in the control system of the Offshore Wind power Plant with Diode Rectifier (DR) based HVDC transmission. These challenges are first reviewed in detail along with the state of the art. Then the offshore system dynamics are analyzed and the control requirements are laid out. Following this, some of the selected control solutions in the literature for this topology are reviewed, compared and assessed by using time domain simulations of a study case. Then, different black start solutions for the offshore AC grid are reviewed and compared using the various qualitative criteria. The various faults in the offshore system are then analyzed and the fault ride through strategies are reviewed in detail. Finally, a brief analysis is done on the challenges for the integration of this OWPP topology into a Multi Terminal DC (MTDC) network.

Keywords: offshore wind power plant, grid forming, voltage control, generation control, black start, High Voltage DC (HVDC)